Hydrogel de nanocapsules lipidiques chargées en gemcitabine : une technologie pharmaceutique pour cibler les ganglions de drainage des cancers

Elodie Moysan

l'université nantes angers le mans
PÔLE DE RECHERCHE ET D'ENSEIGNEMENT SUPÉRIEUR

université angers

Thèse de Doctorat

Elodie Moysan

Mémoire présenté en vue de l'obtention
du grade de Docteur de l'Université d'Angers
Sous le label de l'Université Nantes Angers Le Mans

Spécialité : Pharmacologie expérimentale et clinique
Laboratoire : UMR_S 1066

Soutenue le 21 juin 2013

École doctorale : Biologie Santé
Thèse N°1326

Hydrogel de nanocapsules lipidiques chargées en gemcitabine : une technologie pharmaceutique pour cibler les ganglions de drainage des cancers

JURY

Rapporteurs :	**Mme. Ruxandra GREF**, Directeur de recherche, Université Paris Sud
	M. Sébastien LECOMMANDOUX, Professeur d'Université, Institut Polytechnique de Bordeaux
Examinateurs :	**M. Dominique HEYMANN,** Professeur d'Université, Université de Nantes
	M. Jérôme ABADIE, Maître de conférences, Ecole Vétérinaire de Nantes
Directeur de Thèse :	**M. Jean-Pierre BENOIT**, Professeur d'Université, Université d'Angers
Co-directeur de Thèse :	**M. Guillaume BASTIAT**, Maître de conférences, Université d'Angers

« *Etudie*, *non pour savoir plus*, *mais pour savoir mieux* »

Sénèque

Remerciements

Je voudrais tout d’abord présenter mes plus sincères remerciements à mon directeur de thèse, Jean-Pierre Benoit, pour m’avoir accueillie au sein de son unité pendant ces trois années enrichissantes, pour ses précieux conseils et ses encouragements. Merci d’avoir pris le temps de suivre ce travail régulièrement et d’avoir participé à la correction des publications et de ce manuscrit.

Je tiens également à remercier sincèrement mon co-directeur de thèse, Guillaume Bastiat pour son dévouement. Tout ce que je pourrais écrire ici ne pourrait pas suffire pour te remercier à la hauteur de la qualité de ton encadrement. Merci Guillaume pour ton soutien intarissable, ta grande disponibilité, ton implication personnelle ainsi que tes conseils avisés. Merci d’avoir fait de cette correction de thèse, une priorité dans ton emploi de temps très chargé.

Je tiens à exprimer mes plus sincères remerciements aux membres du jury. Un merci particulier à Mme Ruxandra Gref, et Mr Sébastien Lecommandoux pour me faire l’honneur de participer à ce jury et pour avoir accepté de consacrer du temps à l’évaluation de ce travail de thèse en qualité de rapporteur.

Un grand merci à Mr Sébastien Abadie et Mr Dominique Heymann pour avoir accepté d’évaluer ce travail en tant qu’examinateurs.

Je remercie également Mr Alain Le Pape et Mr José Hureaux pour leur participation à mon comité de suivi de thèse. Merci pour l’enthousiasme dont vous m’avez fait part tout au long de ce travail. Je garderai un très bon souvenir de cette collaboration.

J’adresse de sincères remerciements à tous ceux que j’ai côtoyés au laboratoire pendant 3 ans et qui ont participé à rendre cette thèse aussi agréable.

Nolwenn, toujours là quand on a besoin de toi. On te décrit comme la fille qui court plus vite que son ombre, et je suis bien d’accord avec cette description. Je suis vraiment contente d’avoir passé 3 années à tes cotés et surtout avec une compatriote Bretonne !

Une attention particulière, pour super copine (Anne-Laure), quel dommage que ton changement de bureau se fasse si tard. Merci pour les nombreux échanges scientifiques et personnels, nos repas au RU, nos nombreux mails, nos sms, nos mojitos au soleil place du ralliement, nos soirées. Tu connais déjà la route pour venir me voir, je t'attends très prochainement pour un autre weekend breton et promis Yohann ne te tombera pas dessus en pleine nuit.

Un grand merci à tous les autres pour tous les bons moments passés au labo: Stéphanie ,Alé, Jérôme, Olivier, Edith, Anne-Claire, Audrey, Pauline, Angélique, Nicolas, Jean-Pierre, Florian, Leïla, Samüli, Camille, Kien, Fabien, Amine, Brice… Un grand merci à toi Nathalie pour ton aide précieuse avec les souris.

Merci aux stagiaires qui m'ont accompagné dans ce projet: Anna, Yolanda et Véronika.

Un grand merci à mes collègues de l'IUT, Hélène, Laure, Anthony, Blandine et Caroline. J'ai passé 3 années vraiment enrichissantes à pouvoir enseigner à l'IUT à vos cotés même si la correction des copies était la phase la moins drôle.

Enfin sur un plan plus personnel je tiens à remercier très chaleureusement mes amis pour leur soutien. Lucie, Peggy, Carla, Nicolas, Bertrand, Julie, Maëlenn, David… Un grand merci à mon ancienne chef, Béatrice, quelle déception de ne pas avoir continué en thèse avec toi mais quelle chance de t'avoir connue et d'avoir travaillé avec toi.

Je remercie infiniment mes parents pour leurs encouragements quotidiens tout au long de cette longue route et pour leur affection. Votre dernière fille a enfin fini ses études. Sans vous, je n'en serais pas là.

J'adresse des remerciements sincères à ma famille ; mes sœurs, mon frère, mes petits neveux et petites nièces pour leur soutien inconditionnel, ainsi qu'à ma belle-famille, mes beaux parents, mes belles sœurs, mes beaux frères, et mes petits neveux et nièces pour vos nombreux encouragements.

Le dernier remerciement sera pour toi Yohann. Merci de m'avoir supporté durant ces trois années de thèse (même avant et pour plusieurs années encore). Merci pour ton soutien et pour tes encouragements incessants depuis notre première rencontre. Avec toi une nouvelle vie professionnelle s'ouvre à moi maintenant, j'espère être à la hauteur et ne pas te décevoir! Un grand merci pour notre petite fille qui verra le jour très prochainement. Une nouvelle vie commence pour notre petite famille…

Sommaire

Introduction générale

1. Le cancer du poumon

1.1 Données épidémiologiques

Chaque année 3,45 millions de nouveaux cas de cancer sont diagnostiqués et 1,75 millions de décès sont recensés en Europe, faisant du cancer un problème majeur de santé publique [1]. En France, si les maladies cardio-vasculaires ont longtemps été la première cause de mortalité, depuis les années 2000 le cancer est devenu aujourd'hui la principale cause de mortalité puisque 30% des décès toutes causes confondues sont liés au cancer [2]. Cette tendance reflète l'évolution mondiale, avec le cancer comme cause majeure de mortalité tant dans les pays développés que dans les pays en voie de développement. Les formes de cancer les plus communes sont le cancer du sein (464 000 cas), suivi des cancers colorectaux (447 000) et le cancer du poumon (410 000). Le cancer broncho-pulmonaire, avec un nombre de décès estimé de 353 000 est la cause la plus commune de décès par cancer (Figure 1) [1]. En France, on compte près de 40 000 nouveaux cas de cancer broncho-pulmonaire par an. La mortalité pour ce type de cancer a été divisée par deux en dix ans chez les hommes de 40 ans. En revanche, elle a été multipliée par quatre en quinze ans chez la population féminine qui fume de plus en plus [3].

La gravité des cancers broncho-pulmonaires est reflétée par une mortalité presque égale à une incidence en croissance [4]. Le cancer du poumon compte parmi les cancers les plus agressifs et apparait comme un sujet préoccupant de santé publique avec un taux de survie à 5 ans dans moins de 15% des cas [5]. Ce mauvais pronostic est principalement dû à un diagnostic trop tardif. Pour une tumeur métastatique (Stade IV), moins de 3% des patients seront encore en vie 5 années après le diagnostic.

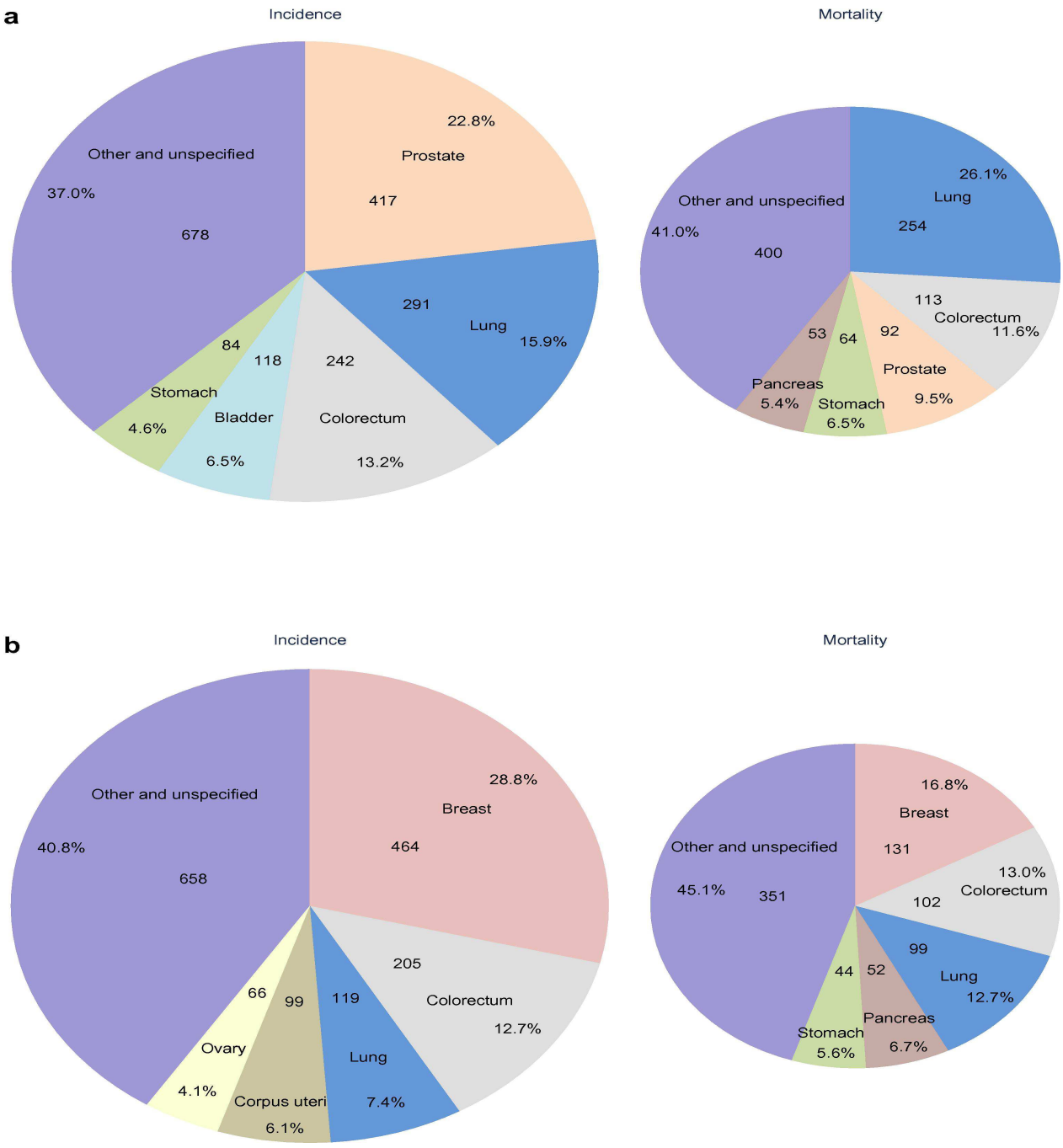

Figure 1: Estimation de l'incidence et de la mortalité des cancers en Europe en 2012 (en milliers). Pour chaque sexe, la zone du segment du diagramme correspond à la proportion du nombre total de cas ou de décès (a : Homme, b : Femme) *(D'après* Ferlay *et al., 2013* [1]*)*

1.2 Classification histologique

L'observation au microscope de la taille et de l'apparence des cellules malignes permet de classer les cancers du poumon en deux grands groupes histologiques :

i. les carcinomes dits « à petites cellules » (Small Cell Lung Carcinoma, SCLC).
ii. les carcinomes dits « non-à petites cellules » (Non-Small Cell Lung Carcinoma, NSCLC)

Les SCLC représentent 15% des cancers brocho-pulmonaires et sont liés dans 95% des cas au tabagisme. Elles ont un haut grade de malignité et sont très invasives avec un fort taux de métastases. Ce type de cancer est traité par chimio ou radiothérapie mais possède généralement un mauvais pronostic. La survie de ces patients n'excède pas 2,5 années [6].

Les NSCLC représentent 85 % des cas [7] et ce groupe contient plusieurs sous-types histologiques adoptant une architecture soit épidermoïde (Squamous Cell Carcinoma, SCC), glandulaire (AdenoCarcinoma, ADC), indifférenciée (Large Cell Carcinoma, LCC) ou toute entité ne présentant pas de caractéristiques "à petites cellules". Ces trois sous-types sont pris en charge et traités de façon similaire.

1.3 Prise en charge des cancers broncho-pulmonaires

Une fois le cancer diagnostiqué, différentes options thérapeutiques sont à la disposition des cliniciens (Tableau 1). Ces options dépendent donc du diagnostic mais aussi du type et du stade de la tumeur, ainsi que de la tolérance du patient aux effets secondaires liés à la thérapie. Plusieurs types de traitement peuvent être proposés pour la prise en charge d'un cancer bronchique : la chirurgie, la radiothérapie (basée sur l'utilisation de rayonnements ionisants : X, alpha, beta ou gamma), la chimiothérapie et la thérapie ciblée (actuellement l'erlotinib, la gefitinie et le cetuximab). Des patients avec SCLC sont habituellement traités par irradiation et/ou chimiothérapie suivant le stade du cancer. L'irradiation crâniale prophylactique (PCI) peut être envisagée, car le risque de développer des métastases du système nerveux central dans les 2 ou 3 années suivant le traitement est élevé. Pour les patients avec NSCLC, le traitement va dépendre du type histologique et de la

classification TNM (Tumor Node Metastasis) d'extension de la maladie (Tableau 2). La chirurgie est le traitement de référence des cancers du poumon non à petites cellules si le stade et l'état du patient le permettent. Les autres modalités thérapeutiques sont la radiothérapie externe (conformationnelle ou stéréotaxique selon les stades) et les chimiothérapies.

Les chimiothérapies sont des traitements systémiques particulièrement indiqués, pour les cancers non-opérables, à fort risque de dissémination ou déjà disséminés. Elles sont très efficaces, mais ne sont pas sélectives des cellules tumorales et sont à l'origine de nombreux effets secondaires (toxicité hématologique, cardiaque, gonadique, digestive, alopécie). Le traitement standard actuel est la bithérapie basée sur un doublet contenant un sel de platine (cisplatine (CYSPLATYL®) ou carboplatine (PARAPLATINE®)). Ce sel est alors associé à une molécule de troisième génération telle que la vinorelbine (NAVELBINE®) (si une cure de radiothérapie concomitante est prévue), la gemcitabine (GEMZAR®) (en absence de radiothérapie) ou le paclitaxel (TAXOL®)[8].

1.4 Choix du modèle

Les cancers bronchiques les plus fréquemment diagnostiqués sont des NSCLC de stade IV, c'est-à-dire métastatiques, et ceux-ci présentent les survies les plus faibles (Tableau 3). Dans ce travail de thèse nous avons choisi de travailler sur un modèle de cancer bronchique à non petites cellules et à haut grade métastatique. Nous avons utilisé un modèle gracieusement offert par le Dr. Konzo de l'Université de Tokushima au Japon. La lignée employée se nomme Ma44-3 et a été obtenue après dilution limite de la lignée mère Ma44 [9]. C'est une lignée appartenant aux NSCLC et adoptant une architecture épidermoïde. Ce modèle est connu pour métastaser rapidement dans les ganglions du médiastin après une implantation orthotopique. Le développement, la caractérisation et l'utilisation de ce modèle pour l'étude d'efficacité de nos formulations seront présentés dans la **publication n°3** .

	TNM	Chirurgie	Radiothérapie	Chimiothérapie ou thérapie ciblée
Stade IA	T1 N0	☒		
Stade IB	T2 N0	☒		○
Stade II	T1,2 N1 T3 N0	☒	○	☒
Stade I ou II Non opérable			☒	○
Stade IIIA	T3 N1	☒	○	○
	T1,3 N2	○	○	○
	T4 N0,1		☒	☒
Stade IIIB	Tous T, N3		☒	☒
	T4, N2		☒	☒
Stade IV	Tous T, N, M1			☒

☒ Modalité thérapeutique de référence, systématique (sauf si contre-indication) ;

○ Selon les situations : peut être parfois envisagée, en association au traitement de référence.

Tableau 1 : Modalités thérapeutiques d'un cancer bronchique non à petites cellules *(D'après l'Institut national du cancer, 2010* [10]*)*

	Fréquence au diagnostic	Survie relative à 5 ans
Cancer localisé STADES I ET II	15 à 30 %	52,6 %
Cancer localement avancé STADE III	20 %	23,7 %
Cancer métastatique STADE IV	40 à 55 %	3,8 %

Tableau 3 : Cancer du poumon à non petites cellules, fréquence et survie par stade *(D'après l'Institut national du cancer, 2010* [11]*)*

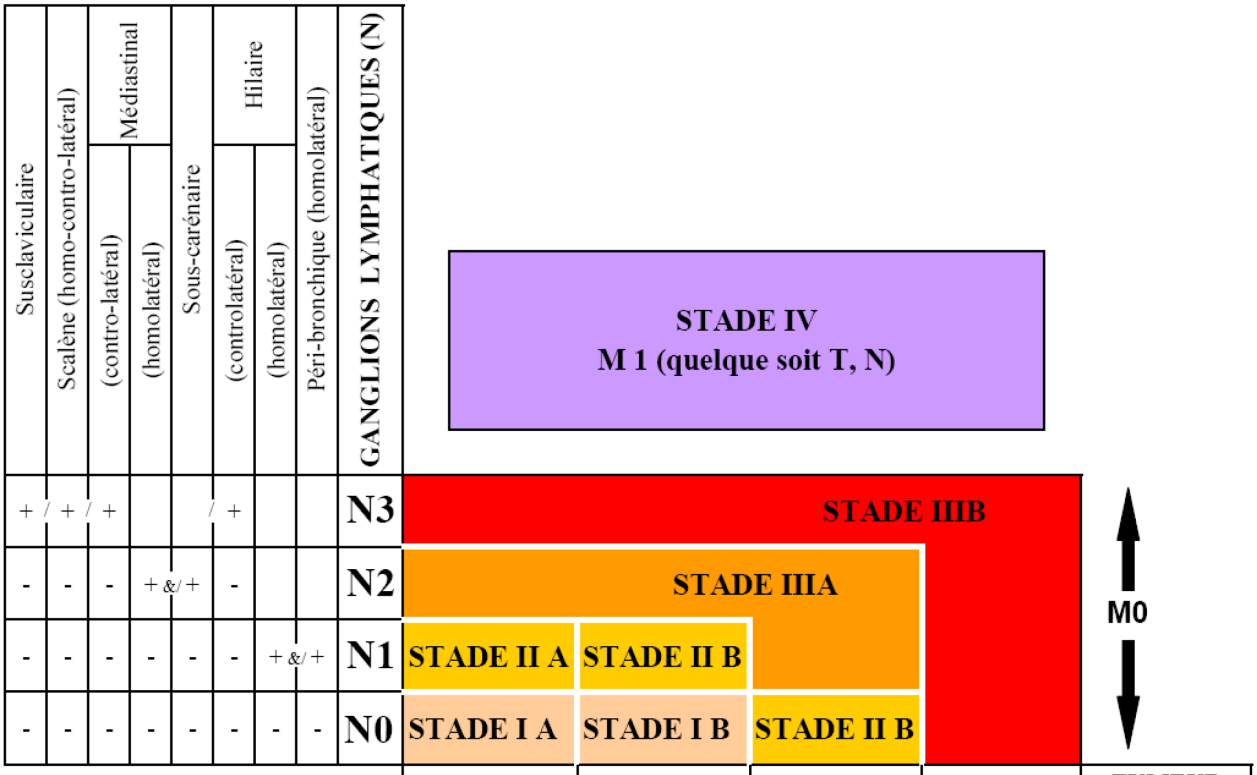

STADE 0
(Tis, N0, M0)

MÉTASTASES (M)

M0 = Absentes
M1 = Présentes

Tis : Carcinome *in situ*

T1	**T2**	**T3**	**T4**	**TUMEUR PRIMITIVE (T)**
a&b&c	a/b/c/d	(a&c)/b/d	(a&c)/d	**Critères**
≤ 3 cm	> 3 cm	quelconque	quelconque	**a. Taille**
Pas d'invasion à proximité de la bronche lobaire	Bronche souche (≥ 2 cm de la carène)	Bronche souche (< 2 cm de la carène)	-	**b. Localisation endo-bronchique**
Entourée par du poumon ou de la plèvre viscérale	Plèvre viscérale	Paroi thoracique/ diaphragme/ plèvre médiastinale/ péricarde pariétal	Médiastin/ trachée/ cœur/ gros vaisseaux/ œsophage/ corps vertébral/ carène	**c. Invasion locale**
-	Atelectasie/ Pneumonie obstructive s'étendant jusqu'à la région hilaire mais ne concerne pas le poumon entier	Atelectasie/ Pneumonie obstructive du poumon entier	Épanchement pleural malin/ péricardique ou nodules tumoraux satellites dans un autre lobe du poumon	**d. Autre**

Tableau 2 : **Classification TNM des cancers bronchopulmonaires selon l'UICC (2002)** (*D'après* Benoit Busser, *2008* [12])

2. Développement des métastases

Toutes les cellules tumorales n'ont pas la capacité de former des métastases. Le potentiel métastatique dépend de multiples facteurs déterminant la croissance des cellules cancéreuses, leur survie, l'angiogénèse et l'invasion. Au cours de son développement, la tumeur met en place des phénomènes d'échappement. L'invasion métastatique est tout d'abord régionale et concerne les ganglions proches du site tumoral puis elle s'étend à certains organes tels que le foie, les os, les poumons et le cerveau. L'angiogenèse et la lymphangiogenèse sont impliquées dans l'invasion des ganglions lymphatiques par les cellules tumorales et la dissémination métastatique en servant de réseau pour le transport des cellules tumorales vers de nouveaux sites. La dissémination métastatique peut être ainsi hématogène ou lymphatique. L'observation de l'envahissement des ganglions lymphatiques reflète généralement un mauvais pronostic pour le patient [13].

Les étapes clés de la dissémination sont les suivantes :

i. Perte de la capacité adhésive des cellules tumorales,
ii. Sécrétion des protéines capables de digérer la matrice extracellulaire des vaisseaux sanguins et lymphatiques avoisinants,
iii. Passage de quelques cellules tumorales qui seront convoyées par le sang ou la lymphe,
iv. Extravasation vers le site secondaire,
v. Développement de tumeurs secondaires au niveau du nouveau site d'invasion.

Le mécanisme général (et simplifié) du rôle de l'angiogenèse et lymphangiogenèse tumorale est représenté sur la figure 2 : (a) en réponse à des facteurs pro-angiogéniques et pro-lymphangiogéniques sécrétés par les cellules tumorales, (b) les cellules endothéliales expriment des intégrines, (c) La liaison de ces intégrines à divers ligands de la matrice extracellulaire permet les phénomènes de prolifération et/ou de migration des cellules endothéliales qui contribuent à la formation et à la maturation des vaisseaux. Ces nouveaux vaisseaux aident à la progression tumorale en éliminant les déchets et en amenant des nutriments. (d) Finalement le phénomène d'angiogenèse provoque la dissémination tumorale, par voie

systémique, vers les organes les plus proches. La lymphangiogenèse, quant à elle, induit la dissémination vers les ganglions lymphatiques les plus proches. Les foyers métastatiques ganglionnaires peuvent envoyer par la suite des emboles néoplasiques dans la circulation sanguine par le canal thoracique et être responsables de nouvelles métastases.

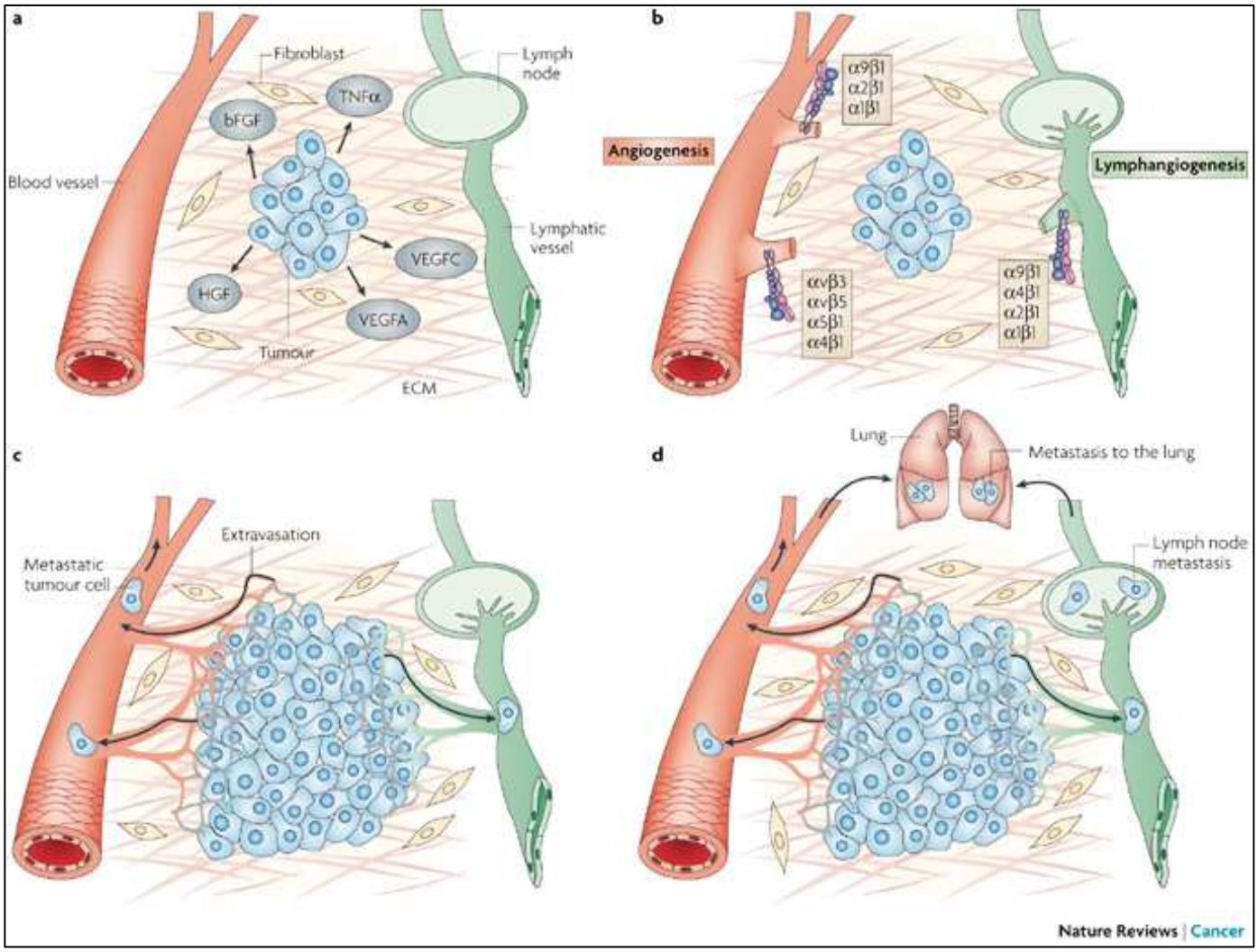

Figure 2 : Mécanismes régulant l'angiogénèse et la lymphangiogénèse tumorale *(D'après* Avraamides *et al*., *2008* [14]*)*

2.1 La lymphangiogénèse

La lymphangiogénèse correspond au développement de nouveaux vaisseaux lymphatiques. Elle est fortement impliquée dans la diffusion des cellules cancéreuses aux ganglions régionaux puis au développement des métastases à distance. L'angiogénèse a longtemps été donnée comme principale cause de dissémination

métastatique, cependant les données impliquant la lymphangiogénèse dans la progression tumorale sont en pleine expansion depuis une décennie. En effet, la mise en évidence de marqueurs protéiques de l'endothélium lymphatique et la découverte de gènes impliqués dans la régulation du système lymphatique ont ouvert la voie à l'analyse de sa régulation.

2.2 Facteurs impliqués dans la lymphangiogénèse

La principale protéine impliquée dans la lymphangiogénèse est le VEGFR-3, récepteur à tyrosine kinase. Ce récepteur est spécifique des cellules endothéliales lymphatiques. Pour induire la lymphangiogénèse, le VEGF-C et le VEGF-D se lient au récepteur VEGFR-3 [15,16]. Cependant, ces deux ligands peuvent aussi stimuler l'angiogénèse par le biais de son affinité pour le récepteur VEGFR2. Des études *in vitro* et *in vivo* ont montré le rôle majeur du système VEGF-C/VEGF-D/VEGFR-3 dans la régulation de la lymphangiogénèse physiologique. Des souris transgéniques surexprimant le VEGF-C au niveau de la peau ont montré une hyperplasie du réseau de vaisseaux lymphatiques [17]. Une étude *in vivo* a montré qu'en utilisant un anticorps bloquant spécifiquement le récepteur VEGFR-3, il était possible d'obtenir une diminution du nombre de métastases dans un modèle orthotopique de cancer du sein [18]. A ce jour, plus de 65 études ont montré que l'expression du facteur VEGF-C était corrélé avec la présence de métastases ganglionnaires et avec un mauvais pronostic de survie dans une large gamme de cancers [19].

L'analyse comparée du transcriptome des cellules endothéliales sanguines et lymphatiques a permis l'identification de nouveaux marqueurs spécifiques de la lignée lymphatique. Ainsi des marqueurs moléculaires spécifiques et/ou privilégiés des cellules endothéliales lymphatiques tels que LYVE-1, Prox-1 et podoplanine ont été découverts [20].

2.3 Implication tumorale

Plusieurs mécanismes de lymphangiogénèse sont actuellement considérés et l'utilisation des modèles animaux ont permis de préciser le rôle de ces facteurs dans la lymphangiogénèse tumorale. La diffusion métastatique lymphatique se manifeste morphologiquement par trois mécanismes : une lymphangiogénèse intra et péritumorale et une lymphangiogénèse intraganglionnaire (à distance). De

nombreuses études considèrent que la diffusion métastatique ganglionnaire ne peut se faire que par l'intermédiaire des vaisseaux lymphatiques péritumoraux, les vaisseaux lymphatiques intratumoraux ne pouvant être fonctionnels en raison de la pression interstitielle élevée régnant au sein de la tumeur rendant les vaisseaux collapsés [21]. Cependant certaines études ont montré une corrélation entre la présence de vaisseaux lymphatiques intratumoraux, l'envahissement ganglionnaire et le mauvais pronostic pour les patients [22,23]. La présence et la fonctionnalisation des vaisseaux lymphatiques intratumoraux dépendent certainement du modèle tumoral étudié. Pour exemple, une étude *in vivo* a démontré une lymphangiogénèse péri et intratumorale après surexpression de VEGF-C chez des souris SCID implantées avec une lignée de cellules de cancer du sein humain (MCF7) transfectées par le gène du VEGF-C [20]. Dans une majorité des cas, une surexpression du VEGF-C et/ou du VEGF-D est associée à une augmentation de la lymphangiogénèse péri et/ou intratumorale, elle-même corrélée à une augmentation de l'incidence des métastases ganglionnaires. Cependant, le développement d'une lymphangiogénèse péritumorale apparaît dans plusieurs cas associée à un meilleur taux de survie, car elle faciliterait le recrutement des cellules dendritiques et la mise en place d'une réponse immunitaire dirigée contre les cellules tumorales [20]. Des travaux récents ont également montré que les cellules tumorales peuvent induire une lymphangiogénèse intraganglionnaire pour préparer à distance la colonisation par les métastases des ganglions. Il semblerait que le VEGF-C joue un rôle prépondérant dans cet envahissement [25].

3. La nanovectorisation

La vectorisation consiste en l'utilisation d'un vecteur pour administrer un principe actif. Aucun médicament ne peut exercer une activité thérapeutique s'il n'est pas capable de franchir les barrières biologiques qui séparent le lieu de son administration de son site d'action. Les intérêts de la vectorisation d'un médicament sont donc nombreux. On parle de nanovectorisation ou nanomédecine lorsque la taille des vecteurs utilisés est comprise entre 1 et 200 nm. De par leurs petites tailles et leurs compositions chimiques, les nanovecteurs (ou nanoparticules) peuvent franchir les barrières biologiques et, par greffage de ligands à la surface des nanoparticules, se diriger spécifiquement vers les cellules cancéreuses et/ou leur environnement proche. La nanovectorisation d'anticancéreux permet de protéger la molécule thérapeutique, d'améliorer son profil pharmacocinétique, de diminuer sa toxicité et accroît ainsi le confort du malade par la réduction du nombre de prises.

La vectorisation va dépendre du type de nanoparticules utilisées, de leur taille, de leur charge, ainsi que du site d'injection [26,27]. On retrouve généralement 5 grands groupes de particules : les liposomes, les dendrimères, les nanoparticules polymères, les nanoparticules métalliques et enfin les nanoparticules lipidiques [28–31].

3.1 Les nanocapsules lipidiques

Parmi les vecteurs nanoparticulaires de principes actifs, notre unité UMR_S U1066 développe depuis plus d'une dizaine d'années des nanocapsules lipidiques (LNCs) biomimétiques ayant une structure proche des lipoprotéines du vivant. Ces LNCs font l'objet de plusieurs brevets [32]. Les nanocapsules lipidiques sont composées d'un cœur lipidique liquide de triglycérides entouré par une coque de tensioactifs amphiphiles et sont dispersées dans un milieu aqueux. Elles sont formulées par un processus d'inversion de phase entre une émulsion huile dans eau (H/E) et une émulsion eau dans huile (E/H) suite à une augmentation et une diminution de la température du milieu réactionnel [33]. Cette technique permet d'obtenir des LNCs sans recours à un solvant organique et sans consommation importante d'énergie. Leur taille monodisperse varie de 20 à 100 nm selon les proportions d'excipients.

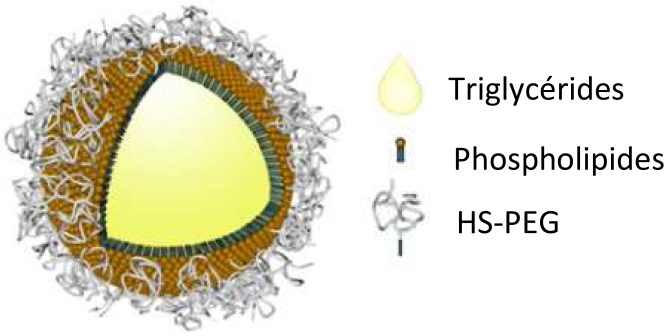

Figure 3 : Structure des nanocapsules lipidiques (LNC). *(D'après* Vanpouille-Box*, 2011* [34]*)*

De nombreux anticancéreux lipophiles, comme l'étoposide, la tripentone, le paclitaxel, le docétaxel ou les dérivés du tamoxifène ont été encapsulés dans les LNCs [35–40],formant des suspensions stables dans le temps et montrant une efficacité *in vitro* équivalente, voire supérieure, à celle de la drogue seule. L'encapsulation de molécules hydrophiles a également récemment été étudiée avec notamment l'encapsulation de la doxorubicine et de l'erlotinib [41–43]. Les LNCs offrent aussi la possibilité d'encapsuler du matériel génétique [44–47] (ADN, siRNA), des composés radioactifs [48–50], ainsi que des fluorophores hydrophobes tel que le DiI (perchlorate de 1,1'-dioctadécyl-3,3,3',3'-tetraméthylindocarbocyanine), le DiD (perchlorate de 1,1'-dioctadécyl-3,3,3',3'-tetraméthylindodicarbocyanine) [46,47,51] afin d'assurer un suivi du devenir des LNCs *in vitro* et *in vivo*.

3.2 Le ciblage tumoral

3.2.1 Le ciblage passif

Le ciblage passif est un mécanisme qui repose sur les propriétés physiologiques des tumeurs. Un principe actif qui normalement démontre peu de spécificité pour les tissus tumoraux peut voir son accumulation tumorale augmenter grâce au phénomène de perméabilité et de rétention vasculaire accrue (ou effet EPR pour « enhanced permeation and retention effect »), une fois celui-ci encapsulé dans un vecteur nanoparticulaire (Figure 4). Cette caractéristique tumorale fut découverte et décrite pour la première fois par l'équipe de Maeda [52]. Les tissus tumoraux sont caractérisés par plusieurs propriétés distinctes, telle qu'une hyper-vascularisation (permettant d'augmenter l'apport en oxygène et en nutriments nécessaires au métabolisme élevé des cellules cancéreuses), une architecture vasculaire

défectueuse et la sécrétion de facteurs qui accentuent la perméabilité des vaisseaux sanguins de la tumeur. En plus de la perméabilité des tissus tumoraux, il existe un deuxième facteur qui influence l'accumulation passive des nanoparticules au niveau de la tumeur. Les tissus tumoraux sont caractérisés par un plus faible drainage lymphatique, en comparaison avec les tissus sains. Par conséquent, les nanoparticules sont retenues pour une période prolongée dans l'interstitium tumoral. Cependant comme décrit dans le paragraphe *§ 2*, les données sur le rôle d'un drainage lymphatique lors du développement tumoral sont en pleine expansion. De plus, des travaux semblent indiquer que l'évaluation du nombre et peut être de la taille des vaisseaux lymphatiques dans la tumeur et autour d'elle, est importante pour déterminer sa capacité à métastaser [21].

Malgré le phénomène de perméabilité et de rétention vasculaire accrue, pour pouvoir s'accumuler au niveau tumoral, la nanoparticule doit avoir un temps de circulation plasmatique prolongé, en échappant aux défenses naturelles de l'organisme et aux différentes voies d'élimination systémiques. Ainsi la nanoparticule doit devenir furtive. L'ajout de PEG (polyéthylène glycol) est largement utilisé pour obtenir des particules furtives [53–55]**.** Le PEG est un matériau neutre et hydrophile permettant de diminuer la reconnaissance par le système immunitaire, et plus particulièrement par le système des phagocytes mononucléés (SPM) [56]**.** La reconnaissance (par opsonisation) et la phagocytose des vecteurs colloïdaux par les macrophages du SPM entraînent leur élimination rapide de la circulation sanguine. L'ajout de PEG à la surface des nanoparticules a pour effet de diminuer l'adsorption des opsonines et ainsi prolonger la durée de circulation des vecteurs colloïdaux. A noter cependant que l'ajout de PEG provoque une augmentation de répulsion stérique entre les particules et les cellules, diminuant ainsi significativement les niveaux de transfection, aussi bien *in vitro* qu'*in vivo* [57,58].

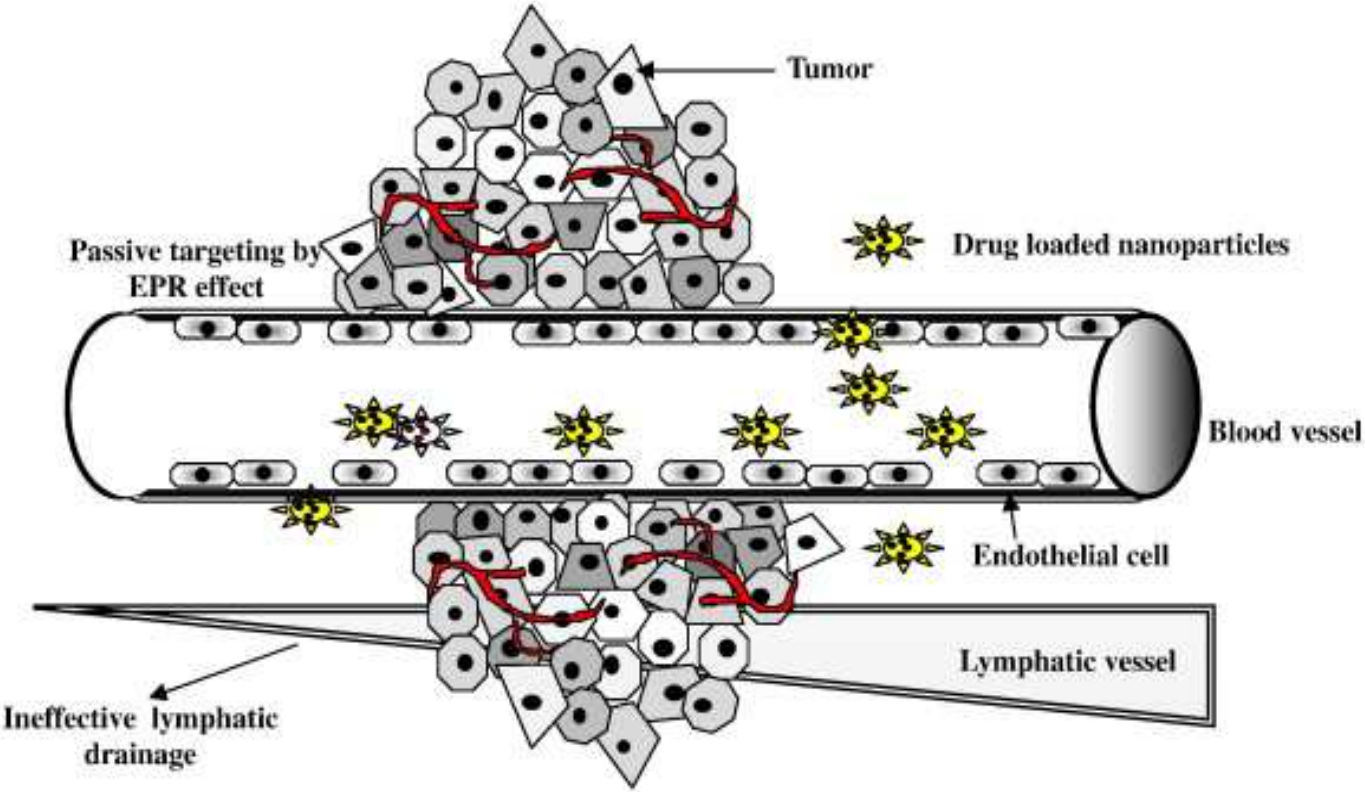

Figure 4 : Représentation schématique du ciblage passif tumoral par effet EPR. *(D'après* Acharya *et al., 2011* [59]*)*

3.2.2 Le ciblage actif

Le concept de thérapie ciblée apparait dans les années 70 avec l'apparition des anticorps monoclonaux, cependant ce concept de ciblage apparait bien plus longtemps avec les nanovecteurs dits de troisième génération. Sachant que les cellules tumorales ou leur microenvironnement surexpriment certains récepteurs, ce sont ces récepteurs qui vont être exploités afin de cibler spécifiquement un agent thérapeutique au sein du foyer tumoral [60]. Les recherches actuelles se développent sur la fonctionnalisation de la surface des nanoparticules pour améliorer l'efficacité du ciblage tumoral et augmenter la biodisponibilité d'agent anticancéreux. Cette approche s'appuie sur des interactions spécifiques telles que ligand-récepteur ou anticorps-antigène. De nombreux ciblages de nanoparticules ont été développés. Ces systèmes emploient des ligands tels que la biotine [61], la galactosamine [62], l'acide folique [63], des aptamères [64,65].

Notre laboratoire a également mis au point des nanocapsules lipidiques fonctionnalisées pour obtenir un ciblage actif. Le premier ciblage actif a été obtenu en greffant l'anticorps monoclonal OX26. Cet anticorps reconnaît spécifiquement le récepteur de la transferrine exprimé à la surface de cellules endothéliales des capillaires cérébraux. Ainsi l'injection systémique de ces LNCs-OX26 contenant un traceur radioactif, le Rhenium 188, chez des rats sains a permis d'augmenter significativement de 1,5 à 2 fois la quantité de Rhenium 188 accumulée au niveau du cerveau 24 heures après injection, comparé aux LNCs natives [66]. Le deuxième ciblage actif a été obtenu en adsorbant un peptide : le NFL-TBS.40-63 (un dérivé provenant de la chaîne légère de neurofilaments) à la surface des LNCs. Ce peptide de 24 acides aminés pénètre préférentiellement dans les glioblastomes, cellules cancéreuses du système nerveux, où il inhibe la formation de microtubules. Ces récents travaux ont montré que les LNCs avec le peptide NFL-TBS.40-63 adsorbé en surface rentrent plus rapidement et de façon plus importante dans les cellules de glioblastome que les LNCs natives. Chez les souris porteuses de gliome, le volume des tumeurs a diminué significativement de 60% après traitement avec les LNCs contenant du paclitaxel, et de 75% pour celle traitées avec les LNCs chargées en paclitaxel et en présence du peptide NFL-TBS.40-63 en surface. [67]

3.3 Le ciblage du système lymphatique

Le système lymphatique joue un rôle majeur dans la défense de l'organisme en permettant la circulation dans l'ensemble de l'organisme des cellules de défense (lymphocytes, macrophages,…) et en filtrant les agents pathogènes grâce aux ganglions. Le système lymphatique est également un système circulatoire unidirectionnel secondaire drainant l'excès de fluide, des protéines et les déchets provenant du métabolisme de nos cellules. Les ganglions lymphatiques jouent un rôle important dans ces deux fonctions.

Le système lymphatique n'est pas facilement accessible par infusion conventionnelle en intraveineux, limitant fortement les quantités d'agents chimiothérapeutiques dans les ganglions lymphatiques atteints par les métastases. Ainsi les nombreuses recherches menées actuellement se portent préférentiellement sur des injections parentérales (injection sous-cutanée, intrapéritonéale, intradermique et intramusculaire) de molécules et de nanoparticules [68,69]. Deux principales

applications chez l'homme sont considérées. Premièrement, le ciblage lymphatique sert d'outil de diagnostic, de détection des métastases ou des ganglions sentinelles. Et deuxièmement, le ciblage lymphatique sert d'outil de traitement, permettant l'accumulation d'agents anticancéreux dans les métastases, limitant ainsi la toxicité sur les tissus sains. Bien que la dissémination métastatique soit la cause la plus fréquente de décès des patients cancéreux, le nombre de médicaments ciblant spécifiquement les ganglions lymphatiques est actuellement très réduit.

Plusieurs facteurs contrôlent l'accumulation de particules dans le système lymphatique dont la taille, la composition, la dose, la charge de surface. La taille est le facteur prédominant dans le comportement *in vivo* des nanoparticules. Pour des injections sous-cutanées, une taille comprise entre 10 et 100 nm semble être optimale pour une capture par les capillaires lymphatiques et ensuite un drainage jusqu'aux ganglions. Les molécules inférieures à 10 nm sont préférentiellement prises en charge par les capillaires sanguins [70].

3.3.1 Le ciblage passif

Des études récentes ont montrées au laboratoire, qu'après injection intraveineuse d'une suspension de nanocapsules lipidiques fluorescentes (au moyen de DiD) à des souris *nudes* porteuses de diverses xénogreffes, une forte accumulation dans les ganglions lymphatiques était observée. Cette accumulation de fluorescence dans les ganglions est 4 à 5 fois plus importante que dans l'ensemble des autres organes (excepté pour le foie, la rate et les intestins) [51,71]. L'influence de la taille (20, 50 et 100 nm), ainsi que celle des polymère de surfaces (PEG, lipodextrane et lipochitosane) ont été testées. Les résultats ne montrent aucune différence entre les diverses formulations, montrant ainsi le fait que les nanocapsules lipidiques ont un fort tropisme pour les ganglions lymphatiques, avec une accumulation qui augmente au cours du temps. La fluorescence des ganglions augmente d'un facteur 4 entre 5h et 24h. L'opsonisation qui est un processus rapide conduisant à une accumulation des nanoparticules dans le foie, la rate et les ganglions lymphatiques, en vue d'une élimination ultérieure, semble être une raison principale de cette accumulation ganglionnaire.

De nombreux autres systèmes nanoparticulaires ont déjà été étudiés dans le cadre du ciblage lymphatique et ganglionnaire. Citons en premier lieu les liposomes, qui ont été les premiers à être étudiés notamment par Oussoren *et al*. Ils ont démontré qu'après une injection sous-cutanée de liposomes (40nm), 80% des liposomes sont éliminés du site d'injection. Cependant seulement une petite fraction, 1 à 2%, se retrouve retenue dans les ganglions lymphatiques [72]. Au contraire, les liposomes s'accumulent dans les ganglions après injection intratumorale ou encore intrapéritonéale. De ce fait, de nombreuses études ont utilisé les liposomes pour délivrer des anticancéreux tels que le méthotrexate, la doxorubicine ou encore le melphalan [73–77]. Les travaux avec des liposomes encapsulant du méthotrexate ont montré que ceux-ci sont localisés principalement dans le foie, la rate et les poumons après administration par voie intraveineuse [78]. Cependant après une injection intramusculaire, les liposomes de méthotrexate sont retrouvés principalement dans les ganglions lymphatiques et dans une moindre mesure dans les reins, le foie et autres tissus par rapport au méthotrexate libre. Une autre étude sur les liposomes encapsulant de la doxorubicine a montré une augmentation de plus de 38 fois de la concentration en drogue dans les ganglions lymphatiques après une injection intrapéritonéale comparativement à une injection intraveineuse. De même, une augmentation jusqu'à 14 fois de la concentration en doxorubicine dans les ganglions est observée après injection de liposomes comparativement à une injection du principe actif seul [79]. Des liposomes encapsulant du vert d'indocyanine (ICG : IndoCyanine Green) ont été formulés pour améliorer la visualisation du flux lymphatique après injection intradermique. L'ICG est un fluorophore d'intérêt pour l'imagerie de fluorescence approuvé depuis 1959, cependant il est instable en solution et rentre rapidement dans les capillaires veineux après injection locale. Proulx *et al*. ont ainsi pu obtenir une capture spécifique des liposomes fluorescents par le système lymphatique et obtenir une meilleure visualisation du flux lymphatique [80].

Des nanoparticules polymères encapsulant des agents de diagnostic ont également été largement étudiées. En 1992, Maincent *et al*. ont montré une accumulation ganglionnaire 70 à 2000 fois plus importante de nanoparticules radiomarquées de polyhéxylcyanoacrylate (PHCA) et de polyméthylméthacrylate (PMMA) injectées intrapéritonéalement comparé à une injection intraveineuse. Plus récemment

Kobayashi *et al*. ont mis au point des dendrimères encapsulant un agent de contraste, le G6 (« generation-6 polyamidoamine ») pour visualiser les canaux lymphatiques et les ganglions lymphatiques drainant des tumeurs mammaires de souris au cours du temps [81]. La détection et la visualisation des ganglions sentinelles plus particulièrement dans le cadre des cancers du sein sont très étudiées par l'utilisation de nanoparticules [82–86]. Actuellement, la détection du ganglion sentinelle consiste en l'injection d'un colorant bleu et d'un colloïde radioactif pour cartographier le ganglion, suivie par son exérèse chirurgicale et son analyse anatomo-pathologique afin de déterminer son statut métastatique. L'imagerie de fluorescence est une alternative intéressante aux traceurs employés actuellement puisque cette technique est hautement sensible, peu coûteuse, facile d'utilisation et les images sont obtenues en temps réel.

3.3.2 Le ciblage actif

La détection de l'invasion lymphatique et des métastases est une étape clé dans le succès des traitements des cancers. Le ciblage actif de nanoparticules vers le système lymphatique est de plus en plus étudié pour augmenter les concentrations ganglionnaires en particules et ainsi en anticancéreux. En effet, après une injection parentérale, on obtient de façon passive une forte accumulation dans les vaisseaux lymphatiques mais une relative faible rétention dans les ganglions. Par un ciblage actif on entend augmenter cette rétention. Le tableau 4 regroupe différents ligands spécifiques expérimentés pour augmenter la visualisation lymphatique et l'accumulation ganglionnaire. Le greffage de polymère de surface, comme par exemple le PEG, le chitosane ou encore le poloxamer, ne sont pas considérés et répertoriés comme ciblage actif dans le tableau 4.

Ligands	Système	Cible	Application	Références
Biotine-Avidine	Liposomes	Ganglions	Vaccins / Anticancéreux	[87]
LyP-1	Nanoparticules / liposomes	Vaisseaux lymphatiques / Tumeur	Anticancéreux	[88,89]
Mannose	Liposomes	Ganglions / Rate	Anticancéreux	[90]
L-sélectine	Microparticules	Ganglions	Agent de contraste	[91]

Tableau 4 : Différents ligands utilisés pour le ciblage lymphatique

4. Le choix des molécules à encapsuler

4.1 La gemcitabine

Nous avons choisi d'encapsuler la gemcitabine dans les nanocapsules lipidiques (Figure 5.a). La gemcitabine, également appelée 2'2'-difluorodéoxycytidine, est un anti-néoplasique cytotoxique appartenant au groupe des antimétabolites pyrimidiques. C'est un analogue synthétique de la déoxycytidine (déoxypyrimidine naturelle) avec laquelle elle rentre en compétition lors de son incorporation dans l'ADN en élongation [92]. Elle est approuvée en clinique depuis 1996 par la FDA, en première intention dans le traitement palliatif de l'adénocarcinome pancréatique localement avancé et métastatique, ainsi qu'en combinaison avec un sel de platine pour le traitement des cancers pulmonaires.

Une des difficultés du traitement par la gemcitabine est l'acquisition au cours du temps d'une résistance qui induit une diminution de sa cytotoxicité [93]. Ainsi, une administration courante et à haute dose est requise ce qui induit de sérieux effets secondaires comme une myélosuppression, une toxicité hépatique et rénale, etc… [94]. Les mécanismes de chimiorésistance de cette molécule étant maintenant bien étudiés, l'encapsulation couplée ou non à des modifications chimiques de cette molécule est aujourd'hui largement étudiée pour diminuer les doses et contrecarrer les phénomènes de résistance. La revue bibliographique : « *Gemcitabine versus modified gemcitabine: a review of several promising chemical modifications* » présentée dans cette thèse, reviendra sur le mode d'action de la gemcitabine et sur les diverses modifications chimiques apportées pour en améliorer son efficacité.

La gemcitabine est une molécule hydrophile, et malgré les études récentes et prometteuses menées au laboratoire sur l'encapsulation de molécules hydrophiles par inclusion de cœur aqueux ou de micelles inverses dans les LNCs, nous avons décidé de partir sur une modification chimique du principe actif (en position 4-(N)). Cette modification par l'ajout d'une chaine laurique aura pour conséquence une augmentation de sa lipophilicité et permettra ainsi son encapsulation dans des LNCs « classiques ». La publication n°1 : « *Gemcitabine-loaded lipid nanocapsule*

hydrogel: when the drug is a key player of the nanomedicine structure » reviendra sur cette modification et ses conséquences sur l'encapsulation dans les LNCs.

4.2 Le DiD

Pour les études de biodistribution, nous avons choisi d'encapsuler le DiD (Figure 5.b). Cette sonde fluorescente (em/ex 644/665 nm) est soluble dans le Labrafac après dissolution préalable dans l'acétone. La méthode de suivi par fluorescence utilisée suit uniquement la biodistribution du fluorophore *in vivo*, qui peut être différente des nanocapsules. Cependant, malgré le fait que l'intégrité des nanocapsules lipidiques ne peut être directement confirmée, le DiD libre n'est pas soluble et ne fluoresce pas dans les milieux aqueux [95]. Ainsi, il nous sera possible de dire que la biodistribution observée sera celle des nanocapsules lipidiques ou du DiD localement capturé par les tissus.

Nous avons utilisé un système d'imagerie appelé Maestro System de CRi. Le système d'imagerie multispectrale Maestro permet l'analyse spectrale *in vivo* de marqueurs fluorescents chez le petit animal. Pour faire cette analyse spectrale, la société CRi a développé un système basé sur l'utilisation d'un filtre variable à cristaux liquides (Liquid Crystal Tunable Filter : LCTF). Ce filtre variable LCTF va permettre d'analyser les longueurs d'onde d'émission dans une gamme de 500 à 950 nm avec un pas inférieur à 10 nm.

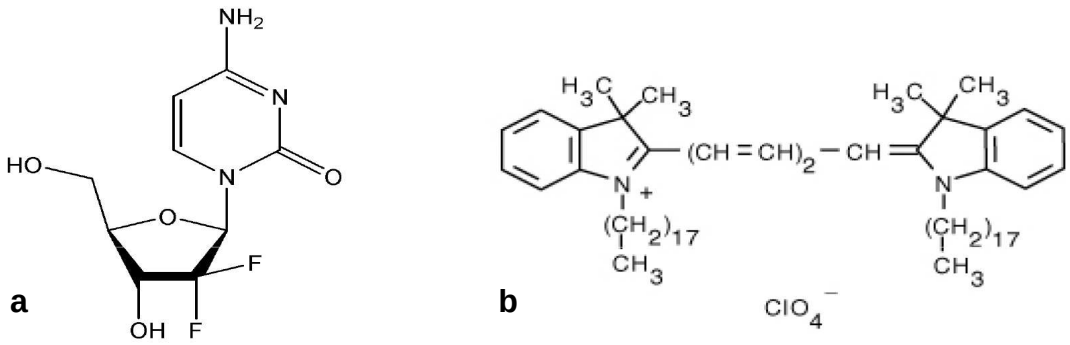

Figure 5 : Structure chimique de la gemcitabine (a) et du DiD (b)

5. Les objectifs de la thèse

Ce travail de thèse s'inscrit dans une stratégie d'optimisation de la chimiothérapie à l'aide des LNCs chargées en gemcitabine.

La gemcitabine étant hydrophile, nous avons dans un premier temps, modifié chimiquement la gemcitabine pour augmenter sa lipophilicité et permettre son encapsulation. Le chapitre 1 (**revue bibliographique)**, reviendra sur le panel de modifications chimiques déjà réalisées sur la gemcitabine ainsi que leurs conséquences sur l'efficacité *in vitro* et *in vivo*.

Le chapitre 2 se concentrera sur la conception, la caractérisation et finalement la biodistribution de ces LNCs chargées en gemcitabine modifiée (appelée Gem-C12). De façon intéressante, une fois la Gem-C12 encapsulée, nous avons obtenu un hydrogel. Celui-ci ainsi que les LNCs seront grandement étudiées dans les **publications n°1 et n°2** .

Dans le chapitre 3, plusieurs axes seront envisagés afin de développer un traitement anticancéreux optimal appliqué au cancer pulmonaire à haut grade métastatique. Dans un premier temps un modèle pulmonaire orthotopique métastasant dans les ganglions du médiastin a été établi et caractérisé. Dans un second temps, deux voies et deux formes d'injections des LNCs ont été étudiées **(publication n°3).**

A la fin, une discussion générale permettra de synthétiser l'ensemble des résultats et d'apporter des informations complémentaires par rapport aux trois publications présentées. Cette discussion tentera de faire ressortir les points forts de nos nanovecteurs afin d'ouvrir de nouvelles perspectives dans le traitement des métastases ganglionnaires.

6. Liste des publications issues de cette thèse

6.1 Revue bibliographique

Gemcitabine versus modified gemcitabine: a review of several promising chemical modifications.
Elodie MOYSAN, Guillaume BASTIAT and Jean-Pierre BENOIT
Molecular Pharmaceutics. 2013 Feb 4; 10(2):430-44.

6.2 Concept, caractérisation et biodistribution

Publication n°1: **Gemcitabine-loaded lipid nanocapsule hydrogel: when the drug is a key player of the nanomedicine structure**
Elodie MOYSAN, Yolanda GONZÁLEZ-FERNÁNDEZ, Nolwenn LAUTRAM, Jérôme BÉJAUD, Guillaume BASTIAT and Jean-Pierre BENOIT

Publication n° 2: **Aqueous suspension and hydrogel of gemcitabine prodrug-loaded lipid nanocapsules: in vitro behavior and in vivo tissuedistribution**
Elodie MOYSAN, Nathalie WAUTHOZ, Yolanda GONZÁLEZ-FERNÁNDEZ, Nolwenn LAUTRAM, Kazuya KONDO, José HUREAUX, Guillaume Bastiat and Jean-Pierre BENOIT

6.3 Efficacité *in vivo*

Publication n° 3: **Evaluation of Lipid Nanocapsules Loaded with Lipophilic Gemcitabine Derivative against Metastases in Mediastinal Lymph Nodes in a Patient-like Lymphogenous Metastatic Model**
Nathalie WAUTHOZ, Elodie MOYSAN, Kazuya KONDO, Marc ZANDECKI, Valérie MOAL, Marie-Christine ROUSSELET, José HUREAUX, Guillaume BASTIAT and Jean-Pierre BENOIT

7. Références

1. Ferlay, J. *et al.* Cancer incidence and mortality patterns in Europe: Estimates for 40 countries in 2012. *Eur. J. Cancer* **49**, 1374-1403 (2013).

2. Aouba, A., Rey, G., Pavillon, G., Jougla, E. & Eb, M. Données sur la mortalité en France : principales causes de décès en 2008 et évolutions depuis 2000. *Bulletin épidémiologique hebdomadaire* **22,** 249–255 (2011).

3. Projection de l'incidence et de la mortalité par cancer en France en 2011. *Institut de veille sanitaire* 78 (2011).

4. Ferlay, J. *et al.* Estimates of worldwide burden of cancer in 2008: GLOBOCAN 2008. *Int. J. Cancer* **127,** 2893–2917 (2010).

5. Jemal, A. *et al.* Cancer statistics, 2008. *CA Cancer J. Clin.* **58,** 71–96 (2008).

6. Lewiński, T. & Żuławski, M. Small cell lung cancer survival: 3 years as a minimum for predicting a favorable outcome. *Lung Cancer* **40,** 203–213 (2003).

7. Herbst, R. S., Heymach, J. V. & Lippman, S. M. Lung cancer. *N. Engl. J. Med.* **359,** 1367–1380 (2008).

8. Schiller, J. H. *et al.* Comparison of four chemotherapy regimens for advanced non-small-cell lung cancer. *N. Engl. J. Med.* **346,** 92–98 (2002).

9. Ishikura, H. *et al.* Artificial lymphogenous metastatic model using orthotopic implantation of human lung cancer. *Ann. Thorac. Surg.* **69,** 1691–1695 (2000).

10. https://www.google.fr/url?sa=t&rct=j&q=&esrc=s&source=web&cd=4&ved=0CD4QFjAD&url=http%3A%2F%2Fwww.e-ancer.fr%2Fcomponent%2Fdocman%2Fdoc_ download%2F9608-cancer-du-poumon-prise-en-charge-therapeutique-du-cancer-du-poumon-non-a-petites-cellules&ei=yfRaUeYR4qnRBZTP gaAI&usg=AFQjCNHvhBl-E42xAGYy1zU68_XOeX88pA). (2 avril 2013).

11. https://www.google.fr/url?sa=t&rct=j&q=&esrc=s&source=web&cd=1&cad=rja&ved= 0CDIQFjAA&url=http%3A%2F%2Fwww.e-cancer.fr%2Fcomponent%2Fdocman%2Fdoc_download%2F9603-cancer-du-poumon-non-a-petites-cellules-formes-localisees-non-operables-localement-avancees-et-metastatiques-recommandations-argumentees&ei=oPZaUd2WOeGc0QWs74DIAQ &usg=AFQjCNEeqxtDy2hy2sSVC1brNnSKCbP-cA&bvm=bv.44442042,d.d2k. (2 avril 2013).

12. Busser, B. Rôle de l'amphiréguline dans la résistance du cancer du poumon non-à petites cellules au gefitinib. (2008).

13. Brown, P. Lymphatic system: Unlocking the drains. *Nature* **436,** 456–458 (2005).

14. Avraamides, C. J., Garmy-Susini, B. & Varner, J. A. Integrins in angiogenesis and lymphangiogenesis. *Nat. Rev. Cancer* **8,** 604–617 (2008).

15. Achen, M. G. *et al.* Vascular endothelial growth factor D (VEGF-D) is a ligand for the tyrosine kinases VEGF receptor 2 (Flk1) and VEGF receptor 3 (Flt4). *Proc. Natl. Acad. Sci. U.S.A.* **95,** 548–553 (1998).

16. Joukov, V. *et al.* A novel vascular endothelial growth factor, VEGF-C, is a ligand for the Flt4 (VEGFR-3) and KDR (VEGFR-2) receptor tyrosine kinases. *EMBO J.* **15,** 290–298 (1996).

17. Jeltsch, M. *et al.* Hyperplasia of Lymphatic Vessels in VEGF-C Transgenic Mice. *Science* **276,** 1423–1425 (1997).

18. Roberts, N. *et al.* Inhibition of VEGFR-3 Activation with the Antagonistic Antibody More Potently Suppresses Lymph Node and Distant Metastases than Inactivation of VEGFR-2. *Cancer Res.* **66,** 2650–2657 (2006).

19. Duong, T., Koopman, P. & Francois, M. Tumor Lymphangiogenesis as a Potential Therapeutic Target. *J. Oncol.* **2012,** 1–23 (2012).

20. Ji, R.-C. Lymphatic endothelial cells, tumor lymphangiogenesis and metastasis: New insights into intratumoral and peritumoral lymphatics. *Cancer Metastasis Rev.* **25,** 677–694 (2006).

21. Pepper, M. Lymphangiogenesis and tumor metastasis: myth or reality? *Clin. Cancer Res.* ***7,*** 462–468 (2001).

22. Maula, S.-M. *et al.* Intratumoral Lymphatics Are Essential for the Metastatic Spread and Prognosis in Squamous Cell Carcinomas of the Head and Neck Region. *Cancer Res* **63,** 1920–1926 (2003).

23. Hall FT, F. J. Intratumoral lymphatics and lymph node metastases in papillary thyroid carcinoma. *Arch. Otolaryngol Head Neck Surg.* **129,** 716–719 (2003).

24. Karpanen, T. *et al.* Vascular endothelial growth factor C promotes tumor lymphangiogenesis and intralymphatic tumor growth. *Cancer Res.* **61,** 1786–1790 (2001).

25. Hirakawa, S. *et al.* VEGF-C–induced lymphangiogenesis in sentinel lymph nodes promotes tumor metastasis to distant sites. *Blood* **109,** 1010 –1017 (2007).

26. Alexis, F., Pridgen, E., Molnar, L. K. & Farokhzad, O. C. Factors affecting the clearance and biodistribution of polymeric nanoparticles. *Mol. Pharm.* **5,** 505–515 (2008).

27. Li, S.-D. & Huang, L. Pharmacokinetics and biodistribution of nanoparticles. *Mol. Pharm.* **5,** 496–504 (2008).

28. Wang, A. Z., Langer, R. & Farokhzad, O. C. Nanoparticle delivery of cancer drugs. *Annu. Rev. Med.* **63,** 185–198 (2012).

29. Huynh, N. T., Passirani, C., Saulnier, P. & Benoit, J. P. Lipid nanocapsules: a new platform for nanomedicine. *Int. J. Pharm.* **379,** 201–209 (2009).

30. Huynh, N. T., Roger, E., Lautram, N., Benoît, J.-P. & Passirani, C. The rise and rise of stealth nanocarriers for cancer therapy: passive versus active targeting. *Nanomedicine (Lond)* **5,** 1415–1433 (2010).

31. Mozafari, M. R. *et al.* Role of nanocarrier systems in cancer nanotherapy. *J. Liposome Res.* **19,** 310–321 (2009).

32. Heurtault, B. *et al.* Lipidic nanocapsules: preparation process and use as Drug Delivery Systems. Patent US8057823 B2 (2000).

33. Heurtault, B., Saulnier, P., Pech, B., Proust, J.-E. & Benoit, J.-P. A novel phase inversion-based process for the preparation of lipid nanocarriers. *Pharm. Res.* **19,** 875–880 (2002).

34. Vanpouille-Box, C. Les nanocapsules lipidiques chargées en Rhénium-188 : nouvel outil pour la radiothérapie interne du carcinome hépatocellulaire et du gliome. (2011).

35. Lamprecht, A. & Benoit, J.-P. Etoposide nanocarriers suppress glioma cell growth by intracellular drug delivery and simultaneous P-glycoprotein inhibition. *J. Control. Release* **112,** 208–213 (2006).

36. Malzert-Fréon, A. *et al.* Formulation of sustained release nanoparticles loaded with a tripentone, a new anticancer agent. *Int. J. Pharm.* **320,** 157–164 (2006).

37. Peltier, S., Oger, J.-M., Lagarce, F., Couet, W. & Benoît, J.-P. Enhanced oral paclitaxel bioavailability after administration of paclitaxel-loaded lipid nanocapsules. *Pharm. Res.* **23,** 1243–1250 (2006).

38. Lacoeuille, F. *et al.* In vivo evaluation of lipid nanocapsules as a promising colloidal carrier for paclitaxel. *Int. J. Pharm.* **344,** 143–149 (2007).

39. Khalid, M. N., Simard, P., Hoarau, D., Dragomir, A. & Leroux, J.-C. Long circulating poly(ethylene glycol)-decorated lipid nanocapsules deliver docetaxel to solid tumors. *Pharm. Res.* **23,** 752–758 (2006).

40. Allard, E. *et al.* Lipid nanocapsules loaded with an organometallic tamoxifen derivative as a novel drug-carrier system for experimental malignant gliomas. *J. Control. Release* **130,** 146–153 (2008).

41. Vrignaud, S., Anton, N., Passirani, C., Benoit, J.-P. & Saulnier, P. Aqueous core nanocapsules: a new solution for encapsulating doxorubicin hydrochloride. *Drug Dev. Ind. Pharm.* (2013)

42. Vrignaud, S., Hureaux, J., Wack, S., Benoit, J.-P. & Saulnier, P. Design, optimization and in vitro evaluation of reverse micelle-loaded lipid nanocarriers containing erlotinib hydrochloride. *Int. J. Pharm.* **436,** 194-200 (2012).

43. Vrignaud, S., Anton, N., Gayet, P., Benoit, J.-P. & Saulnier, P. Reverse micelle-loaded lipid nanocarriers: A novel drug delivery system for the sustained release of doxorubicin hydrochloride. *Eur. J. Pharm. Biopharm.* **79,** 197-204 (2011).

44. David, S. *et al.* siRNA LNCs--a novel platform of lipid nanocapsules for systemic siRNA administration. *Eur. J. Pharm. Biopharm.* **81,** 448–452 (2012).

45. Morille, M. *et al.* Tumor transfection after systemic injection of DNA lipid nanocapsules. *Biomaterials* **32,** 2327–2333 (2011).

46. Morille, M. *et al.* Long-circulating DNA lipid nanocapsules as new vector for passive tumor targeting. *Biomaterials* **31,** 321–329 (2010).

47. David, S. *et al.* DNA nanocarriers for systemic administration: characterization and in vivo bioimaging in healthy mice. *Mol. Ther. Nucleic Acids* **2,** e64 (2013).

48. Allard, E. *et al.* 188Re-loaded lipid nanocapsules as a promising radiopharmaceutical carrier for internal radiotherapy of malignant gliomas. *Eur. J. Nucl. Med. Mol. Imaging* **35,** 1838–1846 (2008).

49. Vanpouille-Box, C. *et al.* Tumor eradication in rat glioma and bypass of immunosuppressive barriers using internal radiation with (188)Re-lipid nanocapsules. *Biomaterials* **32,** 6781–6790 (2011).

50. Vanpouille-Box, C. *et al.* Lipid nanocapsules loaded with rhenium-188 reduce tumor progression in a rat hepatocellular carcinoma model. *PLoS ONE* **6,** e16926 (2011).

51. Hirsjärvi, S. *et al.* Influence of size, surface coating and fine chemical composition on the in vitro reactivity and in vivo biodistribution of lipid nanocapsules versus lipid nanoemulsions in cancer models. *Nanomedicine* **9,** 375–387(2012).

52. Matsumura, Y. & Maeda, H. A New Concept for Macromolecular Therapeutics in Cancer Chemotherapy: Mechanism of Tumoritropic Accumulation of Proteins and the Antitumor Agent Smancs. *Cancer Res.* **46,** 6387–6392 (1986).

53. Huwyler, J., Drewe, J. & Krähenbuhl, S. Tumor targeting using liposomal antineoplastic drugs. *Int. J. Nanomedicine* **3,** 21–29 (2008).

54. Maruyama, K. Intracellular targeting delivery of liposomal drugs to solid tumors based on EPR effects. *Adv. Drug Deliv. Rev.* **63,** 161–169 (2011).

55. Allard-Vannier, E. *et al.* Pegylated magnetic nanocarriers for doxorubicin delivery: a quantitative determination of stealthiness in vitro and in vivo. *Eur. J. Pharm. Biopharm.* **81,** 498–505 (2012).

56. Jokerst, J. V., Lobovkina, T., Zare, R. N. & Gambhir, S. S. Nanoparticle PEGylation for imaging and therapy. *Nanomedicine (Lond)* **6,** 715–728 (2011).

57. Song, L. Y. *et al.* Characterization of the inhibitory effect of PEG-lipid conjugates on the intracellular delivery of plasmid and antisense DNA mediated by cationic lipid liposomes. *Biochim. Biophys. Acta* **1558,** 1–13 (2002).

58. Erbacher, P. *et al.* Transfection and physical properties of various saccharide, poly(ethylene glycol), and antibody-derivatized polyethylenimines (PEI). *J. Gene Med.* **1,** 210–222 (1999).

59. Acharya, S. & Sahoo, S. K. PLGA nanoparticles containing various anticancer agents and tumour delivery by EPR effect. *Adv. Drug Deliv. Rev.* **63,** 170–183 (2011).

60. Jaracz, S., Chen, J., Kuznetsova, L. V. & Ojima, I. Recent advances in tumor-targeting anticancer drug conjugates. *Bioorg. Med. Chem.* **13,** 5043–5054 (2005).

61. Pulkkinen, M. *et al.* Three-step tumor targeting of paclitaxel using biotinylated PLA-PEG nanoparticles and avidin-biotin technology: Formulation development and in vitro anticancer activity. *Eur. J. Pharm. Biopharm.* **70,** 66–74 (2008).

62. Liang, H.-F. *et al.* Paclitaxel-loaded poly(gamma-glutamic acid)-poly(lactide) nanoparticles as a targeted drug delivery system against cultured HepG2 cells. *Bioconjug. Chem.* **17,** 291–299 (2006).

63. Pan, J. & Feng, S.-S. Targeted delivery of paclitaxel using folate-decorated poly(lactide)-vitamin E TPGS nanoparticles. *Biomaterials* **29,** 2663–2672 (2008).

64. Farokhzad, O. C. *et al.* Nanoparticle-aptamer bioconjugates: a new approach for targeting prostate cancer cells. *Cancer Res.* **64,** 7668–7672 (2004).

65. Farokhzad, O. C. *et al.* Targeted nanoparticle-aptamer bioconjugates for cancer chemotherapy in vivo. *Proc. Natl. Acad. Sci. U.S.A.* **103,** 6315–6320 (2006).

66. Béduneau, A. *et al.* Brain targeting using novel lipid nanovectors. *J. Control. Release* **126,** 44–49 (2008).

67. Balzeau, J. *et al.* The effect of functionalizing lipid nanocapsules with NFL-TBS.40-63 peptide on their uptake by glioblastoma cells. *Biomaterials* **34,** 3381–3389 (2013).

68. Xie, Y., Bagby, T. R., Cohen, M. S. & Forrest, M. L. Drug delivery to the lymphatic system: importance in future cancer diagnosis and therapies. *Expert Opin. Drug Deliv.* **6,** 785–792 (2009).

69. Saraf, S., Ghosh, A., Kaur, C. D. & Saraf, S. Novel Modified Nanosystem Based Lymphatic Targeting. *J. Nanosci. Nanotechnol.* **1,** 60–74 (2011).

70. Oussoren, C. & Storm, G. Liposomes to target the lymphatics by subcutaneous administration. *Adv. Drug Deliv. Rev.* **50,** 143–156 (2001).

71. Hirsjärvi, S. *et al.* Surface modification of lipid nanocapsules with polysaccharides: From physicochemical characteristics to in vivo aspects. *Acta Biomater.* **9,** 6686-6693 (2013).

72. Oussoren, C. & Storm, G. Lymphatic uptake and biodistribution of liposomes after subcutaneous injection: III. Influence of surface modification with poly(ethyleneglycol). *Pharm. Res.* **14,** 1479–1484 (1997).

73. Akamo, Y. *et al.* Chemotherapy targeting regional lymph nodes by gastric submucosal injection of liposomal adriamycin in patients with gastric carcinoma. *Jpn. J. Cancer Res.* **85,** 652–658 (1994).

74. Tsuruta, T. *et al.* Liposome encapsulated doxorubicin transfer to the pelvic lymph nodes by endoscopic administration into the bladder wall: a preliminary report. *J. Urol.* **157,** 1652–1654 (1997).

75. Chen, J.-H. *et al.* Effect of small-sized liposomal Adriamycin administered by various routes on a metastatic breast cancer model. *Endocr. Relat. Cancer* **12,** 93–100 (2005).

76. Khato, J., Priester, E. R. & Sieber, S. M. Enhanced lymph node uptake of melphalan following liposomal entrapment and effects on lymph node metastasis in rats. *Cancer Treat. Rep.* **66,** 517–527 (1982).

77. Chong-Kook Kim *et al.* Lymph node targeting and pharmacokinetics of [3H]methotrexate-encapsulated neutral large unilamellar vesicles and immunoliposomes. *Int. J. Pharm.* **98,** 9–18 (1993).

78. Kim, C.-K., Lee, M.-K., Han, J.-H. & Lee, B.-J. Pharmacokinetics and tissue distribution of methotrexate after intravenous injection of differently charged liposome-entrapped methotrexate to rats. *Int. J. Pharm.***108,** 21–29 (1994).

79. Parker, R. J., Hartman, K. D. & Sieber, S. M. Lymphatic absorption and tissue disposition of liposome-entrapped [14C]adriamycin following intraperitoneal administration to rats. *Cancer Res.* **41,** 1311–1317 (1981).

80. Proulx, S. T. *et al.* Quantitative Imaging of Lymphatic Function with Liposomal Indocyanine Green. *Cancer Res.* **70,** 7053–7062 (2010).

81. Kobayashi, H. *et al.* Lymphatic drainage imaging of breast cancer in mice by micro-magnetic resonance lymphangiography using a nano-size paramagnetic contrast agent. *J. Natl. Cancer Inst.* **96,** 703–708 (2004).

82. Wang, Y.-X. J., Wang, D.-W., Zhu, X.-M., Zhao, F. & Leung, K. C. Carbon coated superparamagnetic iron oxide nanoparticles for sentinel lymph nodes mapping. *Quant. Imaging Med. Surg.* **2,** 53–56 (2012).

83. Ravizzini, G., Turkbey, B., Barrett, T., Kobayashi, H. & Choyke, P. L. Nanoparticles in sentinel lymph node mapping. *Nanomed. Nanobiotech.* **1,** 610–623 (2009).

84. Johnson, L., Charles-Edwards, G. & Douek, M. Nanoparticles in Sentinel Lymph Node Assessment in Breast Cancer. *Cancers* **2,** 1884–1894 (2010).

85. Johnson, L., Pinder, S. E. & Douek, M. Deposition of superparamagnetic iron-oxide nanoparticles in axillary sentinel lymph nodes following subcutaneous injection. *Histopathology* **62,** 481–486 (2013).

86. Pan, D. *et al.* Rapid synthesis of near infrared polymeric micelles for real-time sentinel lymph node imaging. *Adv. Healthc. Mater.* **1,** 582–589 (2012).

87. Phillips, W. T., Klipper, R. & Goins, B. Novel method of greatly enhanced delivery of liposomes to lymph nodes. *J. Pharmacol. Exp. Ther.* **295,** 309–313 (2000).

88. Yan, Z. *et al.* LyP-1-conjugated doxorubicin-loaded liposomes suppress lymphatic metastasis by inhibiting lymph node metastases and destroying tumor lymphatics. *Nanotechnology* **22,** 415103 (2011).

89. Luo, G. *et al.* LyP-1-conjugated nanoparticles for targeting drug delivery to lymphatic metastatic tumors. *Int. J. Pharm.* **385,** 150–156 (2010).

90. Kaur, C. D., Nahar, M. & Jain, N. K. Lymphatic targeting of zidovudine using surface-engineered liposomes. *J. Drug Target.* **16,** 798–805 (2008).

91. Hauff, P., Reinhardt, M., Briel, A., Debus, N. & Schirner, M. Molecular targeting of lymph nodes with L-selectin ligand-specific US contrast agent: a feasibility study in mice and dogs. *Radiology* **231,** 667–673 (2004).

92. Hui, Y. F. & Reitz, J. Gemcitabine: a cytidine analogue active against solid tumors. *Am. J. Health Syst. Pharm.* **54,** 162–170; quiz 197–198 (1997).

93. Moysan, E., Bastiat, G. & Benoit, J.-P. Gemcitabine versus Modified Gemcitabine: A Review of Several Promising Chemical Modifications. *Mol. Pharm.* **10,** 430-444 (2012).

94. Storniolo, A. M., Allerheiligen, S. R. & Pearce, H. L. Preclinical, pharmacologic, and phase I studies of gemcitabine. *Semin. Oncol.* **24,** S7–2–S7–7 (1997).

95. Texier, I. *et al.* Cyanine-loaded lipid nanoparticles for improved in vivo fluorescence imaging. *J. Biomed. Opt.* **14,** 054005 (2009).

Revue bibliographique

Avant propos

Ce travail de thèse a consisté à l'encapsulation dans des nanocapsules lipidiques de gemcitabine modifiée par une chaîne aliphatique, pour rendre ce principe actif plus lipophile. Dans la littérature, un grand nombre d'études traite de la modification de cette molécule, par l'ajout de chaînes lipophiles ou hydrophiles, et des améliorations ont été mises en évidence comparativement à la gemcitabine non modifiée. Il nous a semblé nécessaire d'écrire une revue de littérature traitant de ce sujet. En effet, la gemcitabine, un agent anticancéreux qui agit contre un large éventail de tumeurs solides, est connue pour être rapidement désaminée dans le sang en un métabolite inactif, la 2', 2'-difluorodéoxyuridine, et être rapidement excrétée dans les urines. De plus, de nombreux cancers développent des résistances, comme la diminution des transporteurs et des kinases responsables de la première étape de phosphorylation. Pour augmenter son action thérapeutique, la gemcitabine est administrée à dose élevée (1000 mg/m²) causant des effets indésirables (neutropénie, nausées, etc…). Pour améliorer sa stabilité métabolique, son activité cytotoxique et pour limiter les phénomènes de résistance, de nombreuses alternatives ont émergé, telles que la synthèse d'une prodrogue. La modification d'un agent anticancéreux n'est pas une nouveauté, le paclitaxel ou encore l'ara-C ont été synthétisés sous forme de prodrogue. Cette revue résume les différentes modifications chimiques qui peuvent être réalisées sur les positions 4 - (N) - et 5' de la gemcitabine. Elles peuvent fournir (i) une protection contre la désamination, (ii) une meilleure entrée cellulaire, (iii) une libération prolongée dans les cellules, (iv) une utilisation possible en cas de carence en désoxycytidine kinase et (v) en cas d'une déficience en transporteurs. Ces nouvelles prodrogues à base de gemcitabine utilisables en chimiothérapie ont le potentiel d'améliorer les résultats cliniques. Cette revue est parue dans le journal « *Molecular Pharmaceutics* » en février 2013.

molecular pharmaceutics

Review

pubs.acs.org/molecularpharmaceutics

Gemcitabine versus Modified Gemcitabine: A Review of Several Promising Chemical Modifications

Elodie Moysan,[†,‡] Guillaume Bastiat,*[,†,‡] and Jean-Pierre Benoit[†,‡]

[†]LUNAM Université—Micro et Nanomédecines Biomimétiques, F-49933 Angers, France

[‡]INSERM—U1066 IBS-CHU, F-49933 Angers, France

ABSTRACT: Gemcitabine, an anticancer agent which acts against a wide range of solid tumors, is known to be rapidly deaminated in blood to the inactive metabolite 2′,2′-difluorodeoxyuridine and to be rapidly excreted by the urine. Moreover, many cancers develop resistance against this drug, such as loss of transporters and kinases responsible for the first phosphorylation step. To increase its therapeutic levels, gemcitabine is administered at high doses (1000 mg/m^2) causing side effects (neutropenia, nausea, and so forth). To improve its metabolic stability and cytotoxic activity and to limit the phenomena of resistance many alternatives have emerged, such as the synthesis of prodrugs. Modifying an anticancer agent is not new; paclitaxel or ara-C has been subjected to such changes. This review summarizes the various chemical modifications that can be found in the 4-(*N*)- and 5′-positions of gemcitabine. They can provide (i) a protection against deamination, (ii) a better storage and (iii) a prolonged release in the cell, (iv) a possible use in the case of deoxycytidine kinase deficiency, and (v) transporter deficiency. These new gemcitabine-based sysems have the potential to improve the clinical outcome of a chemotherapy strategy.

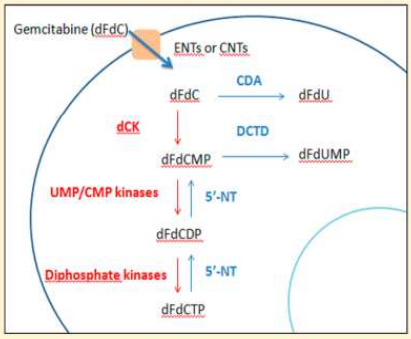

KEYWORDS: *gemcitabine, prodrug, chemical modification, resistance, antitumor effect*

1. INTRODUCTION

Cancer is the leading cause of death in developed countries. A major reason for this high mortality is the failure of current treatment that is in part attributed to the phenomenon of resistance but is also due to ineffective treatment against metastases. The current treatment of cancer using chemotherapy is largely based on the use of nucleoside analogues. These molecules are designed to mimic natural pyrimidine and purine nucleosides. Gemcitabine is one of these nucleoside analogues.

Gemcitabine acts against a wide range of solid tumors such as pancreatic, nonsmall lung, breast, and ovarian cancers.[1−4] One of the major difficulties in cancer therapy is that tumors acquire resistance over time. This resistance is related to the functioning of gemcitabine. Gemcitabine is transported into cells by different transporters, such as hENT1, and a decreased expression of hENT1 is responsible for a lower level of activity of gemcitabine by blocking its uptake.[5] Once in the cell, gemcitabine undergoes a series of phosphorylations to be active; the first of these is carried out by deoxycytidine deaminase (dCK). A low level of dCK is correlated with low gemcitabine cytotoxicity.[6] Furthermore, gemcitabine is rapidly deaminated by cytidine deaminase (CDA) causing a short plasma half-life.[7] Therefore, strategies that provide both enhanced transport and high metabolic bioevasion by chemical modification could potentially lead to new therapeutic strategies.

In this review we look at the pharmacological parameters of gemcitabine and its mode of action (which remains the same even with modified forms), and we describe the state of the art of various chemical modifications of gemcitabine, exclusively on two sites of the molecule (4-(*N*)- and 5′-sites, Figure 1), which have been carried out to improve its efficiency. A prodrug is a biologically inactive derivative of a parent drug molecule that usually requires an enzymatic or chemical transformation within

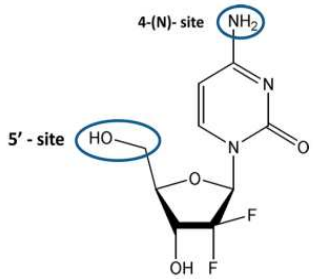

Figure 1. Modification sites in gemcitabine molecule.

Special Issue: Prodrug Design and Target Site Activation

Received: July 10, 2012
Revised: September 9, 2012
Accepted: September 14, 2012
Published: September 14, 2012

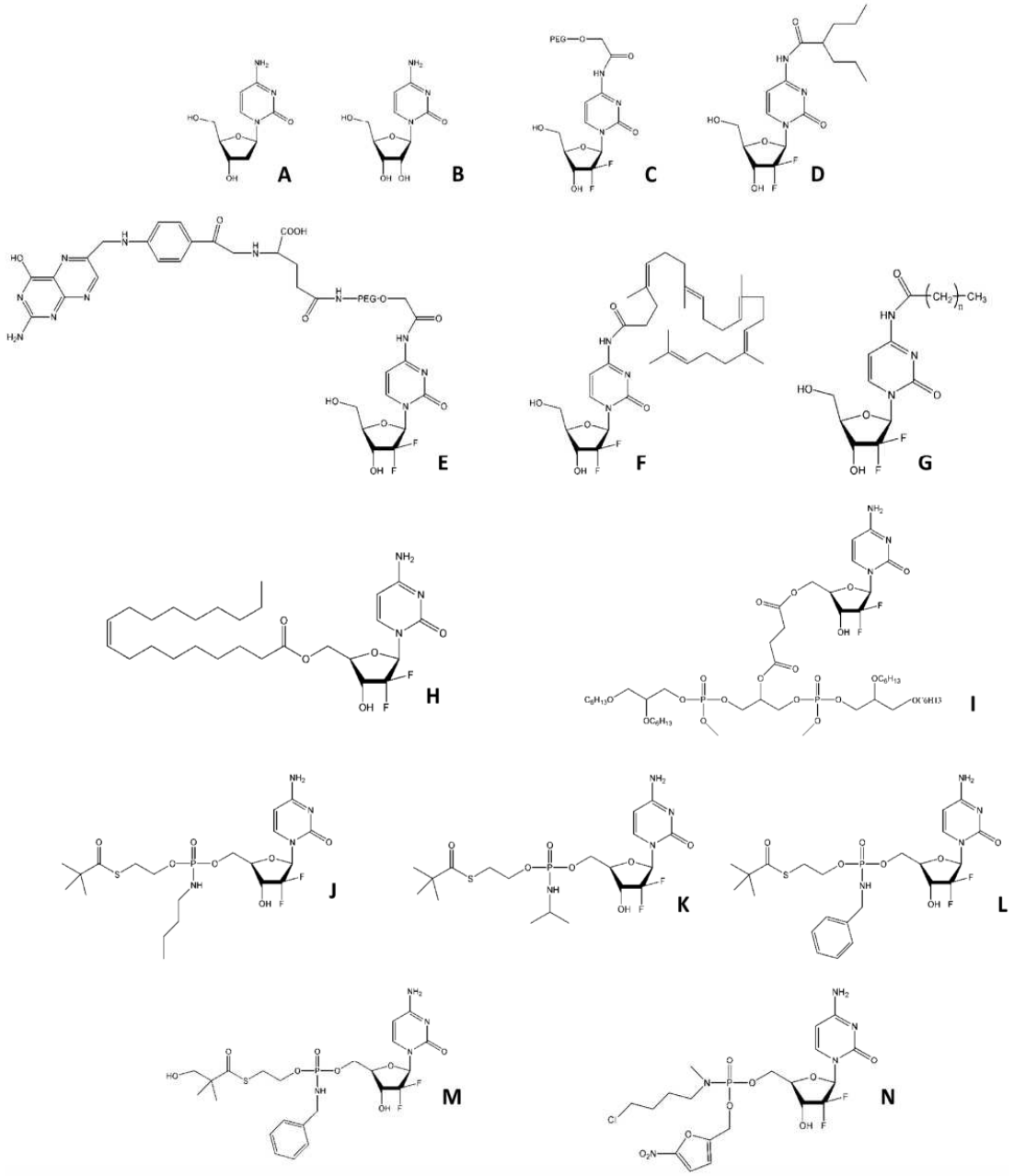

Figure 2. Chemical representation of gemcitabine analogues and modification presented in this review. A: deoxycytidine. B: cytosine arabinoside (AraC). C: PEG-gemcitabine. D: LY2334737. E: folate-PEG-gemcitabine. F: squalenoyl-gemcitabine. G: 4-(*N*)-acyl-gemcitabine. H: CP-4126. I: NEO6002. J: *N*-(*n*-butylamino)-*O*-(*S*-pivaloyl-2-thioethyl)-*O*-5′-gemcitabine phosphoramidate diester (Gem-1). K: *N*-(isopropylamino)-*O*-(*S*-pivaloyl-2-thioethyl)-*O*-5′-gemcitabine phosphoramidate diester (Gem-2). L: *N*-(benzylamino)-*O*-(*S*-pivaloyl-2-thioethyl)-*O*-5′-gemcitabine phosphoramidate diester (Gem-3). M: *N*-(benzylamino)-*O*-(*S*-(2,2-dimethyl-3-hydroxypropionyl)-2-thioethyl)-*O*-5′-gemcitabine phosphoramidate diester (Gem-4). N: 5′-(2′-deoxy-2′,2′-difluorocytidyl) *S*-nitrofurfuryl *N*-methyl-*N*-(4-chlorobutyl) phosphoramidate.

the body to release the active drug and has improved delivery properties in comparison to the parent molecule.[8] Drug modification has already been used with other anticancer drugs to overcome some disadvantages of the parent drug. For example, paclitaxel has been covalently attached to an acyl chain to obtain a lipophilic prodrug of paclitaxel to increase its encapsulation in lipid emulsions.[9] Another example is Ara-C, modified to facilitate Ara-C uptake and prolong its retention in the cell by grafting a fatty-acid chain at the 5′-position of the nucleoside.[10]

In the 4-(*N*)-position of gemcitabine, we will describe modifications with poly(ethylene glycol) (PEG), with valproic acid, with 1,1′,2-tris-nor-squalenoic acid (squalene), and with valeroyl, heptanoyl, lauroyl, and stearoyl linear acyl derivatives.

In the 5′-position, grafting with elaidic acid, with cardiolipin, and a series of phosphoramidates will be reported. All of these new gemcitabine-based molecules have the potential to improve the clinical outcome of traditional therapy.

1.1. Current State of Affairs. Also called 2′,2′-difluorodeoxycytidine (dFdC) (Figure 1), gemcitabine is a cell cycle-dependent (*S*-phase-specific) analogue of deoxycytidine (Figure 2A). Even if it presents some similarities with other nucleoside analogues (cytosine arabinoside; AraC) (Figure 2B), it differs in many properties and in its own spectrum of activity. It was originally investigated for its antiviral effects but has since been developed as an active agent for cancer therapy.[11]

This molecule (Gemzar: commercialized by Eli Lilly and Co.) was approved in 1996 by the Food and Drug Administration as first-line treatment for patients with locally advanced (nonresectable Stage II or Stage III) or metastatic (Stage IV) pancreatic cancer.[1,12] Clinical trials comparing the use of Gemzar and 5-FU for patients with locally advanced or metastatic pancreatic cancer who had received no prior chemotherapy showed that patients treated with Gemzar had significant increases in positive clinical response, survival, and disease progression time compared to 5-FU (Figure 3). In this clinical study, Gemzar was administered intravenously with a 100 mg/m^2-dose for 30 min for 7 of the first 8 weeks as a first cycle. From the second cycle, gemcitabine was given weekly for 3 weeks in 4-week cycles at the same dose. 5-FU was administered intravenously at a 600 mg/m^2-dose for 30 min.[13]

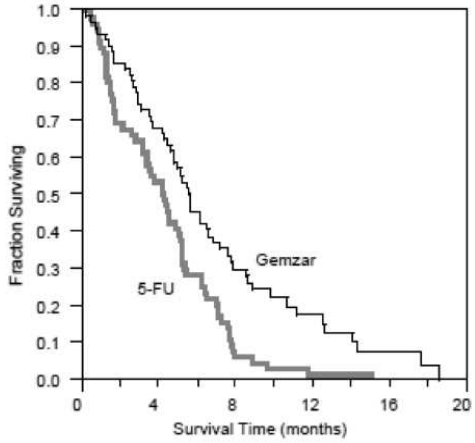

Figure 3. Kaplan–Meier survival curve.[13]

The FDA approved the use of Gemzar in 1996 in combination with cisplatin for the first-line treatment of patients with inoperable, locally advanced (Stage IIIA or IIIB) or metastatic (Stage IV) nonsmall cell lung cancer.[2] Two schedules were investigated, and the optimum schedule was sought. With the 4-week schedule, Gemzar was administered intravenously at a 1000 mg/m^2-dose for 30 min on days 1, 8, and 15 of each 28-day cycle. Cisplatin was administered intravenously at a 100 mg/m^2-dose on day 1 after the infusion of Gemzar. With the 3-week schedule, Gemzar was administered intravenously at 1250 mg/m^2 for 30 min on days 1 and 8 of each 21-day cycle. Cisplatin was administered intravenously at a 100 mg/m^2-dose after the infusion of Gemzar on Day 1.

In 2004, the FDA approved the use of gemcitabine in combination with paclitaxel for the first-line treatment of patients with metastatic breast cancer[3] and in 2006 in combination with carboplatin for the treatment of patients with advanced ovarian cancer.[4] For breast cancer, a 1250 mg/m^2-dose of Gemzar (intravenous infusion for 30 min) was administered on days 1 and 8 of a 21-day cycle with paclitaxel (175 mg/m^2-dose; intravenous infusion for 3 h) administered prior to gemcitabine hydrochloride on day 1 of each cycle. For ovarian cancer, Gemzar was administered at a 1000 mg/m^2-dose on days 1 and 8 of a 21-day cycle with carboplatin (AUC 4) administered on day 1 of each cycle.

Until 2008, Eli Lilly had the exclusive rights of sale of gemcitabine in the United States and Europe, and sales of Gemzar increased constantly with a turnover of 1720 billion dollars. Since 2008, sales have steadily declined with the introduction of generic alternatives. Indeed Gemzar lost effective exclusivity in the U.S. in November 2010 and in major European countries (France, Germany, Italy, Spain ,and the United Kingdom) in March 2009. In 2009 and 2010, sales outside the U.S. decreased by 37% and 31%, respectively; and in 2010 a decrease of 3% in the U.S was observed, driven by reduced demand and lower prices as a result of the entry of generic competition.[14]

1.2. Biodistribution. Gemcitabine has a very short plasma circulation time. The elimination half-life depends upon the infusion time, and the age and the gender of the patient (Table 1). For short infusions, the half-life is from 42 to 94 min. For infusions of 70 min, the half-life is 4 to 10 h and is associated with increased toxicity. At higher doses, major toxicity can be observed, such as neutropaenia, reversible hepatic transaminase increases, proteinuria, nausea and vomiting, mild flulike syndrome, and mild skin rash.[15] Gemcitabine is rapidly cleared from the body upon its enzymatic conversion in the blood, liver, kidney, and various tumor tissues.[16]

Table 1. Gemcitabine Clearance and Half-life for "Typical" Patients[13]

age	clearance men (L/h/m^2)	clearance women (L/h/m^2)	half-life[a] men (min)	half-life[a] women (min)
29	92.2	69.4	42	49
45	75.7	57.0	48	57
65	55.1	41.5	61	73
79	40.7	30.7	79	94

[a]Half-life for patients receiving a short infusion (<70 min).

1.3. Mechanisms of Action. Gemcitabine is transported across the plasma membrane by sodium-dependent (concentrative nucleoside transporter hCNTs) and by sodium-independent (equilibrative nucleoside transporter hENTs) mechanisms.[5,17] Gemcitabine is transported into cells by five nucleoside transporters, two equilibrative nucleoside transporters hENT1 and hENT2 and three concentrative nucleoside transporters hCNT1, hCNT2, and hCNT3. hENTs mediate bidirectional transport of nucleosides across biological membranes down a concentration gradient and are found in most tissues in the body. The hCNT family members are cation-dependent symporters that mediate unidirectional transport of nucleosides into cells.[18] Kinetic studies have shown that gemcitabine intracellular uptake is preferentially directed by hENT1 and, to a lesser extent, by hCNT1 and hCNT3.[19,20] Several studies have shown the importance of the presence of the hENT1 transporter for an optimal response to gemcitabine.[21] One study has shown that, in patients with

pancreatic cancer, those with the highest level of hENT1 mRNA expression had a significant increase in survival time compared with patients expressing low hENT1 levels.[22]

In cells, gemcitabine undergoes a series of phosphorylations, essential to make it active (Figure 4). First it is phosphorylated

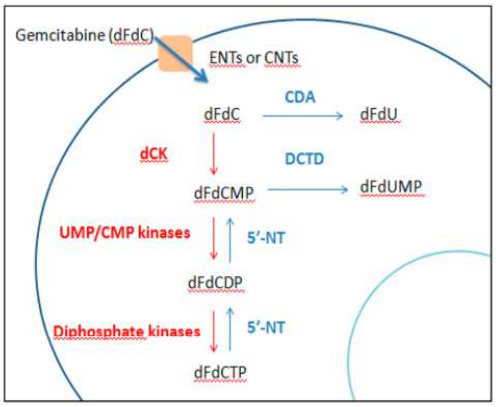

Figure 4. Phosphorylation and dephosphorylation of gemcitabine in the cell. ENTs: equilibrative nucleoside transporters, CNTs: concentrative nucleoside transporters, dFdCMP: gemcitabine monophosphate, dFdCDP: gemcitabine diphosphate, dFdCTP: gemcitabine triphosphate, dFdUMP: 2′-deoxy-2′,2′-difluorouridine monophosphate, dFdU: 2′,2′-difluorodeoxyuridine, CDA: cytidine deaminase, DCTD: deoxycytidylate deaminase, 5′-NT: 5′-nucleotidase, UMP/CMP kinase: nucleoside monophosphate kinase.

to a monophosphate compound (dFdCMP) by deoxycytidine kinase (dCK). It then undergoes a second modification to become gemcitabine diphosphate (dFdCDP) and finally to gemcitabine triphosphate (dFdCTP), all catalyzed by nucleoside monophosphate kinase (UMP/CMP) and diphosphate kinase, respectively. Gemcitabine inactivation is catalyzed by cytidine deaminase (CDA) as well as the deamination of gemcitabine monophosphate, which is catalyzed by deoxycytidylate deaminase (DCTD). Phosphorylated metabolites of gemcitabine are reduced by cellular 5′-nucleotidase (5′-NT), and dFdCMP is also converted, and inactivated, by DCTD into 2′-deoxy-2′,2′-difluorouridine monophosphate (dFdUMP).

The triphosphate form of gemcitabine acts as a competitive substrate of deoxycytidine triphosphate. Its analogy allows it to be incorporated into DNA during replication, thus inhibiting chain elongation of DNA and causing cell death by apoptosis. Once gemcitabine triphosphate is incorporated at the end of the elongated DNA strand, one deoxynucleotide is added, and thereafter the DNA polymerases are unable to proceed. This action, called "masked chain termination", appears to lock the drug into DNA because proof-reading exonucleases are unable to remove gemcitabine nucleotide from this penultimate position.[23,24] The inhibitory action of gemcitabine is enhanced by its nondetection in the DNA chain.

Gemcitabine exhibits a unique property called self-potention which enhances its activation. The diphosphate form (dFdCDP) inhibits ribonucleoside diphosphate reductase (RNR), an enzyme of DNA synthesis, which permits the formation of nucleoside triphosphates. This results in a significant decrease in the concentration of cellular deoxycytidine triphosphate (dCTP) and a change in the ratio of dCTP/dFdCTP in favor of dFdCTP. The accumulation of gemcitabine triphosphate and the intracellular reduction of dCTP results in the inhibition of dFdCMP inactivation by DCTD, which requires sufficient concentrations of dCTP to be active.[25]

Thymidylate synthase (TS), which plays a key role in the synthesis of thymidine monophosphate, has been studied to investigate the possible inhibition of TS by gemcitabine exposure. The natural substrate of TS, 2′-deoxyuridine monophosphate (dUMP), is converted into 2′-deoxythymidine-monophosphate (dTMP). Thereby analogues of dUMP are potential TS inhibitors, and the deaminated product of gemcitabine dFdUMP resembles dUMP.[26] Studies with the human ovarian cancer cell line A2780 and the murine colon carcinoma cell line C26−10 show inhibition of 90% of TS activity after 24 h exposure to gemcitabine.[27] The expression of TS provides an alternative source of substrate for DNA synthesis and positively correlates it with gemcitabine resistance and shortened patient survival time. Another study has proved that removing TS protein expression by siRNA induces a high degree of growth inhibition by gemcitabine, indicating the critical relation of TS to the enhancement of the therapeutic effect of gemcitabine.[28] A final, less well-known, and less studied mode of action of gemcitabine is its incorporation into RNA, which seems to be concentration-dependent.[29]

1.4. Resistance. Many forms of cancer show initial sensitivity to gemcitabine therapy followed by the rapid development of resistance, a feature that essentially characterizes this disease. Thus, a better understanding of the origins of gemcitabine resistance is critical to the development of improved combination therapies to replace gemcitabine or to improve gemcitabine targeting. Resistance to antimetabolic drugs such as gemcitabine can be achieved by various genomic alterations.[29]

A major cause of resistance can be attributed to alterations in the transporter. The development of resistance to gemcitabine correlates strongly with a deficiency of hENT1 expression in human breast and pancreatic cancer cells.[5,30] Many studies have shown that the hENT1 but also hCNT3 expression determination can be used as a prognostic marker to provide prospective evaluations for patients receiving gemcitabine-based adjuvant therapy.[6,31,32]

In L1210 murine leukemia cells made resistant to ara-C and cross-resistant to gemcitabine, altered action of dCK can be observed, due to genomic recombination.[27] These results suggest that a partial deletion of the dCK gene observed after selection in the presence of gemcitabine is involved with resistance to this agent both *in vitro* and *in vivo*. The expression of dCK has been postulated to be correlative to gemcitabine resistance.[33]

Another factor in gemcitabine resistance is the overexpression of ribonucleotide reductase (RR).[34] RR is a dimeric enzyme composed of regulatory subunit M1 (RRM1) and catalytic subunit M2 (RRM2). Ribonucleotide reductase is mainly responsible for the conversion of ribonucleosides to deoxyribonucleoside triphosphates (dNTPs), which are essential for DNA polymerization and repair. RRM1 overexpression through transfection of a lung cancer cell line likewise resulted in gemcitabine resistance. Reduction of RRM1 expression through RNA interference abrogated the induced gemcitabine resistance.[35] Ribonucleotide reductase enzymatic activity is modulated by levels of its M2 subunit. An overexpression of RRM2 is associated with resistance to gemcitabine and down regulation of RRM2 by siRNA enhanced gemcitabine cytotoxicity, both *in vitro* and *in vivo* in pancreatic

dx.doi.org/10.1021/mp300370t | *Mol. Pharmaceutics* 2013, 10, 430−444

adenocarcinoma.[7] Gemcitabine monophosphate and triphosphate are reduced respectively by dCMP deaminase and by 5′-nucleotidase (5′-NT), and gemcitabine itself is inactivated by cytidine deaminase (CDA). High levels of these catabolic enzymes are associated with resistance to the drug.[36]

Apoptosis forms the principal cause of cell death in response to cytotoxic drug treatment. A variety of anticancer drugs have been shown to produce extensive apoptosis in sensitive malignant cells, but it has been suggested that the inability of some cells to undergo apoptosis is similar to the mechanism of gemcitabine resistance. The expression of p53, which plays an important role in apoptosis pathways, induces cell cycle arrest, and in the higher concentration ranges, p53 induces apoptosis. On the other hand, human lung cancer expressing the mutation of the p53 gene does not undergo apoptosis after gemcitabine treatment.[37] The aberrant expression of genes associated with cellular survival and apoptosis is implicated in gemcitabine resistance.

New resistance mechanisms to gemcitabine implicate the stress-response protein Hu antigen R (HuR) which is an RNA-binding protein that post-transcriptionally regulates gene expression. A recent study has shown a relation between HuR and gemcitabine resistance. After treatment of a MiaPaCa-2 cell line with gemcitabine, increased HuR cytoplasmic levels and a reaction to the drug were observed. Since the dCK 3′UTR region contains eight putative hits of an HuR recognition motif, HuR associated with dCK mRNA was tested, and a bond of HuR with the dCK 3′UTR was obtained. A correlation between the level of HuR and the dCK protein levels, but not the dCKA mRNA, was observed. Regulation of dCK protein concentration by HuR and the prediction of gemcitabine response by cytoplasmic HuR levels was suspected.[38] Nevertheless a recent study has shown that HuR binds to VEGF mRNA, implying regulation of VEGF expression in pancreatic ductual andenocarcinoma after gemcitabine exposure.[39] Taken together, these data suggest that the genes encoding proteins involved in the transport and metabolism of gemcitabine and in the metabolism of targets can be potential candidates to predict sensitivity to gemcitabine. Quantitative analyses of these genes can be a potent tool to perform individualized chemotherapy.

Gemcitabine is a polar drug with low membrane permeability and which is extensively degraded by cytidine deaminase into an inactive metabolite in the liver. Moreover, the increasing amount of resistance also reduces its cytotoxicity. Thus, a frequent administration schedule at high drug doses is required, and this leads to serious side effects such as: myelosuppression, high levels of hepatoxicity, renal toxicity, thrombocytopaenia, and anemia.[40] To date, various innovative approaches have been developed to overcome these disadvantages. We will focus on chemical modifications at the 4-(*N*)- and 5′-positions of gemcitabine.

2. 4-(*N*)-MODIFICATION OF GEMCITABINE

2.1. PEG-Gemcitabine. For 40 years, several antitumor agents, either proteins, peptides, or low molecular-weight drugs, have been considered for PEG conjugation. PEGylation can give a number of relevant advantages such as considerable *in vivo* half-life prolongation, a reduction or removal of immunogenicity, and a reduction of aggregation.[41]

The technique has become the leading approach for overcoming most of the aforementioned biological limits, and the number of PEGylated products on the market and in clinical trials is increasing constantly.[42,43] The PEGylation process presents many advantages: (i) PEG is a polymer with high solubility in water and excellent biocompatibility (it is FDA-approved for human administration by mouth, injection, or dermal application[44]), (ii) plasma half-life of the PEGylated product is increased, (iii) it provides enzyme protection, and (iv) it accumulates in tumor zones according to the "enhanced permeability and retention" effect (EPR).[45,46] However, a number of drugs encapsulated or solubilizing with pegylated agents can activate the complement system, the nonspecific, humoral arm of antimicrobial immune defense. Complement activation has been recently proposed as a major underlying or contributing cause of infusion reactions, referred to as complement-activation related pseudoallergy (CARPA). CARPA may be a major underlying cause or contributing factor to the hypersensitivity reactions (HSRs) caused by many successful drugs, such as Taxol and Doxil.[47]

Clinical trials of several derivatives of PEG coupled to anticancer drugs are already under way or have been completed.[43] Pegamotecan (Enzon Pharmaceuticals, Inc.) is a prodrug obtained by coupling two molecules of camptothecin to a PEG of 40 kDa. An amphiphilic polymer-docetaxel conjugate was prepared by attaching PEG to docetaxel through an ester linkage. The PEG-docetaxel was used to form nanosized micelles for the solubilization of free docetaxel. A 1.8-fold higher area under the curve (AUC) for docetaxel equivalent plasma concentration versus time was obtained, in comparison with free docetaxel. The maximum tolerated dose of PEG-docetaxel was also 2.5-fold higher than that for free docetaxel in healthy mice.[48] Studies with paclitaxel were also conducted: PEG (5000 Da) was bound to the 2′-position of paclitaxel through a spacer succinyl group, and this prodrug increased the half-life of PEG-paclitaxel.[49] Other studies have shown the importance of conjugation with PEGs with a molecular weight ≥30 kDa, to prevent rapid elimination by the kidneys.[43] Because of encouraging results from studies with other anticancer agents and because the anticancer effects of gemcitabine is limited by its short half-life, its rapid metabolization, and its low tumor uptake, the addition of PEG on gemcitabine has been tested by several research teams. In a recent paper, a synthesis of a PEG-gemcitabine, by conjugating the amino groups at 4-(*N*)-position of gemcitabine to *N*-hydroxysuccinimide derivative of PEG, has been carried out (Figure 2C).[50]

Confocal analysis showed PEG-gemcitabine colocalization in lysosome and endosome after 24 h incubation and an enhanced retention in cancer cells after 3 days of incubation in comparison to native gemcitabine. It is known that the cellular uptake of PEG-drugs occurs through endocytosis and they are retained in transport vesicles which traffic along the endolysosomal scaffold which are acidic in nature.[51,52] The endolysosomal transport vesicles allow cleavage of the amide bonds between PEG and gemcitabine, thanks to the acidic nature of these vesicles, and thereby allow its prolonged release. Pharmacokinetic studies have shown consistently higher bioavailability (21 times) of PEG-gemcitabine over native gemcitabine, after 1 h of intravenous administration in mice (Figure 5). In MiaPaCA 2 and PANC-1 PEG-gemcitabine was more effective in all cases in comparison with native gemcitabine.

To improve the effect of PEG-gemcitabine, folic acid has recently been conjugated to PEG-gemcitabine (Figure 2E) to evaluate their active targeting and cytotoxic superiority

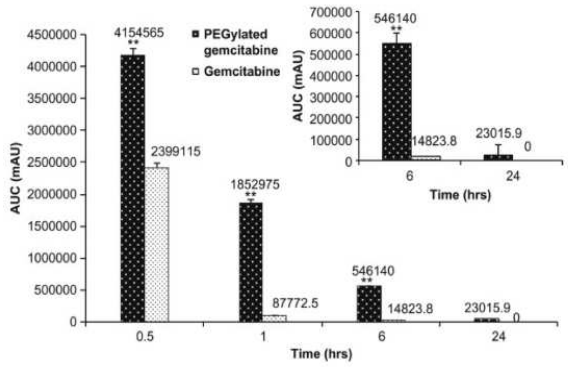

Figure 5. *In vivo* bioavailability of gemcitabine and PEGylated gemcitabine. The mice were divided in two groups. An equivalent concentration of gemcitabine and PEGylated gemcitabine (6.74 mg/kg) was given to group 1 and group 2, respectively. Gemcitabine and PEGylated gemcitabine were administered intravenously, and blood was collected at different time intervals. Serum was separated, and the concentration of gemcitabine was determined by RP-HPLC analysis, as described in materials and methods. (**) $p < 0.005$ and (*) $p < 0.05$ gemcitabine versus PEGylated gemcitabine.[50]

compared the nontargeted PEG-gemcitabine.[53] The drug linkage involved the 4-(*N*)-amino group of gemcitabine and the COOH of PEG, while folic acid was linked through its carboxylic function to PEG amino group. Folic acid was chosen as the targeting agent because its receptor is overexpressed in several types of cancers (lung, breast, kidney, and ovarian),[54−56] while in normal human tissues its receptors may have limited distribution. Effective targeting with folate has been proven by using folate on the surface of many nanocarriers such as gold nanoparticles, liposomes, or magnetic nanoparticles for the detection of cancer cells and the release of anticancer drugs.[57−59]

All conjugates were able to release the drug in a pH-dependent manner with no role played by enzymes. The presence of a plasma enzyme does not accelerate the conversion of different compounds in dFdU, which confirms previous studies showing that the protection of the amino group of gemcitabine prevents this.[60] Polymer conjugation of gemcitabine increases drug plasma half-life, which is dependent on the polymer's molecular weight, by reducing its kidney clearance. An increase of $t_{1/2}\alpha$, $t_{1/2}\beta$, and the area under the curve was obtained. The results of cytotoxicity tests showed no improvement of PEG-gemcitabine (with or without folic acid), compared to native gemcitabine, on tumor cell lines which did not overexpress the folate receptor. Folic acid derivatives are less toxic than PEG derivatives. This is explained by a slower entry into the cell by endocytosis and a cytotoxic activity only after the release of gemcitabine. Moreover, the polymer derivatives targeting folate receptors need a receptor-mediated endocytosis mechanism for cell penetration in cells that do not overexpress the folate receptor. Folate-targeted poly(ethylene glycol) (PEG)-coated nanoparticles are found to bind to folate receptors triggering for caveolae-assisted endocytosis, followed by the formation of intracellular vesicles which can be visualized by confocal microscopy.[61] In contrast, in KB-3-1 cells which overexpress folate receptors, derivatives with folate are certainly less cytotoxic than native gemcitabine but are more cytotoxic than gemcitabine only coupled to PEG.[53]

PEGylation is currently considered to be one of the most successful techniques to prolong the residence time of drugs in the bloodstream. In a few cases, polymer conjugation has also shown that it can confer targeting properties to the disease site, such as tumor masses, by passive diffusion (EPR effect).[62] Different studies have proven the interesting use of PEG-like drug carriers. They permit an increase of drug plasma half-life, prevent the degradation action of cytidine-deaminase enzyme, increase the availability after intravenous injection, and in certain cases increase the cytotoxicity against cancer cells. The easy addition of an agent that specifically targets cancer cells in the case of folic acid is also a benefit of the use of PEGylation.

2.2. LY2334737. Gemcitabine has poor oral bioavailability due to an extensive first pass metabolism by cytidine deaminase. To circumvent this rapid deamination into 2′,2′-difluorodeoxyuridine (dFdU), a gemcitabine prodrug has been developed, LY2334737 (Figure 2D). LY2334737 is an oral gemcitabine prodrug in which gemcitabine is linked to valproic acid via an amide bond at 4-(*N*)-position, enabling it to bypass hydrolysis in enterocytes and portal circulation, thereby avoiding the extensive first pass metabolism that occurs with unmodified gemcitabine. Circulating levels of LY2334737 are detectable several hours after oral administration. In addition, a gradual release of gemcitabine following cleavage of the amide bond should enhance efficacy, since more cancer cells should be exposed to a continuous effective cytotoxic level of gemcitabine. The stability of the prodrug was tested on a pH range from 1 to 8 to check the possibility of delivering an intact prodrug into systemic circulation after passing through the gastrointestinal tract after oral administration. LY2334737 is pH-dependent with about 21% degradation at pH 1 and no degradation between pH 6 to 8, after 4 h of incubation at 40 °C.[63] *In vitro* hydrolysis profiles showed a slow hydrolysis in the liver (subcellular fractions S9 that contain drug-metabolizing enzymes) and in crude homogenates of small intestinal epithelial cells with 27 and 11 pmol/mg·min, respectively. *In vivo* antitumor activity with mice bearing HCT-116 human colon tumor xenografts indicated the same efficacy of LY2334737 after an oral administration at a 7.55 mg/kg-dose for 14 days versus 4 doses of an intraperitoneal administration of gemcitabine at a 160 mg/kg-dose. Phase I trials of LY2334737 either as monotherapy or in combination with other agents are currently under way to determine the maximum tolerated dose and dose limiting toxicities of daily administration.[64]

2.3. Squalenoylation. Squalene is a triterpene that is an intermediate in the cholesterol biosynthesis pathway. Squalene is a structurally unique triterpene compound that is one of the main components (about 13%) of skin surface lipids. It was so-called due to its first historical isolation from shark liver oil, where it is contained in large quantities, and is considered its richest source.[65] In humans, about 60% of dietary squalene is absorbed and is distributed ubiquitously in human tissues in small amounts.[66] Recent *in vitro* and *in vivo* model experiments suggest a tumor-inhibiting role for squalene.[67]

Couvreur's team developed the concept of squalenoylation involving the chemical linkage of squalene with various nucleoside analogues which allowed the formation of novel colloidal nanoassemblies of 100−300 nm with a narrow size distribution, after dispersion in an aqueous environment.[68] They were interested in the pharmacological activity of gemcitabine covalently coupled at 4-(*N*)-position with 1,1′,2-Tris-nor-squalenoic acid to obtain Sq-gemcitabine (4-(*N*)-Tris-

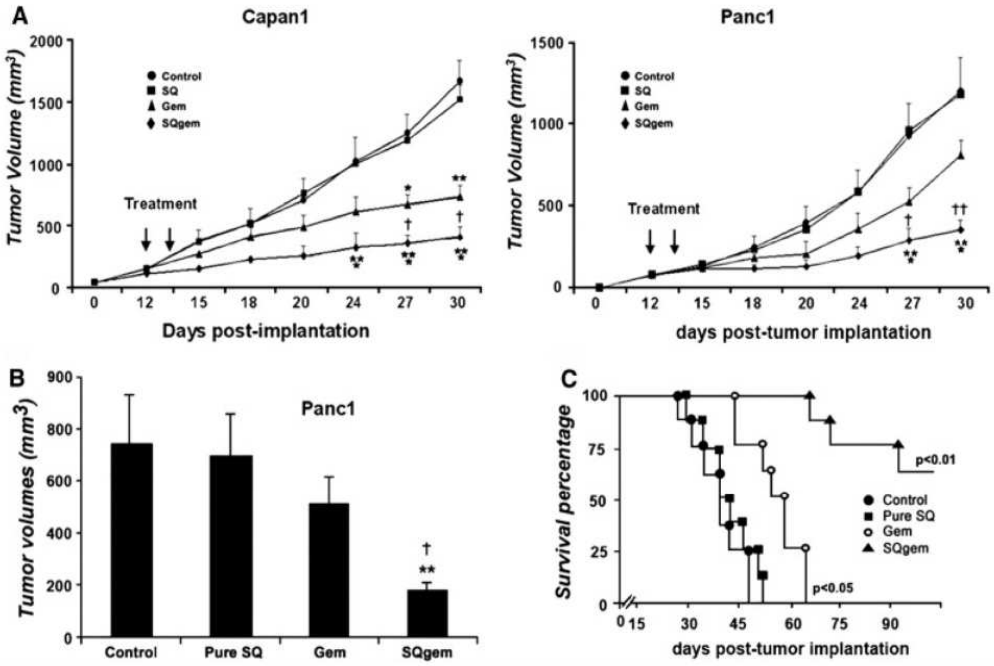

Figure 6. SQ-Gem improves inhibition of tumor growth and increased survival. (A) Mice (n = 8) bearing subcutaneous tumors were treated twice with Gem or SQ-Gem (20 mg/kg). After 1 month, statistical analysis of tumor volumes showed superior antitumor efficacy of SQ-Gem compared to untreated or SQ-treated mice (***$P < 0.001$) and to Gem ($^{\dagger}P < 0.05$, $^{\dagger\dagger}P < 0.001$). (B) The same experiment was performed on a Panc1 orthotopic tumor model (n = 14). Tumors were significantly reduced by SQ-Gem treatment (**$P < 0.01$ vs untreated mice and $^{\dagger}P < 0.05$ vs Gem-treated mice). (C) Kaplan−Meier survival curves of orthotopic Panc1 tumor-bearing mice showed significant enhanced median survival after SQ-Gem treatment (vs Gem-treated mice, $p < 0.5$ and vs control mice, ***$P < 0.001$).[73]

nor-squalenoyl-gemcitabine, SQdFdC) (Figure 2F). A study by X-ray diffraction (SAXS) combined with molecular modeling identified the supramolecular organization of these nanoassemblies, which form an inverse, hexagonal phase, in which the central aqueous core consisting of water and gemcitabine molecules was surrounded by the squalene moieties.[69] They investigated the anticancer activity of Sq-gemcitabine *in vitro* on resistant murine and human leukemia cells (L1210 10K and CEM/ARAC8C, respectively). The L1210 10K cells were characterized by a lower expression of cytoplasmic dCK and CEM/ARAC8C by a deficiency in hENT1 transporters,[70,71] these two ways representing two major resistance factors to gemcitabine. After 72 h of incubation with different concentrations, Sq-gemcitabine demonstrated 3.26 and 3.22-fold higher cytotoxicity compared to gemcitabine with L1210 10K and CEM/ARAC8C, respectively.[72] After intravenous injection of Sq-gemcitabine in aggressive leukemia-bearing mice, an increase in survival time compared to gemcitabine was obtained. This significant increase was attributed to the high degree of localization of Sq-gemcitabine in the liver and spleen which are the major metastatic organs. Sq-gemcitabine was found to be more efficient than gemcitabine, suggesting the considerable potential of this treatment for leukemia.

Studies on human pancreatic adenocarcinoma models were also performed. *In vitro* Sq-gemcitabine showed higher antiproliferative and cytotoxic effects compared to native gemcitabine, on chemoresistant tumor cells (Panc-1) and sensitive cell lines (Capan1 and BxPc3), which were associated with significant DNA synthesis inhibition, S-phase arrest, and higher induction of apoptosis (caspase 3 activation). *In vivo* experiments were performed with subcutaneous tumor models (Panc1 and Capan1) and orthotopic tumors (Panc1). Sq-gemcitabine treatment exerted significant inhibition of tumor growth in all types of tumor models compared to gemcitabine and avoided the formation of metastatis spreading in the peritoneum, and prolonged the survival time of mice with orthotopic pancreatic tumors (Figure 6).[73]

The impact of the encapsulation of Sq-gemcitabine in liposomes on a model of subcutaneous leukemia (L1210wt) was also studied. PEGylated liposomes were employed to modify the drug pharmacokinetics and biodistribution to enhance the anticancer activity (accumulation in tumors due to their ability to extravasate into these tissues by the EPR effect) and to decrease the capture by macrophages in organs of the reticuloendothelial system.[74] PEGylated liposomal formulations exhibited a hydrodynamic diameter of 133 ± 24 nm with a polydispersity index of 0.035 and were stable for 2 weeks. A similar *in vivo* anticancer activity of Sq-gemcitabine in PEGylated-liposomes compared to native gemcitabine was demonstrated, with a drug dosage 5-fold lower than free gemcitabine on a subcutaneous grafted L1210wt leukemia model. They explained this by the protection of gemcitabine from deamination in the blood.

A novel innovative nanoparticle system is currently being developed using Sq-gemcitabine: nanocarriers are able to target the tumor due to the presence of magnetite nanocrystals formed in the self-assembly of the squalenoyl gemcitabine bioconjugate.[75] These particles were thought to be compatible with parenteral administration. After intravenous injection, in L1210 subcutaneous tumor model mice, the new assembly of magnetite-Sq-gemcitabine was guided to the tumor by a magnet placed at the tumor location. Considerable inhibition of tumor

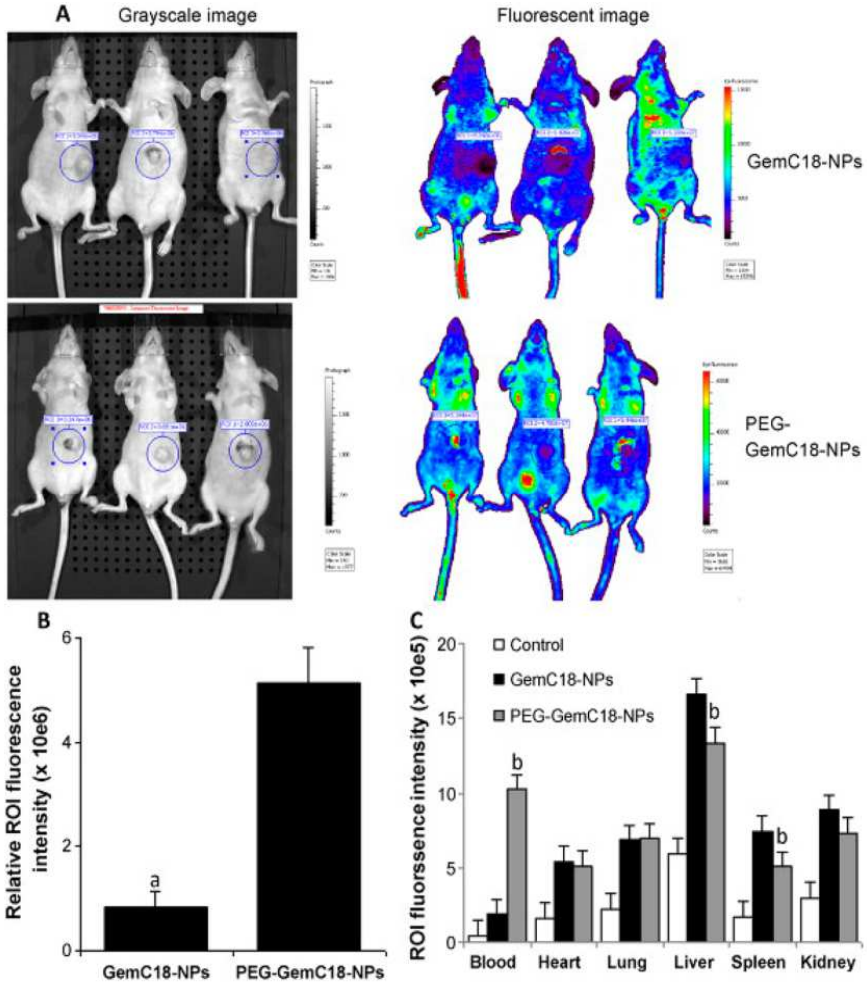

Figure 7. *In vivo* and *ex vivo* imaging of GemC18-NPs and PEG-GemC18-NPs. (A) IVIS images of athymic mice 24 h after injection of fluorescein-labeled GemC18-NPs or PEG-GemC18-NPs. (B) Relative fluorescence intensity values in BxPC-3 tumors (circular ROI in A). [a]p = 0.0006, GemC18-NPs vs PEG-GemC18-NPs. (C) Tissue distribution of fluorescein-labeled GemC18-NPs and PEG-GemC18-NPs 24 h after injection. [b]GemC18-NPs vs PEG-GemC18-NPs, p = 0.003, 0.021, and 0.002 for blood, liver, and spleen, respectively.[93]

growth and an accumulation of the product in the tumor periphery was observed using T_2-weighted imaging in magnetic resonance imaging.

While the mechanism of entry and metabolization of gemcitabine into cells is known, the cellular uptake mechanism of Sq-gemcitabine, its subcellular localization, and its metabolization pathway have only been studied recently. An *in vitro* passive entry in cancer cells (MCF-7: human breast adenocarcinoma) and a preferential accumulation in endoplasmic reticulum, thanks to the high lipophilic level of squalene, were observed.[76] This passive input may explain the efficacy of Sq-gemctiabine on cell lines deficient in active transporters.[72]

In addition to storage, a gradual cleavage of Sq-gemcitabine in native and active form also explains his efficiency. Cathepsin B, a lysosomal enzyme often overexpressed in cancer cells,[77,78] was shown to be responsible for the amidic-linkage degradation of this nanosystem inside the cells. The role of cathepsin B and D in the cleavage of the Sq-gemcitabine has been shown, increasing half-life in blood from 1.5 h to 8 h, for native gemcitabine and Sq-gemcitabine, respectively,[79] thus increasing its anticancer activity through its longer presence in the blood. Two important elements have contributed to the efficiency of this new drug: (i) the storage of gemcitabine in the endoplasmic reticulum have allowed it to be protected from deamination by the presence of squalene and (ii) the progressive cleavage in its native form allowed the metabolisation of the cancer compound. The concept of squalenoylation has also been applied to other nucleoside analogues.[69] Whatever the squalene binding position (heterocycle or sugar), these molecules also self-organize in water as nanoparticles of 100−200 nm. A variety of novel squalene-based prodrugs of the anticancer compound paclitaxel have been synthesized and have produced nanoparticles in water.[80] Preliminary results show a notable cytotoxicity on a murine lung carcinoma cell line (M109).

2.4. Lipophilic Prodrugs. An approach to improve the stability and cytotoxic activity of gemcitabine is to protect the amine group by forming a prodrug and by incorporating it into particles like the Sq-gemcitabine loading in liposomes. Many native gemcitabine-loaded particles have already been studied.

Liposomes, PLGA-, polycyanoacrylate-, chitosan-, or albulmin-nanoparticles, and carbon nanotubes can be cited.[81−85] In addition, the coencapsulation of gemcitabine with other anticancer drugs inside a particle to obtain a synergistic effect has been achieved.[86] Nanoparticles have the advantages of: high stability, high carrier capacity, incorporation of hydrophobic and hydrophilic compounds, and being injectable through various routes of administration. Encapsulation improves the cytotoxic activity of the drug with protection against metabolic inactivation.[87] In addition, extended circulation in the blood by the addition of PEG on the surface of nanocarriers and an active targeting by grafting peptides or antibodies to the shell of nanocarriers result in sustained exposure to tumor cells and enhanced efficacy.[88,89]

In 1998, Eli Lilly patented the synthesis of lipophilic gemcitabine. To protect against the deamination of gemcitabine, it was proposed to covalently link the amino group in position 4 with saturated and monounsaturated, long-chain C18 and C20. The results showed better cytotoxicity of lipophilic derivatives in comparison to native gemcitabine. A few years later, the synthesis of a series of 4-(*N*)-acyl derivative prodrugs of gemcitabine was carried out, first to prevent diffusion through liposome bilayers and later to be encapsulated into other particles.[90] Tokunaga et al. improved metabolic stability with the synthesis of a series of prodrugs of gemcitabine, increasing lipophilicity, by linking the 4-(*N*)-position with valeroyl, heptanoyl, lauroyl, and stearoyl derivatives (Figure 2G) and encapsulated them into liposomes.[91] Liposomal formulations containing these lipophilic prodrugs of gemcitabine increased the drug entrapment efficacy with respect to conventional liposomes, but their encapsulation efficiency (EE) closely depended on the length of the 4-(*N*)-acyl chain, the phospholipids, and the presence of cholesterol. Better results were obtained by incorporating 4-(*N*)-lauroyl-gemcitabine (GemC12) and 4-(*N*)-stearoyl-gemcitabine (GemC18) in liposomes composed by DSPC/DSPG 9:1 (EE of 94.4 ± 7.9% and 97.7 ± 2.3%, respectively). Native gemcitabine is well-known to rapidly convert to inactive metabolite by cytidine deaminase which is widely distributed in plasma, but C12 and C18 derivatives are both stable in plasma. After 24 h, more than 60% of unmodified prodrugs were still present, with GemC12 and GemC18 derivatives, so that after 8 h of incubation in plasma, only 40% of unmodified drug was present with native gemcitabine. pH stability was obtained in the pH range 4−9, which confirms the stable amide linkage. *In vitro* studies have shown that cytotoxicity of free or encapsulated GemC12 and GemC18 derivatives were 2- and 7-fold (in KB and HT-29 cells line, respectively) greater than that of native gemcitabine. Encapsulation of the C18 derivatives into liposomes produced an increase of plasma availability: the AUC was 50 times higher than for native gemcitabine, resulting in the increased accumulation in tumor cells and a high level of antitumoral efficacy in mice grafted with HT-29 and KB 396p cells.[92]

The feasibility of adding GemC18 into other particles to overcome gemcitabine resistance in cancer cells has been evaluated recently in different studies.[93−95] GemC18 was incorporated into lipid nanoparticles (NPs) engineered from lecithin/glycerol monostearate-in-water emulsions.[93] *In vitro* studies were performed with a deficient hENT1 cell line (CCRF-CEM-AraC-8C).[94] Native gemcitabine was not able to enter the cells efficiently, but the GemC18-NPs were able to efficiently deliver the stearoyl gemcitabine into cells by endocytosis and caused apoptosis via caspase-3 activation. Thus in the hENT1 deficient cell line, the GemC18-NPs were 15-fold more cytotoxic than gemcitabine. A second resistant cancer cell line, TC-1-GR, that overexpressed ribonucleotide reductase subunit M1 (RRM1), was tested *in vitro* and *in vivo*. In both cases treatment with GemC18-NPs efficiently inhibited the growth of cancer cells.[96]

PEGylated nanoparticles were also formulated and evaluated *in vitro* and *in vivo* with a pancreatic cancer cell line, BxPc-3.[93] *In vitro*, GemC18-NPs and PEG- GemC18-NPs were less cytotoxic than native gemcitabine, and the addition of PEG did not show any difference in toxicity. However *in vivo*, GemC18-NPs and PEG- GemC18-NPs were more efficient than gemcitabine in controlling the growth of tumors. The *in vitro* decrease in cytotoxicity was explained by a longer uptake into the cell of the particles (by endocytosis), then a gradual release, and finally hydrolysis of the GemC18. This explains a lower cytotoxicity level compared to free gemcitabine with an equivalent incubation time. *In vivo*, PEG-GemC18-NPs significantly increased the accumulation of nanoparticles in the tumors (6.3-fold) and blood circulation (5.3-fold after 24 h) (Figure 7A and B). The addition of PEG also caused a decrease in the accumulation of nanoparticles in the reticulo endothelial system such as the liver and spleen (Figure 7C). Despite an increase in circulation time and tumor accumulation, the PEG-GemC18-NPs did not significantly show different antitumor activities with GemC18-NPs.

In a recent study, the active targeting of nanoparticles has been tested to increase the antitumor effect of the particles. For this, the epithelial growth factor (EGF) was conjugated to the particle surface to target the epidermal growth factor receptor (EGFR).[95] Elevated levels of the EGFR, a growth-factor-receptor tyrosine kinase, was identified as a common component of multiple cancer types and appeared to promote solid tumor growth. The EGFR was found to act as a strong prognostic indicator in head and neck, ovarian, cervical, bladder, and esophageal cancer.[97] The EGFR is overexpressed in 80% of nonsmall cell lung cancer (NSCLC),[98] 80−100% of human head and neck cancer cells, 14−91% of human breast cancer cells, and 30−50% of human pancreatic cancer cells.[95] The EGFR is an important anticancer therapy target that is applicable to many cancer types.[99] Anti-EGFR antibodies and EGF have been conjugated onto liposomes, lipid nanoparticles, chitosan particles, and magnetic particles to target cancer cells overexpressing EGFR and the delivery of anticancer drugs or siRNA. *In vitro* uptake and cytotoxicity of EGF-GemC18-NPs realized with different human breast adenocarcinoma cell lines showed a correlation between EGFR density on the cell surface and cell uptake and toxicity.[86,98,100,101] In cell culture, EGF-GemC18-NPs uptake by tumor cells was correlated to the EGFR density, whereas the uptake of untargeted GemC18-NPs exhibited no difference among those same cell lines. The relative cytotoxicity of the EGF-conjugated GemC18-NPs to tumor cells in cell culture was correlated to EGFR expression as well, with more internalized EGF-GemC18-NPs and higher expected cytotoxicity. *In vivo* efficacy, with mice bearing MDA-MB-468 tumors (human breast adenocarcinoma cell lines overexpress EGFR with 1×10^6 receptors per cell), confirmed the effectiveness of EGF-GemC18-NPs. Mice treated with EGF-GemC18-NPs had a longer life and significantly slower tumor growth than mice treated with untargeted GemC18-NPs, due to the EGF's ability to increase the accumulation of EGF-GemC18-NPs in the tumors.

The increase of anticancer activity observed with these lipophilic derivatives compared with native gemcitabine was obtained at the expense of their solubility in aqueous media. Indeed, with their highly lipophilic properties, these compounds proved difficult to reconcile with intravenous administration, and hence encapsulation is necessary. The modification of lipophilic behavior and encapsulation could be considered a good and versatile antitumoral approach against several tumors which become less sensitive to the native drug.

3. 5′-MODIFICATIONS OF GEMCITABINE

3.1. CP-4126. To enhance cellular uptake, to prolong cell retention, and increase the half-life of gemcitabine with a less hydrophilic drug, derivatives containing a fatty acid side chain have been developed.[102,103] Gemcitabine containing a fatty acid chain at the 5′-position of the nucleoside (CP-4126) has been developed (Figure 2H). The fatty acid was esterified to the 5′-position on a sugar moiety. CP-4126 contains a fatty acid with a chain length of 18 carbon atoms and one trans-double bond (elaidic acid) in position 9. Due to its different molecular design, CP-4126 is absorbed by cancer cells independent of hENT1 levels, which improves its efficacy in tumors with low or no hENT1 expression. Altered membrane transport is also a mechanism of 1-β-D-arabinofuranosylcytosine (Ara-C) resistance. Similarly, to facilitate ara-C uptake and prolong retention in the cell, lipophilic prodrugs have been synthesized and in particular CP-4055 with the same modification as CP-4126.[10] CP-4055 showed a higher activity compared to Ara-C in several human solid tumors and leukemia xenografts. *In vitro* studies with inhibitors of nucleoside carrier-dependent transport, nitrobenzylmercaptopurine riboside and dipyridamol, strongly reduce the cellular sensitivity to Ara-C, but not to CP-4055, indicating that CP-4055 uses an alternative/additional mechanism for internalization into the cell compared with Ara-C.[104] CP-4055 or ELACYT is currently being tested in several clinical studies: phase II in acute myeloid leukemia (AML), phase I in hematology in combination with idarubicin (Idamycin), phase II in colorectal cancer, phase II in malignant melanoma in combination with sorafenib (Nexavar), and phase II in ovarian cancer.[105−107]

In vitro tests have shown that IC50 of gemcitabine increased up to 200-fold in deficient nucleoside transport cell lines, but there was no difference with CP-4126, suggesting a nucleoside transporter-independent transport in the cell of the fatty acid derivative.[108] Inside the cell, CP-4126 was localized in the membrane and the cytosolic fraction, leading to long retention after removal of the cell culture medium. This accumulation caused a slower and prolonged release of the gemcitabine from the lipophilic analogue. CP-4126 needs to be converted into gemcitabine by nonidentified esterases, releasing the fatty acid, to be phosphorylated.[109] CP-4126 is active in cells with deficient nucleoside membrane transport.[110] On the other hand, activity of native gemcitabine and CP-4126 was comparable in the cell lines without resistance, while in dCK-deficient cells both compounds were inactive. CP-4126 is, like native gemcitabine, dependent upon activation by dCK. *In vivo* studies have also shown highly effective action of gemcitabine and CP-4126 in sarcoma, lung, prostate, pancreatic, and breast cancer. In contrast to native gemcitabine which was highly toxic via the oral route, CP-4126 was administered orally with various schedules and an efficient antitumor activity (Figure 8).[111] CP-4126 was also evaluated for a potential synergy with several clinically active cytotoxic drugs such as docetaxel, oxaliplatin, and pemetrexed.[112] *In vitro* preliminary results have shown a synergistic effect in the lung cancer cell line (A549) and the colon cancer cell line (WiDR) with the combination of CP-4126 and oxaliplatin. Furthermore, the combination of docetaxel with CP-4126 induced an accumulation in the G2/M phase in the A549 cell line, but a G0/G1 phase accumulation in the WiDR cell line. Pemetrexed with CP-4126 induced in the A549 cell line an increase of cells in the G0/G1 phase and the S phase.

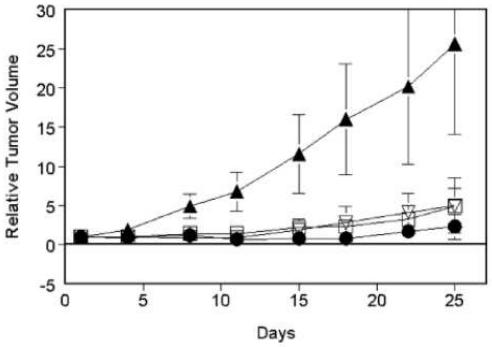

Figure 8. Antitumor efficacy of CP-4126 as an oral drug in the human colon cancer xenograft Co6044. Mice treated with saline, qd 1−5 (▲), 100 mg/kg CP-4126 (●), 20 mg/kg CP-4126 (▽), and 10 mg/kg CP-4126 (□). The curve for the optimal schedule of gemcitabine (not shown) was in between that of the control and q3d schedule (from ref 102).

CP-4126 is currently in a phase II clinical trials in solid tumor patients.[109] This trial will investigate the use of CP-4126 as a second-line treatment for advanced, metastatic pancreatic cancer in patients refractory to first line gemcitabine treatment, where the resistance mechanism is likely to be due to impaired drug entry into tumor cells. The trial is progressing in Europe, the United States, South America, and Australia, and results are anticipated for the end of 2012.

3.2. NEO6002. To enhance the uptake and efficacy by a prolonged release of gemcitabine in cancer cells, NeoPharm has synthesized a novel gemcitabine-cardiolipin conjugate.[113] This approach was to conjugate the ether analogue of synthetic cardiolipin with gemcitabine via a succinate linker. Cardiolipin (CL) is a major membrane phospholipid specifically localized in mitochondria. At the cellular level, CL has been shown to have a role in mitochondrial energy production, mitochondrial membrane dynamics, and the triggering of apoptosis.[114] The conjugate is called NEO6002 (Figure 2I).

In vitro studies showed that NEO6002 can improve the efficacy and potentially overcome NT-deficient (nucleoside transporters) gemcitabine-resistant tumors, indicating a different internalization route of NEO6002.[115] NeoPharm's studies on NEO6002 showed evidence of cytotoxicity against various cancer cell lines, including A549 (human lung); BxPC-3 (human pancreas); MX-1 (human breast); HT-29 (human colon), and P388 (murine leukemia).[116] Mice bearing or not BxPC-3 tumor xenografts were treated with NEO6002 or Gemzar and the toxicities for each were evaluated by the mortality, body weight loss, peripheral blood cell counts, and plasma levels of the liver enzymes at the end of the study. Mice treated with Gemzar for six daily 27 μmol/kg-doses were all moribund, whereas no mouse treated with NEO6002 died. This suggested that NEO6002 was less toxic at equimolar dosage when compared with Gemzar. In mice-bearing BxPC-3 tumors,

at a dose of 18 μmol/kg, NEO6002 inhibited the growth of BxPC-3 xenografts by 52%, while only 32% of tumor inhibition was achieved with Gemzar.

3.3. Phosphoramidate Gemcitabine. The obligatory phosphorylation is often the rate-limiting step in the activation process of many anticancer drugs and is therefore still one of the limiting factors for the therapeutic use of nucleoside analogues. Hence, different strategies to improve the antitumor efficacy of nucleoside analogues are being investigated.

The use of modified nucleotide prodrugs incorporating a phosphate function protecting group, has led to the selective release of the monophosphorylated nucleoside analogue.[117] This is the case of AraC grafted with an *S*-pivaloyl-2-thioethyl (tBuSATA).[118] This prodrug has been found to be more efficient than native Ara-C against L1210 10K cells, being totally dCK-deficient. This modification was tested on gemcitabine to get (i) resistance to chemical degradation, (ii) passive diffusion across a cell membrane, and (iii) release of the monophosphorylated metabolite, independent of kinase expression. These prodrugs are designed to undergo intracellular activation to generate an unstable phosphoramidate intermediate anion, followed by a spontaneous cyclization and P−N bond cleavage by water to liberate the nucleoside monophosphate.[119] In a patent from 2009, Perigaud et al. explained the synthesis of four derivatives of gemcitabine, *N*-(*n*-butylamino)-*O*-(*S*-pivaloyl-2-thioethyl)-*O*-5′-gemcitabine phosphoramidate diester (Gem-1), *N*-(isopropylamino)-*O*-(*S*-pivaloyl-2-thioethyl)-*O*-5′-gemcitabine phosphoramidate diester (Gem-2), *N*-(benzylamino)-*O*-(*S*-pivaloyl-2-thioethyl)-*O*-5′-gemcitabine phosphoramidate diester (Gem-3), and *N*-(benzylamino)-*O*-(*S*-(2,2-dimethyl-3-hydroxypropionyl)-2-thioethyl)-*O*-5′-gemcitabine phosphoramidate diester (Gem-4) (Figure 2J−M). A better cytotoxicity level was obtained in preliminary *in vitro* tests with Gem-1, Gem-2, and Gem-3 compared to the native gemcitabine in L1210 10K cell line (23.7 ± 1.2 μM, 18.3 ± 1.5 μM, 9.7 ± 9.0 μM, 36.7 ± 11.6 μM, respectively).[120]

Another approach to deliver nucleoside 5′-monophosphate intracellularly was developed by using other phosphoramidate conjugations. Many phosphoramidate prodrugs have been synthesized with an increase of biological activity in various therapeutic domains like fluoro-2′-deoxyuridine. The cytostatic activity of NUC-3073, a phosphoramidate prodrug of 5-fluoro-2′-deoxyuridine, has been found to be independent from activation by thymidine kinase and nonsensitive to degradation by phosphorolytic enzymes.[121] Recently INX-08189 has entered human clinical trials. INX-08189 is a phosphoramidate motif and a 6-*O*-methoxy based-prodrug moiety which are combined to generate lipophilic prodrugs of the guanine monophosphate nucleoside.[122] The *in vitro* and *in vivo* data indicated that INX-08189 was a highly potent inhibitor of the hepatitis C virus with a high barrier for resistance and good oral pharmacokinetic properties.[123] This approach was extended to Ara-C, and *in vitro* studies indicated that the phosphoramidate Ara-C was significantly more potent than native Ara-C against transport- and kinase-deficient CEM leukemia cell lines.[124] Finally, this approach was used with 2′-β-D-Arabinouridine (AraU), the uridine analogue of the anticancer agent AraC. Unfortunately, neither the parent compound (AraU) nor any phosphoramidate drugs showed antiviral activity, or potent inhibitory activity against any of the cancer cell lines.[125] The phophoramidate prodrug approach was extented to gemcitabine to form 5′-(2′-deoxy-2′,2′-difluorocytidyl) 5-nitrofurfuryl *N*-methyl-*N*-(4-chlorobutyl) phosphoramidate (Figure 2N). The purpose of this modification was to overcome resistance in tumors deficient in dCK by delivering intracellulary a gemcitabine 5′-monophosphate, entering the cell by passive diffusion.[126] *In vitro* tests on many cancer cell lines have shown that the prodrug is less active than native gemcitabine in wild-type cell lines but more active than native gemcitabine in dCK-deficient cell lines (AG6000 and CEM-dCK). However, after blocking the equilibrative nucleoside transport, the inhibition of tumor growth was no longer observed with the prodrug, indicating that the prodrug antitumor activity was mediated by cell entry implying equilibrative nucleoside transport.

4. CONCLUSION

Since the 1990s, gemcitabine has become the standard treatment for pancreatic cancer. Studies show a therapeutic benefit from the use of gemcitabine compared to fluorouracil and have led to the prescription of gemcitabine as a standard treatment in advanced or metastatic pancreatic cancer.[127] It is also widely used in combination for other solid cancers such as lung, bladder, ovary, or breast.

Gemcitabine undergoes a series of phosphorylations to become active and thus brings the cell into apoptosis. However, the rapid deamination after intravenous injection of gemcitabine induces the formation of its inactive metabolite (dFdU) which is then excreted, mainly in urine. Thus repeated injections and high concentrations to maintain a sufficient concentration for antitumor activity cause a number of side effects.[40] Repeated exposition does not directly lead to clinical improvement. The current clinical are relies on a balance of anticancer activity versus toxicity to normal tissue, to achieve an efficient therapeutic scheme. The short half-life is not the only drawback; numerous tumors develop resistance mechanisms: resistance by a lack of transporters and resistance by a lack of kinase required for phosphorylation and thus activation. The chemical modification of a drug is a smart solution to try to override this resistance and improve the resulting pharmacokinetic parameters.

All changes at 4-(*N*)-position with PEG, squalene, valproic acid, and linear acyl derivatives (valeroyl, heptanoyl, lauroyl, and stearoyl) have been characterized to protect the amine function and thus block CDA action. The enhanced bioavailability of prodrugs, thanks to the storage in various cytosolic fractions followed by a prolonged release, has been obtained by the addition of PEG, squalene in the 4-(*N*)-position, and elaidic acid in the 5′-position. Increased plasma availability is also observed due to the encapsulation of lipophilic GemC18 in liposomes. An independent nucleoside transporter route can be observed with PEG, squalene, elaidic acid, and derivatives, limiting the phenomenon of resistance. Finally, only the phosphoramidate function on the 5′-position provides a monophosphate gemcitabine, initiating pathway activation.

In conclusion, gemcitabine prodrugs have beneficial antitumoral effects by using independent nucleoside transport, by reducing the catabolic effect of CDA, by prolonging the release of the native or monophosphate gemcitabine, and finally by enhancing the cytotoxicity effect. Gemcitabine modification seems to be an innovative and interesting approach to treat less-sensitive cancers.

AUTHOR INFORMATION

Corresponding Author

*LUNAM University, INSERM U1066, IBS-IRIC, CHU Angers, 4 rue Larrey, F-49933 Angers, France. E-mail: guillaume.bastiat@univ-angers.fr. Tel.: +33244688531. Fax: +33244688546.

Notes

The authors declare no competing financial interest.

ACKNOWLEDGMENTS

This work has been realized in the research program LYMPHOTARG financially supported by EuroNanoMed ERA-NET 09 and by Région Pays de la Loire.

REFERENCES

(1) Carmichael, J.; Fink, U.; Russell, R. C.; Spittle, M. F.; Harris, A. L.; Spiessi, G.; Blatter, J. Phase II study of gemcitabine in patients with advanced pancreatic cancer. *Br. J. Cancer* **1996**, *73*, 101−105.

(2) Hoang, T.; Kim, K.; Jaslowski, A.; Koch, P.; Beatty, P.; McGovern, J.; Quisumbing, M.; Shapiro, G.; Witte, R.; Schiller, J. H. Phase II study of second-line gemcitabine in sensitive or refractory small cell lung cancer. *Lung Cancer* **2003**, *42*, 97−102.

(3) Yardley, D. A. Gemcitabine plus paclitaxel in breast cancer. *Semin. Oncol.* **2005**, *32* (4 Suppl 6), S14−21.

(4) Ozols, R. F. Gemcitabine and carboplatin in second-line ovarian cancer. *Semin. Oncol.* **2005**, *32* (4 Suppl 6), S4−8.

(5) Rauchwerger, D. R.; Firby, P. S.; Hedley, D. W.; Moore, M. J. Equilibrative-sensitive nucleoside transporter and its role in gemcitabine sensitivity. *Cancer Res.* **2000**, *60*, 6075−6079.

(6) Farrell, J. J.; Elsaleh, H.; Garcia, M.; Lai, R.; Ammar, A.; Regine, W. F.; Abrams, R.; Benson, A. B.; Macdonald, J.; Cass, C. E.; Dicker, A. P.; Mackey, J. R. Human equilibrative nucleoside transporter 1 levels predict response to gemcitabine in patients with pancreatic cancer. *Gastroenterology* **2009**, *136*, 187−195.

(7) Duxbury, M. S.; Ito, H.; Zinner, M. J.; Ashley, S. W.; Whang, E. E. RNA interference targeting the M2 subunit of ribonucleotide reductase enhances pancreatic adenocarcinoma chemosensitivity to gemcitabine. *Oncogene* **2004**, *23*, 1539−1548.

(8) Zacchigna, M.; Cateni, F.; Drioli, S.; Bonora, G. M. Multimeric, multifunctional derivatives of poly(ethylene glycol). *Polymers* **2011**, *3*, 1076−1090.

(9) Lundberg, B. B.; Risovic, V.; Ramaswamy, M.; Wasan, K. M. A lipophilic paclitaxel derivative incorporated in a lipid emulsion for parenteral administration. *J. Controlled Release* **2003**, *86*, 93−100.

(10) Bergman, A. M.; Kuiper, C. M.; Voorn, D. A.; Comijn, E. M.; Myhren, F.; Sandvold, M. L.; Hendriks, H. R.; Peters, G. J. Antiproliferative activity and mechanism of action of fatty acid derivatives of arabinofuranosylcytosine in leukemia and solid tumor cell lines. *Biochem. Pharmacol.* **2004**, *67*, 503−511.

(11) Bianchi, V.; Borella, S.; Calderazzo, F.; Ferraro, P.; Chieco Bianchi, L.; Reichard, P. Inhibition of ribonucleotide reductase by 2′-substituted deoxycytidine analogs: possible application in AIDS treatment. *Proc. Natl. Acad. Sci. U.S.A.* **1994**, *91*, 8403−8407.

(12) Stathis, A.; Moore, M. J. Advanced pancreatic carcinoma: current treatment and future challenges. *Nat. Rev. Clin. Oncol.* **2010**, *7*, 163−172.

(13) Eli Lilly and Company Gemzar (Gemcitabine HCL) for injection 2005. http://www.fda.gov/ohrms/dockets/ac/06/briefing/2006-4254b_11_04_KP%20GemcitabineFDAlabel42005.pdf; accessed 10-8-2012.

(14) Eli Lilly and Company Annual Report and Proxy Statement 2010. http://files.shareholder.com/downloads/LLY/2107551369x0x447905/6281D413-C258-488B-ADBE-B35289495F26/English.PDF; accessed 10-8-2012.

(15) Reid, J. M.; Qu, W.; Safgren, S. L.; Ames, M. M.; Krailo, M. D.; Seibel, N. L.; Kuttesch, J.; Holcenberg, J. Phase I trial and pharmacokinetics of gemcitabine in children with advanced solid tumors. *J. Clin. Oncol.* **2004**, *22*, 2445−2451.

(16) Abbruzzese, J. L.; Grunewald, R.; Weeks, E. A.; Gravel, D.; Adams, T.; Nowak, B.; Mineishi, S.; Tarassoff, P.; Satterlee, W.; Raber, M. N.; et al. A phase I clinical, plasma, and cellular pharmacology study of gemcitabine. *J. Clin. Oncol.* **1991**, *9*, 491−498.

(17) Griffith, D. A.; Jarvis, S. M. Nucleoside and nucleobase transport systems of mammalian cells. *Biochim. Biophys. Acta* **1996**, *1286*, 153−181.

(18) Paproski, R. J.; Ng, A. M.; Yao, S. Y.; Graham, K.; Young, J. D.; Cass, C. E. The role of human nucleoside transporters in uptake of 3′-deoxy-3′-fluorothymidine. *Mol. Pharmacol.* **2008**, *74*, 1372−1380.

(19) Ueno, H.; Kiyosawa, K.; Kaniwa, N. Pharmacogenomics of gemcitabine: can genetic studies lead to tailor-made therapy? *Br. J. Cancer.* **2007**, *97*, 145−151.

(20) Hodge, L. S.; Taub, M. E.; Tracy, T. S. Effect of its deaminated metabolite, 2′,2′-difluorodeoxyuridine, on the transport and toxicity of gemcitabine in HeLa cells. *Biochem. Pharmacol.* **2011**, *81*, 950−956.

(21) Mori, R.; Ishikawa, T.; Ichikawa, Y.; Taniguchi, K.; Matsuyama, R.; Ueda, M.; Fujii, Y.; Endo, I.; Togo, S.; Danenberg, P. V.; Shimada, H. Human equilibrative nucleoside transporter 1 is associated with the chemosensitivity of gemcitabine in human pancreatic adenocarcinoma and biliary tract carcinoma cells. *Oncol. Rep.* **2007**, *17*, 1201−1205.

(22) Giovannetti, E.; Del Tacca, M.; Mey, V.; Funel, N.; Nannizzi, S.; Ricci, S.; Orlandini, C.; Boggi, U.; Campani, D.; Del Chiaro, M.; Iannopollo, M.; Bevilacqua, G.; Mosca, F.; Danesi, R. Transcription analysis of human equilibrative nucleoside transporter-1 predicts survival in pancreas cancer patients treated with gemcitabine. *Cancer Res.* **2006**, *66*, 3928−3935.

(23) Plunkett, W.; Huang, P.; Gandhi, V. Preclinical characteristics of gemcitabine. *Anticancer Drugs* **1995**, *6*, 7−13.

(24) Barton-Burke, M. Gemcitabine: a pharmacologic and clinical overview. *Cancer Nurs.* **1999**, *22*, 176−183.

(25) Heinemann, V.; Xu, Y. Z.; Chubb, S.; Sen, A.; Hertel, L. W.; Grindey, G. B.; Plunkett, W. Cellular elimination of 2′,2′-difluorodeoxycytidine 5′-triphosphate: a mechanism of self-potentiation. *Cancer Res.* **1992**, *52*, 533−539.

(26) Jansen, R. S.; Rosing, H.; Schellens, J. H. M.; Beijnen, J. H. Deoxyuridine analog nucleotides in deoxycytidine analog treatment: secondary active metabolites? *Fundam. Clin. Pharmacol.* **2011**, *25*, 172−185.

(27) Bergman, A. M.; Pinedo, H. M.; Peters, G. J. Determinants of resistance to 2′,2′-difluorodeoxycytidine (gemcitabine). *Drug Resist. Updat.* **2002**, *5*, 19−33.

(28) Komori, S.; Osada, S.; Mori, R.; Matsui, S.; Sanada, Y.; Tomita, H.; Tokuyama, Y.; Takahashi, T.; Yamaguchi, K.; Yoshida, K. Contribution of thymidylate synthase to gemcitabine therapy for advanced pancreatic cancer. *Pancreas* **2010**, *39*, 1284−1292.

(29) Ruiz van Haperen, V. W.; Veerman, G.; Vermorken, J. B.; Peters, G. J. 2′,2′-Difluoro-deoxycytidine (gemcitabine) incorporation into RNA and DNA of tumour cell lines. *Biochem. Pharmacol.* **1993**, *46*, 762−766.

(30) Clarke, M. L.; Mackey, J. R.; Baldwin, S. A.; Young, J. D.; Cass, C. E. The role of membrane transporters in cellular resistance to anticancer nucleoside drugs. *Cancer Treat. Res.* **2002**, *112*, 27−47.

(31) Maréchal, R.; Mackey, J. R.; Lai, R.; Demetter, P.; Peeters, M.; Polus, M.; Cass, C. E.; Young, J.; Salmon, I.; Devière, J.; Van Laethem, J.-L. Human equilibrative nucleoside transporter 1 and human concentrative nucleoside transporter 3 predict survival after adjuvant gemcitabine therapy in resected pancreatic adenocarcinoma. *Clin. Cancer Res.* **2009**, *15*, 2913−2919.

(32) Santini, D.; Schiavon, G.; Vincenzi, B.; Cass, C. E.; Vasile, E.; Manazza, A. D.; Catalano, V.; Baldi, G. G.; Lai, R.; Rizzo, S.; Giacobino, A.; Chiusa, L.; Caraglia, M.; Russo, A.; Mackey, J.; Falcone, A.; Tonini, G. Human equilibrative nucleoside transporter 1 (hENT1) levels predict response to gemcitabine in patients with biliary tract cancer (BTC). *Curr. Cancer Drug Targets* **2011**, *11*, 123−129.

(33) Sebastiani, V.; Ricci, F.; Rubio-Viqueira, B.; Kulesza, P.; Yeo, C. J.; Hidalgo, M.; Klein, A.; Laheru, D.; Iacobuzio-Donahue, C. A.

Immunohistochemical and genetic evaluation of deoxycytidine kinase in pancreatic cancer: relationship to molecular mechanisms of gemcitabine resistance and survival. *Clin. Cancer Res.* **2006**, *12*, 2492−2497.
(34) Zhou, B. S.; Tsai, P.; Ker, R.; Tsai, J.; Ho, R.; Yu, J.; Shih, J.; Yen, Y. Overexpression of transfected human ribonucleotide reductase M2 subunit in human cancer cells enhances their invasive potential. *Clin. Exp. Metastasis* **1998**, *16*, 43−49.
(35) Zhou, J.; Oliveira, P.; Li, X.; Chen, Z.; Bepler, G. Modulation of the ribonucleotide reductase-antimetabolite drug interaction in cancer cell lines. *J. Nucleic Acids* **2010**, 597098.
(36) Fujita, H.; Ohuchida, K.; Mizumoto, K.; Itaba, S.; Ito, T.; Nakata, K.; Yu, J.; Kayashima, T.; Souzaki, R.; Tajiri, T.; Manabe, T.; Ohtsuka, T.; Tanaka, M. Gene expression levels as predictive markers of outcome in pancreatic cancer after gemcitabine-based adjuvant chemotherapy. *Neoplasia* **2010**, *12*, 807−817.
(37) Tolis, C.; Peters, G.; Ferreira, C. G.; Pinedo, H. M.; Giaccone, G. Cell cycle disturbances and apoptosis induced by topotecan and gemcitabine on human lung cancer cell lines. *Eur. J. Cancer* **1999**, *35*, 796−807.
(38) Costantino, C. L.; Witkiewicz, A. K.; Kuwano, Y.; Cozzitorto, J. A.; Kennedy, E. P.; Dasgupta, A.; Keen, J. C.; Yeo, C. J.; Gorospe, M.; Brody, J. R. The role of HuR in gemcitabine efficacy in pancreatic cancer: HuR-upregulates the expression of the gemcitabine metabolizing enzyme deoxycytidine kinase. *Cancer Res.* **2009**, *69*, 4567−4572.
(39) Richards, N. G.; Rittenhouse, D. W.; Freydin, B.; Cozzitorto, J. A.; Grenda, D.; Rui, H.; Gonye, G.; Kennedy, E. P.; Yeo, C. J.; Brody, J. R.; Witkiewicz, A. K. HuR status is a powerful marker for prognosis and response to gemcitabine-based chemotherapy for resected pancreatic ductal adenocarcinoma patients. *Ann. Surg.* **2010**, *252*, 499−505, Discussion: 505−506.
(40) Storniolo, A. M.; Allerheiligen, S. R.; Pearce, H. L. Preclinical, pharmacologic, and phase I studies of gemcitabine. *Semin. Oncol.* **1997**, *24* (2 Suppl 7), S7-2−7-7.
(41) Mero, A.; Clementi, C.; Veronese, F. M.; Pasut, G. Covalent conjugation of poly(ethylene glycol) to proteins and peptides: strategies and methods. *Methods Mol. Biol.* **2011**, *751*, 95−129.
(42) Pasut, G.; Veronese, F. M. State of the art in PEGylation: The great versatility achieved after forty years of research. *J. Controlled Release* **2012**, *161*, 461−472.
(43) Pasut, G.; Veronese, F. M. PEG conjugates in clinical development or use as anticancer agents: An overview. *Adv. Drug Delivery Rev.* **2009**, *61*, 1177−1188.
(44) Sawant, R. M. Polyethylene glycol (peg) as a key component of long-circulating delivery systems for therapy and imaging. *Pharm. Sci. Dissert.* **2008**, 1−107.
(45) Caliceti, P.; Veronese, F. M. Pharmacokinetic and biodistribution properties of poly(ethylene glycol)−protein conjugates. *Adv. Drug Delivery Rev.* **2003**, *55*, 1261−1277.
(46) Maeda, H.; Wu, J.; Sawa, T.; Matsumura, Y.; Hori, K. Tumor vascular permeability and the EPR effect in macromolecular therapeutics: a review. *J. Controlled Release* **2000**, *65*, 271−284.
(47) Szebeni, J. Complement activation-related pseudoallergy: A new class of drug-induced acute immune toxicity. *Toxicology* **2005**, *216*, 106−121.
(48) Liu, J.; Zahedi, P.; Zeng, F.; Allen, C. Nano-sized assemblies of a PEG-docetaxel conjugate as a formulation strategy for docetaxel. *J. Pharm. Sci.* **2008**, *97*, 3274−3290.
(49) Li, C.; Yu, D.; Inoue, T.; Yang, D. J.; Milas, L.; Hunter, N. R.; Kim, E. E.; Wallace, S. Synthesis and evaluation of water-soluble polyethylene glycol-paclitaxel conjugate as a paclitaxel prodrug. *Anticancer Drugs* **1996**, *7*, 642−648.
(50) Vandana, M.; Sahoo, S. K. Long circulation and cytotoxicity of PEGylated gemcitabine and its potential for the treatment of pancreatic cancer. *Biomaterials* **2010**, *31*, 9340−9356.
(51) Chuang, K.-H.; Wang, H.-E.; Chen, F.-M.; Tzou, S.-C.; Cheng, C.-M.; Chang, Y.-C.; Tseng, W.-L.; Shiea, J.; Lin, S.-R.; Wang, J.-Y.; Chen, B.-M.; Roffler, S. R.; Cheng, T.-L. Endocytosis of PEGylated agents enhances cancer imaging and anticancer efficacy. *Mol. Cancer Ther.* **2010**, *9*, 1903−1912.
(52) Bareford, L. M.; Swaan, P. W. Endocytic mechanisms for targeted drug delivery. *Adv. Drug Delivery Rev.* **2007**, *59*, 748−758.
(53) Pasut, G.; Canal, F.; Dalla Via, L.; Arpicco, S.; Veronese, F. M.; Schiavon, O. Antitumoral activity of PEG-gemcitabine prodrugs targeted by folic acid. *J. Controlled Release* **2008**, *127*, 239−248.
(54) Basal, E.; Eghbali-Fatourechi, G. Z.; Kalli, K. R.; Hartmann, L. C.; Goodman, K. M.; Goode, E. L.; Kamen, B. A.; Low, P. S.; Knutson, K. L. Functional folate receptor alpha is elevated in the blood of ovarian cancer patients. *PLoS ONE* **2009**, *4*, e6292.
(55) Iwakiri, S.; Sonobe, M.; Nagai, S.; Hirata, T.; Wada, H.; Miyahara, R. Expression status of folate receptor alpha is significantly correlated with prognosis in non-small-cell lung cancers. *Ann. Surg. Oncol.* **2008**, *15*, 889−899.
(56) Hartmann, L. C.; Keeney, G. L.; Lingle, W. L.; Christianson, T. J.; Varghese, B.; Hillman, D.; Oberg, A. L.; Low, P. S. Folate receptor overexpression is associated with poor outcome in breast cancer. *Int. J. Cancer* **2007**, *121*, 938−942.
(57) Shmeeda, H.; Amitay, Y.; Gorin, J.; Tzemach, D.; Mak, L.; Ogorka, J.; Kumar, S.; Zhang, J. A.; Gabizon, A. Delivery of zoledronic acid encapsulated in folate-targeted liposome results in potent in vitro cytotoxic activity on tumor cells. *J. Controlled Release* **2010**, *146*, 76−83.
(58) Yang, S.-J.; Lin, F.-H.; Tsai, K.-C.; Wei, M.-F.; Tsai, H.-M.; Wong, J.-M.; Shieh, M.-J. Folic acid-conjugated chitosan nanoparticles enhanced protoporphyrin IX accumulation in colorectal cancer cells. *Bioconjugate Chem.* **2010**, *21*, 679−689.
(59) Kaaki, K.; Herve, K.; Chiper, M.; Shkilnyy, A.; Soucé, M.; Benoit, R.; Paillard, A.; Dubois, P.; Saboungi, M.-L.; Chourpa, I. Magnetic nanocarriers of doxorubicin coated with poly(ethylene glycol) and folic acid: relation between coating structure, surface properties, colloidal stability and cancer cell targeting. *Langmuir* **2011**, *28*, 1496−1505.
(60) Schiavon, O.; Pasut, G.; Moro, S.; Orsolini, P.; Guiotto, A.; Veronese, F. M. PEG-Ara-C conjugates for controlled release. *Eur. J. Med. Chem.* **2004**, *39*, 123−133.
(61) Dauty, E.; Remy, J.-S.; Zuber, G.; Behr, J.-P. Intracellular delivery of nanometric DNA particles via the folate receptor. *Bioconjugate Chem.* **2002**, *13*, 831−839.
(62) Harris, J. M.; Chess, R. B. Effect of pegylation on pharmaceuticals. *Nat. Rev. Drug Discovery* **2003**, *2*, 214−221.
(63) Bender, D. M.; Bao, J.; Dantzig, A. H.; Diseroad, W. D.; Law, K. L.; Magnus, N. A.; Peterson, J. A.; Perkins, E. J.; Pu, Y. J.; Reutzel-Edens, S. M.; Remick, D. M.; Starling, J. J.; Stephenson, G. A.; Vaid, R. K.; Zhang, D.; McCarthy, J. R. Synthesis, crystallization, and biological evaluation of an orally active prodrug of gemcitabine. *J. Med. Chem.* **2009**, *52*, 6958−6961.
(64) Koolen, S. L.; Witteveen, P. O.; Jansen, R. S.; Langenberg, M. H.; Kronemeijer, R. H.; Nol, A.; Garcia-Ribas, I.; Callies, S.; Benhadji, K. A.; Slapak, C. A.; Beijnen, J. H.; Voest, E. E.; Schellens, J. H. Phase I study of oral gemcitabine prodrug (LY2334737) alone and in combination with erlotinib in patients with advanced solid tumors. *Clin. Cancer Res.* **2011**, *17*, 6071−6082.
(65) Huang, Z.-R.; Lin, Y.-K.; Fang, J.-Y. Biological and pharmacological activities of squalene and related compounds: potential uses in cosmetic dermatology. *Molecules* **2009**, *14*, 540−554.
(66) Kelly, G. S. Squalene and its potential clinical uses. *Altern. Med. Rev.* **1999**, *4*, 29−36.
(67) Newmark, H. L. Squalene, olive oil, and cancer risk: a review and hypothesis. *Cancer Epidemiol. Biomarkers Prev.* **1997**, *6*, 1101−1103.
(68) Couvreur, P.; Stella, B.; Reddy, L. H.; Hillaireau, H.; Dubernet, C.; Desmaële, D.; Lepêtre-Mouelhi, S.; Rocco, F.; Dereuddre-Bosquet, N.; Clayette, P.; Rosilio, V.; Marsaud, V.; Renoir, J.-M.; Cattel, L. Squalenoyl nanomedicines as potential therapeutics. *Nano Lett.* **2006**, *6*, 2544−2548.

(69) Desmaële, D.; Gref, R.; Couvreur, P. Squalenoylation: A generic platform for nanoparticular drug delivery. *J. Controlled Release* **2012**, *161*, 609−618.
(70) Jordheim, L. P.; Cros, E.; Gouy, M.-H.; Galmarini, C. M.; Peyrottes, S.; Mackey, J.; Perigaud, C.; Dumontet, C. Characterization of a gemcitabine-resistant murine leukemic cell line: reversion on *in vitro* resistance by a mononucleotide prodrug. *Clin. Cancer Res.* **2004**, *10*, 5614−5621.
(71) Gourdeau, H.; Clarke, M. L.; Ouellet, F.; Mowles, D.; Selner, M.; Richard, A.; Lee, N.; Mackey, J. R.; Young, J. D.; Jolivet, J.; Lafrenière, R. G.; Cass, C. E. Mechanisms of uptake and resistance to troxacitabine, a novel deoxycytidine nucleoside analogue, in human leukemic and solid tumor cell lines. *Cancer Res.* **2001**, *61*, 7217−7224.
(72) Reddy, L. H.; Dubernet, C.; Mouelhi, S. L.; Marque, P. E.; Desmaële, D.; Couvreur, P. A new nanomedicine of gemcitabine displays enhanced anticancer activity in sensitive and resistant leukemia types. *J. Controlled Release* **2007**, *124*, 20−27.
(73) Réjiba, S.; Reddy, L. H.; Bigand, C.; Parmentier, C.; Couvreur, P.; Hajri, A. Squalenoyl gemcitabine nanomedicine overcomes the low efficacy of gemcitabine therapy in pancreatic cancer. *Nanomedicine* **2011**, *7*, 841−849.
(74) Pili, B.; Reddy, L. H.; Bourgaux, C.; Lepêtre-Mouelhi, S.; Desmaële, D.; Couvreur, P. Liposomal squalenoyl-gemcitabine: formulation, characterization and anticancer activity evaluation. *Nanoscale* **2010**, *2*, 1521−1526.
(75) Arias, J. L.; Reddy, L. H.; Othman, M.; Gillet, B.; Desmaële, D.; Zouhiri, F.; Dosio, F.; Gref, R.; Couvreur, P. Squalene based nanocomposites: a new platform for the design of multifunctional pharmaceutical theragnostics. *ACS Nano* **2011**, *5*, 1513−1521.
(76) Bildstein, L.; Dubernet, C.; Marsaud, V.; Chacun, H.; Nicolas, V.; Gueutin, C.; Sarasin, A.; Bénech, H.; Lepêtre-Mouelhi, S.; Desmaële, D.; Couvreur, P. Transmembrane diffusion of gemcitabine by a nanoparticulate squalenoyl prodrug: An original drug delivery pathway. *J. Controlled Release* **2010**, *147*, 163−170.
(77) Podgorski, I.; Sloane, B. F. Cathepsin B and its role(s) in cancer progression. *Biochem. Soc. Symp.* **2003**, *70*, 263−276.
(78) Yang, Z.; Cox, J. L. Cathepsin L increases invasion and migration of B16 melanoma. *Cancer Cell Int.* **2007**, *7*, 8.
(79) Celia, C.; Cosco, D.; Paolino, D.; Fresta, M. Gemcitabine-loaded innovative nanocarriers vs GEMZAR: Biodistribution, pharmacokinetic features and *in vivo* antitumor activity. *Expert Opin. Drug Deliv.* **2011**, *8*, 1609−1629.
(80) Dosio, F.; Reddy, L. H.; Ferrero, A.; Stella, B.; Cattel, L.; Couvreur, P. Novel nanoassemblies composed of squalenoyl−paclitaxel derivatives: synthesis, characterization, and biological evaluation. *Bioconjugate Chem.* **2011**, *21*, 1349−1361.
(81) Jantscheff, P.; Ziroli, V.; Esser, N.; Graeser, R.; Kluth, J.; Sukolinskaya, A.; Taylor, L. A.; Unger, C. Massing, U. Anti-metastatic effects of liposomal gemcitabine in a human orthotopic LNCaP prostate cancer xenograft model. *Clin. Exp. Metastasis* **2009**, *26*, 981−992.
(82) Aggarwal, S.; Yadav, S.; Gupta, S. EGFR targeted PLGA nanoparticles using gemcitabine for treatment of pancreatic cancer. *J. Biomed. Nanotechnol.* **2011**, *7*, 137−138.
(83) Yang, F.; Jin, C.; Yang, D.; Jiang, Y.; Li, J.; Di, Y.; Hu, J.; Wang, C.; Ni, Q.; Fu, D. Magnetic functionalised carbon nanotubes as drug vehicles for cancer lymph node metastasis treatment. *Eur. J. Cancer* **2011**, *47*, 1873−1882.
(84) Ventura, C. A.; Cannavà, C.; Stancanelli, R.; Paolino, D.; Cosco, D.; La Mantia, A.; Pignatello, R.; Tommasini, S. Gemcitabine-loaded chitosan microspheres. Characterization and biological *in vitro* evaluation. *Biomed. Microdevices* **2011**, *13*, 799−807.
(85) Stella, B.; Arpicco, S.; Rocco, F.; Marsaud, V.; Renoir, J. M.; Cattel, L.; Couvreur, P. Encapsulation of gemcitabine lipophilic derivatives into polycyanoacrylate nanospheres and nanocapsules. *Int. J. Pharmaceutics* **2007**, *344*, 71−77.
(86) Arya, G.; Vandana, M.; Acharya, S.; Sahoo, S. K. Enhanced antiproliferative activity of Herceptin (HER2)-conjugated gemcitabine-loaded chitosan nanoparticle in pancreatic cancer therapy. *Nanomedicine* **2011**, *7*, 859−870.
(87) Cattel, L.; Ceruti, M.; Dosio, F. From conventional to stealth liposomes: a new frontier in cancer chemotherapy. *Tumori* **2003**, *89*, 237−249.
(88) Tardi, P.; Choice, E.; Masin, D.; Redelmeier, T.; Bally, M.; Madden, T. D. Liposomal Encapsulation of topotecan enhances anticancer efficacy in murine and human xenograft models. *Cancer Res.* **2000**, *60*, 3389−3393.
(89) Milla, P.; Dosio, F.; Cattel, L. PEGylation of proteins and liposomes: a powerful and flexible strategy to improve the drug delivery. *Curr. Drug Metab.* **2012**, *13*, 105−109.
(90) Immordino, M. L.; Brusa, P.; Rocco, F.; Arpicco, S.; Ceruti, M.; Cattel, L. Preparation, characterization, cytotoxicity and pharmacokinetics of liposomes containing lipophilic gemcitabine prodrugs. *J. Controlled Release* **2004**, *100*, 331−346.
(91) Tokunaga, Y.; Iwasa, T.; Fujisaki, J.; Sawai, S.; Kagayama, A. Liposomal sustained-release delivery systems for intravenous injection. IV. Antitumor activity of newly synthesized lipophilic 1-beta-D-arabinofuranosylcytosine prodrug-bearing liposomes. *Chem. Pharm. Bull. (Tokyo)* **1988**, *36*, 3574−3583.
(92) Brusa, P.; Immordino, M. L.; Rocco, F.; Cattel, L. Antitumor activity and pharmacokinetics of liposomes containing lipophilic gemcitabine prodrugs. *Anticancer Res.* **2007**, *27*, 195−199.
(93) Sloat, B. R.; Sandoval, M. A.; Li, D.; Chung, W.-G.; Lansakara-P, D. S.; Proteau, P. J.; Kiguchi, K.; DiGiovanni, J.; Cui, Z. *In vitro* and *in vivo* anti-tumor activities of a gemcitabine derivative carried by nanoparticles. *Int. J. Pharmaceutics* **2011**, *409*, 278−288.
(94) Chung, W.-G.; Sandoval, M. A.; Sloat, B. R.; Lansakara-P, D. S.; Cui, Z. Stearoyl gemcitabine nanoparticles overcome resistance related to the over-expression of ribonucleotide reductase subunit M1. *J. Controlled Release* **2012**, *157*, 132−140.
(95) Sandoval, M. A.; Sloat, B. R.; Lansakara-P, D. S.; Kumar, A.; Rodriguez, B. L.; Kiguchi, K.; DiGiovanni, J.; Cui, Z. EGFR-targeted stearoyl gemcitabine nanoparticles show enhanced anti-tumor activity. *J. Controlled Release* **2012**, *157*, 287−296.
(96) Batrakova, E. V. Sensitizing of gemcitabine-resistant human leukemia cells by stearoyl gemcitabine nanoparticles. *Nanomedicine (London)* **2011**, *6*, 1491−1492.
(97) Nicholson, R. I.; Gee, J. M.; Harper, M. E. EGFR and cancer prognosis. *Eur. J. Cancer* **2001**, *37*, S9−S15.
(98) Yokoyama, T.; Tam, J.; Kuroda, S.; Scott, A. W.; Aaron, J.; Larson, T.; Shanker, M.; Correa, A. M.; Kondo, S.; Roth, J. A.; Sokolov, K.; Ramesh, R. EGFR-targeted hybrid plasmonic magnetic nanoparticles synergistically induce autophagy and apoptosis in non-small cell lung cancer cells. *PLoS ONE* **2011**, *6*, e25507.
(99) Song, S.; Liu, D.; Peng, J.; Sun, Y.; Li, Z.; Gu, J.-R.; Xu, Y. Peptide ligand-mediated liposome distribution and targeting to EGFR expressing tumor *in vivo*. *Int. J. Pharmaceutics* **2008**, *363*, 155−161.
(100) Gao, J.; Yu, Y.; Zhang, Y.; Song, J.; Chen, H.; Li, W.; Qian, W.; Deng, L.; Kou, G.; Chen, J.; Guo, Y. EGFR-specific PEGylated immunoliposomes for active siRNA delivery in hepatocellular carcinoma. *Biomaterials* **2012**, *33*, 270−282.
(101) Benhabbour, S. R.; Luft, J. C.; Kim, D.; Jain, A.; Wadhwa, S.; Parrott, M. C.; Liu, R.; DeSimone, J. M.; Mumper, R. J. *In vitro* and *in vivo* assessment of targeting lipid-based nanoparticles to the epidermal growth factor-receptor (EGFR) using a novel Heptameric ZEGFR domain. *J. Controlled Release* **2011**, *158*, 63−71.
(102) Bergman, A. M.; Adema, A. D.; Balzarini, J.; Bruheim, S.; Fichtner, I.; Noordhuis, P.; Fodstad, O.; Myhren, F.; Sandvold, M. L.; Hendriks, H. R.; Peters, G. J. Antiproliferative activity, mechanism of action and oral antitumor activity of CP-4126, a fatty acid derivative of gemcitabine, in *in vitro* and *in vivo* tumor models. *Invest. New Drugs* **2011**, *29*, 456−466.
(103) Adema, A. D.; Bijnsdorp, I. V.; Sandvold, M. L.; Verheul, H. M.; Peters, G. J. Innovations and opportunities to improve conventional (deoxy)nucleoside and fluoropyrimidine analogs in cancer. *Curr. Med. Chem.* **2009**, *16*, 4632−4643.

(104) Breistøl, K.; Balzarini, J.; Sandvold, M. L.; Myhren, F.; Martinsen, M.; De Clercq, E.; Fodstad, O. Antitumor activity of P-4055 (elaidic acid-cytarabine) compared to cytarabine in metastatic and s.c. human tumor xenograft models. *Cancer Res.* **1999**, *59*, 2944−2949.
(105) ELACYT Clinical Update - Clavis Pharma. http://www.clavispharma.com/news-events/2008-press-releases/elacyt-clinical-update (accessed Jan 4, 2012).
(106) Dueland, S.; Aamdal, S.; Lind, M. J.; Thomas, H.; Sandvold, M. L.; Gaullier, J.-M.; Rasch, W. Intravenous administration of CP-4055 (ELACYT) in patients with solid tumours. A Phase I study. *Acta Oncol.* **2009**, *48*, 137−145.
(107) Pignata, S.; Amant, F.; Scambia, G.; Sorio, R.; Breda, E.; Rasch, W.; Hernes, K.; Pisano, C.; Leunen, K.; Lorusso, D.; Cannella, L.; Vergote, I. A phase I-II study of elacytarabine (CP-4055) in the treatment of patients with ovarian cancer resistant or refractory to platinum therapy. *Cancer Chemother. Pharmacol.* **2011**, *68*, 1347−1353.
(108) Adema, A. D.; Smid, K.; Losekoot, N.; Honeywell, R. J.; Verheul, H. M.; Myhren, F.; Sandvold, M. L.; Peters, G. J. Metabolism and accumulation of the lipophilic deoxynucleoside analogs elacytarabine and CP-4126. *Invest. New Drugs* **2012**, *30*, 1908−1916.
(109) Galmarini, C. M.; Myhren, F.; Sandvold, M. L. CP-4055 and CP-4126 are active in ara-C and gemcitabine-resistant lymphoma cell lines. *Br. J. Hamaetol.* **2009**, *144*, 273−275.
(110) Sandvold, M. L.; Galmarini, C.; Myhren, F.; Peters, G. The activity of the lipophilic nucleoside derivatives elacytarabine and CP-4126 in a panel of tumor cell lines resistant to nucleoside analogues. *Nucleosides Nucleotides Nucleic Acids* **2010**, *29*, 386−393.
(111) Gagnadoux, F.; Le Pape, A.; Urban, T.; Montharu, J.; Vecellio, L.; Dubus, J.-C.; Leblond, V.; Diot, P.; Grimbert, D.; Racineux, J.-L.; Lemarié, E. Safety of pulmonary administration of gemcitabine in rats. *J. Aerosol Med.* **2005**, *18*, 198−206.
(112) Adema, A. D.; Laan, A. C.; Myhren, F.; Fichtner, I.; Verheul, H. M.; Sandvold, M. L.; Peters, G. J. Cell cycle effects of fatty acid derivatives of cytarabine, CP-4055, and of gemcitabine, CP-4126, as basis for the interaction with oxaliplatin and docetaxel. *Int. J. Oncol.* **2010**, *36*, 285−294.
(113) Ali, S. M.; Khan, A. R.; Ahmad, M. U.; Chen, P.; Sheikh, S.; Ahmad, I. Synthesis and biological evaluation of gemcitabine-lipid conjugate (NEO6002). *Bioorg. Med. Chem. Lett.* **2005**, *15*, 2571−2574.
(114) Sakamoto, T.; Inoue, T.; Otomo, Y.; Yokomori, N.; Ohno, M.; Arai, H.; Nakagawa, Y. Deficiency of cardiolipin synthase causes abnormal mitochondrial function and morphology in germ cells of Caenorhabditis elegans. *J. Biol. Chem.* **2012**, *287*, 4590−4601.
(115) Chien, P.-Y.; Khan, A. R.; Miller, B.; Sheikh, S.; Ali, S. M.; Ahmad, M. U.; Ahmad, I. A novel gemcitabine-cardiolipin conjugate induced cytotoxicity in cancer cells through an equilibrative nucleoside transporter-independent pathway. *AACR Meeting Abstracts* **2005**.
(116) Chen, P.; Chien, P.-Y.; Khan, A. R.; Sheikh, S.; Ali, S. M.; Ahmad, M. U.; Ahmad, I. *In-vitro and in-vivo* anti-cancer activity of a novel gemcitabine-cardiolipin conjugate. *Anticancer Drugs* **2006**, *17*, 53−61.
(117) Galmarini, C. M.; Warren, G.; Senanayake, M. T.; Vinogradov, S. V. Efficient overcoming of drug resistance to anticancer nucleoside analogs by nanodelivery of active phosphorylated drugs. *Int. J. Pharmaceutics* **2010**, *395*, 281−289.
(118) Bazzanini, R.; Manfredini, S.; Durini, E.; Gröschel, B.; Cinatl, J.; Balzarini, J.; De Clercq, E.; Imbach, J. L.; Périgaud, C.; Gosselin, G. Prodrugs of Ara-CMP and Ara-AMP with a S-acyl-2-thioethyl (SATE) biolabile phosphate protecting group: synthesis and biological evaluation. *Nucleosides Nucleotides* **1999**, *18*, 971−972.
(119) Tobias, S. C.; Borch, R. F. Synthesis and biological studies of novel nucleoside phosphoramidate prodrugs. *J. Med. Chem.* **2001**, *44*, 4475−4480.
(120) Perigaud, C.; Peyrottes, S.; Dumontet, C. Gemcitabine phosphoester prodrugs as anticancer agents. Patent Application WO/2009/053654, 2009.
(121) Vande Voorde, J.; Liekens, S.; McGuigan, C.; Murziani, P. G.; Slusarczyk, M.; Balzarini, J. The cytostatic activity of NUC-3073, a phosphoramidate prodrug of 5-fluoro-2′-deoxyuridine, is independent of activation by thymidine kinase and insensitive to degradation by phosphorolytic enzymes. *Biochem. Pharmacol.* **2011**, *82*, 441−452.
(122) McGuigan, C.; Madela, K.; Aljarah, M.; Gilles, A.; Brancale, A.; Zonta, N.; Chamberlain, S.; Vernachio, J.; Hutchins, J.; Hall, A.; Ames, B.; Gorovits, E.; Ganguly, B.; Kolykhalov, A.; Wang, J.; Muhammad, J.; Patti, J. M.; Henson, G. Design, synthesis and evaluation of a novel double pro-drug: INX-08189. A new clinical candidate for hepatitis C virus. *Bioorg. Med. Chem. Lett.* **2010**, *20*, 4850−4854.
(123) Vernachio, J. H.; Bleiman, B.; Bryant, K. D.; Chamberlain, S.; Hunley, D.; Hutchins, J.; Ames, B.; Gorovits, E.; Ganguly, B.; Hall, A.; Kolykhalov, A.; Liu, Y.; Muhammad, J.; Raja, N.; Walters, C. R.; Wang, J.; Williams, K.; Patti, J. M.; Henson, G.; Madela, K.; Aljarah, M.; Gilles, A. McGuigan, C. INX-08189, a phosphoramidate prodrug of 6-O-methyl-2′-C-methyl guanosine, is a potent inhibitor of hepatitis C virus replication with excellent pharmacokinetic and pharmacodynamic properties. *Antimicrob. Agents Chemother.* **2011**, *55*, 1843−1851.
(124) Tobias, S. C.; Borch, R. F. Synthesis and biological evaluation of a cytarabine phosphoramidate prodrug. *Mol. Pharmaceutics* **2004**, *1*, 112−116.
(125) Mehellou, Y.; Valente, R.; Mottram, H.; Walsby, E.; Mills, K. I.; Balzarini, J.; McGuigan, C. Phosphoramidates of 2′-*β*-d-arabinouridine (AraU) as phosphate prodrugs; design, synthesis, *in vitro* activity and metabolism. *Bioorg. Med. Chem.* **2010**, *18*, 2439−2446.
(126) Wu, W.; Sigmond, J.; Peters, G. J.; Borch, R. F. Synthesis and biological activity of a gemcitabine phosphoramidate prodrug. *J. Med. Chem.* **2007**, *50*, 3743−3746.
(127) Burris, H. A., III; Moore, M. J.; Andersen, J.; Green, M. R.; Rothenberg, M. L.; Modiano, M. R.; Cripps, M. C.; Portenoy, R. K.; Storniolo, A. M.; Tarassoff, P.; Nelson, R.; Dorr, F. A.; Stephens, C. D.; Von Hoff, D. D. Improvements in survival and clinical benefit with gemcitabine as first-line therapy for patients with advanced pancreas cancer: a randomized trial. *J. Clin. Oncol.* **1997**, *15*, 2403−2413.

Concept, caractérisation et biodistribution

Publication N°1

Avant-propos

Une forme lipophile de la gemcitabine (modifiée par une chaîne aliphatique en C_{12}), un agent anticancéreux, a été encapsulée dans des nanocapsules lipidiques (LNCs), en utilisant un procédé d'inversion de phase couramment utilisé dans notre laboratoire depuis une dizaine d'années. Ce principe actif, modifié ou non, n'a jamais été testé avec cette forme pharmaceutique et il nous semblait intéressant de tester son potentiel thérapeutique. De manière surprenante, un gel s'est formé spontanément à la fin du procédé de formulation. Les propriétés viscoélastiques du gel ont été mesurées en fonction des concentrations en LNCs et en gemcitabine modifiée. Les études de tensiométrie de surface ont montré que la gemcitabine modifiée est localisée à l'interface huile/eau des LNCs, avec la tête de la gemcitabine exposée vers la phase aqueuse. Cette disposition permet l'interaction entre LNCs via des liaisons hydrogène entre les groupements polaires de la gemcitabine modifiée pour aboutir à une structure gélifiée, sans matrice polymère, similaire à un « collier de perles ». La dissolution de ce gel physique permet de casser les interactions inter-nanoparticules et obtenir des LNCs chargées en gemcitabine modifiée en suspension dans l'eau, sans aucun résidu. Ces nanoparticules présentent une activité cytotoxique intéressante comparativement à la gemcitabine native sur plusieurs lignées cancéreuses. Ainsi, une nouvelle méthode d'obtention d'un hydrogel de nanoparticules a été rapportée avec une action clé du principe actif encapsulé dans les nanoparticules. L'injection du gel par des seringues a été vérifiée avec succès et ouvre plusieurs perspectives à l'utilisation de ce nouveau système (injection intratumorale ou sous-cutanée). Cette publication sera soumise prochainement dans le journal « *Acta Biomaterialia* »

Gemcitabine-loaded lipid nanocapsule hydrogel: when the drug is a key player of the nanomedicine structure

Elodie MOYSAN [a,b], Yolanda GONZÁLEZ-FERNÁNDEZ [a,b] Nolwenn LAUTRAM [a,b], Jérôme BÉJAUD [a,b], Guillaume BASTIAT [a,b,*] and Jean-Pierre BENOIT [a,b]

a) LUNAM Université – Micro et Nanomédecines Biomimétiques, F-49933 Angers, France
b) INSERM – U1066 IBS-CHU, F-49933 Angers, France ;

*) Corresponding author: guillaume.bastiat@univ-anger.fr, phone number +33(0)2 44 68 85 31, Fax +33() 02 44 68 85 46, Université d'Angers – UMR_S1066 (MINT), IBS-CHU Angers, 4 rue Larrey, 49933 Angers Cédex 9

Abstract

A new method to form a nanoparticle-structured hydrogel was reported based on the loaded drug in the nanoparticles to form the solid structure. A lipophilic form of gemcitabine (lauroyl modification), an anti-cancer drug, was encapsulated in lipid nanocapsules (LNC), using a phase inversion temperature process. A gel was spontaneously formed, depending on LNC concentration and drug loading, with total entrapment efficiency and the rheological properties of the gel were assessed. Physical studies (surface tension measurements) showed that modified Gemcitabine was localized at the oil/water interface of the LNC, with the gemcitabine moieties of the prodrug exposed to the water phase. This particular assembly promoted the inter-LNC interaction via hydrogen bonds between gemcitabine moieties to lead to a LNC gel structure in water, without matrix, like a pearl necklace. The dilution of the physical gel gave gemcitabine-loaded LNC suspension in water and these nanoparticles presented a cytotoxic activity in regards of various cancer cell lines, higher than the native drug. Finally, syringeability of the formulation was successfully tested and perspectives of use as a nanomedicine depot (intratumoral or subcutaneous injection) could be envisaged.

Keywords: Physical hydrogel, gemcitabine prodrug, lipid nanocapsules, cancer, nanomedicine, syringeability

1. Introduction

Gemcitabine, a nucleoside analogue of cytidine, acts against a wide range of solid tumors such as pancreatic, non-small cell lung, breast and ovarian cancers as a single agent or in combination [1]. Its action mechanisms are based on intracellular phosphorylation into its active phosphate derivative (by deoxycytidine kinase; dCK) after an entry into the cells by nucleoside transporters. Analogy with deoxycytidine triphosphate allows gemcitabine to be incorporated into DNA during replication, thus inhibiting chain elongation of DNA and causing cell death by apoptosis [2]. However, tumor cells often acquire resistance during gemcitabine treatment [3]. A lower expression of nucleoside transporters and dCK are correlated with low gemcitabine cytotoxicity [4] and [5]. Another drawback is its rapid deamination (cytidine deaminase action) to an inactive form in the blood, liver, kidney and other tissues [6].

To increase its therapeutic levels, gemcitabine is administered at high dose (1000mg/m²) causing sides effects [1]. To improve metabolic stability and cytotoxic activity of gemcitabine and to limit the phenomena of resistance (lack of transporters [7], alteration of dCK [8], overexpression of ribonucleotide reductase [9], etc), many alternatives have emerged, such as the synthesis of prodrugs [10], [11], [12] and [13] and the encapsulation of these prodrugs [1] and [14]. Couvreur's team developed squalenoyl-gemcitabine loaded in PEGylated liposomes. These nanocarriers presented, on a subcutaneous grafted L1210wt leukemia cell line model, a similar *in vivo* anticancer activity with a drug dosage 5-fold lower that free gemcitabine [15]. Deamination in the blood was inhibited so the cytotoxic efficacy was increased at lower drug concentration.

Lipophilic forms of gemcitabine were synthesized to improve stability and cytotoxicity. Gemcitabine was covalently linked to various acyl derivatives (4-(N) position modification) and loaded in liposomes or lipid nanoparticles. These prodrugs were found to be more stable in plasma than the native drug and more active on KB and HT-29 cell lines (human oropharyngeal and colon carcinoma, respectively) [1]. Lipid nanoparticles loaded with 4-(N)-stearoyl-gemcitabine were able to deliver the prodrug into CCRF-CEM-AraC-8C cell line (human leukemia), a deficient nucleoside transporter cancer cell line, whereas the native gemcitabine was unable to enter.

Moreover, the loaded nanoparticle caused a cytotoxic effect 15-fold higher than native gemcitabine [16].

Our group has developed and patented a novel nanoscale system, the so-called lipid nanocapsules (LNCs) [17]. They are composed of lipids (triglycerides) as the core surrounded by a surfactant shell (lecithin and pegylated surfactant) and exhibit good dispersion stability. These biomimetic particles (analog to lipoproteins) are obtained using a free-organic solvent phase inversion process and their size can be tuned within the range of 20–100 nm [18]. Cancer treatment was the main application for the LNCs with the loading of a large variety of drugs : lipophilic anticancer drugs [19] and [20], radionucleides [21] and [22] and genetic materials [23] and [24]. The *in vivo* main properties of these nano-objects are : the biological barrier crossing [25], their accumulation in tumors via the EPR effect (enhanced permeability and retention) and the passive targeting of lymph nodes [26]. Moreover, LNCs can be functionalized and combined to thiolated proteins including monoclonal mAbs [27] and [28].

The aim of this work was to successfully encapsulate gemcitabine for the first time in LNCs with an easy and free-organic solvent process. In order to optimize the cytotoxic effect of gemcitabine, the amine group was protected against the deamination by adding a single 12-carbon length (C12) alkyl chain. This chemical modification permits to obtain a more lipophilic drug (Gem-C12) for its loading into LNCs. The lipophilic form was added during the LNC formulation process. Unfortunately, liquid LNC suspensions were not obtained as usual. The final product was a gel-like system. Gel properties were determined using rheological measurements *vs.* drug concentration, LNC concentration, temperature, and with additives such as urea, ethanol and NaCl. Interestingly, LNC suspensions were recovered after gel dilution. The stability of the nanocarrier and its protective effect for Gem-C12 were determined. Location of Gem-C12 inside LNC was assessed using tensiometry and explained the implication of the drug in the gel formation. Finally, cytotoxicity of diluted nanocarriers and syringeability of concentrated nanocarriers, *i.e.* gel-like structure, were tested for potential use in therapeutics as a new nanomedicine.

2. Materials and methods

2.1. Chemicals

Labrafac® WL 1349 (caprylic-capric acid triglycerides) (Labrafac) was generously provided by Gattefossé S.A. (Saint-Priest, France). Kolliphor® HS15 (formerly Solutol® HS15; mixture of free polyethylene glycol 660 and polyethylene glycol 660 hydroxystearate) (Kol) were kindly supplied by BASF (Ludwigshafen, Germany). Gemcitabine base was provided by Carbosynth (Berkshire, United Kingdom). Deionized water was obtained from a Milli-Q plus system (Millipore, Paris, France). Span® 80 (Span 80), Tween® 80 (Tween 80), dodecanoic anhydride, sodium chloride, urea, acid lauric, gemcitabine hydrochloride and antibiotics solution were purchased from Sigma (St Quentin-Fallavier, France). Dulbecco's modified Eagle's medium, RMPI 1640, fetal bovine serum and horse serum were obtained from Lonza (BioWhittaker, Verviers, Belgium). (3-(4,5-dimethylthiazol-2-yl)-5-(3-carboxymethoxyphenyl)-2-(4-sulfophenyl)-2H-tetrazolium (MTS) was purchased from Promega (Charbonnières-Les-Bains, France). Ethanol, dichloromethane and methanol were purchased from Fischer Scientific (Loughborough, United Kingdom).

2.2. Synthesis of 4-(N)-lauroyl gemcitabine

Synthesis of 4-(N)-lauroyl gemcitabine (Gem-C12) was already described [11]. Briefly, gemcitabine base (1mmol, 263mg) was mixed with dioxane (16mL) and dodecanoic anhydride (2mmol, 765mg) dissolved in water (4mL) under magnetic stirring at 40℃ during 48h. The reaction was monit ored by thin layer chromatography (dichloromethane/ethanol 96/4 *v/v*). Evaporation under vacuum was performed at room temperature after 24 hours to remove reaction solvents. The residue was purified by silica gel column flash chromatography (elution with a mixture dichloromethane/ethanol 96/4 *v/v*). Pure fractions were gathered and evaporated under vacuum to obtain a white product: Gem-C12 as the main product. Molecular weight was analysed using a microToFQII apparatus (Bruker Daltonics GmbH, Bremen, Germany) in electronspray positive ionization mode. ^{1}H-NMR spectra were recorded on a Avance DRX 500 MHz (Bruker Daltonics GmbH, Bremen, Germany) in deuterated dimethylsulfoxide. Elemental analysis was performed using a homemade organic microanalysis apparatus ("Service Central d'Analyse", Solaize, France).

Gem-C12 yield: 53 %

^{1}H-NMR ($(CD_3)_2SO$) 10.99 (1H, s, NHCO), 8.22 (1H, d, 6-CH), 7.27 (1H, d, 5-CH), 6.33 (1H, m, 1'-CH), 4.16 (1H, m, 3'-CH), 3.88-3.78 (2H, m, 5'-CH), 3.65 (1H, m, 4'-CH), 2.39 (1H, t, CO-CH_2), 1.52 (2H, t, CO-CH_2-CH_2), 1.22 (16H, m, $CH_2(CH_2)_8CH_3$), 0.84 (3H, t, CH_3).

Elemental analysis found: C 55.32 H 7.23 N 8.99 F 8.7. Calculated for $C_{21}H_{33}O_5N_3F_2$: C 56.63 H 7.42 N 9.44 F 8.54%.

$(M+H)^+$ m/z found: 446.25. Calculated: 446.23

2.3. LNC preparation

LNC formulation was based on a phase inversion process and was thoroughly described [17] and [29]. The quantities of oil phase (Labrafac), aqueous phase (water and NaCl) and surfactant (Kol and Span 80) for each formulation were precisely weighted. For 30 nm-Z-Ave LNC, $m_{Labrafac}$ = 0.75g m_{Kol} = 1.25g, m_{Span80} = 0.25g, m_{Water} = 1.02g and m_{NaCl} = 0.045g; for 65 nm-Z-Ave LNC, $m_{Labrafac}$ = 1.24g, m_{Kol} = 0.967g, m_{Span80} = 0.25g, m_{Water} = 1.02g and m_{NaCl} = 0.045g.

For loaded-LNC formulation, Gem-C12 or lauric acid was first solubilized in a mixture of Labrafac and Span 80 at concentrations from 1 to 10% (ratio Gem-C12 or lauric acid/Labrafac *w/w*) at room temperature, before the addition of Kol and aqueous phase. Mixtures were heated to 75℃ under magnetic stirring followed by cooling to 45℃ (rate of 5℃/min). This cycle was repeated thr ee times and during the last temperature decrease at the phase inversion temperature, *i.e.* 55℃, an irreversible shock was induced by dilution with 2.12 g of pure water, urea aqueous solutions (5, 10 and 15 urea/Gem-C12 *molar ratio*), NaCl aqueous solutions (5, 15 and 20 NaCl/Gem-C12 *n/n*), or ethanol/water mixtures (5, 10 and 25 ethanol/Gem-C12 *n/n*). Afterwards, a slow magnetic stirring was applied to the suspension of LNCs at room temperature.

2.4. Gel preparation

During the slow magnetic stirring at room temperature, a hydrogel spontaneously formed, with a waxy aspect. Gelation process was considered as completed after 24h at 4℃. The hydrogel was diluted by a factor 60 (*v/v*) with pure water before hydrodynamic diameter (Z-Ave), polydispersity index (PdI) and zeta potential (Pz) measurements, to confirm the LNC presence in diluted suspensions. In addition,

directly after the last dilution step of the LNC formulation, syringes with 18 Gauge (Ø 1,2mm) and 21 Gauge (Ø 0.8mm)-needles were fulfilled with the liquid suspension (before the gel formation) and stored at 4℃ during 24h. Gels, before and after extrusion through the needles, were analyzed in terms of rheological behavior.

2.5. Lipid nanocapsule characterization

Hydrodynamic diameter: Z-average (Z-ave), polydispersity index (PdI) and zeta potential (Pz) of LNCs were determined by dynamic light scattering on a Zetasizer® Nano serie DTS 1060 (Malvern Instruments S.A., Worcestershire, United Kingdom). The helium–neon laser, 4 mW, operates at 633 nm, with the scatter angle fixed at 173° and the temperature maintained at 25 ℃. The c urve fittings of the correlation functions were performed using exponential fit (Cumulant approach) for Z-ave and PdI determinations for LNC suspensions. Smoluchowski's approximation was used to determine electrophoretic mobility for Pz determination.

2.6. Evaluation of drug loading efficacy

The drug loading and entrapment efficiency were determined using UPLC method. Gem-C12 loaded in LNCs was determined after dialysis: 2mL of LNC preparation was filtered (0.2µm) and was filled into a dialysis tube (cutoff of 100 kDa) and inserted in a 4000-mL flask containing water at 25°C under magnetic stirring (300 rpm). The amount of drug in the dialysis tube was determined after disruption of LNC using methanol (1:36 v/v). For control, total quantities of Gem-C12 added in the formulation were determined without filtration and dialysis, by disruption of LNC using methanol.

UPLC apparatus was equipped with UV spectroscopy detection. The samples were injected into a C18 column (1.7 x100mm, ACQUITY UPLC BEH C18) equipped with a column guard. The column was eluted (methanol as elution solvent) with at 0.343 mL/min-flow rate. The detection wavelength was 248 and 266 nm. Peak heights were recorded and processed on MPower software (Waters, USA). The drug concentration was calculated from linear titration curve, with freshly Gem-C12 methanol solutions at concentration range from 1 to 100 µg/mL.

2.7. Rheological properties

The viscoelastic properties of the gels at room temperature were measured using a Kinexus® rheometer (Malvern Instruments S.A., United Kingdom), with a cone plate geometry (diameter 40 mm, angle: 2°). Parallel plate geometry (diameter 20 mm, gap: 700 µm) was used for temperature experiments. Oscillatory strain sweeps at 1Hz-constant frequency was performed to determine the linear regime characterized by constant dynamic moduli (storage modulus: G' and loss modulus: G''), independent of strain amplitude. In this regime (0.1% constant strain), G' and G'' were measured as a function of angular frequency (0.1 to 100 Hz). Solid-to-liquid temperature (T_{SL}) transition was determined at constant frequency and strain, 1 Hz and 0.01%, respectively, in a range of temperatures from 4 to 60°C and a heating rate of 2°C/min. All these experiments were repeated three times. G', G'' and T_{GS} values were expressed as mean ± standard deviation (SD).

2.8. Tensiometry

Absorption kinetics were obtained at Labrafac-water interface by means of a rinsing drop method using a drop tensiometer device (Tracker Teclis, Longessaigne, France). For this study, Gem-C12 was diluted in Labrafac, from 0 to 6 mg/g (Gem-C12/Labrafac *w/w*). Basically, a Labrafac drop (5 µL) was formed with an Exmire microsyringe (Prolabo, Paris, France) into an optical glass bowl (Hellma, Paris, France) containing a water phase. The axial symetric shape (Laplacian profile) of the drop was analyzed by use of a video camera connected to a microcomputer. From numerical image analysis, with the Laplace equation integrating the drop profile points, the interfacial tension, the surface area and the volume of the drop were recorded in real time (five measurements per sec). Piston movements of the syringe were controlled by a stepping motor connected to a microcomputer, to control the drop volume and to keep the surface area constant. Absorption kinetics consisted of the formation of a monolayer by the gradual diffusion of the amphiphilic molecules from drop core to the interface, until complete saturation was achieved. Saturation was reached when surface tension stabilized. For each Gem-C12 concentration, experiments were repeated in triplicate and surface tension was expressed as a mean ± SD.

2.9. Cell cultures

Human pancreatic carcinoma Mia PaCa-2 and BxPc-3, and human lung cancer H460 cell lines were obtained from ATCC (Manassas, VA, USA). Mia PaCa-2 cells were cultured in Dulbecco's modified Eagle's fortified medium containing glucose (4.5 g/L) whereas BxPc-3 and H460 cells were cultured in RPMI 1610. All media were completed with fetal bovine serum (10% *v/v*), horse serum (2.5% *v/v*, only for Mia PaCa-2 culture), penicillin (100 UI/mL), streptomycin (100 µg/mL) and amphotericin B (0.250 µg/mL)**.** Fresh medium was substituted every 48 h. When cells reached 80% confluence, dissociation was performed using trypsine and replated in 75-cm^2 flasks, at 37℃ in CO_2/air mixture (5/95 *v/v*)**.**

2.10. Proliferation assay

The cytotoxicity of diluted Gem-C12-loaded LNCs was determined using MTS test. Fresh medium, non-loaded LNCs, gemcitabine hydrochloride and pure Gem-C12 (in water/ethanol/Tween 80 87.6/5.5/6.9 *(v/v)*) mixture were used as control. Cells were seeded into 96-well plates (15,000 cells/well) and incubated at 37℃ under CO_2/air mixture (5/95 *v/v*) overnight. Various amounts of drugs (maximum concentration values of 250, 100 and 50µM for Mia PaCa-2, BxPc-3 and H460, respectively) and LNCs were added into the wells, and the cells were incubated for 48h.

The number of living cells was determined using a MTS assay (colorimetric assay based on conversion of a tetrazolium salt into formazan). Formazan absorbance was measured at 492 nm and 750 nm, directly from 96-well plates using a spectrophotometer (Multiscan Ascent MP reader, Thermo Scientific, Courtaboeuf, France), after exposition to MTS (20 µL/well) for 2.5 h at 37 ℃. The percentage of cell viability was calculated according to the following equation:

$$\text{Cell viability}\,(\%) = \frac{\text{Abs}\,(\text{T})}{\text{Abs}\,(\text{C})} \times 100$$

with Abs (T) and Abs (C), the absorbance values of treated and untreated cells (with fresh medium), respectively. The quantity of formazan is proportional to the number of living cells in culture. Relative percentage of living cells (compared to living cells with fresh medium control) was reported as the mean ± SD of three different experiments.

2.11. Statistical analysis

All results were expressed as mean ± SD. Normal distributions were assumed for the rheological moduli G' and G''. Significant differences between means of rheological moduli were analyzed by one-way analysis of variance (ANOVA 1F), followed by Scheffe's *post hoc* test for pairwise comparisons. Differences were considered statistically significant for $p < 0.05$.

3. Results

3.1. Gem-C12-loaded LNC gel technology

The phase-inversion temperature (PIT) method was first described by Shinoda, *et al* [30] and developed by Heurtault, *et al* [29] to obtain nano-objects based on an oily core (Labrafac) surrounded by an organized assembly made up of lecithin molecules and PEGylated surfactants (Kol) with the PEG chains oriented towards the aqueous phase [17] and [29]. A Similar process was used changing lecithin with Span80. After the temperature cycles and the rapid cold dilution, LNC suspensions were obtained (Fig. 1. insert A). Changing Labrafac and surfactant compositions, LNC-hydrodynamic diameters (Z-Ave) were modified: 30.0 ± 0.5 and 67.0 ± 2.0 nm. PdI was lower than 0.1 for all these nano-objects (0.047 ± 0.012 and 0.037 ± 0.010, respectively), characteristic to a monomodal and thin size distribution. Pz values were -9.3 ± 4.6 mV and -7.5 ± 3.0 mV, respectively, and corresponded to classical value obtained for LNCs [17].

Gemcitabine hydrochloride, a hydrophilic drug, is not easy to encapsulate inside LNCs. Due to the lipophilic core, encapsulation strategies have to be developed for this purpose as already performed in our group (reverse micelle, aqueous core LNCs) for other molecules [31] and [32]. Hydrophobization of gemcitabine could also be an appropriate approach as described in literature [11] and [33]. Lauroyl-modified gemcitabine (Gem-C12) was synthesized and the characterization data are given in the "Materials and Methods" section. To obtain Gem-C12-loaded LNCs, the drug was first added to the initial mixture before the first temperature cycle. Drug concentration was modified from 1 to 10% (Gem-C12/Labrafac *w/w*). After the rapid cold dilution, suspensions were obtained but they turned into a waxy aspect gel state (Fig. 1. insert

B) for drug concentrations higher than 5%. Below this drug concentration value, no gelation occurred and a LNC suspension was always obtained.

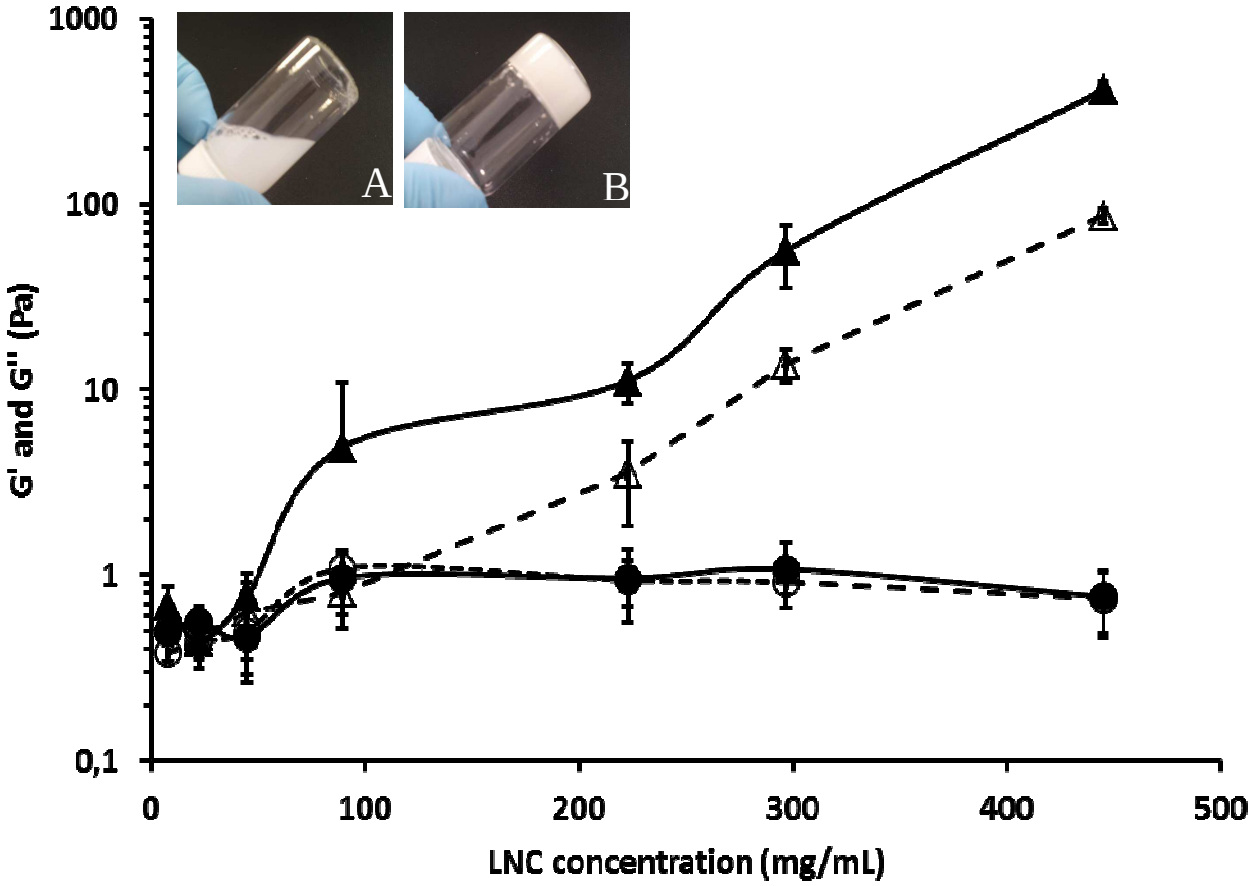

Fig. 1. Storage modulus G' (closed symbol, solid line) and loss modulus G'' (open symbol, dotted line) *vs.* LNC concentration for Gem-C12 5% loaded (Gem-C12/Labrafac *w/w*) (▲,△) and non-loaded LNC (Z-Ave = 67 nm) (●,○). (n=3, mean ± SD). Non-loaded LNC suspension (Insert A) and Gem-C12-loaded LNC gel (Insert B) pictures at room temperature (LNC concentration 445 mg/mL; 5% Gem-C12/Labrafac *w/w*).

Gels could be dissolved in an excess of water and nano-objects were still visible showing the physical character of the gel association. For the corresponding 67 nm-Z-Ave blank LNC composition, loaded nano-object Z-Ave was 55.5 ± 2.0 nm, with a PdI and Pz of 0.05 ± 0.01 and -8.0 ± 2.5 mV, respectively. For the corresponding 30 nm-Z-Ave blank LNC composition, loaded nano-object Z-Ave was similar: 29.0 ± 1.0 nm, with a PdI and Pz of 0.030 ± 0.02 and -3.0 ± 0.3 mV, respectively.

Gem-C12 encapsulation rates were determined using UPLC method after LNC disruption in methanol, with and without filtration and dialysis. Whatever Gem-C12 concentration, the drug was totally encapsulated in the nano-objects. No difference in Gem-C12 loading was observed: (i) directly after the formulation process (initial Gem-C12 loading) and (ii) after the filtration (large Gem-C12 aggregate elimination) followed by the dialysis process (residual micelle elimination). The total encapsulation rate, size, PdI and Pz of nano-objects were constant over time (1 year) at 4℃, whatever the storage form of this innovativ e pharmaceutical technology: gel state or diluted state.

3.2. Rheological characterization

Rheological analysis (viscoelastic property characterization) was performed for Gem-C12-loaded LNCs in gel state, changing the applied strain at a constant oscillation frequency of 1 Hz. Whatever the drug loading, all gels presented a linear regime corresponding to strain-independent storage (G') and loss (G'') moduli up to a critical strain value of about 1%. Beyond this critical value, G' and G'' decreased.

The viscoelastic properties of the gels were then studied at 25℃, within the linear regime (0.1% strain), as a function of the oscillation frequency. Constant values were obtained from 0.02 to 8.0 Hz, characteristic of a gel state**.** G' and G'' profiles *vs.* Gem-C12-loaded LNC (5% Gem-C12/Labrafac *w/w*) concentration were illustrated in Fig. 1. Without any additional volume for shock dilution at the end of the formulation process**,** *i.e.* Gem-C12-loaded LNC concentration of 445 mg/mL, G' and G'' values were 410 ± 40 and 90 ± 10 Pa, respectively. Ratio G'/G'' was about 4.55, showing the strong elasticity of the gel.

Similar results were obtained by dilution of the gel or using various volumes of shock dilution at the end of the formulation process. When the gel was diluted, G' and G'' significantly decreased ($p<0.01$) up to 5 ± 6 and 1 ± 0.5 Pa, respectively, for Gem-C12-loaded LNC concentration of 89 mg/mL**.** Gel hardness was lost with dilution but elasticity remained constant: G'/G'' were about 5 for C12-loaded LNC concentration of 89 mg/mL. No gelation and no elastic behavior were observed with the corresponding non-loaded LNC, considering the same LNC concentration rage. At concentration lower than 89 mg/mL, Gem-C12-loaded and non-loaded LNC have the

same rheological behavior: G' and G" values close to 1 Pa corresponding to the absence of gelation and consequently the absence of elastic behavior.

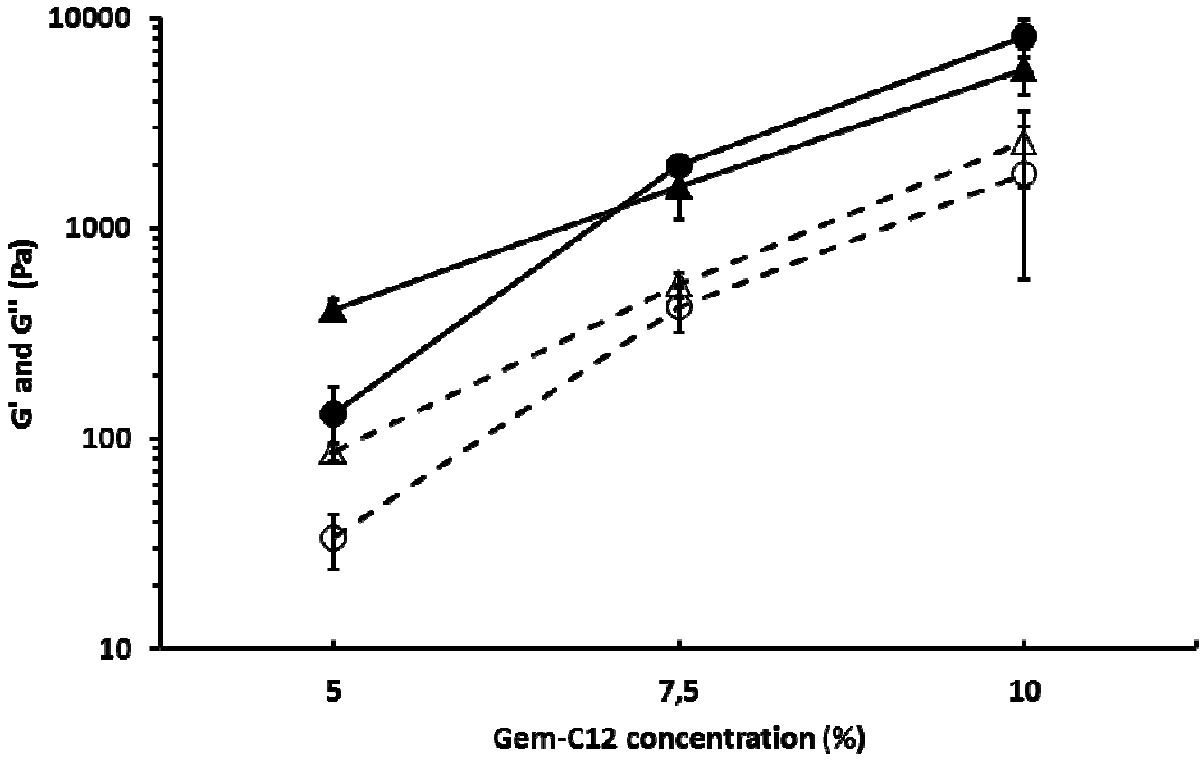

Fig. 2. Storage modulus G' (closed symbol, solid line) and loss modulus G'' (open symbol, dotted line) *vs.* Gem-C12 concentration (Gem-C12/Labrafac *w/w*) for 29 nm-Z-Ave (●,○) and 55 nm-Z-Ave (▲,△) Gem-C12-loaded LNC. (n=3, mean ± SD).

G' and G'' profiles, *i.e.* the gel hardness, was dependent on Gem-C12 concentration (Gem-C12/Labrafac *w/w*) (Fig. 2.). G' and G" values increased of about 1 decade when drug concentration increased from 5 to 10%, whatever studied C12-loaded LNC size. Drug concentrations: 5%, 7.5% and 10%, had no effect on gel elasticity, with a relatively constant G'/G" ratio at about 4.55, 2.90 and 2.20, respectively, for LNC Z-Ave of 55 nm and 3.90, 4.7 and 4.50, respectively, for LNC Z-Ave of 29 nm. Moreover, gel properties were independent on Gem-C12-loaded LNC size. Similar G' and G'' moduli values were observed for Gem-C12-loaded LNC Z-Ave of 29 nm and 55 nm, at constant Gem-C12 concentration from 5 to 10% (Gem-C12/Labrafac *w/w*).

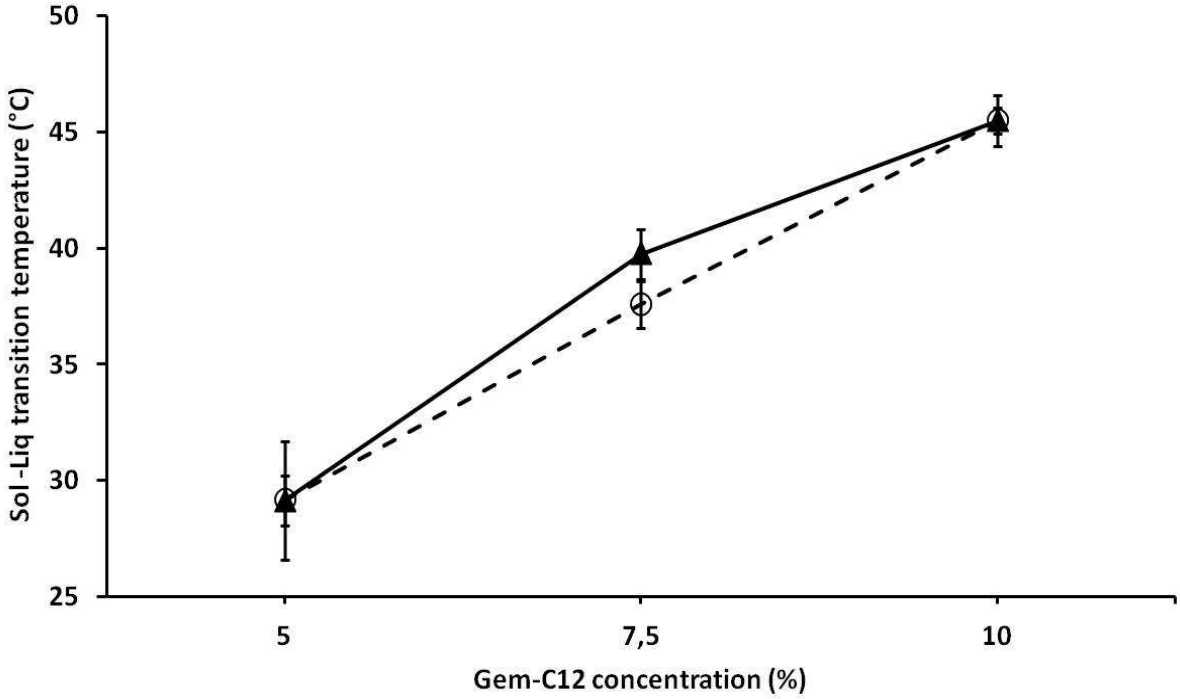

Fig. 3. Solid-to-liquid transition temperature T_{SL} *vs.* Gem-C12 concentration (Gem-C12/Labrafac *w/w*) for 29 nm-Z-Ave (○) and 55 nm-Z-Ave LNC (▲) Gem-C12-loaded LNC. (n=3, mean ± SD).

Gel properties (G' and G'') were studied *vs.* temperature at a constant oscillation frequency (1 Hz) and constant strain (0.01%). A Solid-to-liquid temperature (T_{SL}) transition (G' and G'' crossing) was observed, depending on Gem-C12 concentration (data not shown). From 5 to 10% drug concentration (Gem-C12/Labrafac *w/w*), T_{SL} linearly increased from about 30 to 45℃ (Fig. 3.). While drug concentration effect was observed, no dependence with Gem-C12-loaded LNC Z-Ave was shown (Fig. 3.). T_{SL} were about 45 ± 1 and 46 ± 1 ℃ for 29 and 55-nm Z -Ave of loaded LNC, respectively (10% Gem-C12/Labrafac *w/w*).

To sum up, Gem-C12 concentration in LNC and Gem-C12-loaded LNC concentration influenced the G' and G'' gel properties and T_{SL}, *i.e.* the gel state to LNC suspension transition, while no influence was shown with Gem-C12-loaded LNC size.

3.3. Surface tension measurements

Labrafac-water interface was performed using a 5 µL-Labrafac drop in water. Surface tension was measured at the interface Labrafac-water *vs.* Gem-C12 concentration (Gem-C12/Labrafac *w/w*), when the drug was solubilized in the Labrafac drop (Fig.

4.). When drug concentration was increased from 0 to 6 mg/g, surface tension was significantly decreased from 34.6 ± 1.5 to 14.0 ± 1.0 mN/m, respectively. Gem-C12 behaves as an amphiphilic molecule and moves from the oil drop to the Labrafac-water interface.

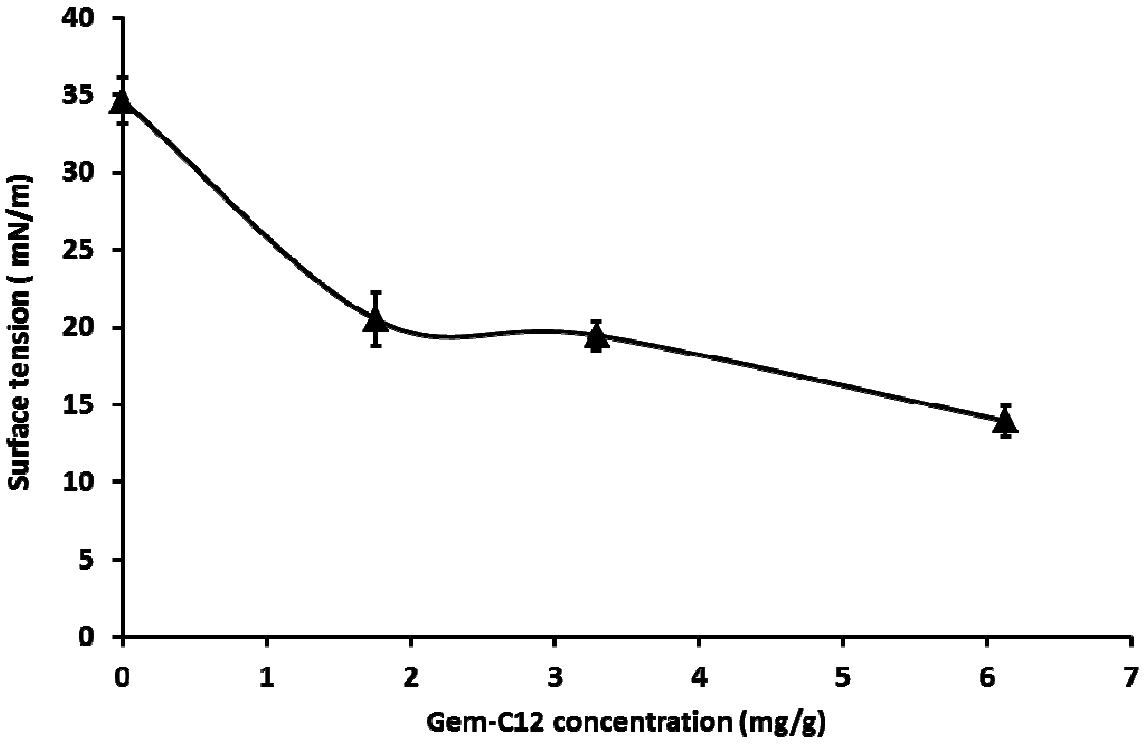

Fig. 4. Surface tension of Labrafac-water interface of a 5 µL-Labrafac drop in water *vs.* Gem-C12 concentration (Gem-C12/Labrafac *w/w*). (n=3, mean ± SD).

3.4. Interaction characterization in the gel state

Lauric acid was encapsulated in a similar manner that for Gem-C12. LNC suspension was obtained at the end of the process, without any gelation. G' and G'' values for 5% lauric acid-loaded LNC (lauric acid/Labrafac *w/w*, Z-Ave = 62.5 ± 0.4 nm) suspension were about 1 Pa, similar to values obtained with blank LNC (Fig. 1.). So gemcitabine moiety, from Gem-C12 molecule, was responsible of the nano-object gelation.

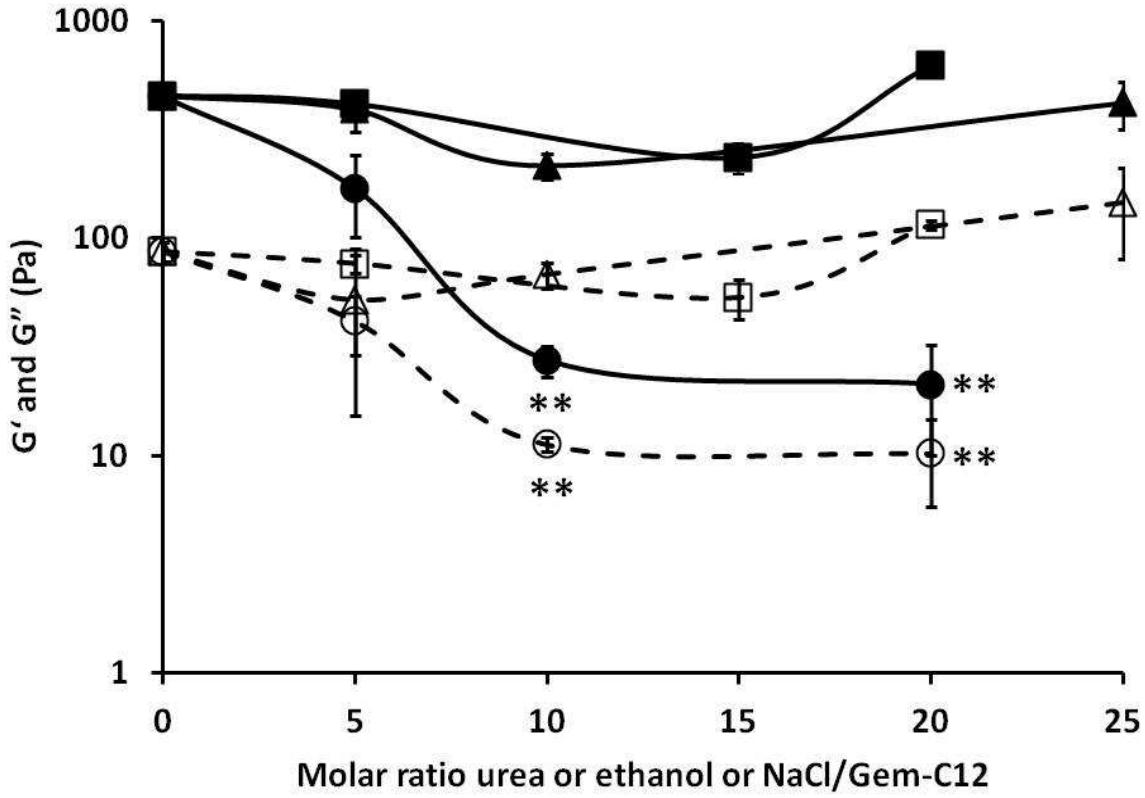

Fig. 5. Storage modulus G' (closed symbol, solid line) and loss modulus G'' (open symbol, dotted line) for Gem-C12 loaded LNC (Z-Ave = 55nm, Gem-C12 concentration = 5% Gem-C12/Labrafac *w/w*) *vs*. the molar ratio of urea (●,○) or ethanol (▲,△) or NaCl (■, □) with Gem-C12. (n=3, mean ± SD; **: p<0.01).

Ethanol, NaCl or urea was added during the formulation process (in the shock dilution water) of 5% Gem-C12-loaded LNC (Gem-C12/Labrafac *w/w*, Z-Ave = 55.0 ± 0.2 nm) to characterize the LNC interactions implied during gelation. While no significant difference was observed when ethanol or NaCl was added, the urea addition significantly decreased the gel hardness (Fig. 5.). Modulus values decreased from 410 ± 40 (G') and 90 ± 10 (G'') without urea to 21 ± 10 (G') and 10 ± 4 Pa (G'') with molar ratio urea/Gem-C12 of 20. Therefore, gelation between Gem-C12-loaded LNC was due to H-bond. Electrostatic or van der Walls interaction can be rejected (no effect of NaCl and ethanol, respectively) [34] and [35].

3.5. Gel property and in vitro *syringe injection*

In a content of pharmaceutical development, this innovative gel form could be subcutaneously or locally injected to patients. To avoid surgery, this form should be

injected using a syringe and gel property has to be recovered after extrusion through thin needles. Feasibility was performed fulfilling syringes directly after the shock dilution at the end of the formulation (before gelation occurred). Then, once the gel was formed inside the syringe, the material was directly extruded through 18 and 21G needles in a rheometer.

Fig. 6. reported G' and G" values for Gem-C12-loaded LNC gel (445 g/mL constant LNC concentration) with various drug concentrations: 5, 7.5 and 10% (Gem-C12/Labrafac *w/w*) and for 29 and 55-mn LNC Z-Ave. Comparisons were assessed without and after extrusion. Whatever LNC Z-Ave and needle size, no significant difference was observed before and after extrusion when drug concentrations were 7.5 and 10% (Gem-C12/Labrafac *w/w*). For 5%-drug concentration, a significant G' and G" decrease were observed before and after extrusion through needles. Nevertheless, the liquid form was not recovered. For 29 and 55-nm Z-Ave loaded LNC gel, G' and G" values were 1 and 2 decades higher than for non-loaded LNCs, respectively. Feasibility with 55-nm Z-Ave loaded LNC gel with 10% drug concentration (Gem-C12/Labrafac *w/w*) was not performed due to the instantaneous gelation process directly after the shock dilution at the end of the formulation, and so the impossibility to fill up syringes.

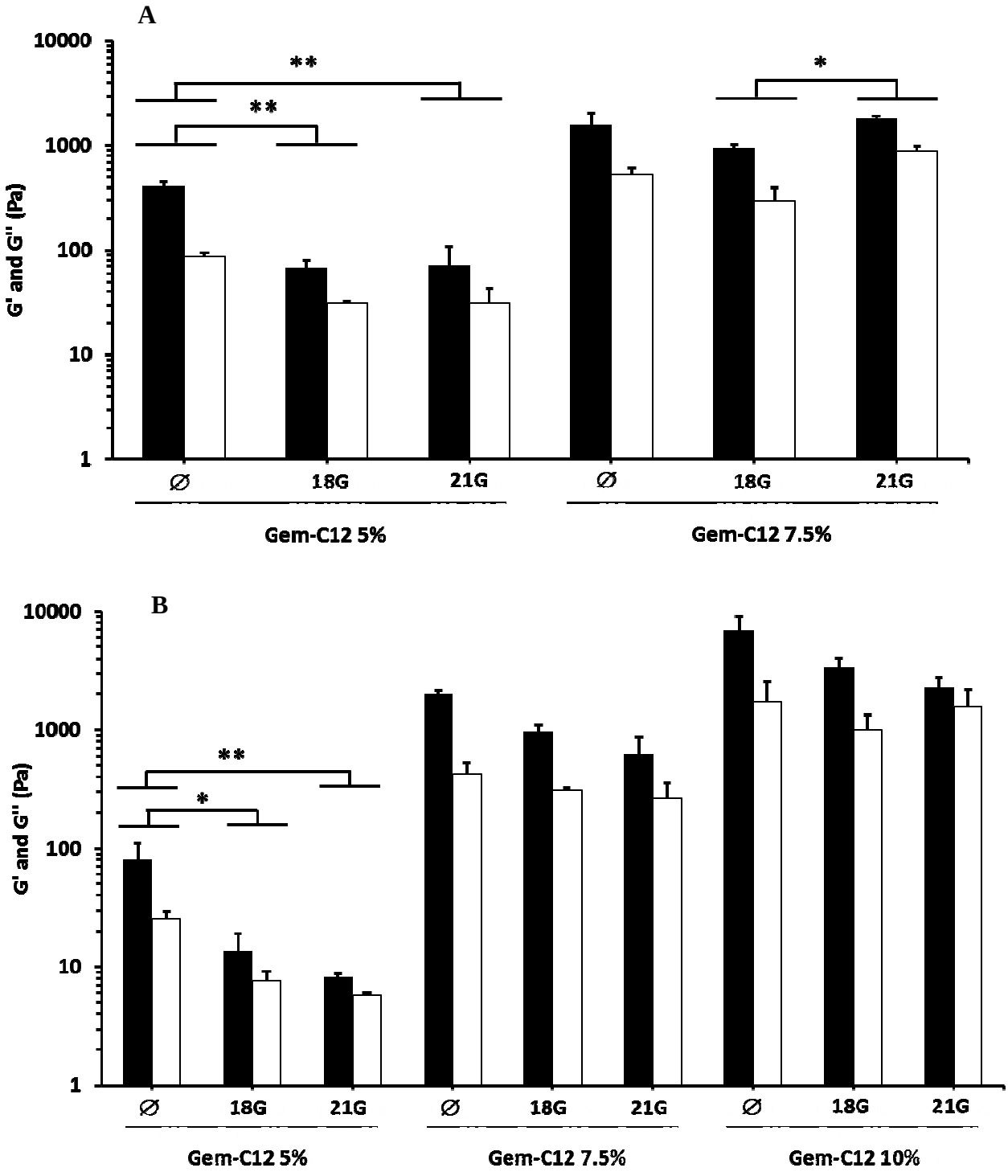

Fig. 6. Storage modulus G' (black bar) and loss modulus G'' (white bar) for Gem-C12-loaded LNC (Z-Ave = 55 (panel A) and 29 nm (panel B), Gem-C12 concentration = 5, 7.5 and 10% Gem-C12/Labrafac *w/w*, LNC concentration 445mg/mL) before (∅) and after extrusion through 18G and 21G-needles. (n=3, mean ± SD; *: $p<0.05$, **: $p<0.01$).

3.6. In vitro *cytotoxicity of Gem-C12-loaded LNCs on tumor cells*

In vitro cytotoxicity was tested *vs.* Gem-C12 concentration on three tumor cell lines: a human lung cancer: H460, and two pancreatic cancers: BxPc-3 and Mia PaCa-2. Mia PaCa-2 is known to be resistant to gemcitabine while BxPc-3 and H460 seem more sensitive to this drug [36] and [37]. Four formulations were tested: gemcitabine hydrochloride in aqueous solution, Gem-C12 in a mixture of water/ethanol/Tween 80 (87.6/5.5/6.9 *v/v*), non-loaded LNC (Z-Ave = 67 nm) and Gem-C12-loaded LNC (Z-Ave = 55 nm, Gem-C12 concentration = 5% Gem-C12/Labrafac *w/w*) in a liquid form after gel dilution (Fig. 7. A, B and C).

After 48 h of exposure with Gem-C12-loaded LNCs at 37℃, cell viability decreased. The half maximal inhibitory concentrations (IC_{50}) were measured at 125, 1 and 0.5 µM when Gem-C12-loaded LNC were incubated with Mia PaCa-2, BxPc-3 and H460, respectively. No cytotoxicity was observed for non-loaded LNC in the concentrations studied. To extrapolate with Gem-C12 concentration, this non-loaded nanocarrier suspension was similarly diluted to Gem-C12-loaded LNC. *In vitro* cytotoxicity observed with Gem-C12-loaded LNC was due to the drug and not the nanocarrier alone. After incubation with Gem-C12 without LNC nanocarrier, close IC_{50} values that for Gem-C12-loaded LNC were observed. Gemcitabine hydrochloride presented a high cytotoxic behavior on BxPc-3 cell line, with IC_{50} value at about 1µM (Fig. 7. B). On the other hand, no cytotoxic effect was found when gemcitabine hydrochloride was incubated with Mia PaCa-2 until 250 µM of drug concentration. With these three cancers cell lines, a significantly increase of sensitivity was observed with Gem-C12 alone or Gem-C12-loaded LNCs compared to the commercialized drug (gemcitabine hydrochloride).

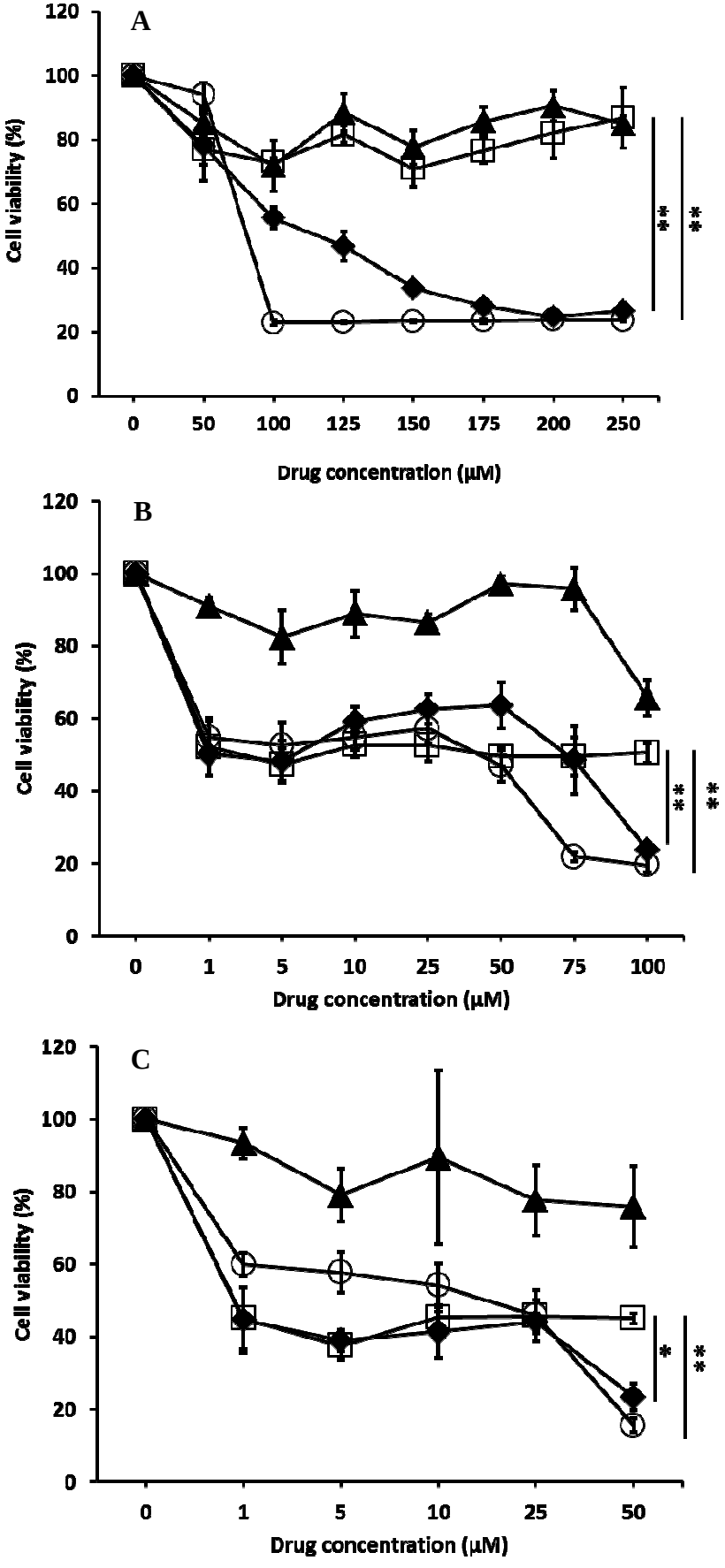
A
Cell viability (%)
120
100
80
60
40
20
0
0
50
100
125
150
175
200
250
Drug concentration (µM)
**
**
B
Cell viability (%)
120
100
80
60
40
20
0
0
1
5
10
25
50
75
100
Drug concentration (µM)
**
**
C
Cell viability (%)
120
100
80
60
40
20
0
0
1
5
10
25
50
Drug concentration (µM)
*
**

Fig. 7. Cell viability of Mia PaCa-2 (panel A), BxPc-3 (panel B) and H460 (panel C) cell lines *vs*. drug concentration after 48h-incubation with Gem-C12 (○) (solution in water/ethanol/Tween 80 87.6/5.5/6.9 *v/v/v*), gemcitabine hydrochloride (□) (solution in PBS), Gem-C12-loaded LNC (◆) (Z-Ave = 55 nm, Gem-C12 concentration = 5% Gem-C12/Labrafac *w/w*) and non-loaded LNC (▲) (Z-Ave = 67 nm). There is no Gem-C12 inside non-loaded LNC, but dilutions were performed in the same way that for Gem-C12-loaded LNC for comparison. (n=3, mean ± SD; * $p<0.05$, **: $p<0.01$).

4. Discussion

In the 90's, innovative gel materials were reported in the field of pharmaceutical technology. These materials, called organogels, are ternary mixtures of oil, water and low molecular weight molecules (lecithin, sorbitan monostearate or monopalmitate) and the ternary composition was adjusted to obtain solid-like systems [38], [39], [40], [41], [42] and [43]. *In vitro* release and *in vivo* efficacy were assessed for propanolol [44], cyclosporin A [45] and antigen models (bovine serum albumin and haemagglutin) [40], [41] and [46] for nasal, oral, subcutaneous and intramuscular administration. Clinical trials for transdermal diclofenac administration were also reported [47], [48] and [49]. Similar systems were obtained with the ternary mixture of Labrafac (oil), water, Kolliphor/Span 80 (low molecular weight molecules) when Gem-C12 was added in the formulation. Nevertheless, the innovation of this system is the re-obtention of nanoparticles after dilution of the gels. No dilution matrix description was reported for the organogel described previously. The nature of the gel architecture, *i.e.* a gelling network composed of entangled rod-shaped tubules (entangled cylindrical reverse micelle) was described [39], [43] and [50] and the organogel dilution should lead to an oil/water phase separation. The gel architecture developed in this study was new. It consisted of the inter-nanoparticle association of Gem-C12-loaded LNC, with H-bond crosslinkings between the gemcitabine moieties of Gem-C12 located at the oil/water interface of LNCs (Fig. 4. and 5.). Gemcitabine moiety of Gem-C12, oriented to the water phase, was therefore responsible to the gel formation and a schematic representation of the gel structure could be a tridimensional pearl necklace immobilizing the water phase. Once diluted, the necklace broke and the pearls (Gem-C12-loaded LNCs) were recovered in the water phase, with the loss of gel rheological properties (Fig. 1.). In the present study, the

gelation between Gem-C12-loaded LNC is due to physical interactions and a reversible gel-to-solution temperature (T_{GS}) transition temperature was observed (Fig. 3.), confirming the presence of H-bonds [51].

The gel material developed in this study could be considered as a hydrogel. Indeed, hydrogels may be defined as a semi-solid formulation having an external polar phase, immobilized within the spaces available of a three dimensional network structure [52]. In industrial and medical applications, hydrogels received a considerable attention for the development of new controlled delivery systems [53]. Coupling hydrogel and nanoparticles appears like a new promising nanoparticulate drug delivery systems. Nanoparticle hydrogel were performed with liposomes [54] and [55], solid lipid nanoparticle [56] and [57] or micelle [58]. Nevertheless, all nanoparticle-based hydrogels were obtained by adding synthetic or natural polymers to induce the gelation. These polymers alone led to the gel formations and the nanoparticles were dispersed in the matrix, without any interaction with the tridimensional polymer network. A challenge is to limit the addition of polymers to avoid any additional side effects and to simplify the formulation. In this study, a rapid gelation was observed once the formulation process was achieved and the gel structure was obtained without the addition of any polymer. The hydrogel property was not found with non-loaded LNCs, but only with the loading of Gem-C12. This drug participated actively to the structuration of the gel.

In literature, loading of lipophilic gemcitabine prodrug into nanoparticle was already studied but the gelation effect was never observed. Zhu, *et al* used polymeric micelles (micelle concentration of 10mg/mL) for stearoyl-modified gemcitabine loading [59]. Cui's group incorporated stearoyl-modified gemcitabine into nanoemulsions (particle concentration from 0.5 to 1 mg/mL) [13], [16] and [33]. Similar concentrations of Gem-C12-loaded LNC we developed are in liquid state and the gel effect was observed at higher concentration. The stearoyl chain is longer than the lauroyl one and the lipophilicity of the prodrug is certainly improved. Therefore, another explanation of the non-gelation effect could be the location of modified gemcitabine inside the nanoparticle core *versus* the oil/water interface observed in this study. Immordino, *et al* studied the encapsulation of lipophilic (from valeroyl to stearoyl) gemcitabine prodrug into liposomes [11]. The prodrug, due to the amphiphilic assembly of liposomes, should be located in a similar way that for LNCs

(with gemcitabine moiety of the prodrug oriented to the aqueous phase), but the gelation effect was not observed. With liposomes, the molar ratio prodrug/lipid is 0.04 at maximum. In the present study, gelation was observed at a higher molar ratio prodrug/surfactant (Kol and Span 80), *i.e.* about 0.1, corresponding to Gem-C12 concentration of 5% (GemC12/Labrafac *w/w*). The gelation effect is strongly dependent on Gem-C12 and nanocapsule concentrations (Fig. 1. and 2.).

An advantage of a hydrogel drug delivery system is the possibility to inject directly the preparation. No surgical procedure is required for the insertion of gels into the body and the gels are administered by simple injection [60]. With respect to implantable systems which request slight surgery, an injectable hydrogel is particularly attractive. Gem-C12-loaded LNC hydrogel can be administered in a straightforward manner using a syringe without loss of viscoelastic gel properties (Fig. 6.). Seo, *et al* used an injectable system containing an anti-cancer drug for the treatment of a primary tumor: B16F10 melanoma cells (via intratumoral injection) [61]. Cytotoxicity assays have demonstrated the efficiency of GemC12-loaded LNCs on pancreatic and lung cancer cells (Mia PaCa-2, BxPc-3 and H460 cell line). This was particularly impressive with Mia Paca-2 cell line which is known to be resistant to gemcitabine [62]. This innovative material could be useful for cancer therapy. After subcutaneous administration, the Gem-C12-loaded LNC hydrogel should be diluted progressively and the Gem-C12-loaded LNC could passively target the lymph nodes to prevent metastasis as described in the review of Cai, *et al* [63].

5. Conclusion

An innovative nanomedicine approach was developed for the encapsulation of modified gemcitabine in LNCs. A hydrogel was spontaneously formed depending on the LNC and prodrug concentrations. This material assembly was totally new in regards of organogels already developed, due to the inter-LNC association via H-bonds, and this property is directly caused by the prodrug encapsulated at the oil/water interface of LNC. In addition, after the dilution of the material, gemcitabine-loaded LNC were recovered in suspension in water, with a strong cytotoxic activity with respect to pancreatic and lung cancer cell lines, higher than the native commercialized drug. The present pharmaceutical technology offers the following

advantages: (i) it is easy to perform (scale-up possibility); (ii) the gelation reaction occurs rapidly in absence of template or gelator; (iii) the loaded drug is protected against any degradation process such as deamination in the current study; (iv) once diluted, the cytotoxic activity of loaded-LNCs was confirmed, without LNC surface modification; and finally (v) the hydrogel can be injected using a syringe. Using this system as depot after intratumoral or subcutaneous administration could be interesting to develop new therapeutics.

Acknowledgements

The authors would like to thank Benjamin Siegler (Plateforme d'Ingénierie et Analyses Moléculaires (PIAM), Angers, France) for RMN analysis. We also thank the Service Central d'Analyse (Solaize, France) for molecular weight and elemental analysis. This work has been realized within the research program LYMPHOTARG financially supported by EuroNanoMed ERA-NET 09 and by the Région Pays de la Loire.

References

[1] E. Moysan, G. Bastiat, J.-P. Benoit, Gemcitabine versus Modified Gemcitabine: A Review of Several Promising, Mol Pharm, 10 (2012), pp. 430-44

[2] W. Plunkett, P. Huang, V. Gandhi, Preclinical characteristics of gemcitabine, Anticancer Drugs, 6 (1995), pp. 7‑13

[3] A.M. Bergman, H.M. Pinedo, G.J. Peters, Determinants of resistance to 2′,2′-difluorodeoxycytidine (gemcitabine), Drug Resistance Updates, 5 (2002), pp. 19‑33

[4] D.R. Rauchwerger, P.S. Firby, D.W. Hedley, M.J. Moore, Equilibrative-sensitive nucleoside transporter and its role in gemcitabine sensitivity, Cancer Res, 60 (2000), pp. 6075‑6079

[5] J.J. Farrell, H. Elsaleh, M. Garcia, R. Lai, A. Ammar, W.F. Regine, et al., Human equilibrative nucleoside transporter 1 levels predict response to gemcitabine in patients with pancreatic cancer, Gastroenterology, 136 (2009), pp. 187‑195

[6] J.L. Abbruzzese, R. Grunewald, E.A. Weeks, D. Gravel, T. Adams, B. Nowak, et al., A phase I clinical, plasma, and cellular pharmacology study of gemcitabine, J Clin Oncol, 9 (1991), pp. 491‑498

[7] M.L. Clarke, J.R. Mackey, S.A. Baldwin, J.D. Young, C.E. Cass, The role of membrane transporters in cellular resistance to anticancer nucleoside drugs, Cancer Treat Res, 112 (2002), pp. 27‑47

[8] V. Sebastiani, F. Ricci, B. Rubio-Viqueira, B. Rubio-Viquiera, P. Kulesza, C.J. Yeo, et al., Immunohistochemical and genetic evaluation of deoxycytidine kinase in pancreatic cancer: relationship to molecular mechanisms of gemcitabine resistance and survival, Clin Cancer Res, 12 (2006), pp. 2492‑2497

[9] B.S. Zhou, P. Tsai, R. Ker, J. Tsai, R. Ho, J. Yu, et al., Overexpression of transfected human ribonucleotide reductase M2 subunit in human cancer cells enhances their invasive potential, Clin Exp Metastasis, 16 (1998), pp. 43‑49

[10] L.H. Reddy, P. Couvreur, Novel approaches to deliver gemcitabine to cancers, Curr Pharm Des, 14 (2008), pp. 1124‑1137

[11] M.L. Immordino, P. Brusa, F. Rocco, S. Arpicco, M. Ceruti, L. Cattel, Preparation, characterization, cytotoxicity and pharmacokinetics of liposomes containing lipophilic gemcitabine prodrugs, J ControlRelease, 100 (2004), pp. 331‑346

[12] S.M. Ali, A.R. Khan, M.U. Ahmad, P. Chen, S. Sheikh, I. Ahmad, Synthesis and biological evaluation of gemcitabine-lipid conjugate (NEO6002), Bioorganic Med Chem Lett, 15 (2005), pp. 2571‑2574

[13] M.A. Sandoval, B.R. Sloat, D.S.P. Lansakara-P., A. Kumar, B.L. Rodriguez, K. Kiguchi, et al., EGFR-targeted stearoyl gemcitabine nanoparticles show enhanced anti-tumor activity, J Control Release, 157 (2012), pp. 287-296

[14] C. Celia, D. Cosco, D. Paolino, M. Fresta, Gemcitabine-loaded innovative nanocarriers vs GEMZAR: Biodistribution, pharmacokinetic features and in vivo antitumor activity, Expert Opin Drug Deliv, 8 (2011), pp. 1609‑1629

[15] B. Pili, L.H. Reddy, C. Bourgaux, S. Lepêtre-Mouelhi, D. Desmaële, P. Couvreur, Liposomal squalenoyl-gemcitabine: formulation, characterization and anticancer activity evaluation, Nanoscale, 2 (2010), pp. 1521‑1526

[16] W.-G. Chung, M.A. Sandoval, B.R. Sloat, D.S.P. Lansakara-P, Z. Cui, Stearoyl gemcitabine nanoparticles overcome resistance related to the over-expression of ribonucleotide reductase subunit M1, J Control Release, 157 (2012), pp. 132-140

[17] B. Heurtault, P. Saulnier, B. Pech, J.-E. Proust, J.-P Benoit, A novel phase inversion-based process for the preparation of lipid nanocarriers, Pharm Res, 19 (2002), pp. 875‑880

[18] B. Heurtault, P. Saulnier, B. Pech, M.-C. Venier-Julienne, J.-E. Proust, R. Phan-Tan-Luu, et al., The influence of lipid nanocapsule composition on their size distribution, Eur J Pharm Sci, 18 (2003), pp. 55‑61

[19] S. Vrignaud, J. Hureaux, S. Wack, J.-P. Benoit, P. Saulnier, Design, optimization and in vitro evaluation of reverse micelle-loaded lipid nanocarriers containing erlotinib hydrochloride, Int J Pharm, 436 (2012), pp. 194-200

[20] A.-L. Laine, N.T. Huynh, A. Clavreul, J. Balzeau, J. Béjaud, A. Vessieres, et al., Brain tumour targeting strategies via coated ferrociphenol lipid nanocapsules, Eur J Pharm Biopharm, 81 (2012), pp. 690‑693

[21] E. Allard, F. Hindre, C. Passirani, L. Lemaire, N. Lepareur, N. Noiret, et al., 188Re-loaded lipid nanocapsules as a promising radiopharmaceutical carrier for internal radiotherapy of malignant gliomas, Eur J Nucl Med Mol Imaging, 35 (2008), pp. 1838‑1846

[22] C. Vanpouille-Box, F. Lacoeuille, C. Belloche, N. Lepareur, L. Lemaire, J.-J. LeJeune, et al., Tumor eradication in rat glioma and bypass of immunosuppressive barriers using internal radiation with (188)Re-lipid nanocapsules, Biomaterials, 32 (2011), pp. 6781‑6790

[23] S. David, P. Resnier, A. Guillot, B. Pitard, J.-P. Benoit, C. Passirani, siRNA LNCs--a novel platform of lipid nanocapsules for systemic siRNA administration, Eur J Pharm Biopharm, 81 (2012), pp. 448‑452

[24] M. Morille, C. Passirani, S. Dufort, G. Bastiat, B. Pitard, J.-L. Coll, et al., Tumor transfection after systemic injection of DNA lipid nanocapsules, Biomaterials, 32 (2011), pp. 2327‑2333

[25] A. Paillard, F. Hindré, C. Vignes-Colombeix, J.-P. Benoit, E. Garcion, The importance of endo-lysosomal escape with lipid nanocapsules for drug subcellular bioavailability, Biomaterials, 31 (2010), pp. 7542‑7554

[26] S. Hirsjärvi, S. Dufort, J. Gravier, I. Texier, Q. Yan, J. Bibette, et al., Influence of size, surface coating and fine chemical composition on the in vitro reactivity and in vivo biodistribution of lipid nanocapsules versus lipid nanoemulsions in cancer models, Nanomedicine, 9 (2012), pp. 375-387

[27] E. Bourseau-Guilmain, J. Béjaud, A. Griveau, N. Lautram, F. Hindré, M. Weyland, et al., Development and characterization of immuno-nanocarriers targeting the cancer stem cell marker AC133, Int J Pharm, 423 (2012), pp. 93‑101

[28] A. Béduneau, P. Saulnier, F. Hindré, A. Clavreul, J.-C. Leroux, J.-P. Benoit, Design of targeted lipid nanocapsules by conjugation of whole antibodies and antibody Fab' fragments, Biomaterials, 28 (2007), pp. 4978‑4990

[29] Béatrice Heurtault, P. Saulnier, J.-E. Proust, B. Pech, J. Richard, J.-P. Benoit, Lipidic nanocapsules: preparation process and use as Drug Delivery Systems, U.S. Patent WO02688000, 2000

[30] K. Shinoda, H. Saito, The Stability of O/W type emulsions as functions of temperature and the HLB of emulsifiers: The emulsification by PIT-method, J Colloid Interface Sci, 30 (1969), pp. 258‑263

[31] N. Anton, P. Saulnier, C. Gaillard, E. Porcher, S. Vrignaud, J.-P. Benoit, Aqueous-core lipid nanocapsules for encapsulating fragile hydrophilic and/or lipophilic molecules, Langmuir, 25 (2009), pp. 11413‑11419

[32] S. Vrignaud, J.-P. Benoit, P. Saulnier, Strategies for the nanoencapsulation of hydrophilic molecules in polymer-based nanoparticles, Biomaterials, 32 (2011), pp. 8593‑8604

[33] B.R. Sloat, M.A. Sandoval, D. Li, W.-G. Chung, D.S.P. Lansakara-P, P.J. Proteau, et al., In vitro and in vivo anti-tumor activities of a gemcitabine derivative carried by nanoparticles, Int J Pharm, 409 (2011), pp. 278-288

[34] X.. Shu, K.. Zhu, W. Song, Novel pH-sensitive citrate cross-linked chitosan film for drug controlled release, Int J Pharm, 212 (2001), pp. 19‑28

[35] S. Hwang, Q. Shao, H. Williams, C. Hilty, Y.Q. Gao, Methanol strengthens hydrogen bonds and weakens hydrophobic interactions in proteins--a combined molecular dynamics and NMR study, J Phys Chem B, 115 (2011), pp. 6653‑6660

[36] M. Humbert, N. Castéran, S. Letard, K. Hanssens, J. Iovanna, P. Finetti, et al., Masitinib Combined with Standard Gemcitabine Chemotherapy: In Vitro and In Vivo Studies in Human Pancreatic Tumour Cell Lines and Ectopic Mouse Model, PLoS ONE, 5 (2010), pp. e9430

[37] W. Wang, X. Liu, G. Liu, C. Tang, L. Qu, W. Wang, The difference between multi-drug resistant cell line H460/Gem and its parental cell NCI-H460, Chinese-German J Clin Oncol, 7 (2011), pp. 615‑619

[38] Jurgen-Hinrich Fuhrhop, W. Helfrich, Fluid and solid fibers made of lipid molecular bilayers, Chem Rev, 93 (1993), pp. 1565‑1582

[39] Y.-A. Shchipunov, Self-organising structures of lecithin, Russian Chem Rev, 66 (1997), pp. 301‑322

[40] S. Murdan, G. Gregoriadis, A.T. Florence, Non-ionic surfactant based organogels incorporating niosomes, STP Pharm Sci, 6 (1996), pp. 44‑48

[41] S. Murdan, B. van den Bergh, G. Gregoriadis, A.T. Florence, Water-in-sorbitan monostearate organogels (water-in-oil gels), J Pharm Sci, 88 (1999), pp. 615‑619

[42] S. Murdan, G. Gregoriadis, A.T. Florence, Interaction of a nonionic surfactant-based organogel with aqueous media, Int J Pharm, 180 (1999), pp. 211-214

[43] S. Murdan, G. Gregoriadis, A.T. Florence, Novel sorbitan monostearate organogels, J Pharm Sci, 88 (1999), pp. 608-614

[44] S. Pisal, V. Shelke, K. Mahadik, S. Kadam, Effect of organogel components on in vitro nasal delivery of propranolol hydrochloride, AAPS Pharm Sci Tech, 5 (2004), pp. e63

[45] S. Murdan, T. Andrýsek, D. Son, Novel gels and their dispersions--oral drug delivery systems for ciclosporin, Int J Pharm, 300 (2005), pp. 113-124

[46] S. Murdan, G. Gregoriadis, A.T. Florence, Sorbitan monostearate/polysorbate 20 organogels containing niosomes: a delivery vehicle for antigens?, Eur J Pharm Sci, 8 (1999), pp. 177-186

[47] D. Grace, J. Rogers, K. Skeith, K. Anderson, Topical diclofenac versus placebo: a double blind, randomized clinical trial in patients with osteoarthritis of the knee, J Rheumatol, 26 (1999), pp. 2659-2663

[48] P. Mahler, F. Mahler, H. Duruz, M. Ramazzina, V. Liguori, G. Mautone, Double-blind, randomized, controlled study on the efficacy and safety of a novel diclofenac epolamine gel formulated with lecithin for the treatment of sprains, strains and contusions, Drugs Exp Clin Res, 29 (2003), pp. 45-52

[49] G. Spacca, A. Cacchio, A. Forgács, P. Monteforte, G. Rovetta, Analgesic efficacy of a lecithin-vehiculated diclofenac epolamine gel in shoulder periarthritis and lateral epicondylitis: a placebo-controlled, multicenter, randomized, double-blind clinical trial, Drugs Exp Clin Res, 31 (2005), pp. 147-154

[50] S. Murdan, G. Gregoriadis, A.T. Florence, Inverse toroidal vesicles: precursors of tubules in sorbitan monostearate organogels, Int J Pharm, 183 (1999), pp. 47‑49

[51] C. Bhattacharya, N. Kumar, S. Sagiri, K. Pal, S. Ray, Development of span 80-tween 80 based fluid-filled organogels as a matrix for drug delivery, J Pharm Bioallied Sci, 4 (2012), pp. 155

[52] T.R. Hoare, D.S. Kohane, Hydrogels in drug delivery: Progress and challenges, Polymer, 49 (2008), pp. 1993‑2007

[53] D. Seliktar, Designing Cell-Compatible Hydrogels for Biomedical Applications, Science, 336 (2012), pp. 1124‑1128

[54] N. MacKinnon, G. Guérin, B. Liu, C.C. Gradinaru, P.M. Macdonald, Liposome−Hydrogel Bead Complexes Prepared via Biotin−Avidin Conjugation, Langmuir, 25 (2009), pp. 9413‑9423

[55] S. Mourtas, S. Fotopoulou, S. Duraj, V. Sfika, C. Tsakiroglou, S.G. Antimisiaris, Liposomal drugs dispersed in hydrogels. Effect of liposome, drug and gel properties on drug release kinetics, Colloids Surf B Biointerfaces, 55 (2007), pp. 212‑221

[56] A.C. Silva, M.H. Amaral, E. González-Mira, D. Santos, D. Ferreira, Solid lipid nanoparticles (SLN) - based hydrogels as potential carriers for oral transmucosal delivery of Risperidone: Preparation and characterization studies, Colloids Surf B Biointerfaces, 93 (2012), pp. 241‑248

[57] M.A. Casadei, F. Cerreto, S. Cesa, M. Giannuzzo, M. Feeney, C. Marianecci, et al., Solid lipid nanoparticles incorporated in dextran hydrogels: A new drug delivery system for oral formulations, Int J Pharm, 325 (2006), pp. 140‑146

[58] D. Ma, H.-B. Zhang, K. Tu, L.-M. Zhang, Novel supramolecular hydrogel/micelle composite for co-delivery of anticancer drug and growth factor, Soft Matter, 8 (2012), pp. 3665‑3672

[59] S. Zhu, D.S.P. Lansakara-P., X. Li, Z. Cui, Lysosomal Delivery of a Lipophilic Gemcitabine Prodrug Using Novel Acid-Sensitive Micelles Improved Its Antitumor Activity, Bioconjugate Chem, 23 (2012), pp. 966‑980

[60] T. Dipen, P. Amit, P. Vipul P., A. Samir A., D. Tusharbindu R., Trend of injectable hydrogel in formulation and research., American J PharmTech Research, 2 (2012), pp. 1‑13

[61] H.W. Seo, D.Y. Kim, D.Y. Kwon, J.S. Kwon, L.M. Jin, B. Lee, et al., Injectable intratumoral hydrogel as 5-fluorouracil drug depot, Biomaterials, 34 (2013), pp. 2748‑2757

[62] D. Chen, M. Niu, X. Jiao, K. Zhang, J. Liang, D. Zhang, Inhibition of AKT2 Enhances Sensitivity to Gemcitabine via Regulating PUMA and NF-κB Signaling Pathway in Human Pancreatic Ductal Adenocarcinoma, Int J Mol Sci, 13 (2012), pp. 1186‑1208

[63] S. Cai, Q. Yang, T.R. Bagby, M.L. Forrest, Lymphatic drug delivery using engineered liposomes and solid lipid nanoparticles, Adv Drug Deliv Rev, 63 (2011), pp. 901‑908

Publication N°2

Avant-propos

Cette partie traite des propriétés *in vitro* et *in vivo* de l'hydrogel de LNCs chargées en gemcitabine modifiée (Gem-C12). Différentes caractérisations *in vitro* ont montré une relation entre la dureté du gel et la libération des LNCs à partir de celui-ci. De plus, des études de stabilité (taille des LNCs, taux d'encapsulation en Gem-C12) ont été effectuées sur la forme hydrogel en présence d'huile, pouvant simuler en première intention la présence de tissu adipeux autour de l'hydrogel suite à une injection sous-cutanée. Les formes LNCs gélifiées et LNCs en suspension (une fois diluées dans un tampon aqueux) ont été utilisées pour suivre le devenir de ces nanocapsules lipidiques (LNCs) après injection sous-cutanée (*s.c.*) ou intraveineuse (*i.v.*) chez la souris immunodéficiente non porteuse de tumeur. De façon intéressante, les LNCs se sont fortement localisées dans les ganglions lymphatiques répartis autour du site d'injection après administration *s.c* et dans les ganglions lymphatiques de l'organisme entier après injection *i.v*.. De plus, l'injection *s.c.* sous forme de gel a empêché une accumulation des LNCs dans le foie et la rate. Le ciblage ganglionnaire par des nanoparticules est un moyen potentiel de traiter les cancers métastatiques. Ces résultats suggèrent que l'hydrogel après injection sous-cutanée pourrait être une formulation utilisable en chimiothérapie pour le traitement du cancer pulmonaire métastatique. La cytotoxicité des LNCs chargées en Gem-C12 a ainsi été testée sur une lignée cancéreuse : Ma44-3, lignée cellulaire connue pour former des métastases dans le médiastin après l'implantation intrapulmonaire. Il a été démontré une cytotoxicité supérieure à la gemcitabine native. Cette publication sera soumise prochainement dans le journal « *European Journal of Pharmaceutics and Biopharmaceutics* »

Aqueous suspension and hydrogel of gemcitabine prodrug-loaded lipid nanocapsules: *in vitro* behavior and *in vivo* tissue distribution

Elodie MOYSAN [1, 2], Nathalie WAUTHOZ[1, 2], Yolanda GONZÁLEZ-FERNÁNDEZ [1, 2], Nolwenn LAUTRAM[1, 2], Kazuya KONDO [3], José HUREAUX[1,4], Guillaume BASTIAT [1, 2, *] and Jean-Pierre BENOIT [1, 2]

[1] LUNAM Université – Micro et Nanomédecines Biomimétiques, F-49933 Angers, France

[2] INSERM – U1066 IBS-CHU, F-49933 Angers, France

[3] Department of Oncological and Regenerative Surgery, School of Medicine, University of Tokushima, Kuramoto-cho, Tokushima 770-8503, Japan

[4] Pneumology Department, Academic Hospital, Angers, F-49933, France

***** To whom correspondence should be addressed:

Tel : +33 244688531 ; Fax: +33 244688546 ; E-mail adresse : guillaume.bastiat@univ-angers.fr

Abstract

Gem-C12, a lipophilic form of gemcitabine (modified with lauroyl chain), one of the widely used anticancer agents, was encapsulated in lipid nanocapsules (LNCs) and a hydrogel was spontaneously formed depending on prodrug loading and LNC concentration. *In vitro* study of the hydrogel dissolution showed a relationship between the gel hardness and the LNC release liberation in the aqueous buffer. The modification of the LNC surface with longer PEG chains did not improve the furtivity of the nanocarrier but the Gem-C12 located in the surfactant shell of LNCs did, observed after *in vitro* CH50 experiments. Cytotoxicity of LNCs loaded with Gem-C12 was higher than free non-modified gemcitabine on a Ma44-3 cell line (lung cancer cells). This cell line is known to rapidly develop metastases in the mediastinum after intrapulmonary implantation. Finally, the *in vivo* behaviors of Gem-C12-loaded LNCs in hydrogel and in suspension forms were investigated after subcutaneous and intravenous injection in healthy nude mice. Interestingly, LNCs accumulated strongly in lymph nodes close to the injection site after subcutaneous administration. In addition, injection of the hydrogel form prevented the LNC accumulation in liver and spleen. These results suggested that Gem-C12-loaded LNCs in hydrogel form could be subcutaneously injected for metastatic lung cancer therapy.

Keywords : Hydrogel, gemcitabine prodrug, lipid nanocapsules, biodistribution, lymph nodes.

1. Introduction

Nanomedicine, an emerging new field created by the application of nanotechnology to medicine, is one of the most promising areas for the development of targeted therapies for cancer treatment [1]. Preclinical evaluation such as *in vivo* biodistribution of nanomedicines is one of the essential steps to decide the pursuit of the development, and *in vivo* nanoparticle behaviors depended on the size, shape, composition, surface chemistry and administration routes of the nanocarrier [2].
Our group had developed and patented synthetic particles called lipid nanocapsules (LNCs) with tunable size between 20 and 100 nm [3]. The liquid core of the spherical nanoparticles is made up of triglycerides, surrounded by a compact surfactant shell made of pegylated-hydroxystearate and phospholipids. LNCs structure was obtained by a solvent free low-energy process and surface modification can be performed by post-insertion of amphiphilic molecules [4]. Various drugs can be encapsulated inside LNCs [5-8], and the accumulation of the nanocarriers in tumors or in lymph nodes after intravenous injection was already demonstrated [4,9-11].

Gemcitabine, an anticancer drug [12], was chemically modified with lauroyl chain (Gem-C12) to improve its hydrophobicity and this prodrug was successfully encapsulated inside LNCs [13]. A hydrogel was spontaneously formed depending on the LNC and prodrug concentrations. The gel form was due to inter-nanoparticle association of Gem-C12-loaded LNCs, with interactions between the gemcitabine moieties (because of H-bond formation) of Gem-C12 located at the LNC interface. This hydrogel was obtained without the addition of synthetic or natural polymers. The hydrogel can be injected by a syringe avoiding any surgical procedure and this gel form could be stored directly in syringes because a high stability of Gem-C12-loaded LNCs was observed. Finally, after gel dissolution in an excess of buffer, LNCs in suspension were found and their size was similar to non-loaded LNC ones, and the cytotoxic activity of Gem-C12-loaded LNC was confirmed against pancreas and lung cancer cell lines [13].

In this study, *in vitro* behaviors of hydrogel and suspension of Gem-C12-loaded LNCs were studied. Gem-C12 loading rate was followed as a function of time and gel dissolution properties were determined at different gel hardness, to mimic the

behavior of a hydrogel after subcutaneous administration. Post-insertion of a lipid PEG derivative, 1,2-distearoyl-sn-glycero-3-phosphoethanolamine-N-[maleimide(polyethyleneglycol)-2000] (DSPE-mPEG$_{2000}$) into the LNC membrane was assessed to make the LNCs more stealthy, and therefore to mimic the behavior of a pegylated LNC suspension after intravenous administration. *In vitro* cytotoxicity of diluted nanocarriers was tested on a highly metastatic lung carcinoma cell line (Ma44-3). Finally, *in vivo* biodistribution of fluorescent LNCs and pharmacokinetic studies were performed in healthy nude mice. The effects of LNCs form (suspension and gel) and injection routes (intravenous and subcutaneous) were assessed.

2. Materials and methods

2.1. Chemicals and biochemicals

Labrafac® WL 1349 (caprylic-capric acid triglycerides) (Labrafac) was generously provided by Gattefossé S.A. (Saint-Priest, France). Kolliphor® HS15 (formerly Solutol® HS15; mixture of free polyethylene glycol 660 and polyethylene glycol 660 hydroxystearate) (Kol) were kindly supplied by BASF (Ludwigshafen, Germany). Deionized water was obtained from a Milli-Q plus system (Millipore, Paris, France). Nile Red, Span® 80 (Span 80), Tween® 80 (Tween 80), sodium chloride, gemcitabine hydrochloride were purchased from Sigma (St Quentin-Fallavier, France). 3-(4,5-dimethylthiazol-2-yl)-5-(3-carboxymethoxyphenyl)-2-(4-sulfophenyl)-2H-tetrazolium (MTS) was purchased from Promega (Charbonnières-les-Bains, France). 1,1'-Dioctadecyl-3,3,3',3'-tetramethylindodicarbocyanine 4-chlorobenzenesulfonate salt (DiD) was provided by Life Technologies (Saint-Aubin, France). Methanol was purchased from Fischer Scientific (Loughborough, United Kingdom). 4-(*N*)-lauroyl-gemcitabine (Gem-C12) was synthesized as described elsewhere [13]. All reagents and solvents were used as received.

2.2. Ma44-3 cell line and culture conditions

Ma44-3 cells (a human lung carcinoma cell line which forms lymph node metastases in the mediastinum) were kindly provided by Dr. Kondo (Department of Oncological and Regenerative Surgery, School of Medicine, University of Tokushima, Japan). This cell line was cultured in RPMI 1640 with 10% (*v/v*) heat-inactivated fetal bovine serum (BioWhittaker, Verviers, Belgium) and maintained at 37℃ in CO_2/air mixture

(5/95 *v/v*). Medium was complemented with fetal bovine serum (10% *v/v*), penicillin (100 U/mL), streptomycin (100 µg/mL) and amphotericin B (0.250 µg/mL) from Sigma (St Quentin-Fallavier, France).

2.3. LNC and PEGylated LNC preparation

LNC formulations were based on a phase inversion process as already described [14]. For loaded-LNC formulations, Gem-C12 was first solubilized in a mixture of Labrafac and Span 80 at concentrations from 5 to 7.5% (ratio Gem-C12/Labrafac *w/w*) at room temperature, before the addition of Kol, NaCl and water. For 29nm-Z-Ave LNC, $m_{Labrafac}$ = 0.75g, m_{Kol} = 1.25g, m_{Span80} = 0.25g, m_{water} = 1.02g and m_{NaCl} = 0.045g. For 55nm-Z-Ave LNC, $m_{Labrafac}$ = 1.24g, m_{Kol} = 0.967g, m_{Span80} = 0.25g, m_{water} = 1.02g and m_{NaCl} = 0.045g. Mixtures were heated to 75°C under magnetic stirring followed by cooling to 45°C (rate of 5°C/min). This cycle was repeated three times [13]. In the last temperature decrease, 2.12 g of water was added. Afterward, a slow magnetic stirring was applied to the LNC suspension at room temperature and a hydrogel formed spontaneously, with a waxy aspect. Gelation process was considered as achieved after 24h at 4°C. In addition, syringes with 19 Gauge (Ø 1.1mm) needles were fulfilled with the LNC suspension (before the gel formation) and stored at 4°C. This hydrogel was due to Gem-C12 loading as already described [13] and non-loaded LNCs at the similar concentrations were in suspension form. Gem-C12-loaded LNC hydrogel can be dissolved with water to obtain nanoparticles in suspension (transition hydrogel/suspension at LNC concentration of about 90 mg/mL).

To obtain fluorescent dye-labeled LNCs, a solution of DiD in acetone or Nile Red directly in powder was incorporated in Labrafac (0.1% dye/Labrafac *w/w*). Acetone was evaporated before starting the formulation process. The incorporation of fluorescent dyes did not prevent the hydrogel formation.

To perform the post-insertion, 18mg of DSPE–$mPEG_{2000}$ (Avanti Polar Lipids, Alabaster, USA) were incubated at 60 °C during 1h45 with 89 mg/mL of LNCs in suspension. The resulting mixture (2 mL) was dialysed (cutoff of 15 kDa, Spectrum Laboratories, Breda, The Netherlands) against water at 25°C under magnetic stirring to separate the post-inserted LNCs from free DSPE–$mPEG_{2000}$ micelles. The

outcome of the surface modification was verified by size and zeta potential measurements.

2.4. Physicochemical characterization

Hydrodynamic diameter: Z-Average (Z-Ave), polydispersity index (PdI) and zeta potential (Pz) of LNCs were determined by dynamic light scattering on a Zetasizer® Nano serie DTS 1060 (Malvern Instruments S.A., Worcestershire, United Kingdom). The helium–neon laser, 4 mW, operates at 633 nm, with the scatter angle fixed at 173° and the temperature maintained at 25 ℃. The c urve fittings of the correlation functions were performed using an exponential fit (Cumulant approach) for Z-Ave and PdI determinations for LNC suspensions. Smoluchowski's approximation was used to determine electrophoretic mobility for Pz determination. The measurements were performed in triplicate, with LNC concentration at 7.5 mg/mL after dilution in deionized water.

2.5. Evaluation of drug loading efficacy

The entrapment efficiency was determined by an UPLC method already described [13]. Total quantities of Gem-C12 in the LNC suspension were determined without filtration and dialysis, by methanol disruption of LNC (1/36 *v/v*). These solutions were injected into a C18 column (1.7 x 100mm, ACQUITY UPLC BEH C18) equipped with a column guard, with a flow rate of 0.343 mL/min (methanol as elution solvent). The drug concentration was calculated from a linear titration curve, with freshly Gem-C12 methanol solutions at concentration ranging from 1 to 100 µg/mL.

2.6. Complement activation

The complement consumption was evaluated in normal human serum (NHS) (provided by the Etablissement Français du Sang, CHU, Angers, France) by measuring the residual haemolytic capacity of the serum complement after contact with LNCs. The technique consisted in determining the amount of serum able to hemolyze 50% of a fixed number of sensitized sheep erythrocytes in presence of rabbit anti-sheep erythrocyte antibodies (CH50) [15]. In order to compare nanoparticles with different mean diameters, the results were expressed in terms of surface area. Nanoparticle surface area was calculated by the following equation:

$S = n \times 4\pi R^2$ and $V = n \times \frac{4\pi R^3}{3}$ leading to $S = \frac{3 \times m}{R \times \rho}$

where S is the surface area (cm^2) and V the volume (cm^3) of n spherical LNCs in suspension (1 mL) of average radius R (cm). m the total weight (g) of the n spherical LNCs in suspension (1 mL) and ρ the density (taken as ρ = 1 g/cm^3) [16]. All experiments were performed in triplicate.

2.7. Proliferation assay

The cytotoxicity of diluted GemC12-loaded LNCs was determined using MTS test. Non-loaded LNCs, gemcitabine hydrochloride and pure Gem-C12 (in water/ethanol/Tween 80 87.6/5.5/6.9 *v/v/v*) were used as control. Ma44-3 cells were seeded into 96-well plates (15,000 cells/well) and incubated at 37℃ under CO_2/air mixture (5/95 *v/v*) overnight. On day 2, cells were treated with free Gem-C12, gemcitabine hydrochloride, non-loaded LNCs and Gem-C12-loaded LNCs in the drug concentration ranging from 1 to 100 µmol/L. There was no prodrug inside non-loaded LNC, but dilutions were performed in the same way that for Gem-C12-loaded LNC for comparison purposes. The number of cells alive was determined using a MTS assay (colorimetric assay based on the conversion of a tetrazolium salt into formazan). Formazan absorbance was measured at 492 nm and 750 nm, directly from 96-well plates by spectrophotometry (Multiskan, Ascent, Thermo Fisher Scientific, Courtaboeuf, France), after exposition to MTS (20 µL/well) for 2.5 h at 37 ℃. The maximal absorbance was determined by incubating cells with culture media and was considered as 100% survival. These experiments were repeated three times.

2.8. In vitro transfer of Gem-C12 against a lipophilic phase

Encapsulation stability of Gem-C12 in LNCs was determined in lipophilic condition. An excess amount of oily phase (Labrafac) was added to screw-capped test tube containing Gem-C12-loaded LNCs in suspension or in gel state. After sealing, tubes were vigorously shaken at 25℃ or 37℃ until 48h. E ach tube was centrifuged at 14,000 rpm for 30 min to separate the LNCs from the excess of Labrafac and the amount of Gem-C12 in the supernatant (Labrafac) was determined by UPLC. The size of LNCs in suspension was measured at each time point and all the experiments were repeated 3 times.

2.9. LNC release from the gel dissolution

Gem-C12-loaded LNCs in gel form, containing Nile Red, were used to study the release of LNCs from the gel. Directly after LNCs formulation, 200 µL of LNC suspension were placed into a spectrometry cuvette to form a hydrogel (one night at 4°C). PBS (1.8 mL at pH 6.5 or 7.4), preheated at 37 °C, was added on top of the hydrogel and the cuvettes were incubated at 37°C. Samples of 200 µL of buffer were collected and replaced by 200µL of pre-heated PBS to maintain constant volume. Hydrogel dissolution (presence of LNCs in buffer) was followed by fluorescence (Fluoroskan, Ascent, Thermo Fisher Scientific, Courtaboeuf, France) (ex/em 515/590 nm) and the size distribution was measured. The total hydrogel dissolution (100% of LNCs in suspension) was obtained by fluorescence, mixing 200µl of Gem-C12-loaded LNCs containing Nile Red in suspension (directly after LNCs formulation) with 1.8 mL of PBS. All the experiments were repeated 3 times.

2.10. In vivo biodistribution and pharmacokinetics

Nine weeks-old female nude SWISS mice (Harlan, Gannat, France) were housed and maintained at the University animal facility (SCAHU). All the animal experiments were performed in agreement with the EEC guidelines and the "Principles of Laboratory Animal Care" (NIH Publication No. 86-23, revised 1985) and with the agreement of Comité d'Ethique pour l'Expérimentation Animale des Pays-de-la-Loire (authorization CEEA; 2012-37). Mice ($n = 5$ for each group) were anesthetized (isoflurane). 110µL of Gem-C12-loaded LNC containing DiD in gel form (Z-Ave = 55nm) were injected subcutaneously behind the neck. 110µL of non-loaded LNC suspension and containing DiD (no prodrug, Z-Ave = 55nm) were injected either intravenously in the tail vein or subcutaneously behind the neck. LNC concentrations were the same in hydrogel and suspension forms. After various times, from 1h to 2 weeks, the mice were sacrificed and the organs (liver; spleen; kidneys; lung; heart; stomach; intestine; and inguinal, axillary, cervical and brachial nodes) and blood (cardiac puncture) were removed. Fluorescence imaging and analysis were performed using a fluorescence imaging system (CRI Maestro^{TM}, Woburn, MA, USA). Semi-quantitative data were obtained by using a time exposition of 10 ms between 630 and 600 nm, unmixing the generated cube, extracting the background and drawing the regions of interest (ROI) from fluorescent images. The number of

photons collected into each ROI was then used to calculate the average signal. The results of organ fluorescence quantifications were expressed in phot/cm²/s.

Each blood sample was centrifuged for 10 min at 2000 g in a venous blood collection tube containing Li-heparin (Tube Micro, 1.3 mL, Sarstedt, Marnay, France). One hundred µL of the supernatant (plasma) were deposited in a black 96-well plate (Greiner Bio-one, Frickenhausen, Germany). Fluorescence was measured using Fluoroskan (ex/em 646/678 nm). The injected dose was normalized as a function of animal weight, assuming the blood represents 7.5% of mouse body weight [17]. DiD concentration in plasma was calculated from linear titration curve, using LNC containing DiD in plasma at concentration range from 0.006 to 12 µg/mL. Pharmacokinetic data were treated by IV bolus and extravascular non-compartmental analysis (for intravenous and subcutaneous administration, respectively) of the quantity of the injected dose versus time profiles with Kinetica 4.1.1 software (Thermo Fisher Scientific, Villebon-sur-Yvette, France). The trapezoidal rule was used to calculate the area under the curve (AUC) during the whole experimental period (from 1 to 336 h) without extrapolation. The half-lifes $t_{1/2}$ were calculated from 1 to 8h for $t_{1/2}$ distribution and from 8 to 336h (suspension intravenous and hydrogel subcutaneous administrations) and from 4 to 336h (suspension subcutaneous administration) for $t_{1/2}$ elimination.

2.11. Statistical analysis

All results were expressed as mean ± SD. Normal distributions were assumed. Statistical analysis was performed by one-way analysis of variance (ANOVA 1F), followed by Scheffe's *post hoc* test for pairwise comparisons. The differences were considered as significant with $p < 0.05$.

3. Results

3.1. Hydrogel preparation and LNC post-insertion

The physico-chemical properties of Gem-C12-loaded LNCs were already examined [13]. Briefly, after the phase-inversion process comprising temperature cycles and water addition during the last phase inversion, LNC suspensions were obtained. Changing Labrafac and Kol compositions, LNC-hydrodynamic diameters (Z-Ave)

were modified and non-loaded LNC of 30.0 ± 0.5 and 67.0 ± 2.0 nm in size were obtained. For all formulations, the polydispersity index was low, meaning a monomodal size distribution. With the encapsulation of Gem-C12 into LNCs, a hydrogel with a waxy aspect was obtained. The gel state was not obtained with non-loaded LNCs or with the encapsulation of other drugs [5-8, 10, 18]. The dissolution of this physical hydrogel led to the LNC separation allowing to recover a suspension of LNCs. For the corresponding 30 and 67-nm non-loaded LNC sizes, Gem-C12-loaded LNC sizes were 29.0 ± 1.0 and 55.5 ± 2.0 nm, respectively. Encapsulation of fluorescent dyes: Nile Red and DiD in addition to Gem-C12 did not change the Z-Ave of LNCs.

DSPE-mPEG$_{2000}$ molecules were post-inserted into the membrane of LNCs as already performed [19] to recover the LNC surface with longer PEG chains. LNC sizes were significantly higher with a charge surface much more negative, proving the success of PEG surface modification. The non-loaded LNCs (67 ± 4 nm) and Gem-C12-loaded LNCs (55.5 ± 2.0 nm) reached 86 ± 4 nm and 66 ± 2 nm after post-insertion, respectively. Pz decreased until -46 ± 7 mV and -43 ± 5 mV for PEG covered non-loaded and Gem-C12-loaded LNCs, respectively (*vs.* -7.5 ± 3.0 mV and -8.0 ± 2.5 mV for non-covered LNCs, respectively).

3.2. Gem-C12 transfer and LNC stability against a lipophilic phase

In vitro Gem-C12 transfer studies were performed in order to test the stability of encapsulation of the drug in the LNCs. LNC size and Gem-C12 encapsulation rate were already described in aqueous medium [13]. Here, the influence of a lipophilic phase in contact with Gem-C12-loaded LNC hydrogel or in suspension was investigated. When LNCs in suspension were vigorously mixed with pure Labrafac as the lipophilic phase during 48h, an increase of LNC sizes from 55 to 95 ± 21 nm (PdI of 0.265) and 142 ± 26 nm (PdI of 0.286) at 25°C and 37°C, respectively, were obtained (Fig. 1A and 1B). The stirring was responsible of the larger LNC size, because after 1 month at 37°C without agitation, LNC sizes were stable (data not shown). This size increase led to LNC destabilization and a transfer of Gem-C12 to the oily phase. At 25°C after 48-h shaking (Fig. 1 A), a slight transfer was observed: 86% of the Gem-C12 was always present into the LNCs. A higher transfer was observed at 37°C (Fig. 1B) for LNCs in suspension: about 50% of Gem-C12 was

present in LNCs after 5h. The behavior of hydrogel and suspension forms was different. At 37℃, Gem-C12 transfer was immediate for LNCs in suspension whereas the transfer of the prodrug started after 5h for the hydrogel.

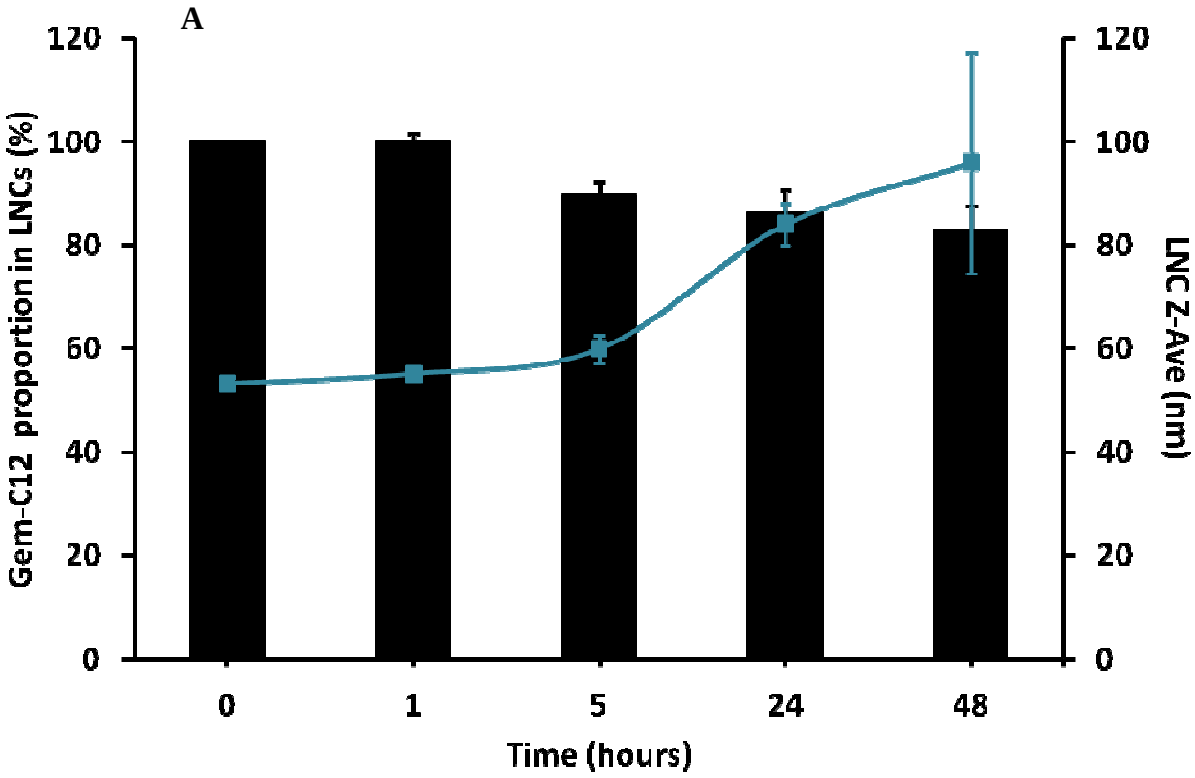

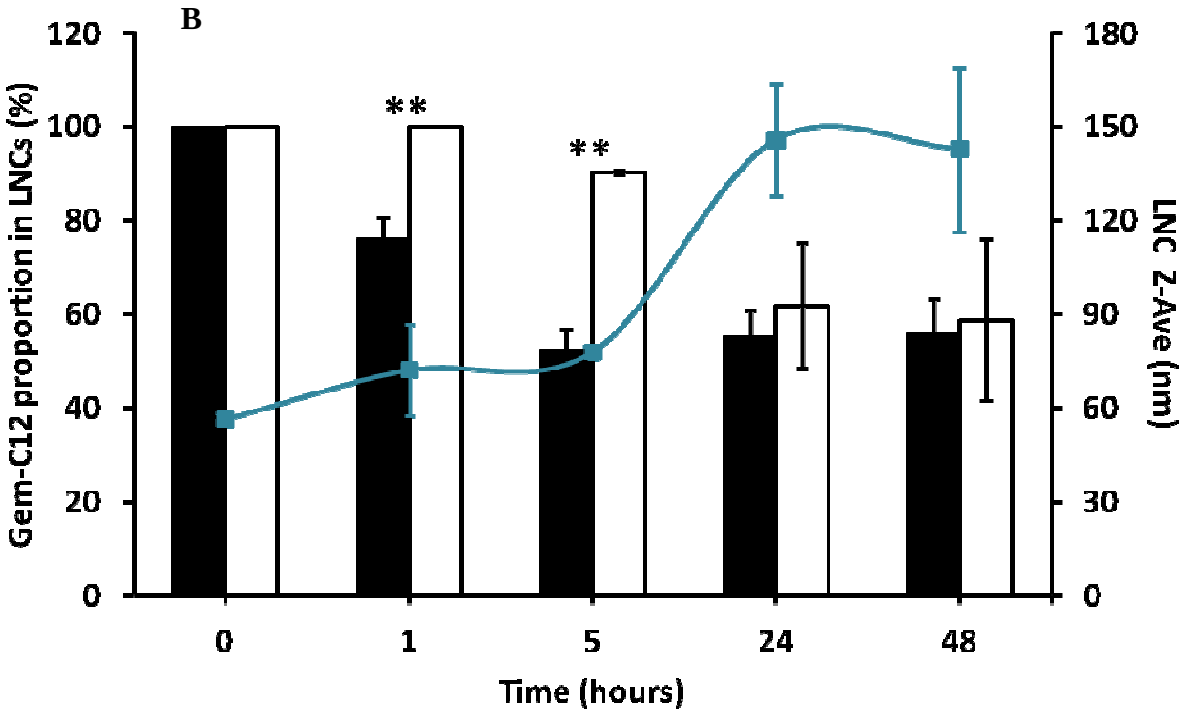

Fig. 1. LNC Z-Ave (blue square) of Gem-C12-loaded LNCs in suspension and Gem-C12 content in LNCs *vs.* time after the contact under stirring of Gem-C12-loaded LNC hydrogel (white bar) and Gem-C12-loaded LNCs in suspension (black bar) with a lipophilic phase (Labrafac), at 25℃ (A) and 37℃ (B). (n=3, mean ± SD, **: $p < 0.01$).

3.3. In vitro hydrogel dissolution

In vitro hydrogel dissolution studies were performed in order to follow the release of LNC from the hydrogel. When the hydrogel of LNCs loaded with 5% of Gem-C12 (Gem-C12/Labrafac *w/w*) was in contact with PBS, a rapid dissolution occurred and reached 100% of LNCs in suspension at 6h and 24h with LNC Z-Ave of 29 and 55 nm, respectively (Fig. 2A and B). No difference was observed by changing the pH: 7.4 and 6.5. For LNC loaded with 7.5% of Gem-C12, (Gem-C12/Labrafac *w/w*), a slower dissolution was observed. About 50% of LNCs were in suspension after 48h for the two LNC Z-Aves. After 1 week, about 70 % of LNC were in suspension with LNC Z-Ave of 29 nm whatever pH, while about 60 and 50% of LNCs in suspension at pH 6.5 and pH 7.4, respectively, were observed for LNC Z-Ave of 55 nm. There was no change in LNC Z-Ave in suspension over the time and whatever the pH (6.5 and 7.4) when the hydrogel was dissolved (data not shown).

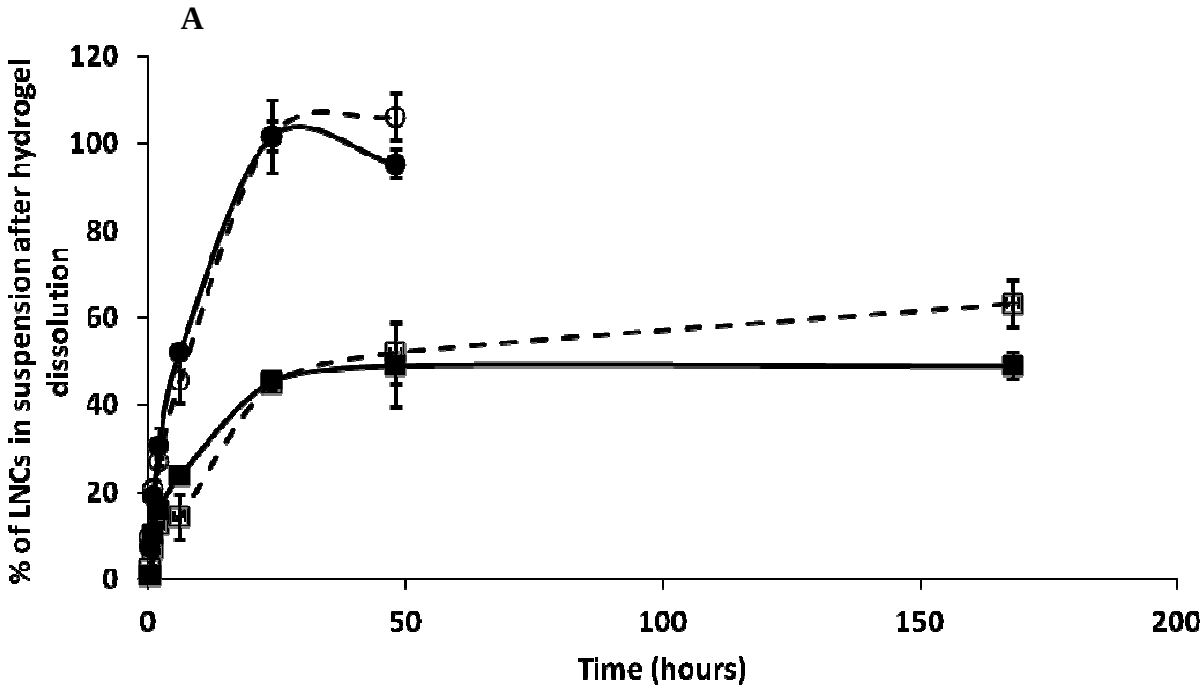

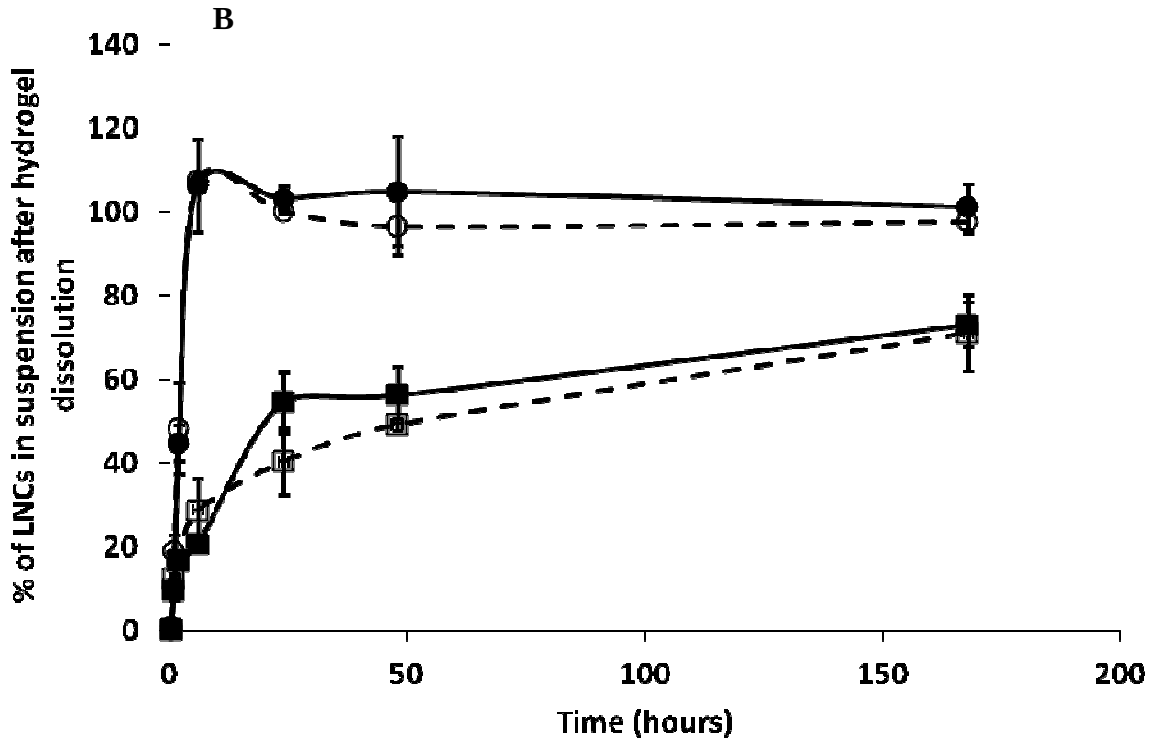

Fig. 2. % of LNCs generated from hydrogel dissolution after incubation in PBS at 37 ℃, at pH = 7.4 (closed symbol, solid line) and pH = 6.5 (open symbol, dotted line). LNC Z-Ave of 55 (A) and 29 nm (B) were loaded with various concentrations of Gem-C12 (●○: 5% and ■□: 7.5% Gem-C12/Labrafac *w/w*). (n=3, mean ± SD).

3.4. Complement activation evaluation

Complement consumption was evaluated as the lytic capacity of the serum towards 50% of antibody-sensitized sheep erythrocytes (CH50 units) after exposure to non-loaded LNCs (Z-Ave of 30 and 67 nm), Gem-C12-loaded LNCs (Z-Ave of 29 and 55 nm), and non-loaded and Gem-C12-loaded LNCs coated with DSPE-mPEG$_{2000}$ (Z-Ave of 66 and 86 nm, respectively). PMMA nanoparticles (Z-Ave of 150 nm), already described as strong complement activator nanoparticles (*e.g.* no PEGylation in surface), were used as control [16].

As already described in literature, LNCs were less complement activator than PMMA nanoparticles [19]. The consumption of CH50 units reached a maximum of 100 % for a low nanoparticle surface area for PMMA, in comparison to all tested LNCs (Fig. 3). Gem-C12 located in the surfactant shell of LNCs decreased the complement activation for LNC Z-Ave of 55 nm in comparison to non-loaded LNCs. The influence

of Gem-C12 was not so clear for lower LNC Z-Ave and the complement activation was similar for non-loaded and Gem-C12-loaded LNCs with LNC Z-Ave of 29 and 30 nm and Gem-C12-loaded LNCs with LNC Z-Ave of 55 nm. The coating of LNC surface with DSPE-mPEG$_{2000}$ led to a slight decrease of complement activation but this effect was not so significant as compared to Gem-C12 effect.

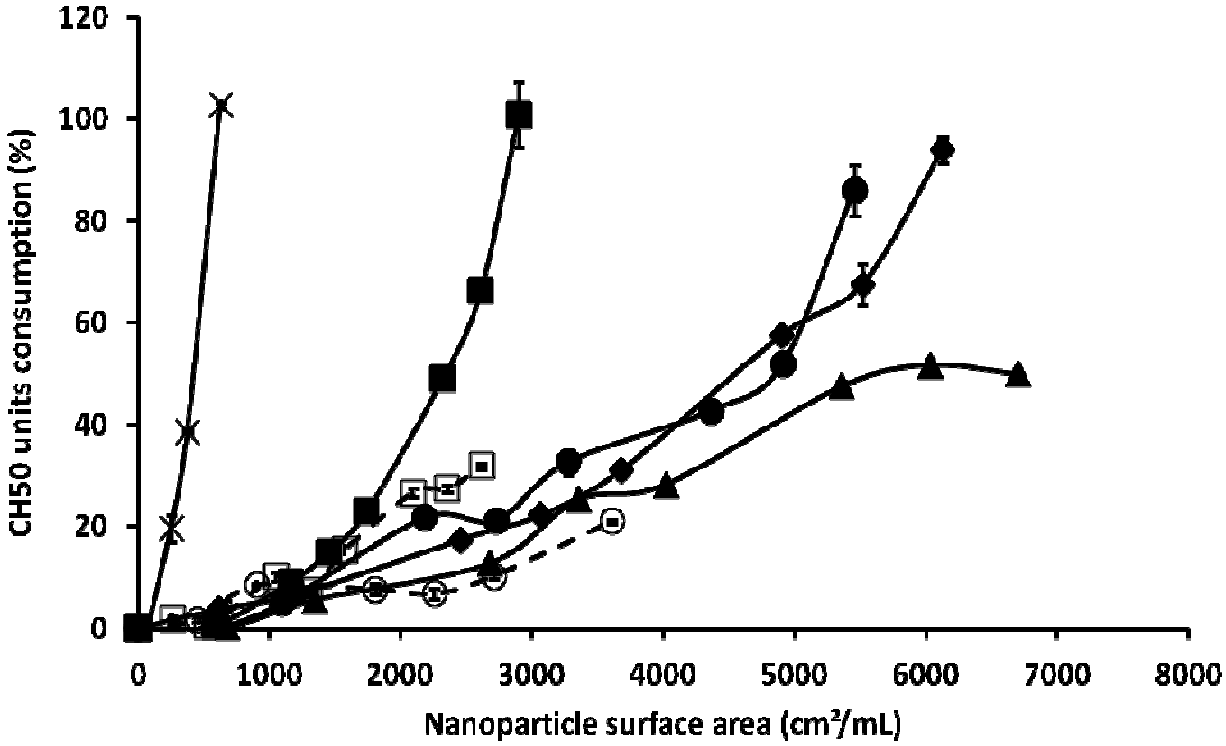

Fig. 3. Complement activation (CH50 units consumption at 37℃ with 1-h incubation) *vs.* nanoparticle surface area (cm^2/mL) of PMMA (×: Z-Ave = 150 nm), non-loaded LNCs (■: Z-Ave = 67 nm and ▲: Z-Ave = 30 nm), Gem-C12-loaded LNC (5% Gem-C12/Labrafac *w/w*) (●: Z-Ave = 55 nm and ◆: Z-Ave = 29 nm), DSPE-mPEG$_{2000}$-covered non-loaded LNCs (□: Z-Ave = 86 nm) and DSPE-mPEG$_{2000}$-covered Gem-C12-loaded LNCs (○: Z-Ave = 66 nm). (n=3, mean ± SD).

3.5. Cytotoxicity on Ma44-3 cell line

In vitro cytotoxicity of LNC loaded with Gem-C12 was tested on a human lung carcinoma cells (Ma44-3). The cells were exposed for 48 h to various concentrations of free gemcitabine hydrochloride, free Gem-C12 (in water/ethanol/Tween 80 87.6/5.5/6.9 *v/v/v*), Gem-C12-loaded LNC (55 nm), or non-loaded LNC (67 nm). The

cell viability profiles are shown in Fig. 4. The negative control: non-loaded LNCs did not reach IC50 in the studied LNC dilution meaning the non toxicity of the empty LNC for Ma44-3 cell line. Gem-C12-loaded LNC, free Gem-C12 and gemcitabine hydrochloride had similar cytotoxicity profiles with a significantly greater cell death for Gem-C12 (loaded in LNCs or not) at high drug concentration than for gemcitabine hydrochloride.

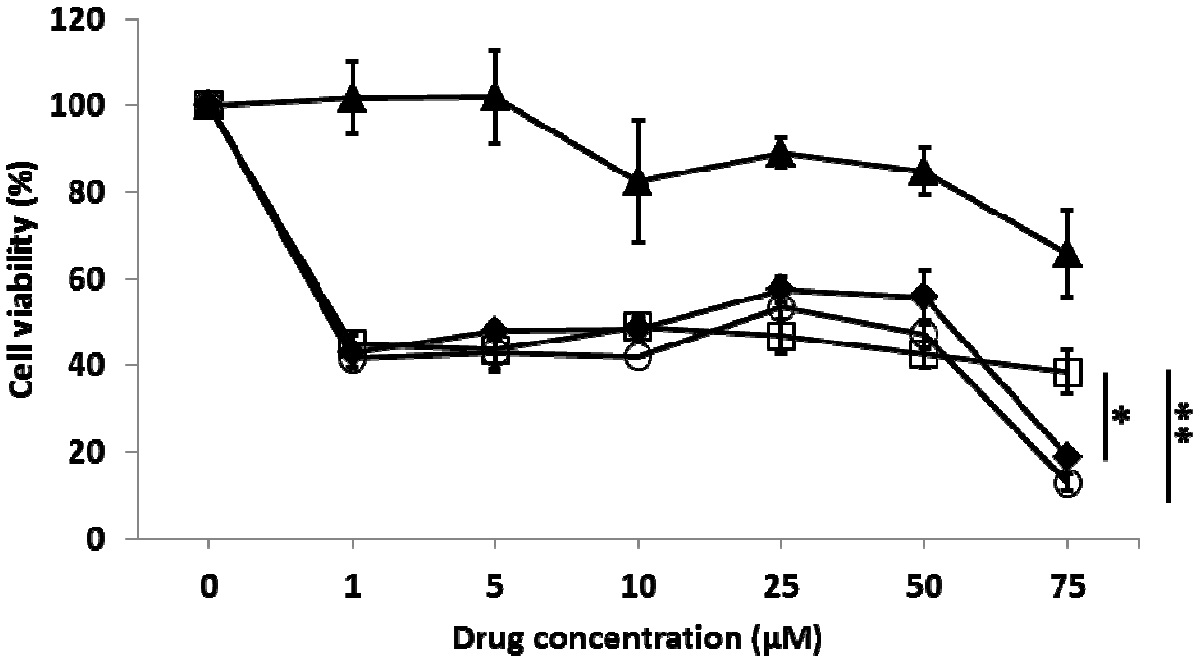

Fig. 4. Cell viability of Ma44-3 cell line *vs*. drug concentration after 48h-incubation with Gem-C12 (○) (solution in water/ethanol/Tween 80 87.6/5.5/6.9 *v/v/v*), gemcitabine hydrochloride (□) (solution in PBS), Gem-C12-loaded LNC (◆) (5% Gem-C12/Labrafac *w/w*) and non-loaded LNCs (▲). There was no Gem-C12 inside non-loaded LNC, but dilution was performed in the same way that for Gem-C12-loaded LNC for comparison. (n=3, mean ± SD; *: $p < 0.05$; **: $p < 0.01$).

3.6. In vivo biodistribution and pharmacokinetics

Fluorescent LNCs were used to evaluate tissue biodistributions and pharmacokinetics after intravenous (*i.v.*) and subcutaneous (*s.c.*) administration in nude SWISS mice. A fluorescent probe, DiD (a near-infrared fluorophore used to limit the autofluorescence wavelength emitted by animals), was encapsulated into LNCs, as already published [4, 9, 20]. Moreover, DiD was used because the dye is weakly

fluorescent in aqueous media, but highly fluorescent in lipophilic vehicles [21]. Images of the extracted organs (Fig. 5) were taken 1, 4, 8, 48, 96, and 336 hours after administration (Fig. 6). Fluorescent-labeled LNCs were injected at a DiD dose of 1.2 mg/kg of animal weight. Gem-C12-loaded LNCs were used to study the hydrogel form (*s.c.* administration) and the LNC suspension form was studied with non-loaded LNCs (*s.c.* and *i.v.* administration) with the same injected LNC concentration.

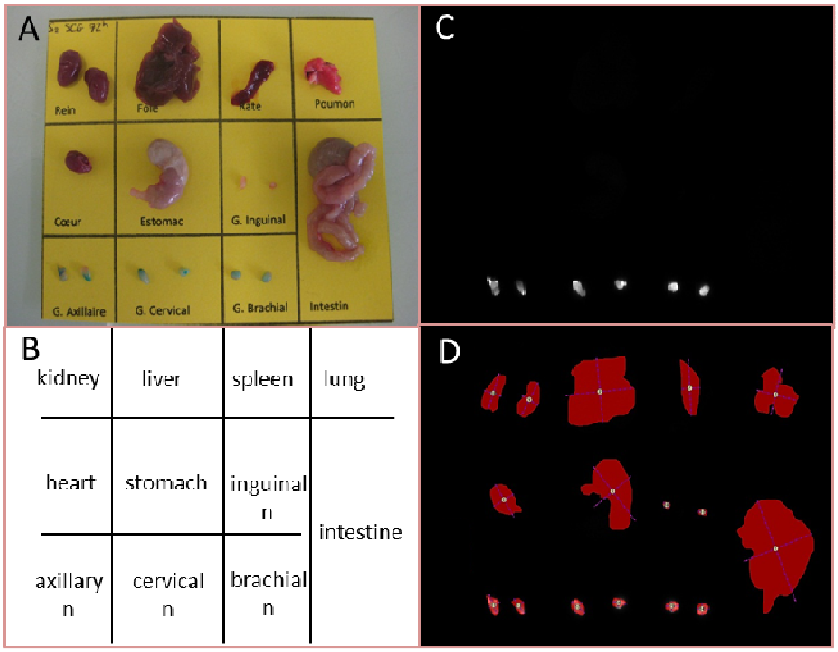

Fig. 5. (A) Extracted organs 72h after subcutaneous injection of Gem-C12-loaded LNCs (5% Gem-C12/Labrafac *w/w*) in hydrogel state. (B) Scheme of extracted organs. (C) Fluorescence signal in the organs (10-ms exposure) (ex: 436 nm; em: 630-800 nm). (D) Regions of interest (ROIs) defined for the extracted organs in order to semi-quantify the amount of photons detected per pixel.

An immediate accumulation in liver and spleen after 4h and 8h was observed when LNC suspension was *i.v.* administered. After 48h, a decrease of the accumulation was observed for these organs to totally disappear after 336h (Fig. 6). A weak accumulation was observed in the liver and spleen for LNCs in suspension injected by *s.c* at 8h and 48h whereas no accumulation was observed with LNCs in hydrogel state. All formulations were homogeneously and rapidly distributed in lymph nodes. However, higher accumulations in the lymph nodes the nearest of the injection site (axillary, brachial and cervical lymph nodes) were obtained after *s.c* injection

comparatively to *i.v* injection. LNCs did not accumulate in the inguinal lymph nodes after *s.c.* hydrogel administration while fluorescence was observed in these lymph nodes after LNC suspension administration, a higher accumulation for *i.v* compared to *s.c.* administration. No significant difference was observed for lymph node biodistribution after these various administrations.

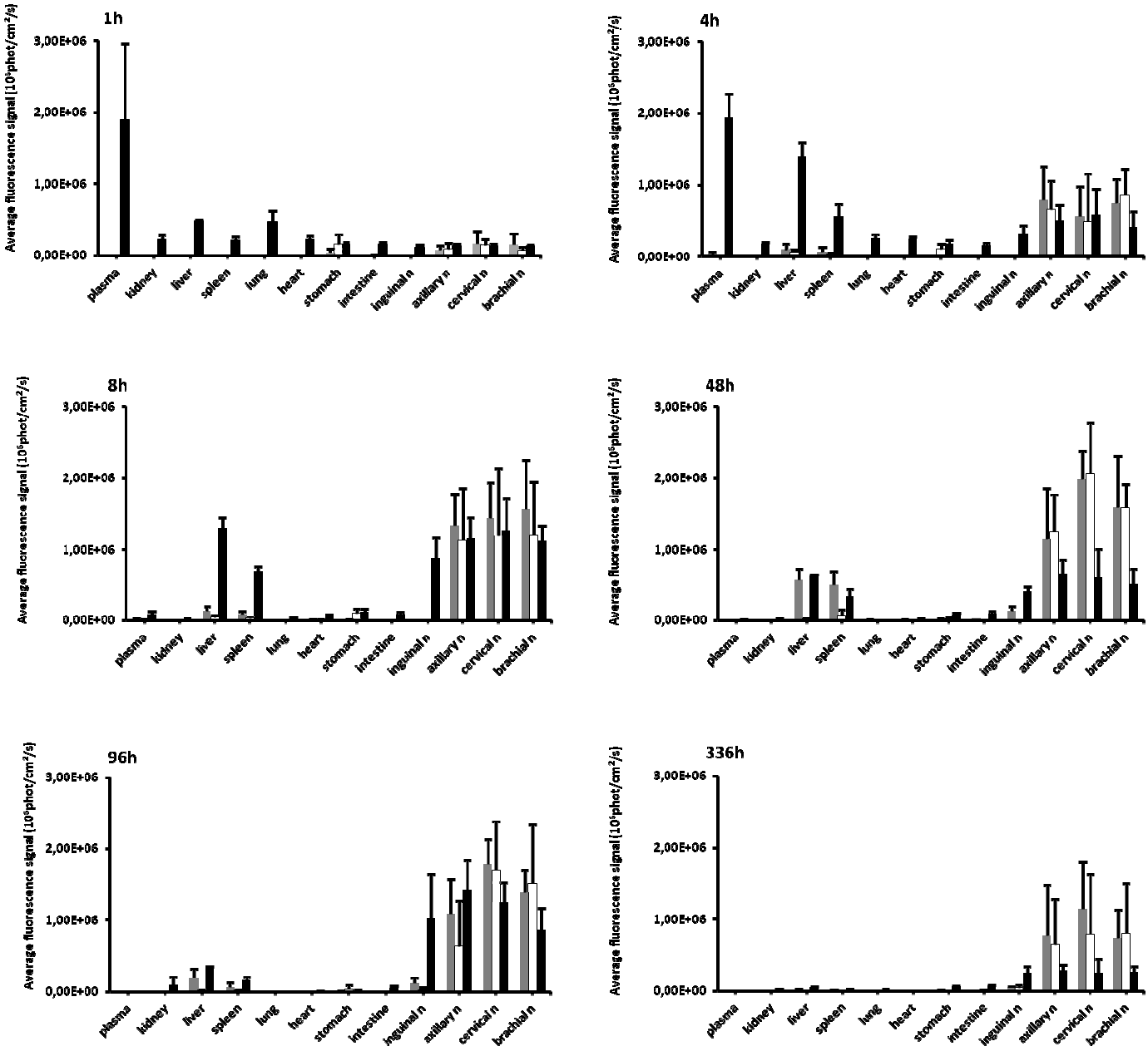

Fig. 6. *In vivo* biodistribution of DiD-labeled LNCs in healthy nude mice, after intravenous injection (tail vein) of LNCs in suspension (no Gem-C12) (Black bar), subcutaneous injection (behind the neck) of LNCs in suspension (no Gem-C12) (Grey bar), and subcutaneous injection (behind the neck) of LNC hydrogel (5% Gem-

C12/Labrafac *w/w*) (White bar). Quantification of the fluorescence signals of the different organs and plasma using fluorescence images (10 ms integration time) (Fig. 5) at various times *post* LNC administrations (1, 4, 8, 48, 96 and 336h). (n after inguinal, axillary, cervical and brachial means nodes). (n=5, mean ± SD).

As described in Table 1 and Fig. 6, a stronger LNC presence was observed in plasma after *i.v* injection with an AUC of 174 µg/mL/h. However, LNCs were quite rapidly cleared from the systemic circulation after their administration with a $t_{1/2}$ elimination of 19h. After *s.c.* injection, lower quantities of fluorescent-LNCs were detected in plasma: AUC of 11 and 4 µg/mL/h for LNCs in suspension and hydrogel form, respectively. Nevertheless, these *s.c* injections exhibited an increase of the $t_{1/2}$ of elimination to reach 32h. With *s.c* injection of LNCs in suspension, a higher C_{max} was obtained comparatively to LNCs injected in the hydrogel state (0.24 *versus* 0.1 µg/mL). While these formulations were *s.c.* administered, the LNCs can reach the systemic circulation, and these results were in agreement with a higher fluorescence found in both liver and spleen with *s.c.* injection of LNCs in suspension.

	T_{max} (h)	C_{max} (µg/mL)	$t_{1/2}$ distribution (h)	$t_{1/2}$ elimination (h)	AUC (µg/mL/h)
***i.v.* LNC suspension**	-	-	1,29	19	174,2
***s.c* LNC suspension**	4	0,24 ± 0,2	N.D	32	10,94
***s.c* LNC hydrogel**	8	0,1 ± 0,03	N.D	32	4,4

Table 1. Main LNC pharmacokinetic characteristics after intravenous (*i.v*) injection (tail vein) of LNC suspension, and subcutaneous (*s.c.*) injections (behind the neck) of LNC suspension or in hydrogel form. LNCs in suspension were non-loaded LNCs and LNCs in hydrogel form were Gem-C12-loaded LNCs (5% Gem-C12/Labrafac *w/w*). (n=5, mean ± SD).

4. Discussion

Nanotechnology is one of the 21st century's most promising technologies [22]. Conventional anticancer treatments, as gemcitabine for pancreas and lung cancers, are nonspecific and at the origin of systemic toxicity, accompanied with undesirable side effects such as damage to the liver and bone marrow [23]. Among these news

technologies, nanovectorization is a promising strategy to enhance the pharmacological properties, the therapeutic index and the targeting of therapeutic agents [2,24]. The present study was conducted to understand the *in vitro* and *in vivo* behaviors of gemcitabine modified-loaded LNC, obtained in hydrogel form or in suspension after hydrogel dissolution, for a future use in lung cancer.

One of the most troublesome obstacles for the treatment of lung cancer is the presence of metastasis in the mediastinal lymph nodes from the primary lesion [25]. The inability to remove all the lymph node metastases remains the primary cause of cancer death [26]. Recent studies in our laboratory have demonstrated the capacity of LNCs to passively target the lymph nodes after intravenous injection in mice bearing different tumors [4,9]. However the lymphatic system is not easily accessible by intravenous administration, thus limiting the amount of drug that reaches lymphatic tissues including lymph node metastases. After intravenous administration, nanoparticles are rapidly removed from the circulation and accumulate mainly in the liver and spleen due to the opsonization process and the subsequent recognition by the mononuclear phagocyte system (MPS) [27]. A way to overcome this recognition was the addition of PEG chains in particle surface using the post-insertion approach [19]. In this study, LNCs non-covered with DPSE-mPEG$_{2000}$ were used for the biodistribution experiments for a number of reasons. Firstly, Gem-C12-loaded-LNCs covered with DSPE-mPEG$_{2000}$ were not stable 1 month after post-insertion (data not shown). In other words, the surface modification led to LNC destabilization. Secondly, non-covered Gem-C12-loaded LNCs exhibited low complement activation, and the addition of DSPE-mPEG$_{2000}$ did not significantly decrease the CH50 consumption (Fig. 3). It has to be noted that the higher consumption of CH50 units with non-loaded-LNCs (67nm) than for Gem-C12-loaded LNCs (55nm) was correlated with an increase of the nanoparticle size [19]. Thirdly, the lipid nanocapsules were already covered with PEG 660 Da at high density leading to a low macrophage uptake [11]. Nanoparticle steric stabilization with PEG improve nanocarrier way through the interstitium (after subcutaneous injection) to reach lymph circulation by reducing non-specific interactions [28]. However, their increased stealth nature could also reduce the nanocarrier uptake in lymph nodes (macrophage internalization) but it was recently shown that dendritic cells (DCs) were capable of taking up nanoparticles present in the lymph nodes [29, 30].

The biodistribution profiles of these nanocarriers presented interesting behaviors as a function of the injection site and/or the final form. When injected intravenously, nanocapsules were rapidly cleared from the blood circulation and predominantly trapped in the liver and the spleen while these accumulations were weak after subcutaneous injection. Nevertheless at 48h, presence of DiD fluorescence in these two organs was detected after *s.c* injection of LNCs in suspension, probably explained by a stronger way of LNCs in suspension in blood circulation than for the hydrogel form. After *i.v* and *s.c* injections, a sustained fluorescence was detected in lymph nodes. However, more nanocarriers were found in lymph nodes after *s.c* injection compared to *i.v* one. Previously, histological analysis of these lymph nodes demonstrated that most of the fluorescent signal was located in the trabeculae and paracortex [9]. This localization is in correlation which another study which demonstrated that macrophages of paracortex were mainly responsible for particle capture from the lymph [31]. An ongoing study is focusing on the efficiency of the Gem-C12-loaded LNCs on lung metastatic cancer. This *in vitro* test was performed on the same artificial lymphogenous metastatic model, Ma44 cell line. This human non–small cell lung cancer cell line is known to be sensitive to gemcitabine [32] but when obtained by the limiting dilution method to develop its metastatic potential, its sensitivity to this drug still unknown. *In vitro* experiments allowed to observe the absence of toxicity of non-loaded LNCs (67 nm). Only composed of GRAS excipients, this result was predictable. Cytotoxicity assays demonstrated also the efficiency of GemC12-loaded LNCs against Ma44-3 cell line. Moreover, free Gem-C12 was comparable to Gem-C12-loaded LNC efficacy, meaning that Gem-C12 encapsulation into LNCs did not affect the efficacy of the prodrug.

The particularity of this new formulation was to obtain nanocapsules in a hydrogel form. In a previous study, visco-elasticity studies demonstrated a gel hardness depending of the Gem-C12 and LNCs concentration. Elastic (G') and viscous (G'') modulus values were 410 ± 40 and 90 ± 10 Pa, respectively for LNCs (Z-Ave = 55 nm) loaded with 5% of prodrug (Gem-C12/Labrafac *w/w*) and 1580 ± 500 and 480 ± 70 Pa for LNCs loaded with 7.5% of Gem-C12 (Gem-C12/Labrafac *w/w*). Similar G' and G'' values were observed with Gem-C12-loaded LNCs with Z-Ave of 29 nm [13]. To follow the release of LNCs from the gel, *in vitro* dissolutions in PBS at pH 7.4 and pH 6.5 were performed (Fig. 2). The extracellular pH is known to be lower in many

tumors than in normal tissues. The extracellular pH of malignant solid tumors is in the range of 6.5 to 6.9, whereas the pH of normal tissues is significantly more alkaline, 7.2 to 7.5 [33, 34]. No difference of LNC release from hydrogels, was observed at both pH = 7.4 and 6.5, with a constant LNC size released along the dissolution. However, with 5% of prodrug (Gem-C12/Labrafac *w/w)*, a slower release was obtained with LNCs of Z-Ave = 55 nm comparatively to 29 nm (100% of hydrogel dissolution at 24h *vs.* 6h, respectively). With stronger gel hardness, the hydrogel dissolution was slower (Fig. 2). These experiments showed the possible application of the nanocapsule-based hydrogel as a sustained delivery system after subcutaneous injection and particularly with LNCs (Z-Ave = 55 nm) loaded with 5% of Gem-C12 (Gem-C12/Labrafac *w/w)*.

Finally, to complete the characterization and to mimic LNC destabilization after subcutaneous administration of the hydrogel (possible interaction with lipophilic compartments), Gem-C12 transfer study was performed with Gem-C12-loaded LNCs in hydrogel form and in suspension. This experiment did not mimic the exact *in vivo* behavior due to hard stirring condition but it was a first approach in the stability study against complex medium, and complementary to the stability of LNCs and encapsulation rate in aqueous buffer. In the most hostile conditions of agitation, a slight release of the drug to a lipophilic phase was observed at 37℃ with LNCs in hydrogel form, while when LNCs were in suspension a higher transfer of the drug was observed. This transfer could be attributed to the destabilization of LNCs due to presence of external Labrafac phase and the high agitation. As already showed, Gem-C12 prodrug was trapped at the oil/water interface of LNCs in the surfactant shell, causing the high stability of the encapsulation rate [13].

5. Conclusion

A hydrogel was spontaneously obtained after the encapsulation of modified gemcitabine (Gem-C12) in lipid nanocapusles (LNCs) using a phase inversion process. Dissolution of the hydrogel permitted the progressive release of LNCs whose profile was dependent on gel hardness. Lymph nodes targeting was observed with subcutaneous injection of the hydrogel, with no accumulation in liver and spleen. Only lymph nodes close to the injection site were targeted which was not the case

after intravenous injection of LNC suspension where a global targeting (all the lymph nodes) was observed but with a loss of nanocarriers in the liver and spleen. Moreover, a lymph node sustained accumulation was observed after the hydrogel injection in agreement with the progressive release of LNCs from the hydrogel. This new technology could be used to target metastases in lymph nodes. *In vitro* cell-proliferation assays showed that the LNC loaded with Gem-C12 adversely affected the proliferation of Ma44-3, a highly metastatic lung cancer cell line. Thus, this novel hydrogel is a promising implant material for prolonged *in vivo* residence time in lymph nodes and temporal release of gemcitabine. Local delivery of anticancer drugs to lymph nodes invaded by metastases could have several advantages over systemic treatment, such as higher local doses and lower systemic concentrations.

Acknowledgements

This work has been realized in the research program LYMPHOTARG financially supported by EuroNanoMed ERA-NET 09 and by the Région Pays de la Loire.

References

[1] N.T. Huynh, C. Passirani, P. Saulnier, J.P. Benoit, Lipid nanocapsules: A new platform for nanomedicine, Int. J. Pharm. 379 (2009) 201‑209.

[2] S.M. Moghimi, A.C. Hunter, J.C. Murray, Nanomedicine: current status and future prospects, FASEB J. 19 (2005) 311‑330.

[3] B. Heurtault, P. Saulnier, B. Pech, M.-C. Venier-Julienne, J.-E. Proust, R. Phan-Tan-Luu, J.-P. Benoît, The influence of lipid nanocapsule composition on their size distribution, Eur. J. Pharm. 18 (2003) 55‑61.

[4] S. Hirsjärvi, S. Dufort, G. Bastiat, P. Saulnier, C. Passirani, J.-L. Coll, J.-P. Benoît, Surface modification of lipid nanocapsules with polysaccharides: From physicochemical characteristics to in vivo aspects, Acta Biomater. 9 (2013) 6683-6693.

[5] S. Vrignaud, J. Hureaux, S. Wack, J.-P. Benoit, P. Saulnier, Design, optimization and in vitro evaluation of reverse micelle-loaded lipid nanocarriers containing erlotinib hydrochloride, Int. J. Pharm. 436 (2012) 194-200.

[6] A.-L. Laine, N.T. Huynh, A. Clavreul, J. Balzeau, J. Béjaud, A. Vessieres, J.-P. Benoit, J. Eyer, C. Passirani, Brain tumour targeting strategies via coated ferrociphenol lipid nanocapsules, Eur. J. Pharm. Biopharm. 81 (2012) 690‑693.

[7] E. Allard, F. Hindre, C. Passirani, L. Lemaire, N. Lepareur, N. Noiret, P. Menei, J.-P. Benoit, 188Re-loaded lipid nanocapsules as a promising radiopharmaceutical carrier for internal radiotherapy of malignant gliomas, Eur. J. Nucl. Med. Mol. Imaging 35 (2008) 1838‑1846

[8] S. David, P. Resnier, A. Guillot, B. Pitard, J.-P. Benoit, C. Passirani, siRNA LNCs--a novel platform of lipid nanocapsules for systemic siRNA administration, Eur. J. Pharm. Biopharm. 81 (2012) 448‑452.

[9] S. Hirsjärvi, S. Dufort, J. Gravier, I. Texier, Q. Yan, J. Bibette, L. Sancey, V. Josserand, C. Passirani, J.-P. Benoit, J.-L. Coll, Influence of size, surface coating

and fine chemical composition on the in vitro reactivity and in vivo biodistribution of lipid nanocapsules versus lipid nanoemulsions in cancer models, Nanomedicine 9 (2012) 375-387.

[10] M. Morille, C. Passirani, S. Dufort, G. Bastiat, B. Pitard, J.-L. Coll, J.-P. Benoit, Tumor transfection after systemic injection of DNA lipid nanocapsules, Biomaterials 32 (2011) 2327‑2333.

[11] M. Morille, T. Montier, P. Legras, N. Carmoy, P. Brodin, B. Pitard, J.-P. Benoît, C. Passirani, Long-circulating DNA lipid nanocapsules as new vector for passive tumor targeting, Biomaterials 31 (2010) 321‑329.

[12] E. Moysan, G. Bastiat, J.-P. Benoit, Gemcitabine versus Modified Gemcitabine: A Review of Several Promising Chemical Modifications, Mol. Pharm. 10 (2012) 430-44.

[13] E. Moysan, Y. Gonzalez-Fernandez, N. Lautram, J. Béjaud, G. Bastiat, J.-P. Benoit, Gemcitabine-loaded lipid nanocapsule hydrogel: when the drug is a key player of the nanomedicine structure

[14] B. Heurtault, P. Saulnier, J.-E. Proust, B. Pech, J. Richard, J.-P. Benoit Lipidic nanocapsules: preparation process and use as Drug Delivery Systems U.S. Patent WO02688000 (2000)

[15] M. Socha, P. Bartecki, C. Passirani, A. Sapin, C. Damgé, T. Lecompte, J. Barré, F. El Ghazouani, P. Maincent, Stealth nanoparticles coated with heparin as peptide or protein carriers, J. Drug. Target. 17 (2009) 575‑585.

[16] C. Passirani, G. Barratt, J.P. Devissaguet, D. Labarre, Interactions of nanoparticles bearing heparin or dextran covalently bound to poly(methyl methacrylate) with the complement system, Life Sci. 62 (1998) 775‑785.

[17] P. Calvo, B. Gouritin, H. Chacun, D. Desmaële, J. D'Angelo, J.P. Noel, D. Georgin, E. Fattal, J.P. Andreux, P. Couvreur, Long-circulating PEGylated polycyanoacrylate nanoparticles as new drug carrier for brain delivery, Pharm. Res. 18 (2001) 1157‑1166.

[18] C. Vanpouille-Box, F. Lacoeuille, C. Belloche, N. Lepareur, L. Lemaire, J.-J. LeJeune, J.-P. Benoît, P. Menei, O.F. Couturier, E. Garcion, F. Hindré, Tumor eradication in rat glioma and bypass of immunosuppressive barriers using internal radiation with (188)Re-lipid nanocapsules, Biomat. 32 (2011) 6781‑6790.

[19] A. Vonarbourg, C. Passirani, P. Saulnier, P. Simard, J.C. Leroux, J.P. Benoit, Evaluation of pegylated lipid nanocapsules versus complement system activation and macrophage uptake, J. Biomed. Mater. Res. A. 78 (2006) 620‑628.

[20] S. David, N. Carmoy, P. Resnier, C. Denis, L. Misery, B. Pitard, J.-P. Benoit, C. Passirani, T. Montier, In vivo imaging of DNA lipid nanocapsules after systemic administration in a melanoma mouse model, Int. J. Pharm. 423 (2012) 108‑115.

[21] I. Texier, M. Goutayer, A. Da Silva, L. Guyon, N. Djaker, V. Josserand, E. Neumann, J. Bibette, F. Vinet, Cyanine-loaded lipid nanoparticles for improved in vivo fluorescence imaging, J. Biomed. Opt. 14 (2009)

[22] M. Fakruddin, Z. Hossain, H. Afroz, Prospects and applications of nanobiotechnology: a medical perspective, J Nanobiotech. 10 (2012) 31.

[23] M.K. Kwak, K. Hur, J.E. Yu, T.S. Han, K. Yanagihara, W.H. Kim, S.M. Lee, S.-C. Song, H.-K. Yang, Suppression of in vivo tumor growth by using a biodegradable thermosensitive hydrogel polymer containing chemotherapeutic agent, Invest. New Drugs 28 (2010) 284‑290.

[24] A. Swami, J. Shi, S. Gadde, A.R. Votruba, N. Kolishetti, O.C. Farokhzad, Nanoparticles for Targeted and Temporally Controlled Drug Delivery, Multifunctional Nanoparticles Drug, Deliv. Appli. (2012) 9‑29.

[25] O. Schillaci, A. Spanu, F. Scopinaro, F. Monteleone, M.E. Solinas, P. Volpino, P. Pirina, P. Marongiu, V. Cangemi, G. Madeddu, Mediastinal lymph node involvement in non-small cell lung cancer: evaluation with 99mTc-tetrofosmin SPECT and comparison with CT, J. Nucl. Med. 44 (2003) 1219‑1224.

[26] P.O. Van Trappen, M.S. Pepper, Lymphatic dissemination of tumour cells and the formation of micrometastases, Lancet Oncol. 3 (2002) 44-52.

[27] D.E. Owens III, N.A. Peppas, Opsonization, biodistribution, and pharmacokinetics of polymeric nanoparticles, Int. J. Pharm. 307 (2006) 93-102.

[28] C. Oussoren, G. Storm, Lymphatic uptake and biodistribution of liposomes after subcutaneous injection: III. Influence of surface modification with poly(ethyleneglycol), Pharm. Res. 14 (1997) 1479-1484.

[29] V. Manolova, A. Flace, M. Bauer, K. Schwarz, P. Saudan, M.F. Bachmann. Nanoparticles target distinct dendritic cell populations according to their size, Eur. J. Immunol. 38 (2008) 1404-1413.

[30] S.T. Reddy, A. Rehor, H.G. Schmoekel, J.A. Hubbell, M.A. Swartz, In vivo targeting of dendritic cells in lymph nodes with poly(propylene sulfide) nanoparticles, J. Control. R. 112 (2006) 26-34.

[31] S.M. Moghimi, B. Bonnemain, Subcutaneous and intravenous delivery of diagnostic agents to the lymphatic system: applications in lymphoscintigraphy and indirect lymphography, Adv. Drug Deliv. Rev. 37 (1999) 295-312.

[32] M. Matsumoto, Y. Takeda, H. Maki, K. Hojo, T. Wada, Y. Nishitani, R. Maekawa, T. Yoshioka, Preclinical in vivo antitumor efficacy of nedaplatin with gemcitabine against human lung cancer, Jpn. J. Cancer Res. 92 (2001) 51-58.

[33] I.F. Robey, B.K. Baggett, N.D. Kirkpatrick, D.J. Roe, J. Dosescu, B.F. Sloane, A.I. Hashim, D.L. Morse, N. Raghunand, R.A. Gatenby, R.J. Gillies, Bicarbonate Increases Tumor pH and Inhibits Spontaneous Metastases, Cancer Res. 69 (2009) 2260-2268.

[34] E.K. Rofstad, B. Mathiesen, K. Kindem, K. Galappathi, Acidic Extracellular pH Promotes Experimental Metastasis of Human Melanoma Cells in Athymic Nude Mice, Cancer Res. 66 (2006) 6699-6707.

Efficacité *in vivo*

Publication N°3

Avant-propos

Une étude d'efficacité de notre nouvelle forme pharmaceutique : hydrogel de LNCs chargées en gemcitabine modifiée (Gem-C12) nous a semblé nécessaire afin de mettre en évidence tout le potentiel de cette technologie. La plupart des patients atteints de cancer du poumon non à petites cellules meurent suite à des métastases progressives en dépit des modalités de multithérapies. Un modèle de cancer pulmonaire a été établi suite à l'implantation de façon orthotopique de cellules Ma44-3. Cinq jours après l'implantation, des études en fluorescence et des coupes histologiques ont confirmé la présence de métastases dans les ganglions médiastinaux. Des injections intraveineuses et sous-cutanées de nanocapsules lipidiques chargées en Gem-C12, en suspension et à l'état gel, respectivement ont été testées et comparées avec une injection intraveineuse de gemcitabine à 40mg/kg (équivalent Gemzar®). Aucune différence significative de survie n'a été observée. Néanmoins, une myélosuppression a été observée avec le traitement Gemzar® et une hépato-toxicité a été retrouvé avec la prodrogue libre. Les LNCs chargées en Gem-C12 n'ont provoqué aucun de ces deux symptômes, quelles que soient leurs voies d'administration. Ces résultats sont prometteurs du fait que le modèle tumoral est extrêmement agressif en terme de survie. Ainsi, les LNCs encapsulant la Gem-C12 pourraient être une nouvelle forme utilisable en chimiothérapie pour le traitement du cancer pulmonaire métastatique.

Evaluation of Lipid Nanocapsules Loaded with Lipophilic Gemcitabine Derivative against Metastases in Mediastinal Lymph Nodes in a Patient-like Lymphogenous Metastatic Model

Nathalie WAUTHOZ [1, 2], Elodie MOYSAN [1, 2], Kazuya KONDO [3], Marc ZANDECKI [4], Valérie MOAL [5], Marie-Christine ROUSSELET [6], José HUREAUX[1,7], Guillaume BASTIAT [1, 2, *] and Jean-Pierre BENOIT [1, 2]

[1] LUNAM Université – Micro et Nanomédecines Biomimétiques, F-49933 Angers, France

[2] INSERM – U1066 IBS-CHU, F-49933 Angers, France

[3] Department of Oncological and Regenerative Surgery, University of Tokushima, Kuramoto-cho, Tokushima 770-8503, Japan

[4] Hematology Department, Academic Hospital, Angers, F-49933, France

[5] Biochemistry Department, Academic Hospital, Angers, F-49933, France

[6] Cell and Tissue Pathology Department, Academic Hospital, Angers, F-49933, France

[7] Pneumology Department, Academic Hospital, Angers, F-49933, France

* Corresponding author: guillaume.bastiat@univ-anger.fr, phone number +33(0)2 44 68 85 31, Fax +33()02 44 68 85 46, Université d'Angers – UMR_S1066 (MINT), IBS-CHU Angers, 4 rue Larrey, 49933 Angers Cédex 9

Abstract

Most of patients with non-small cell lung cancer (NSCLC) are diagnosed in advanced stage and present a dismal prognosis despite of multi-therapeutic modalities. Gemcitabine, one of the widely anticancer agents used at this stage, undergoes deamination in blood and tissue that implies the delivery of high dose inducing myelosuppression. The purpose of this study is the evaluation of the antitumor efficacy of a lauroyl derivative of gemcitabine (Gem-C12) encapsulated in lipid nanocapsules (LNC), delivered as a liquid or a gel form by intravenous and/or subcutaneous route, in severe combined immunodeficiency mice with a CB17 genetic background (SCID-CB17) grafted with a lymphogenous metastatic model obtained from the orthotopic implantation of human Ma44-3 cells. Lung tumor and involvement of metastases in mediastinum are characterized by fluorescence at day 5, 9 and 12 post-tumor graft using 5-aminolevulinic acid. Gem-C12 loaded in LNC delivered twice a week as a gel by subcutaneous route showed specific accumulation in mediastinal lymph nodes and similar survival rate as the commercial gemcitabine hydrochloride delivered by intravenous route three times a week at the same total and final dose of 20 or 40 mg/kg of molar equivalent. Moreover, Gem-C12 loaded in LNC did not induce significant myelosuppresion (decrease of platelet count) in comparison to the control saline group in contrary to the gemcitabine hydrochloride treated group ($p < 0.05$).

Keywords: non-small-cell lung cancer, lymphatic targeting, nanomedicine, nanoparticles, mediastinum

1. Introduction

Lung cancers remain not only the leading cause of cancer-related mortality (both in males and females) in the United States, with an estimated 228,190 new cases diagnosed and 159,480 deaths predicted in 2013 [1] but also around the world [2]. Lung cancers are divided in small cell lung cancers (SCLC) and non-small cell lung cancers (NSCLC), which represent 15% and 85% of all cases of lung cancers, respectively [3]. NSCLC constituted of lung cancer histology differing from SCLC [4] and are mainly represented by adenocarcinomas (~50%), squamous cell carcinomas (~20%) and large cell carcinomas (~10%) [5]. Diagnosed NSCLC are present in local, regional but, in most cases, in advanced extent for 15%, 22% and 56% of patients, respectively [6]. Once diagnosed, NSCLC 5-year survival rate reaches globally 15% with the different therapeutic modalities such as surgery, radiotherapy, and chemotherapy [3]. The prognostic mainly depends on the stage of the NSCLC with a 5-year survival rate of 53% for local, 24% for regional and only 4% for advanced stage [6]. For most patients, NSCLC had spread in mediastinal and supraclavicular lymph nodes (N2 disease, stage III) or in the contralateral lung, pleural cavity or beyond lung (M1 disease, stage IV) [7]. These advanced stages are generally treated using sequential or concurrent chemotherapy and radiotherapy (stage III) [8] or combined chemotherapies (stage IV) [9]. Platinum–based doublet-third generation agent chemotherapy is the first-line chemotherapy having proven improved survival, response rates, and quality of life for advanced NSCLC patients presenting good performance status. This gold standard is generally based on a platinum compound (cisplatin or carboplatin) and associated with a third-generation agent such as a taxane (paclitaxel or docetaxel), gemcitabine, or vinorelbine [3], which present a similar efficacy [10].

Since 1996, commercial gemcitabine hydrochloride (Gemzar®) have been approved by FDA in combination with cisplatin for the first-line treatment of patients with inoperable, locally-advanced (Stage III), or metastatic (Stage IV) NSCLC [11]. According to pharmacoeconomic data, cisplatin and gemcitabine regimen is associated with the lowest total treatment-related costs among platinum-based combinations with third-generation cytotoxic drugs [12]. In addition, because cisplatin administration induce severe toxicities and also because a therapeutic plateau is

reached, a lot of nonplatinum-based regimens are explored with gemcitabine as the most investigated third-generation drug but also in combination with targeted agents, respectively [12]. Gemcitabine hydrochloride also called 2'deoxy-2'2'-difluorocytidine hydrochloride, is a potent and specific pyrimidine nucleoside antimetabolite which is structurally analogous to deoxycytidine [11,12]. Due to its hydrophilic nature and low membrane permeability but also its extensive deamination in plasma and tissues by cytidine deaminase, its plasma elimination half-life after 30 min-perfusion is extremely short (e.i., 42-94 min) [11], which requires high dose regimen and leads mainly to dose-limiting myelosuppression in approximately two-thirds of patients [12]. Moreover, different mechanisms of resistance against gemcitabine were developed by cancer cells and chemically modified gemcitabine emerged [11].

Because conventional chemotherapies are not specific and selective enough and are not able to reach the site of metastases, a therapeutic plateau with cytotoxic drugs has been reached for many years. In aim to protect the drug until the site of action, target the lymph nodes invaded by metastases and decrease the related systemic toxicities, nanomedicine could be of interest [13]. Indeed, some examples of nanotechnology in clinics demonstrated these abilities: liposome-encapsulated doxorubicin (Doxil™) protects patients with ovarian cancer, breast cancer or Karposi's sarcoma from the cardiotoxicity of the unencapsulated drug, paclitaxel-based albumin nanoparticles (Abraxane®), approved for metastatic breast cancer, have showed an increased drug uptake in tumor, iron oxide-based nanoparticles (Ferumoxytol®) is able to stage early lymph node metastasis in patients with prostate and testicular cancers [13].

A new nanocarrier system, lipid nanocapsules (LNC), loaded with a lipophilic derivative of gemcitabine (Gem-C12) have been developed and have demonstrated the ability to form a hydrogel when the prodrug is encapsulated in LNC [14], which could be delivered as a gel by the subcutaneous route or as a suspension (after dilution) for intravenous administration, to reach passively the lymph nodes *in vivo* [15]. The purpose of this study is to evaluate the antitumor efficacy of this new nanocarrier system in a lymphogenous metastatic model of human NSCLC, which mimics the spreading of metastases in mediastinum from the primary tumor implanted in the lung of severe combined immunodeficiency mice with CB17 genetic background

(SCID-CB17) [16], but also the tolerance (myelosupression and hepatotoxicity) of this new treatment delivered either as a gel by subcutaneous route or as a suspension by intravenous route.

2. Materials and methods

2.1. Chemicals and biochemicals

The Labrafac® WL 1349oil (caprylic–capric acid triglycerides) was provided by Gattefossé S.A. (Saint-Priest, France). Kolliphor® HS15 (mixture of free polyethyleneglycol 660 and polyethyleneglycol 660 hydroxystearate) was supplied by BASF (Ludwigshafen, Germany). Sodium chloride, acetone and ethanol were purchased from VWR (Fontenay-sous-bois, France). Span® 80 (Span 80), Tween® 80 (Tween 80) and 5-aminolevulinic acid (ALA) were purchased from Sigma (St Quentin Fallavier, France). 1,1'-Dioctadecyl-3,3,3',3'-tetramethylindodicarbocyanine (DiD) was provided by Life Technologies (Saint Aubin, France). Methanol was analytical grade purchased from Fischer Scientific (Loughborough, United Kingdom). Water was obtained from a MilliQ filtration system (Millipore, Paris, France). 4-(*N*)-lauroyl-gemcitabine (Gem-C12) was synthesized and characterized as described elsewhere [14] .

2.2. Preparation of Formulations

LNC were prepared following the phase inversion temperature (PIT) process [17] patented by our group a decade ago [18], which has recently been slightly adapted to encapsulate Gem-C12 in LNC [14,15]. Briefly, Gem-C12 was first solubilized (5 %, ratio Gem-C12/Labrafac *w/w*) in a mix of Labrafac, Span 80 and acetone that was evaporated before the addition of Kolliphor®, NaCl and water (Gem-C12 : 0.062g, Labrafac : 1.24g, Kolliphor® : 0.967g, Span 80 : 0.25g, water : 1.02g and NaCl : 0.045g). All were then mixed and heated to 75 °C under magnetic stirring at 500 rpm followed by cooling to 45°C (rate of 5°C/min). Three cycles were performed and at the last cooling phase, a sudden dilution with 2.12g room-temperature water was carried out at 60°C. LNC loaded with Gem-C12 form spontaneously a hydrogel with a waxy aspect. Gelation process was considered as achieved after 24h at 4°C. Fluorescent LNC were obtained by adding the fluorescent probe (DiD) with the other reagents at a final concentration of 0.1% of Labrafac (*w/w*). LNC loaded with the

prodrug (Gem-C12) and used in a liquid form was acquired by the dilution of the formulation directly after the process before the establishment of the hydrogel. Non-loaded LNC were prepared by mixing first all components (Labrafac : 1.24g, Kolliphor® : 0.967g, Span 80 : 0.25g, water : 1.02g and NaCl : 0.045g) and then heated to 75 ℃ under magnetic stirring at 500 rpm followed by cooling to 45℃ (rate of 5℃/min). Three cycles were performed and at the last cooling phase, a sudden dilution with 2.12g room-temperature water was carried out at 60℃. Free Gem-C12 was dissolved in ethanol, Tween 80 and water (87.6/5.5/6.9 *v/v/v*) for *in vivo* experiments. Commercial gemcitabine hydrochloride used was Gemcitabine Hospira 38 mg/mL diluted at the required concentration with NaCl 0.9%.

2.3. Characterizations of LNC-based Formulations

Hydrodynamic diameter (Z-average), polydispersity index (PDI) and zeta potential of LNC were determined by dynamic light scattering using a Zetasizer® Nano serie DTS 1060 (Malvern Instruments S.A., Worcestershire, UK). LNC were diluted 1:60 (*v/v*) in deionised water in order to ensure a convenient scattered intensity on the detector. Each measurement was done in triplicate at 25℃. The drug loading was determined using an UPLC apparatus with UV spectroscopy detection as previously described [14]. Briefly, the LNC samples (after disruption of LNC in methanol (1:36 *v/v*)) were injected into a C18 column (1.7 x100 mm, ACQUITY UPLC BEH C18) equipped with a column guard. The detection wavelengths were 248 and 266 nm. The drug concentration was calculated from linear calibration curve range from 1 to 100 µg/mL of Gem-C12 in methanol solutions. Each measurement was done in triplicate.

2.4. Cell Cultures and Inoculum Preparation for Lung Implantation

Ma44-3 cell line derived from the human NSCLC carcinoma cancer cell line Ma44 by limit dilution method was kindly provided by Prof. Kondo (Department of Oncological and Regenerative Surgery, School of Medicine, University of Tokushima, Japan) and was cultured in RPMI 1640 (Lonza, Verviers, Belgium) supplemented with 10% heat-inactivated fetal bovine serum (Lonza, Verviers, Belgium), 100 U/mL of penicillin, 100 µg/mL of streptomycin and 0.250 µg/mL of amphotericin B from Sigma (St Quentin Fallavier, France) at 37℃ in a humidified incubator with 5% CO_2. The medium was routinely changed every 3 days and the cells were separated by trypsinization before reaching confluency. For lung implantation, the cells were harvested at 70-80%

confluence using trypsin that was inactivated by the culture medium. Then, the cell suspension was centrifuged at 1400 rpm during 5 min and the supernatant was removed and replaced by RPMI 1640 containing 0.1% of bovine serum albumin fraction V pH 7.0 (PAA GmbH, Pasching, Austria) which are then mixed to Matrigel® (DB biosciences, Bedford, MA) to obtain an inoculum of 2.0×10^6 tumor cells/mL with 400 µg/mL of Matrigel®. The inoculum is kept on ice during maximum 2 hours.

2.5. Animals

Male SCID-CB17 mice (4-5 weeks of age) were purchased from Charles River (L'Arbresle, France) and housed and maintained at the University animal facility (SCAHU) in disposable plastic cages with hardwood chips bedding in an air-conditioned room with a 12-hour-light–12-hour-dark cycle. All the animal experiments were performed in agreement with the EEC guidelines and the "Principles of Laboratory Animal Care" (NIH Publication No. 86-23, revised 1985) and with the agreement of "Comité d'Ethique pour l'Expérimentation Animale des Pays-de-la-Loire" (authorization CEEA; 2012-73).

2.6. Orthotopic Intrapulmonary Implantation Procedure

The orthotopic intrapulmonary implantation procedure was performed as previously reported [16]. The 6 weeks-aged mice were maintained in the right lateral decubitus and anesthetized by isoflurane inhalation. A 1-cm transverse incision was made on the left lateral skin just below the inferior border of the scapula of the SCID-CB17 mice. The muscles were separated from the ribs by sharp dissection, and intercostal muscles were visible. 10 µL of cell suspension (2.0×10^4 cells) were inoculated with a 30-gauge needle to a depth of about 3-5 mm into the lung through the intercostal muscles and after, the needle was promptly pulled out. Mice were maintained in the right lateral decubitus position after injection and the skin incision was closed with 3-0 silk (Ethicon, St-Stevens-Woluwe, Belgium). Mice were observed until complete recovery. Mice were then randomly divided into the different groups to evaluate the *in vivo* antitumor efficacy.

2.7. Evaluation of Primary Lung Tumor and Mediastinal Metastases

To control the apparition of the metastases or lung tumor, 5-aminolevulinic acid (ALA) was used at day 5, 9 and 12 post-tumor graft. ALA was freshly dissolved in

phosphate buffer saline (PBS) medium (Lonza, Verviers, Belgium) and was orally delivered at a dose of 400 mg/kg body weight 4 hours before sacrificed. This substance is metabolized into a fluorescent photosensitizing protophorphyrin IX (PpIX) that is highly accumulated by cancer cells. At day 5, 9 and 12, three SCID mice were killed under deep anesthesia and the chest was opened. Lung and mediastinal organs were immediately observed by means of CRI Maestro system (Woburn, USA) with an excitation range from 500 to 635 nm.

For histopathological examination, the lung and mediastinal organs were removed and immediately immersed in 10% neutral buffered formalin and fixed for a minimum period of 48 h and then placed in cassettes. Tissues in cassettes were processed into paraffin, embedded in a paraffin block, sectioned on a microtome to a thickness of 5 microns, placed on a microscope slide and stained with hematoxylin and eosin.

2.8. *Visualization of Fluorescent LNC in Lung after IV or SC Administrations*

The visualization of the same amount of LNC loaded with a fluorescent probe DiD injected *iv* or *sc* was performed on six SCID-CB17 mice grafted with Ma44-3 cells. At day 5 post tumor graft, a group of 3 mice received orally 400 mg/kg of ALA in PBS (200 µL) and an intravenous injection of LNC loaded with DiD (in liquid form) in the tail vein, and the other group (n=3) received orally 400 mg/kg of ALA in PBS (200 µL) and a subcutaneous injection of LNC loaded with DiD and Gem-C12 (in gel form) behind the neck. Four hours after the injection, the mice were killed and dissected for imaging the lung and the mediastinum area. Fluorescence imaging was performed using the CRI Maestro system between 500 and 635 nm (for Protoporphyrin IX (Pp IX) visualization) and 630 and 800 nm (for DiD visualization) using the automatic exposition.

2.9. In Vivo Antitumor Efficacy

In both experiments, treatments were started 5 days after the intrapulmonary implantation of Ma44-3 cells. Each group contained 10 mice. Mice were observed each day and body weight measurements were performed daily during the treatment period and then three times a week. By applying the criteria for euthanasia of

experimental animals, mice were sacrificed when they lost 20% of body weight and/or associated with a high degree of respiratory depression.

Experiment 1

The first experiment evaluated the impact on survival of GemC12 loaded in LNC and delivered by *iv* or *sc* routes in comparison to negative controls (saline or not-loaded LNC) and positive controls (gemcitabine hydrochloride and free GemC12).. At day 5, 7 and 9, NaCl 0.9% (saline *iv*) solution, non-loaded LNC (non-loaded LNC *iv*), commercial gemcitabine hydrochloride (Gemcitabine *iv*), Gem-C12 (Gem-C12 *iv*) and liquid form of Gem-C12 loaded LNC (LNC Gem-C12 *iv*) were intravenously administered by the tail vein (145 µL at each injection). At day 5 and 9, non-loaded LNC (non-loaded LNC *sc*) and gel form of Gem-C12 loaded LNC (LNC Gem-C12 *sc*) were subcutaneously administered behind the neck (55 µL at each injection). The total LNC delivered dose of non-loaded LNC was the same that Gem-C12 loaded LNC for *iv* or *sc* administrations. In groups treated by gemcitabine hydrochloride and Gem-C12 (in LNC or not), the total dose delivered in mice was 40 mg (molar equivalent gemcitabine hydrochloride) per kilo of body weight.

Experiment 2

The second experiment evaluated the impact on survival of GemC12 loaded in LNC and delivered by *sc* routes with or without intravenous gemcitabine hydrochloride at two different doses in comparison to negative controls (saline or not-loaded LNC) and at two different doses of gemcitabine hydrochloride as positive controls. At day 5, 7 and 9, NaCl 0.9% (saline *iv*) solution and commercial gemcitabine hydrochloride at a dose of 20 mg/kg (Gemcitabine *iv* 20 mg/kg) or 40 mg/kg (Gemcitabine *iv* 40 mg/kg), were intravenously administered by the tail vein (145 µl at each injection). At day 5 and 9, non-loaded LNC (non-loaded LNC *sc*) and gel form of Gem-C12 loaded LNC at a dose of 20 mg/kg (LNC Gem-C12 *sc* 20 mg/kg) or 40 m/kg (LNC Gem-C12 *sc* 40 mg/kg) were subcutaneously administered behind the neck (27.5 and 55 µL at each injection, respectively). Combined groups were also tested with commercial gemcitabine hydrochloride delivered intravenously at a dose of 20 mg/kg (145 µL at each injection) at day 5, 7 and 9 and Gem-C12 loaded LNC delivered subcutaneously at a dose of 20 mg/kg (27.5 µL at each injection) at day 5 and 9, or commercial gemcitabine hydrochloride delivered intravenously at a dose of 30 mg/kg

(145 µL at each injection) at day 5, 7 and 9 and Gem-C12 loaded LNC delivered subcutaneously at a dose of 10 mg/kg (13.8 µL at each injection) at day 5 and 9. The total LNC delivered dose of non-loaded LNC was the same that Gem-C12 loaded LNC at 40 mg/kg for *sc* administrations. In groups treated by gemcitabine hydrochloride and Gem-C12 (in LNC or not), the total dose delivered in mice was 20 or 40 mg (molar equivalent gemcitabine hydrochloride) per kilo of body weight.

2.10. Evaluation of the Mediastinum Weight

Treatments were started 5 days after the intrapulmonary implantation of Ma44-3. Twenty-five mice (5 per group) received 145 µL of an intravenous injection of saline (saline *iv*), gemcitabine hydrochloride (Gemcitabine *iv*), Gem-C12 (Gem-C12 *iv*) solutions or non-loaded LNC (non-loaded LNC *iv*) or liquid form of Gem-C12 loaded LNC (LNC Gem-C12 *iv*) dispersions at day 5, 7 and 9. Ten mice (5 per group) received 55 µL of a subcutaneous injection of non-loaded LNC (non-loaded LNC *sc*) or gel form of Gem-C12 loaded LNC (LNC Gem-C12 *sc*) at day 5 and 9. The total LNC delivered dose of non-loaded LNC was the same that Gem-C12 loaded LNC for *iv* or *sc* administrations. In groups treated by gemcitabine hydrochloride and Gem-C12 (in LNC or not), the total dose delivered in mice was 40 mg (molar equivalent gemcitabine hydrochloride) per kilo of body weight. At day 9 post-tumor graft for control groups (saline, LNC *iv* and LNC *sc*) and at day 21 post-tumor graft for groups treated by gemcitabine hydrochloride or Gem-C12 (loaded or not in LNC), mice were sacrificed by lethal anesthesia, lung and mediastinum were removed in bloc, mediastinum are separated from the lungs to determine their weight.

2.11. In vivo Hematologic and Hepatic Toxicity Evaluation

Twenty-five mice (5 per group) received 145 µL of an intravenous injection of saline (saline *iv*), gemcitabine hydrochloride (Gemcitabine *iv*), Gem-C12 (Gem-C12 *iv*) solutions or non-loaded LNC (non-loaded LNC *iv*) or liquid form of Gem-C12-loaded LNC (LNC Gem-C12 *iv*) dispersions at day 5, 7 and 9. Ten mice (5 per group) received 55 µL of a subcutaneous injection of non-loaded LNC (non-loaded LNC *sc*) or gel form of Gem-C12-loaded LNC (LNC Gem-C12 *sc*) at day 5 and 9. The total LNC delivered dose of non-loaded LNC was the same that Gem-C12 loaded LNC for *iv* or *sc* administrations. In groups treated by gemcitabine hydrochloride and Gem-C12 (in LNC or not), the total dose delivered in mice was 40 mg (molar equivalent

gemcitabine hydrochloride) per kilo of body weight. Hematology and biochemical assays on blood were done for each mouse 8 days after the first injection to assess the tolerability of treatments. Blood sampling was performed by cardiac puncture in deeply anaesthetized mice, the half of blood sample was placed in a venous blood collection tube containing heparin lithium (Tube Micro from SARSTEDT, Marnay, France) for hematology studies and the other half on ethylene-diamine-tetraacetic acid (EDTA) tube (K2E tube from BD Microtainer, NJ, USA) which are then centrifuged at 10,000 × g for 10 min to remove the plasma and evaluate the blood biochemical markers. The hematological parameters were determined in the Haematology Ward of the Academic Hospital of Angers with an XE-2100 haematology analyser (Sysmex) and plasma biochemistry analyses were carried out at the Biochemistry Ward of the Academic Hospital of Angers on a Modular P® (Roche diagnostics).

2.12. Statistical analysis

Survival analyses were carried out by means of Kaplan-Meier curves and the log-rank test. Statistical comparisons of more than three independent groups of data were made using the Kruskal-Wallis test (a nonparametric one-way analysis of variance). When this multi-group test was significant, post-hoc tests (Dunn's procedure) were used to avoid multiple comparison effects when comparing the group pairs of interest. All statistical analyses were performed using Statistica (Statsoft, Tulsa, OK).

3. Results

3.1. LNC-based Formulations

To protect gemcitabine against blood and tissue deamination and make it accumulate in lymph nodes, a lipophilic derivative of gemcitabine (Gem-C12) was synthesized and encapsulated in LNC [14,15]. By mixing Gem-C12 with excipients at well-characterised concentrations described by a ternary diagram and by applying the phase inversion process [17,18] , LNC loaded with Gem-C12 were obtained. The physicochemical characteristics of non-loaded LNC, Gem-C12-loaded LNC and DiD-Gem-C12-loaded LNC (Z average, PDI, zeta potential and drug payload) are presented in Table 1. With the addition of Gem-C12 into LNC, a hydrogel was formed

and can be injected by syringe [14]. Once the gel was diluted in water, nanoparticles dispersion was obtained. Non–loaded LNC for *iv* and *sc* injection, Gem-C12 loaded LNC for *iv* and *sc* injection, DiD-non-loaded LNC for *iv* and DiD-Gem-C12 loaded LNC for *sc* injection formulated by the PIT method have Z-average mean (*e.i.,* hydrodynamic diameter) of 68 ± 3 nm, 67 ± 2 nm, 53 ± 2 nm, 53 ± 1 nm, 55 ± 2 nm and 56 ± 2 nm, respectively, and a polydispersity index in all cases less than 0.1, which means that very monodispersed distributions were obtained. In all cases, the zeta potential was slightly negative, from −5 to −10 mV. Similar to many hydrophobic drugs [19,20], Gem-C12 was well-encapsulated in LNC with a high encapsulation efficiency of about 100% [14]. The measured drug payload corresponded to what expected theoretically (*e.i.,* 11 mg/mL for the gel form and 2.2 mg/mL for the liquid form).

	Z average (nm)	**Polydispersity index**	**Zeta potential (mV)**	**Drug payload (mg/mL of suspension)**
Non-loaded LNC (*iv*)	68 ± 3	0.08 ± 0.02	- 8 ± 3	/
Non-loaded LNC (*sc*)	67 ± 2	0.07 ± 0.01	- 10 ± 5	/
LNC Gem-C12 (*sc*)	53± 2	0.07 ± 0.01	- 7 ± 4	11 ± 0.2
LNC Gem-C12 (*iv*)	53 ± 1	0.04 ± 0.01	- 7 ± 3	2.75 ± 0.05
DiD-Gem-C12 loaded LNC (*sc*)	56 ± 2	0.04 ± 0.02	- 5 ± 2	11 ± 0.2
DiD-non-loaded LNC (*iv*)	55 ± 2	0.06 ± 0.02	- 7 ± 4	/

Table 1. Physicochemical characteristics of non-loaded LNC for *iv* and *sc* injection, LNC Gem-C12 LNC for *iv* and *sc* injection, non-loaded LNC with DiD for *iv* injection and LNC Gem-C12 with DiD for *sc* injection. Mean Values ± SD are presented (n=3).

3.2. Characterization of the Preclinical model of Lymphogenous Metastases

Ma44-3 is a subpopulation of human squamous NSCLC cell line Ma44 selected by limiting dilution which invades lymphogenously the mediastinum after intrapulmonary graft [16,21]. No surgical deaths caused by implantation were observed and all pulmonary implantations were a success in SCID-CB17 mice as previously reported by Ishikura *et al* [16]. All mice died from the mediastinal metastases and not from the small primary lung tumor (Figure 1A) from the 10-11th day post-tumor graft without drastic change of weight as reported for the saline *iv* groups (Figure 4B and 5B). Indeed, the lung tumor remained at a moderate size at day 5, 9 and 12 post-tumor graft (Figure 2) and until the death of the mice (Figure 1A). On the contrary, the volume of mediastinum could become large enough to cause the death of mice (Figure 1A) as previously reported by Fujino *et al* [22] where the mass of mediastinum and the total metastatic area in the mediastinum and not the primary lung tumor volume at day 14 post-tumor graft showed significant difference between the treated and the control group. This trend was in the negative way of the survival rate as demonstrated by the significance difference in the Kaplan-Meier survival curves [22]. On day 5, 9 and 12 post-tumor graft, tumor tissue could be detected in the mediastinum area and in the left lobe of lung under the fluorescence scope (after oral administration of ALA) (Figure 2). Primary lung tumor was confirmed by histopathological analysis with the high level of mitosis, angiogenesis and large compacted cells present in tumor tissue in comparison to the healthy lung tissue (Figure 1B and 1C). However, for metastatic lymph nodes, histopathological analysis is more complex because the detection of tumor involvement in lymph nodes depends on the modification of the lymph node architecture [23]. In SCID-CB17 that are severe combined immunodefiency mice, lymph nodes are atrophied and do not present architecture well defined which complicates the confirmation of tumor tissue [23]. For this reason, we chose to deliver to mice ALA known to be a precursor to porphyrin in heme synthesis and already used to detect lymph node metastases [24] and pleural malignant metastases [25] from lung cancer in mice or lymph node metastases in mouse rectal cancer [26]. In tumor cells, significant difference in the activities of key enzymes in the heme-synthesis pathway leads to an accumulation of Pp IX from ALA in comparison to normal cells [27]. Nowadays, ALA is approved as photodynamic detection for residual malignant glioma, dermatologic and urogenital

applications and are investigated for many other cancers [27]. In our study, the mediastinal tumor tissue detected in Figure 2 could not be only attributed to mediastinal metastases because spontaneous T-cell thymic lymphomas frequently occur in SCID-CB17 strain [28], which produced an intense red fluorescence (Figure 2). However, the development of thymic lymphomas was slow [28] and therefore not interfered with the Ma44-3 preclinical model. Removing the two atrophic thymus lobes (Figure 2) and examining again the mediastinum under fluorescence scope, low fluorescence was detected. This phenomenon was explained by the small metastatic foci contrary to the detectable primary lung tumor and that the excitation wavelengths range used did not contain the main excitation peak of Pp IX of 405 nm because CRI Maestro system is only able to emit light from 500 nm. However Pp IX presents lower peaks of excitation between 500 and 600 nm, which induces light emission at 635 nm [29].

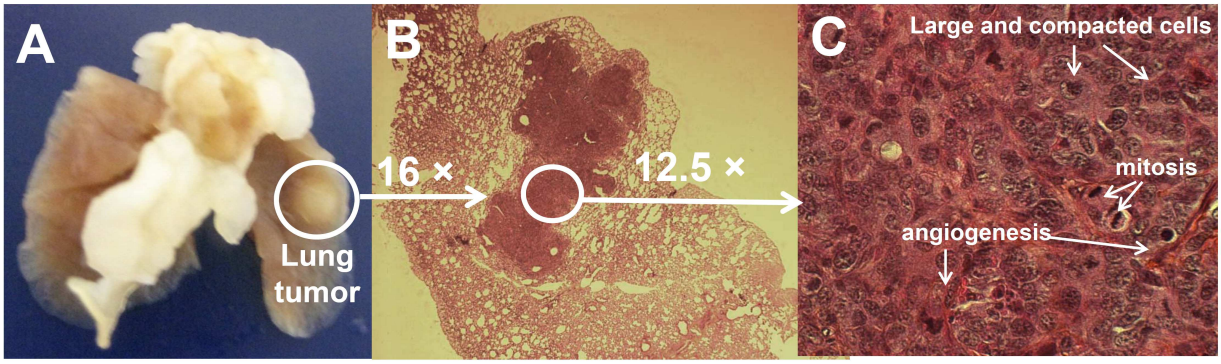

Figure 1. Images of (A) lung and mediastinum (pink and white tissues, respectively) of a dead mouse at day 12 post-tumor graft, histological slide of left lung with the Ma44-3 tumor (B) visualized at a magnification 16× and (C) visualized at a magnification 200× in the tumor area.

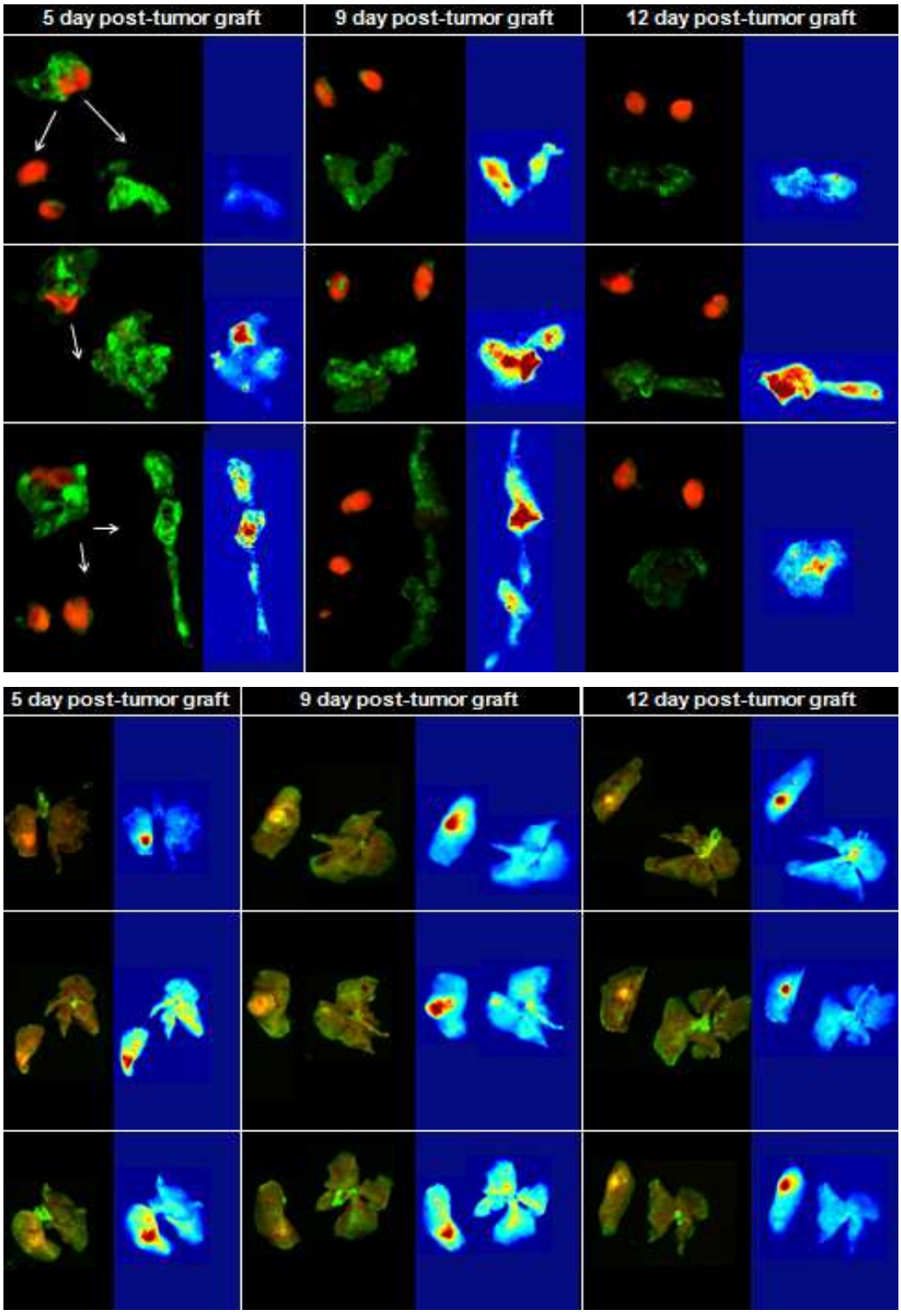

Figure 2. Visualization of mediastinum (at the top) and left and right lung lobes (at the bottom) after administration of 400 mg/kg of 5-aminolevulinic acid to a group of three mice at day 5, 9 and 12 post-tumor graft after 500-640 nm excitation using a CRI Maestro system. Tumor tissue emitted a red fluorescence from the accumulation

of protophorphyrin IX, which is more visible using a rainbow grayscale (intensity: blue to red) for both tissues.

3.3. *Visualization of Fluorescent LNC in Lung after iv or sc Administrations*

The *in vivo* behavior of LNC is then assessed following their intravenous injection in the tail vein and their subcutaneous injection behind the neck of SCID-CB17 bearing Ma44-3 xenografts in their left lung. The fluorescence images obtained 4h after DiD-LNC injections are presented in Figure 3. Thymic lymphoma was detected in red using the ALA protocol in all mice (Figure 3A and C). DiD-LNC were visible in the entire lung of the three mice after intravenous injection (Figure 3B) because at this time, LNC mainly remained in the blood as previously reported [15] and because lung is a highly vascularized organ. On the contrary, DiD-LNC administered by subcutaneous route emitted an intense local accumulation in mediastinal lymph nodes (Figure 3D), which are close to thymus as reported in the literature [30].

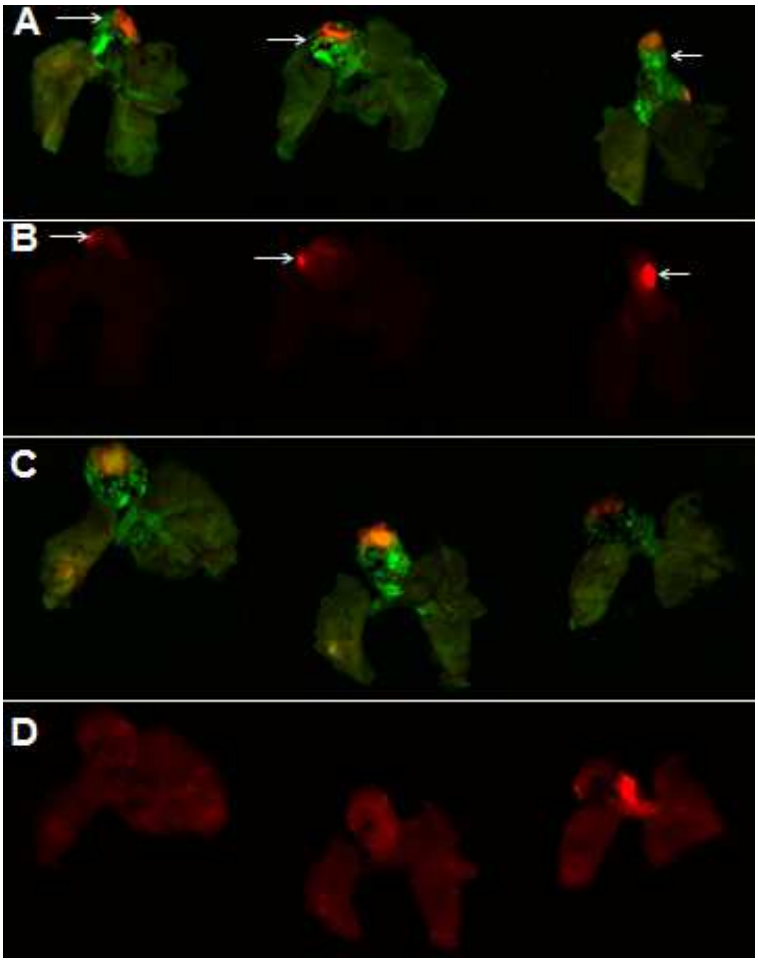

Figure 3. Visualization of lungs of three mice at day 5 after tumor implantation with oral administration of 400 mg/kg of 5-aminolevulinic acid and administration of LNC loaded with DiD delivered *iv* using (A) Pp IX or (B) DiD visualization mode or delivered *sc* using (C) Pp IX or (D) DiD visualization mode using a CRI Maestro system.

3.4. In Vivo Antitumor Efficacy

The patient-like lymphogenous metastatic Ma44-3 preclinical model [16] was used to evaluate the efficacy of Gem-C12 loaded LNC. Five days post-tumor graft in the left lobe of lung, when micrometastatic foci were detected in mediastinum (Figure 2) [16,21], comparative efficacy studies on randomized groups were performed with different treatments and schedule of administration. The total dose of 40 mg (molar equivalent dose of gemcitabine hydrochloride) by kilo of body weight delivered twice by the subcutaneous route or three times a week by the intravenous route was chosen because no weight loss or death was observed in a group of three mice using Gem-C12-loaded LNC (gel form) for subcutaneous route or Gem-C12-loaded LNC (liquid form) for intravenous route, respectively. Higher doses or other schedules caused drastic weight loss or death of mice (data not shown). Survival times of experimental animals were plotted on the Kaplan Meier curves as shown in Figure 4A and Figure 5A. Mice of the control (saline *iv*) and non-loaded LNC (*sc* and *iv*) groups were characterized by a very short and reproducible lifespan after tumor implantation with a median survival time of 13 (Figure 4A) or 14 (Figure 5A), 18 (Figure 4A) or 19 (Figure 5A) and 18 (Figure 4A) days, respectively, without significant difference ($p > 0.05$, log-rank test) in relation to the saline *iv* or LNC groups. In the treated groups by gemcitabine hydrochloride or Gem-C12 loaded in LNC or not, a prolonged lifespan are observed with a close median survival time for the 20 mg/kg treated groups : 19 days for gemcitabine hydrochloride *iv* 20 mg/kg and 20 days for LNC Gem-C12 *iv* 20 mg/kg (Figure 5A), increased for the 40 mg/kg treated groups : 25 or 23 days for gemcitabine hydrochloride *iv* 40 mg/kg (Figure 4A and 5A, respectively), 24 days for Gem-C12 *iv* 40 mg/kg (Figure 4A), 27 days for LNC Gem-C12 *iv* 40 mg/kg (Figure 4A) and, 26 days for LNC Gem-C12 *sc* 40 mg/kg (Figure 4A and 5A), 25 days for gemcitabine hydrochloride *iv* 20 mg/kg combined with LNC Gem-C12 *sc* 20 mg/kg (Figure 5A) and 27 days for gemcitabine hydrochloride *iv* 30 mg/kg combined with LNC Gem-C12 *sc* 10 mg/kg (Figure 5A). In both experiments, significant level (e.i., p

< 0.05, log-rank test) was reached with gemcitabine hydrochloride, free Gem-C12 and Gem-C12 loaded in LNC by *sc* routes at a dose of 20 or 40 mg/kg of molar equivalent of gemcitabine hydrochloride in comparison to the saline *iv* group or to non-loaded LNC by *sc*, respectively. However, there was no significant differences between the survival rate of groups treated by gemcitabine hydrochloride and Gem-C12 loaded in LNC or not ($p > 0.05$, log-rank test), regardless of the dose used, the route of administration and the respective schedule (2 subcutaneous injections and/or 3 intravenous injections). The weight evolution of the different mice groups remained similar during the experiment with a short stabilization during the treatment period (Figure 4B and Figure 5B). However, in the E*xperiment II*, the both groups combining Gem-C12 loaded LNC and Gemcitabine *iv* showed a death of mice at day 10 due to the treatment and not from the metastases. No significant difference was observed for the mediastinum weight at day 9 post-tumor graft for control groups and day 21 post-tumor graft for treated groups by gemcitabine hyrochloride or Gem-C12 loaded in LNC or not (Figure 6), what confirms the non-significant difference observed in Kaplan-Meier survival curves in *Experiment I*.

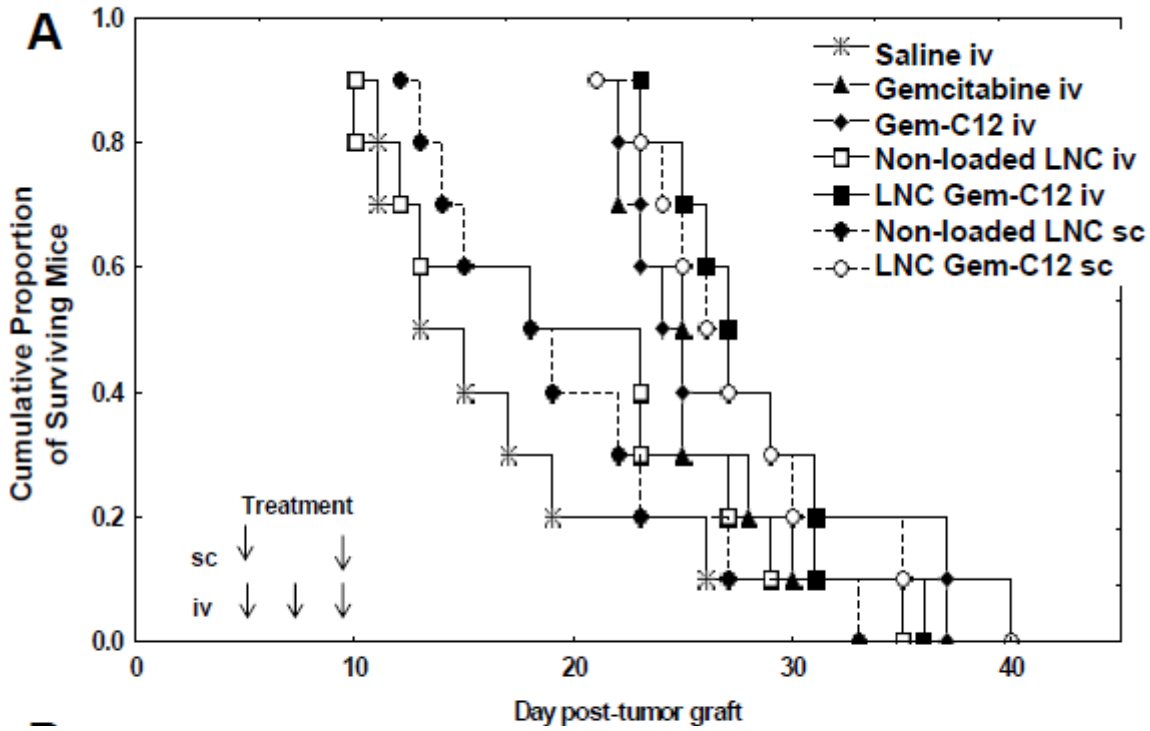

B

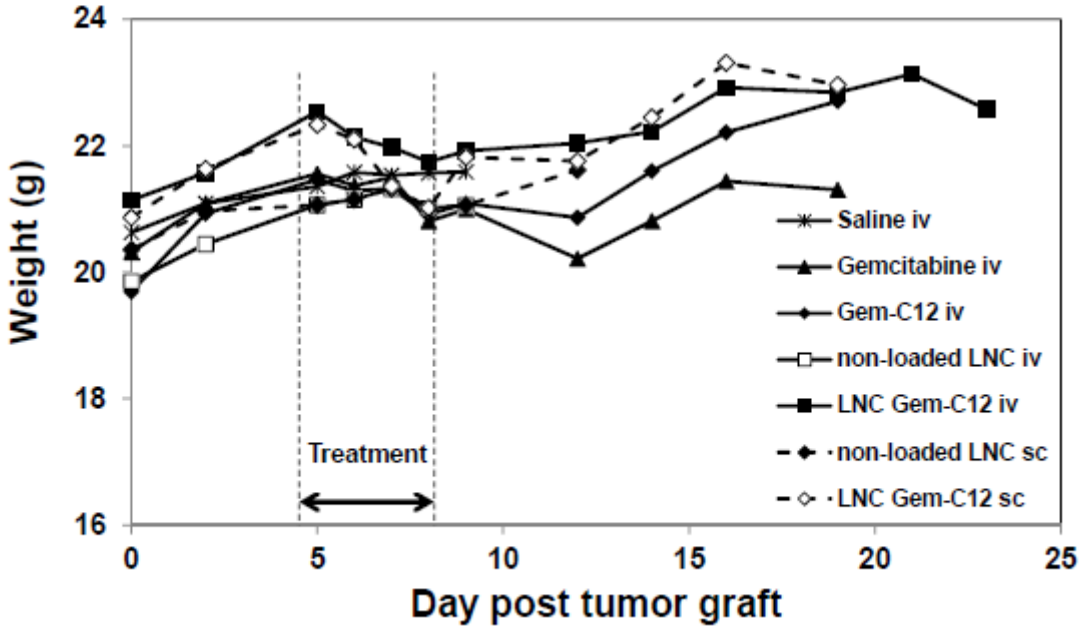

Figure 4. (A) The Kaplan-Meier survival curves and (B) the weight evolution of 6 weeks-aged male SCID-CB17 mice grafted with 2 × 10^4 Ma44-3 cells (implanted in the left lobe) and randomized on day 0. The mice were treated without (star for saline treated group by *iv*, empty square for non-loaded LNC treated group by *iv*, full circle for non-loaded LNC treated group by *sc*) or with gemcitabine hydrochloride (full triangle) or Gem-C12 loaded in LNC (full square by *iv* and empty circle by sc) or not (full diamond) at a final dose of 40 mg (molar equivalent gemcitabine hydrochloride) per kilo of body weight beginning on day 5. The treatments were administered intravenously via the tail vein (*iv*, continuous lines) three times a week or by subcutaneous route (*sc*, dashed lines) twice a week. Each experimental group was composed of 10 animals. The survival time and body weight of each mouse were evaluated each day and three times (each day during the treatment period) per week, respectively.

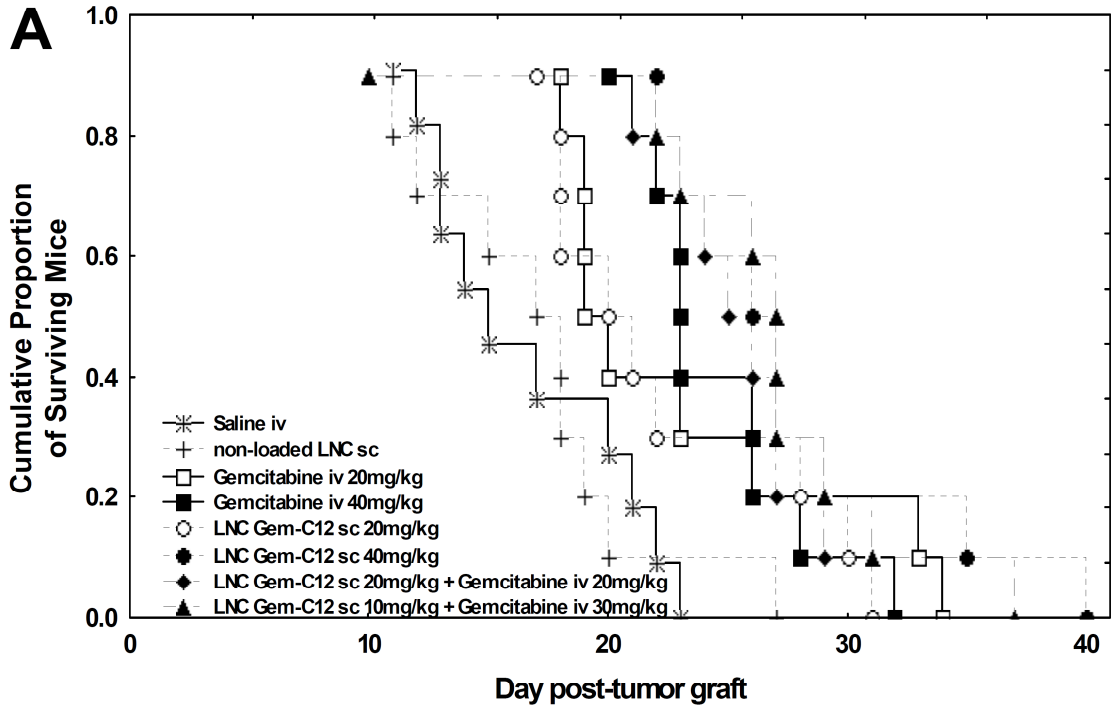
A
Cumulative Proportion of Surviving Mice
1.0
0.8
0.6
0.4
0.2
0.0
0
10
20
30
40
Day post-tumor graft
Saline iv
non-loaded LNC sc
Gemcitabine iv 20mg/kg
Gemcitabine iv 40mg/kg
LNC Gem-C12 sc 20mg/kg
LNC Gem-C12 sc 40mg/kg
LNC Gem-C12 sc 20mg/kg + Gemcitabine iv 20mg/kg
LNC Gem-C12 sc 10mg/kg + Gemcitabine iv 30mg/kg

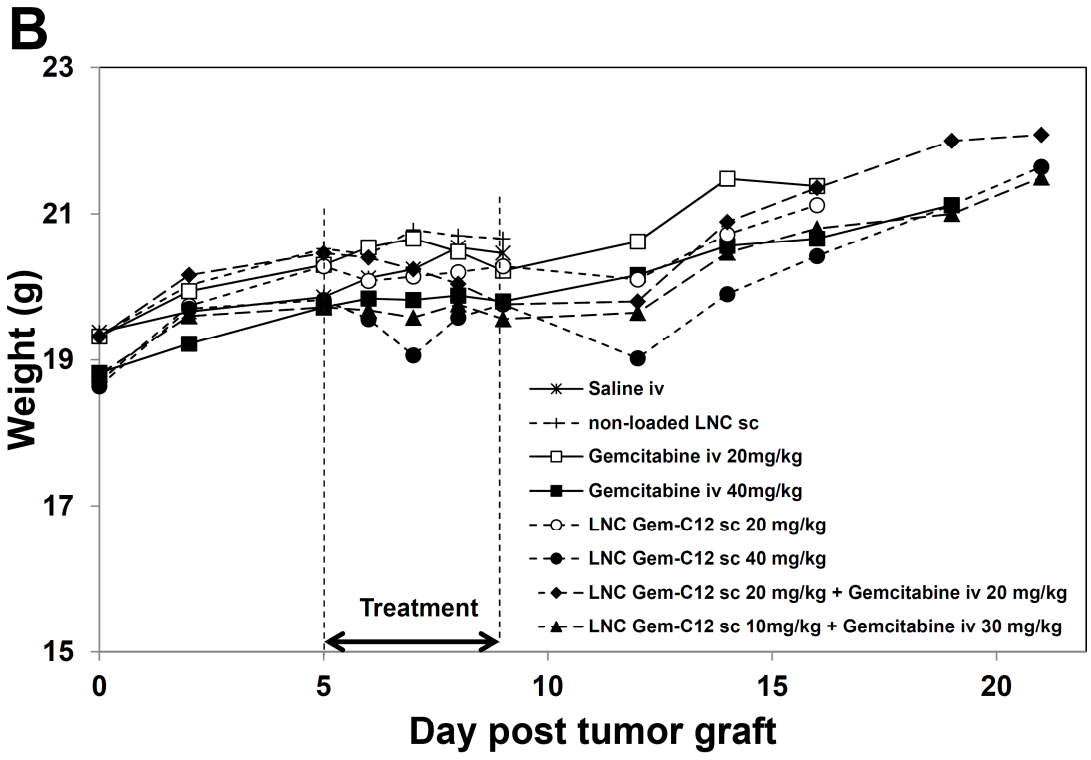
B
Weight (g)
23
21
19
17
15
0
5
10
15
20
Day post tumor graft
Treatment
Saline iv
non-loaded LNC sc
Gemcitabine iv 20mg/kg
Gemcitabine iv 40mg/kg
LNC Gem-C12 sc 20 mg/kg
LNC Gem-C12 sc 40 mg/kg
LNC Gem-C12 sc 20 mg/kg + Gemcitabine iv 20 mg/kg
LNC Gem-C12 sc 10mg/kg + Gemcitabine iv 30 mg/kg

Figure 5. (A) The Kaplan-Meier survival curves and (B) The weight curves of 6 weeks-aged male SCID-CB17 mice were grafted with 2×10^4 Ma44-3 cells (implanted in the left lobe) and randomized on day 0. The mice were treated without (star for saline treated group by *iv* and cross for non-loaded LNC treated group by *sc*) or with gemcitabine hydrochloride at 20 mg/kg (empty square) or at 40 mg/kg (full square) using the intravenous route (continuous line) or Gem-C12 loaded in LNC at 20 mg/kg (empty circle) or at 40 mg/kg (full circle) using the subcutaneous route (dashed line) or a combination of gemcitabine hydrochloride at 20 mg/kg by *iv* and Gem-C12 loaded in LNC at 20 mg/kg by *sc* (full diamond) or gemcitabine hydrochloride at 30 mg/kg by *iv* and Gem-C12 loaded in LNC at 10 mg/kg by *sc* (full triangle). The final dose was either 20 mg or 40 mg (molar equivalent gemcitabine hydrochloride) per kilo of body weight beginning on day 5. The treatments were administered intravenously via the tail vein (*iv*) three times a week or by subcutaneous route (*sc*) twice a week. Each experimental group was composed of minimum of 10 animals. The survival time and body weight of each mouse were evaluated each day and three times (each day during the treatment period) per week, respectively.

A

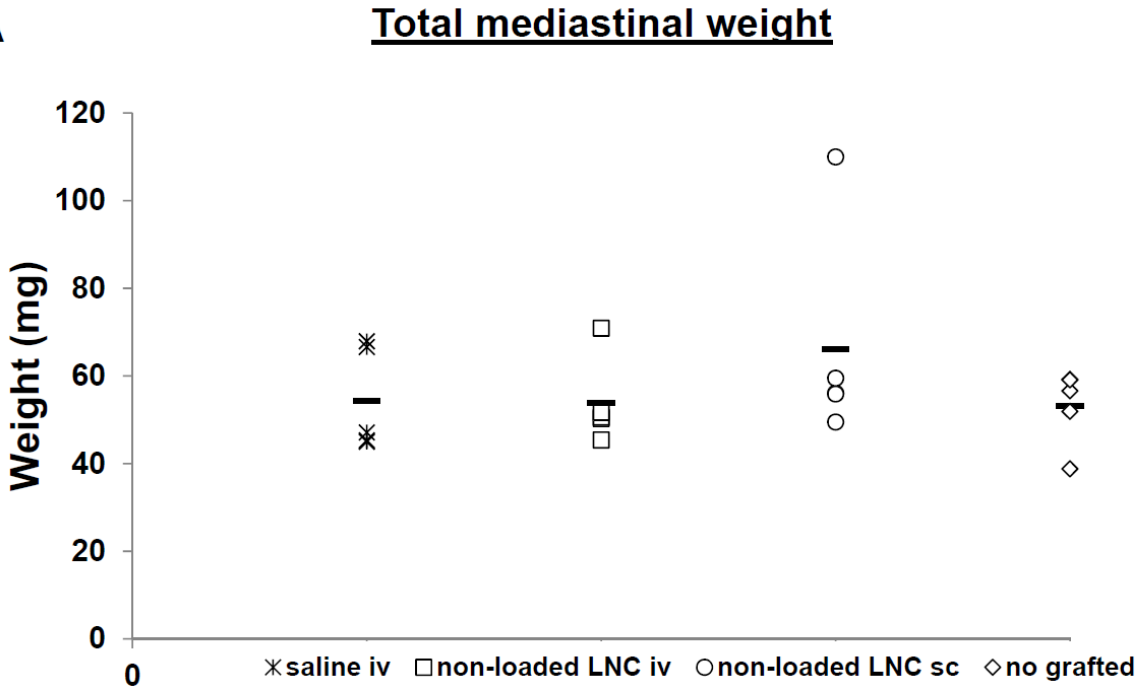
Total mediastinal weight
Weight (mg)
120
100
80
60
40
20
0
0
saline iv
non-loaded LNC iv
non-loaded LNC sc
no grafted

B

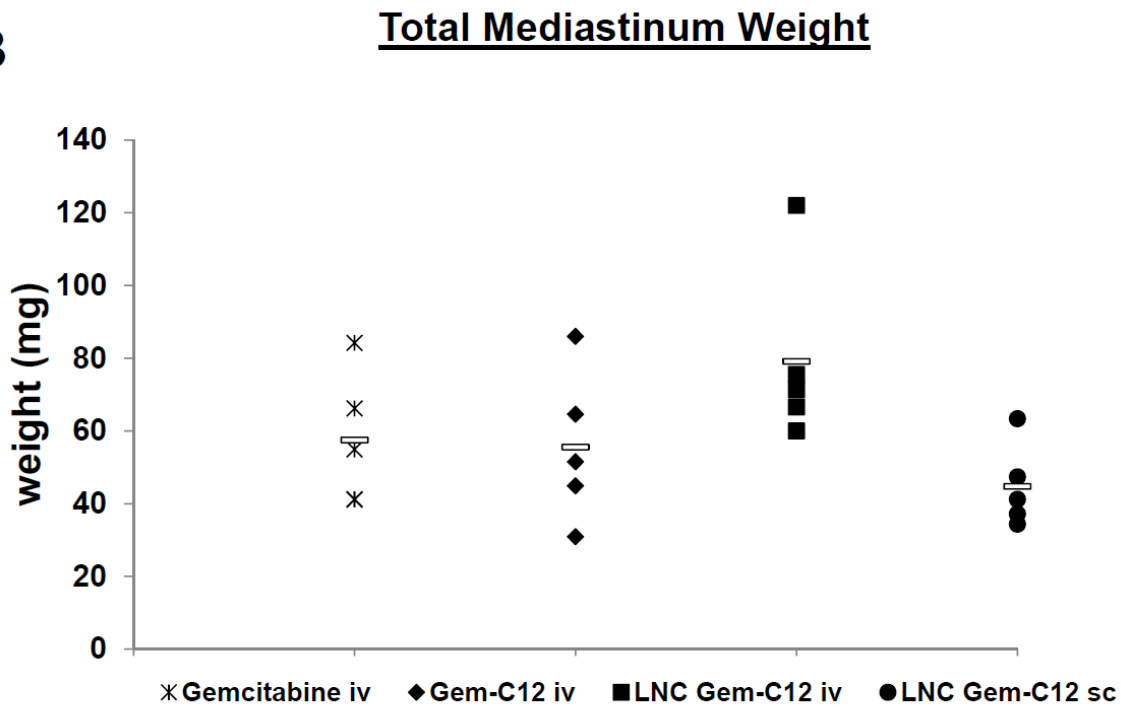
Total Mediastinum Weight
weight (mg)
140
120
100
80
60
40
20
0
Gemcitabine iv
Gem-C12 iv
LNC Gem-C12 iv
LNC Gem-C12 sc

Figure 6. Mediastinum weight of SCID-CB17 mice (A) at day 9 post-tumor graft for control groups (saline *iv*, non-loaded LNC *iv* and non-loaded LNC *sc*) and (B) at day 21 post-tumor graft for treated group (gemcitabine hydrochloride *iv*, Gem-C12 *iv*, Gem-C12 loaded LNC *iv* and Gem-C12-loaded LNC *sc*). 6 weeks-aged male SCID-CB17 mice were grafted with 2×10^4 Ma44-3 cells (implanted in the left lobe) and randomized on day 0. The mice were treated without (star for saline treated group by *iv*, empty square for non-loaded LNC treated group by *iv*, empty circle for non-loaded LNC treated group by *sc*) or with gemcitabine hydrochloride (star) or Gem-C12 loaded in LNC (full square by *iv* and full circle by *sc*) or not (full diamond) at a final dose of 40 mg (molar equivalent gemcitabine hydrochloride) per kilo of body weight beginning on day 5. The treatments were administered intravenously via the tail vein (*iv*) three times a week or by subcutaneous route (*sc*) twice a week. Each experimental group was composed of 5 animals.

3.5. Tolerance of Treatments on SCID-CB17 Mice

Despite the low toxicity profile of gemcitabine hydrochloride in comparison to other cytotoxics used against NSCLC, it presents dose-limiting myelosuppression occuring in approximately 60% or 85% of patients that received the drug as single agent or in combination with cisplatin over a standard 30-min infusion [31,12]. Moreover in 65% of patient, a transient elevation of serum transaminases and phosphatase alcaline is also observed but with no evidence of hepatic toxicity [31]. To evaluate if the different treatments used in SCID-CB17 mice induced myelosuppresion, the complete blood count was performed 8 days after the first injection as in clinic and are presented in Table 2. A significant decrease of platelet count was only observed with the group treated by gemcitabine hydrochloride *iv* in comparison to the saline *iv* control group ($p < 0.05$, Kruskal-Wallis test) and no difference was measured for Gem-C12 non or loaded in LNC and delivered *iv* or *sc* in the respective schedule. No difference was seen in complete granulocyte count because the SCID-CB17 mice are severe combined immunodefiency mice characterized by a severe lymphopenia [28]. In clinical practice, complete granulocyte and platelet counts are the parameters used to evaluate the myelosuppression 8 days after injection to adjust the next dose. If the complete granulocyte and platelet counts are respectively superior to 1000×10^6/L and $100\,000 \times 10^6$/L, 100% of the dose is delivered, comprised between $500\text{-}1000 \times 10^6$/L or $50\,000\text{-}\,100\,000 \times 10^6$/L, only 75% of the dose is administered and if they

are inferior to 500 × 10^6/L or 50 000 × 10^6/L, the treatment is stopped [31]. The limitation of administered dose causing myelosuppression could have an important impact on the response of the treatment in patients.

Plasma biochemical parameters such as aspartate aminotransferase (ASAT), alanine aminotransferase (ALAT), phosphatase alkaline (PH ALK) and serum creatinine are evaluated and presented in Table 3. No significant difference was seen between the different groups in comparison to the control saline *iv* group except a significant decrease of PH ALK for Gem-C12 not loaded in LNC ($p < 0.05$, Kruskal-Wallis test).

	WBC (giga/L)	**RBC (tera/L)**	**HGB (g/dL)**	**HCT (%)**	**PLT (giga/L)**
Saline *iv*	0.2 ± 0.1	9.8 ± 0.3	15.1 ± 0.3	47 ± 1	469 ± 50
Gemcitabine *iv*	0.2 ± 0.1	9.2 ± 0.3	14.0 ± 0.4	45 ± 1	**245 ± 63 ***
Gem-C12 *iv*	0.3 ± 0.2	9.1 ± 0.6	14 ± 1	45 ± 2	275 ± 63
Non-loaded LNC *iv*	0.6 ± 0.3	9.8 ± 0.2	15.1 ± 0.3	47.7 ± 0.9	465 ± 44
LNC Gem-C12 *iv*	0.14 ± 0.03	8.9 ± 0.2	13.7 ± 0.3	43.1 ± 0.9	284 ± 24
Non-loaded LNC *sc*	0.4 ± 0.1	9.4 ± 0.7	14 ± 1	46 ± 3	453 ± 20
LNC Gem-C12 *sc*	0.26 ± 0.06	9.4 ± 0.5	14.5 ± 0.8	45 ± 2	281 ± 83

Table 2. Complete blood counts in different groups. WBC: complete granulocyte count. RBC: red blood cell count. HGB: hemoglobin rate. HCT: hematocrit. PLT: platelet count. Mean values ± SD are presented (n=5). *: $p < 0.05$.

	ASAT (UI/L)	ALAT (UI/L)	PH ALK (UI/L)	Creatinine (mg/L)
Saline *iv*	138 ± 115	24 ± 8	146 ± 8	1.8 ± 0.4
Gemcitabine *iv*	98 ± 27	27 ± 12	129 ± 17	3 ± 3
Gem-C12 *iv*	152 ± 95	23 ± 8	**97 ± 33 ***	2 ± 1
Non-loaded LNC *iv*	77 ± 20	22 ± 4	139 ± 4	1.7 ± 0.5
LNC Gem-C12 *iv*	82 ± 21	18 ± 7	143 ± 14	3 ± 2
Non-loaded LNC *sc*	88 ± 52	24 ± 16	109 ± 5	2 ± 1
LNC Gem-C12 *sc*	157 ± 52	32 ± 10	121 ± 11	4 ± 3

Table 3. Biological analysis in different groups. ASAT: aspartate aminotransferase. ALAT: alanine aminotransferase. PH ALK: phosphatase alkaline. Mean values ± SD (n=5) are presented. *: $p < 0.05$.

4. Discussion

Regional lymph nodes invasion by metastases from the primary tumor is a critical parameter affecting directly the prognosis of patients with NSCLC with a five-year survival rate estimated at 42% for a stage of N0 (without regional lymph node metastases) to 7% for N3 corresponding to the latest stage of lymph node implication [32]. Invasion of the mediastinum lymph nodes corresponds to the N2 and N3 staging with a five-year survival rate of 16% and 7%, respectively [32]. Patients at this stage are considered in the advanced stage III treated mainly by a combination of radiotherapy and chemotherapy with poor improvement in long-term survival and at the expense of a large rise in Grade 3 toxicities [7]. Conventional systemic chemotherapies are not selective and specific enough to combat cancer cells without causing severe systemic side effects. In the case of gemcitabine hydrochloride as a single agent, a high dose of 1250 mg/m^2 is delivered by 30-min intravenous infusion weekly for 2 or 3 weeks followed by a week of rest. This schedule seems to be the best compromise between toxicity and dose intensity to saturate the deoxycitidine kinase responsible to the deamination of gemcitabine [12]. However, it presents dose-

limiting myelosuppression occuring in approximately 60% or 85% of patients that received gemcitabine has single agent or in combination with cisplatin over a standard 30-min infusion [31,12]. In this study, the evaluation of a new nanocarrier system, able to target more specifically the lymph nodes and loaded with a derivative of gemcitabine, Gem-C12, was performed on a patient-like lymphogenous metastatic Ma44-3 preclinical model. Indeed, there are a very few preclinical models of lymphogenous metastatic NSCLC in the literature. Ma44-3 preclinical model developed by Ishikura *et al* [16] was chosen because it (i) is a subpopulation of a human squamous NSCLC grafted in the lung [16], (ii) spreads in the mediastinum [16,21] and (iii) causes the death of mice from the mediastinum metastases and not from the primary tumor [22]. Moreover, this preclinical model was used to evaluate the efficacy of cisplatin or uracil-tegafur delivered when mediastinum metastases were detected (day 5 post-tumor graft) with a significant increase of the lifespan despite the high aggressiveness of the model causing the death of mice from the 10-11th day post-tumor graft [33]. We chose subcutaneous route to deliver the gel because it is the most investigated route for lymphatic targeting [34,35,36,37]. The subcutaneous administration of the gel form of LNC loaded with Gem-C12 released LNC in the interstitial fluid passing in the lymphatic capillary vessels that is drained until lymph nodes as observed by the specific accumulation of LNC in mediastinum lymph nodes (Figure 3B). The systemic exposition of LNC by subcutaneous route is highly limited as previously reported [15]. These results seemed to confirm that absorption by blood capillaries is restricted to water and small molecules and that absorption of nanocarriers inferior to 0.1 µm have direct access to lymphatic capillaries [37]. Despite the presence of primary lung tumor responsible of the cancer cells release to mediastinum, LNC loaded with Gem-C12 only localized in mediastinum lymph nodes were able to exert the same antitumor efficacy than a systemic administration of gemcitabine hydrochloride (Figure 4A and 5A), which exerted a systemic anticancer activity (*e.i.,* on primary lung tumor and mediastinal metastases). Moreover, this similar anticancer activity by targeting lymph nodes was also accompanied by lower systemic side effects. Indeed, Gem-C12 loaded in LNC delivered by *iv* or *sc* routes presented no significant depletion in platelet count, a marker of myelosuppression, contrary to conventional gemcitabine hydrochloride *iv* (Table 2) and no significant depletion in phosphatase alkaline contrary to Gem-C12 not loaded in LNC (Table 3) when compared to the control saline *iv* group, respectively. Nowadays, nanomedicine

approved on the market present a better therapeutic index mainly by decreasing drastically toxicities. For example, Doxil™ (for US) and Caelyx® (for Europe), that are pegylated liposomal doxorubicin, and Myocet™, a non-pegylated liposomal doxorubicin, decrease drastically the cumulative dose-dependent cardiotoxicity but not improve the survival in comparison to conventional doxorubicin [39]. The *nab*-paclitaxel (Abraxane®), albumin-bound paclitaxel, overcomes the toxicities and complications encountered with the conventional formulation based on poly-ethoxylated castor oil (Cremophor® EL) and ethanol, which imply an increase of the administrable dose and therefore a slightly increase of survival [40].

Concerning the similar antitumor activity, the preclinical model used in this study, despite a development of metastases in mediastinum close to those happening in humans, was severe immunodeficiency. Therefore, the immunologic action of gemcitabine was not included in the *in vivo* antitumor activity. Indeed, gemcitabine has shown to increase the expression of class I human leukocyte antigen (HLA) on malignant cells, enhance the cross-presentation of tumor antigens to CD8+ T cells, and selectively kill myeloid-derived suppressor cells (MDSCs), both *in vitro* and *in vivo*, thus facilitating T cell-dependent anti-cancer immunity [41]. Because SCID-CB17 mice present a mutation at the protein kinase, DNA activated, catalytic polypeptide ($Prkdc^{scid}$) locus responsible to non-mature T and B cells [42], that suppress the impact of chemotherapy on immunity but assure a successful human tumor cells engraftment. Good results have been obtained combining gemcitabine and immunotherapy in murine model of pancreatic carcinoma [43] and in non-resectable pancreatic patients during phase II [44]. So, further investigations are required to evaluate the impact of this localized treatment in lymph nodes to enhance immunity against tumor and metastases.

5. Conclusion

The nanocarrier system loaded with a lipophilic derivative of gemcitabine was able to target the mediastinal lymph nodes and exerted a similar antitumor efficacy than the conventional systemic gemcitabine in the lymphogenous metastatic preclinical model with a schedule of twice a week in comparison to the schedule of three times a week for the intravenous route. Moreover, LNC loaded with Gem-C12 and delivered *iv* or

sc route did not induce myelosuppression unlike the conventional systemic gemcitabine.

Acknowledgements

This work has been realized within the research program LYMPHOTARG financially supported by EuroNanoMed ERA-NET 09 and by the Région Pays de la Loire.

References

1. Siegel, R., Naishadham, D., Jemal, A., Cancer Statistics. *A Cancer Journal for Clinicians* **63**, 11-30 (2013).

2. IARC 2008: http://globocan.iarc.fr/ (last visit at 26/03/2013)

3. Molina, J.R., Yang, P, Cassivi, S.D., Schild, S.E., Adjei, A.A.A., Non-Small Cell Lung Cancer: Epidemiology, Risk Factors, Treatment, and Survivorship. *Mayo Clinic Proceeding* **83**, 584-594 (2008).

4. Brambilla, E., Travis, W.D., Colby, T.V., Corrin, B., Shimosato, Y., The new World Health Organization classification of lung tumours. *European Respiratory Journal* **18**, 1059-1068 (2001).

5. Wakelee, H.A., Bernado, P., Johnson, D.H., Schiller, J.H., Changes in the natural history of nonsmall cell lung cancer (NSCLC)-comparison of outcomes and characteristics in patients with advanced NSCLC entered in Eastern Cooperative Oncology Group trials before and after 1990. *Cancer* **106**, 2208-2217 (2006)

6. Howlader, N., Noone, A.M., Krapcho, M., Neyman, N., Aminou, R., Waldron, W., Altekruse, S.F., Kosary, C.L., Ruhl, J., Tatalovich, Z., Cho, H., Mariotto, A., Eisner, M.P., Lewis, D.R., Chen, H.S., Feuer, E.J., Cronin, K.A., Edwards BK (Eds.). SEER Cancer Statistic Review, 1975-2008, National Cancer Institute. Bethesda, MD, http://seer.cancer.gov/csr/1975_2008/, based on November 2010 SEER data submission, posted to the SEER web site, 2011.

7. Fung, S.F.F., Warren, G.W., Singh, A.K., Hope for progress after 40 years of futility? Novel approaches in the treatment of advanced stage III and IV non-small-cell-lung cancer : stereotactic body radiation therapy, mediastinal lymphadenectomy, and novel systemic therapy. *Journal of Carcinogenesis* **11,** 20 (2012)

8. Jett, J.R., Scott, W.J., Rivera, M.P., Sause, W.T., American College of Chest

Physicians, Guidelines on treatment of stage IIIB non-small cell lung cancer. *Chest* **123,** 221S-225S (2003).

9. Socinski, M.A., Morris, D.E., Masters, G.A., Lilenbaum, R., Chemotherapeutic management of stage IV non-small cell lung cancer. *Chest* **123**,226S-243S (2003).

10. Schiller, J.H., Harrington, D., Belani, C.P., Langer, C., Sandler, A., Krook, J., Zhu, J., Johnson, D.H., Comparison of four chemotherapy regimens for advanced non-small-cell lung cancer. The *New England Journal of Medicine* ***346*****,** 92-98 (2002).

11. Moysan, E., Bastiat, G., Benoit, J.-P., Gemcitabine versus Modified Gemcitabine: A Review of Several Promising Chemical Modifications. *Molecular Pharmaceutics*. **10**, 430-44(2012).

12. Toschi, L., Cappuzzo, F., Gemcitabine for the treatment of advanced nonsmall cell lung cancer. *OncoTargets and Therapy* **2,** 209 (2009).

13. Schroeder, A., Heller, D.A., Winslow, M.M., Dahlman, J.E., Pratt, G.W., Langer R., Jacks, T., Anderson, D.G., Treating metastatic cancer with nanotechnology. *Nature Reviews* **12**, 39-50 (2012).

14. Moysan,E., Gonzalez-Fernandez, Y., Lautram, N., Béjaud, J., Bastiat, G., Benoit, J-P., Gemcitabine-loaded lipid nanocapsule hydrogel: when the drug is a key player of the nanomedicine structure

15. Moysan,E., Wauthoz, N., Gonzalez-Fernandez, Y., Lautram, N., Kondo, K., Hureaux, J., Bastiat, G., Benoit, J-P. Aqueous suspension and hydrogel of gemcitabine prodrug-loaded lipid nanocapsules: in vitro behavior and in vivo tissuedistribution

16. Ishikura, H., Kondo, K., Miyoshi, T., Kinoshita, H., Hirose, T., Monden, Y., Artificial lymphogenous metastatic model using orthotopic implantation of human lung cancer. *The Annals of Thoracic Surgery* **69,** 1691–1695 (2000).

17. Heurtault, B., Saulnier, P., Pech, B., Proust, J.-E., Benoit, J.-P., A novel phase inversion-based process for the preparation of lipid nanocarriers. *Pharmaceutical Research* **19,** 875–880 (2002).

18. Heurtault, B., *et al,* Lipidic nanocapsules: preparation process and use as Drug Delivery Systems. (2000).

19. Allard, E., Passirani, C., Garcion, E, Pigeon, P., Vessières, A., Jaouen G., Benoit, J.-P., Lipid nanocapsules loaded with an organometallic tamoxifen derivative as a novel drug-carrier system for experimental malignant gliomas. *Journal of Controlled Release* **130,** 146–153 (2008).

20. Peltier, S., Oger, J.-M., Lagarce, F., Couet, W., Benoit, J.-P., Enhanced oral paclitaxel bioavailability after administration of paclitaxel-loaded lipid nanocapsules. *Pharmaceutical. Research.* **23,** 1243–1250 (2006).

21. Ishikura, H., Kondo, K., Miyoshi, T., Takahashi, Y., Fujino, H., Monden, Y., Green Fluorescent Protein, Expression and Visualization of Mediastinal Lymph Node Metastasis of Human Lung Cancer Cell Line Using Orthotopic Implantation. *Anticancer Research* **24,** 719–724 (2004).

22. Fujino, H., Kondo, K., Ishikura, H., Maki, H., Kinoshita, H., Miyoshi, T., Takahashi, Y., Sawada, N., Takizawa, H., Nagao, T., Sakiyama, S., Monden, Y., Matrix metalloproteinase inhibitor MMI-166 inhibits lymphogenous metastasis in an orthotopically implanted model of lung cancer, *Molecular Cancer Therapeutics* **4**, 1409-1416 (2005).

23. Servais, E.L., Colovos C., Bograd, A.J., White J., Sadelain, M., Adusumilli, P.S., Animal models and molecular imaging tools to investigate lymph node metastases. *Journal of Molecular Medicine* **89**, 753-769 (2011).

24. Takizawa, H., Kondo, K., Toba, H., Kenzaki, K., Sakiyama, S., Tankoku, A., Fluorescence diagnosis of lymph node metastasis of lung cancer in a mouse

model. *Oncology Reports* **22**, 17-21 (2009)

25. Ali, A.H.K., Takizawa, H., Kondo K., Matsuoka, H., Toba, H., Nakagawa, Y., Kenzaki K., Sakiyama, S., Kakiuchi, S., Sekido, Y., Sone, S., Tangoku, A., 5-aminolevulinic acid-induced fluorescence diagnosis of pleural malignant tumor. *Lung cancer* **74**, 48-54 (2011).

26. Murayama, Y., Harada, Y., Imaizumi, K., Dai P., Nakano, K., Okamoto, K., Otsuji, E., Takamatsu, T., Precise detection of lymph node metastases in mouse rectal cancer by using 5-aminolevulinic acid. *International Journal of Cancer* **125**, 2256-2263 (2009).

27. Nokes, B., apel, M., Jones, C., Brown, G., Lang, J.E., Aminolevulinic acid (ALA): photodynamic detection and potential therapeutic applications. *Journal of Surgical Research* **In press**, 1-10 (2013).

28. Custer, R. P., Bosma, G. C., Bosma, M. J., Severe Combined Immunodeficiency (SCID) in the Mouse. Pathology, Reconstitution, Neoplasms. *Am J Patho*l **120**, 464-477 (1985).

29. Shepherd, M., Dailey, H.A., A continuous fluorimetric assay for protoporphyrinogen oxidase by monitoring porphyrin accumulation. *Analytical Biochemistry* **344**, 115-121 (2005).

30. Van den Broeck, W., Derore, A., Simoens, P., Anatomy and nomenclature of murine lymph nodes: Descriptive study and nomenclatory standardization in BALB/cAnNCrl mice. *Journal of Immunological Methods* **312**, 12-19 (2006).

31. Gemcitabine FDA-approved label, 2005. http://www.accessdata.fda.gov/drugsatfda_docs/label/2005/020509s033lbl.pdf

32. Detterbeck, F.C., Boffa, D.J., Tanoue, L.T., The new lung cancer staging system. *Chest* **136**, 260-271 (2009).

33. Ishikura, H., Kondo, K., Miyoshi, T., Kinoshita, H., Takahashi, Y., Fujino, H., Monden, Y., Suppression of Mediastinal Metastasis by Uracil-Tegafur or cis-Diamminedichloroplatinum(II) Using a Lymphogenous Metastatic Model in a Human Lung Cancer Cell Line. *Clinical Cancer Research* **7,** 4202–4208 (2001).

34. Trubetskoy, V. S., Cannillo, J. A., Milshtein, A., Wolf, G. L., Torchilin, V. P., Controlled delivery of Gd-containing liposomes to lymph nodes: surface modification may enhance MRI contrast properties. *Magnetic Resonance Imaging* **13,** 31–37 (1995).

36. Xie, Y., Bagby, T. R., Cohen, M., Forrest, M. L., Drug delivery to the lymphatic system: importance in future cancer diagnosis and therapies. *Expert Opinion on Drug Delivery* **6,** 785–792 (2009).

37. Chen, J., Yao, Q., Li, D., Zhang, B., Li, L., Wang, L., Chemotherapy targeting regional lymphatic tissues to treat rabbits bearing VX2 tumor in the mammary glands. *Cancer Biology & Therapy* **7,** 721–725 (2008).

38. Oussoren, C., Storm, G., Liposomes to target the lymphatics by subcutaneous administration. *Advanced Drug Delivery Reviews* **50,** 143–156 (2001).

39. Leonard, R.C.F., Williams, S., Tulpule, A., Levine, A.M., Oliveros, S., Improving the therapeutic index of anthracycline chemotherapy: Focus on liposomal doxorubicin (Myocet^{TM}), *The Breast* **18**, 218-224 (2009).

40. Hawkins, M.J., Soon-shiong P., Desai, N., Protein nanoparticles as drug carriers in clinical medicine, *Advanced Drug Delivery Reviews* **60**, 876-885 (2008).

41. Galluzi, L., Senovilla, L., Zitvogel, L., Kroemer, G., The secret ally:immunostimulation by anticancer drugs, *Nature Reviews Drug Discovery* **11**, 215-233 (2012).

42. Shultz, L., Ishikawa, F., Greiner, D.L., Humanized mice in translational biomedical research, *Nature Reviews Immunology* **7**, 118-130 (2007).

43. Ghansah, T., Vohra, N.,Kinney, K., Weber, A., Kodumudi, K., Springett, G., Sarnaik, A.A., Pilon-Thomas S., Dendritic cell immunotherapy combined with gemcitabine chemotherapy enhances survival in a murine model of pancreatic carcinoma, *Cancer Immunol Immunother,* DOI 10.1007/s00262-013-1407-9 (2013).
44. Yanagimoto, H., Shiomi, H., Satoi, S., Mine, T., Toyokawa H., Yamamoto, T., Tani, T., Yamada, A., Kwon A-H, Komatsu, N., Itoh, K., Noguchi, M., A phase II study of personalized peptide vaccination combined with gemcitabine for non-resectable pancreatic cancer patients, *Oncology Reports* **24**, 795-801 (2010).

Discussion générale et perspectives

Le cancer est une maladie caractérisée par une prolifération anormale de cellules d'un tissu ou d'un organe, par leur pouvoir envahissant local et leur capacité à métastaser à distance du foyer primitif. La dissémination des métastases peut se faire par voie sanguine mais aussi par voie lymphatique. En empruntant la voie lymphatique, voie majeure de dissémination métastatique, les cellules tumorales envahissent les ganglions et conduisent à la formation d'un foyer secondaire. Dans le cadre des cancers présentant une dissémination par voie lymphatique, un traitement systémique post-opératoire pour diminuer le risque de rechute métastatique est délivré. Cependant, une fois que les cellules tumorales atteignent les ganglions, le pronostic de survie devient mauvais. Différentes stratégies ont été développées et sont aujourd'hui utilisées pour améliorer l'activité des agents anticancéreux en général. Les plus courantes sont : i) l'association des drogues entre elles, (ii) la synthèse de nouveaux dérivés (prodrogues) [1–4] et iii) la vectorisation.

Dans ce contexte, l'objectif de cette thèse a été d'évaluer le potentiel thérapeutique d'une nanovectorisation, des nanocapsules lipidiques chargées en gemcitabine, et d'en optimiser son utilisation au sein d'un modèle orthotopique de cancer pulmonaire formant des métastases dans le médiastin. Dans cette partie, i) les points les plus importants concernant les résultats obtenus seront repris, ii) certains résultats non publiés seront décrits, et ii) des améliorations à apporter aux résultats générés seront discutées.

1. Encapsuler la gemcitabine

1.1 Microémulsion

La solubilisation du principe actif dans les excipients est une étape nécessaire à une encapsulation dans des vecteurs colloïdaux. La modification chimique de la gemcitabine ne fut pas tout de suite réalisée pour encapsuler la drogue. Dans un premier temps des microémulsions eau dans huile ont été réalisées pour encapsuler la gemcitabine. Ce procédé est tiré d'un brevet du laboratoire (US 2012/0027825 A1). Cette invention consiste en un procédé permettant d'encapsuler des actifs à caractère hydrophile.

Plus précisément cette formulation se décompose en 2 étapes. La première étape est la formulation d'une microémulsion, comprenant une phase huileuse, au moins un tensioactif lipophile, une phase polaire ou hydrophile, et contenant au niveau de sa phase polaire ou hydrophile au moins un actif à caractère hydrophile. La deuxième étape consiste à formuler des nanocapsules lipidiques de façon classique et d'y insérer la première microémulsion, contenant le principe hydrophile, juste avant la trempe.

Les tests n'ont pas été réalisés avec la gemcitabine pour des raisons économiques mais avec une sonde fluorescente hydrophile, la rhodamine B. Dans un premier temps la rhodamine B a été préalablement dissoute dans l'eau pour arriver à une concentration finale de 1 à 11 $mg.mL^{-1}$. A 15 mg d'eau ont été ajouté le Labrafac, l'Imwitor® 308 et le Tween® 80. L'ensemble a été chauffé à 37℃ pendant 24h. C ette microémulsion a été ajoutée pendant la formulation de nanocapsules lipidiques classiques de 50 nm juste avant l'étape de trempe. Une séparation par exclusion stérique a ensuite été réalisée à l'aide d'une colonne Sephadex®, qui constitue un moyen fiable, facile et rapide de déterminer le rendement d'encapsulation. Après purification des LNCs sur la colonne et analyse par fluorescence, la rhodamine B n'a pas été retrouvée dans les LNCs.

Constituants	Quantité (mg)	Quantité (mg)
Imwitor® 308	35	35
Tween® 80	15	15
Labrafac	35	35
Eau	15	15
Rhodamine B (dans l'eau)	11 $mg.mL^{-1}$	1 $mg.mL^{-1}$
Taille de la microémulsion	**5,50 nm**	**5,10 nm**
Taille des LNCs	**75 nm**	**50 nm**
PdI des LNCs	**0,23**	**0,05**
Encapsulation (%)	**0**	**0**

Tableau 1 : Récapitulatif des constituants des microémulsions, des tailles et du taux d'encapsulation de la rhodamine B.

Malgré de nombreux changements dans le procédé des microémulsions : nature et proportions des surfactants, influence de la température ou encore de la concentration en actif hydrophile, aucune encapsulation de la rhodamine B n'a été obtenue avec cette technique. Cette voie d'encapsulation n'a pas été poursuivie dans le cadre de cette thèse. De très récents résultats ont été obtenus avec l'encapsulation de la gemcitabine à l'aide de ce type de microémulsion au laboratoire (non publié pour le moment). Jusqu'à 30% de gemcitabine ont été encapsulés, mais ces résultats préliminaires demandent à être confirmés et améliorés.

1.2 Changement d'huile et de surfactant

Dans un deuxième temps, après l'abandon des microémulsions, l'investigation d'une huile et/ou d'un surfactant pouvant solubiliser la gemcitabine a été conduite. La gemcitabine base, insoluble dans l'eau, a été choisie comme principe actif. Un précédent travail de thèse a inspiré cette méthode. En effet plusieurs huiles et surfactants avaient été étudiés pour trouver un composé capable de solubiliser du Sn38 (métabolite actif de l'irinotécan) [5]. Le tableau 2 récapitule tous les candidats testés pour solubiliser la gemcitabine base. Une insolubilité de cette molécule dans une multitude d'huile à été retrouvée ($C_{gemcitabine\ base} < 1 mg.mL^{-1}$). Cependant deux surfactants ont montré une capacité à la solubiliser, il s'agit du Labrasol® et du Transcutol®. Après la mise au point de formulation blanche (sans principe actif), stable et monodisperse, l'encapsulation de la gemcitabine base a été réalisée, une fois celle-ci solubilisée à 1 $mg.mL^{-1}$ dans les deux surfactants. Malgré la solubilisation de la gemcitabine base, aucune encapsulation n'a été obtenue. Il a été compris par la suite (lors de la synthèse de la prodrogue) que la gemcitabine base devenait soluble dans l'eau à haute température. Le fait de chauffer la gemcitabine base a certainement provoqué sa solubilisation dans l'eau par création de sel de gemcitabine empêchant ainsi son encapsulation dans la phase huileuse des LNCs.

Excipients	Solubilité
Labrasol®	Oui
Transcutol®	Oui
Captex® 500	Non
Captex® 8000	Non
Huile d'olive	Non
Huile de ricin	Non
Plurol oléique	Non
Captex ® 200	Non
Lauroglycol	Non
Labrafil M1944	Non
Huile de sésame	Non

Tableau 2. Listes des huiles et surfactants testés.

1.3 Modification chimique

Après les différents échecs d'encapsulation dans des microémulsions et autres formulations, l'augmentation de la lipophilie de la drogue a été retenue comme solution pour envisager son encapsulation dans les nanocapsules lipidiques. Dans un premier temps, la gemcitabine a été greffée avec une chaine en C18, mais des problèmes de purification ont amené au greffage d'une chaine plus courte, une chaine laurique (C12), sur la fonction amine. Une étude de stabilité de la Gem-C12 à 85℃ pendant 5 min a été réalisée (Analyse par RMN ^{1}H). Les figures 1a et b montrent que cette molécule ne subit aucune dégradation en atteignant, pour un court laps de temps, la température de 85℃. Dans l e cas des formulations avec la gemcitabine modifiée, la température n'est jamais montée plus haut que 75℃. Ainsi la drogue reste intacte une fois encapsulée dans les nanocapsules lipidiques.

La synthèse de ce travail d'encapsulation met en évidence les difficultés que l'on rencontre lorsque l'on encapsule une molécule hydrophile. Quelle que soit la stratégie choisie, il en ressort que l'obtention d'une encapsulation en principe actif suffisante requiert une importante étape d'optimisation du procédé. Dans ce travail, l'augmentation de la lipophilie a semblé être la meilleure option. Ainsi, des nanocapsules lipidiques hautement chargées en gemcitabine modifiée, grâce à la participation active de la prodrogue au processus de formulation, ont été obtenues.

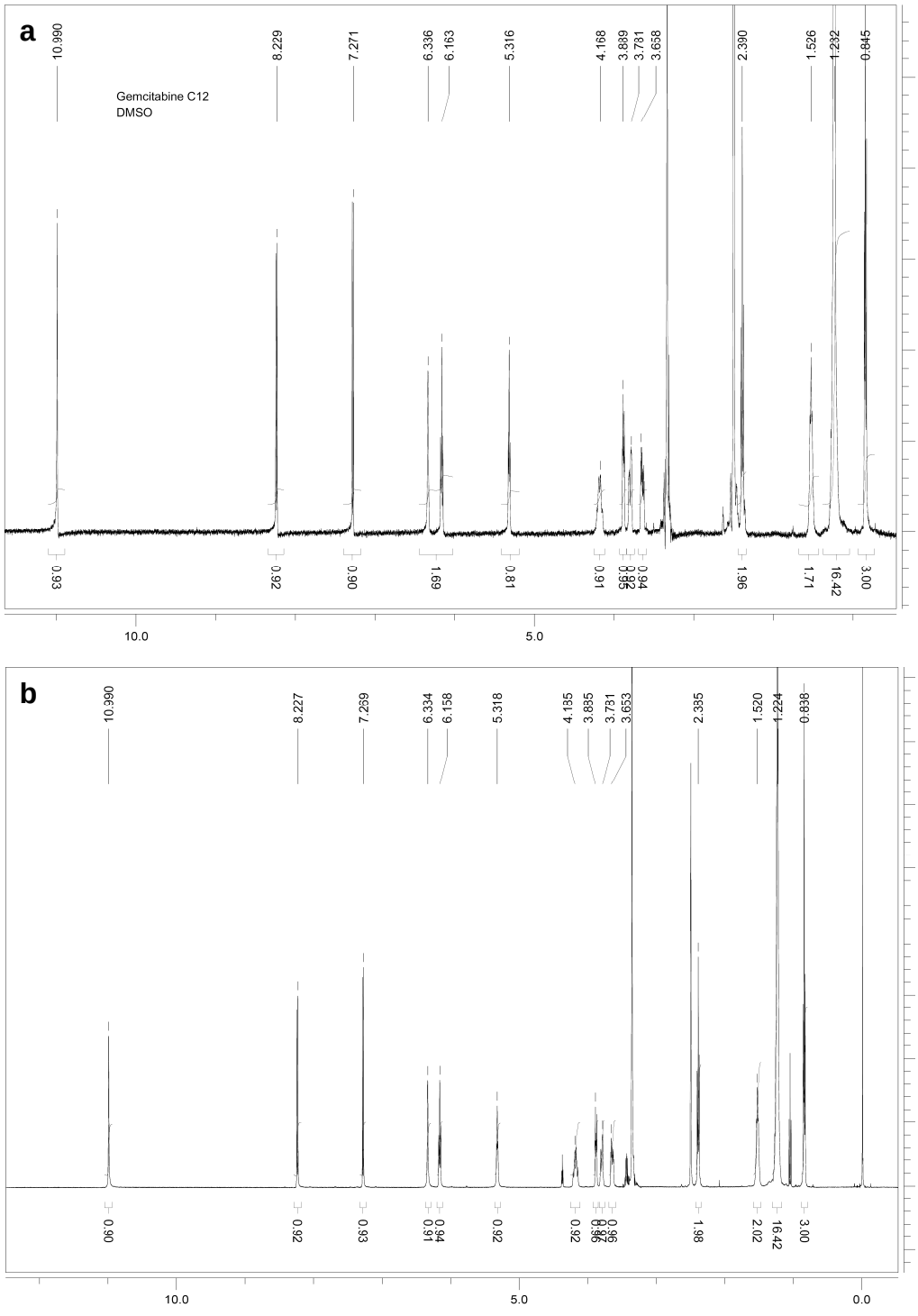

Figure 1 : Spectre RMN ^{1}H de la Gem-C12 dans du DMSO avant (a) et après (b) chauffage à 85℃ pendant 5min.

2. Obtention d'un hydrogel

Il a été démontré par tensiométrie de surface que la Gem-C12 se met à l'interface entre le Labrafac et l'eau, jouant ainsi le rôle d'un surfactant. Néanmoins, la participation active de la Gem-C12 à la formulation n'est pas sa seule action. En effet, de manière surprenante et très intéressante, une gélification des LNCs a été obtenue après incorporation de la Gem-C12. C'est la première fois au laboratoire qu'une gélification est obtenue après encapsulation d'une molécule. De plus, une fois le gel dilué, nous retrouvons les LNCs en suspension. L'obtention d'un gel après mélange d'huile, d'eau et de surfactant n'est pas nouveau. En effet, ce type de gel, appelé organogel, a été très étudié dès les années 90 et plus particulièrement par le Dr. Murdan [6–10]. Cependant, il n'a jamais été retrouvé à notre connaissance dans la littérature d'études comparables à celle-ci, où la dilution du gel permet d'obtenir des systèmes nanoparticulaires en suspension. En effet, le plus souvent les organogels adoptent une architecture tridimensionnelle composée de micelles cylindriques, qui une fois dilués se désassemblent pour former d'une part une phase polaire et de l'autre une phase apolaire [11]. La figure 2 représente de façon schématique l'arrangement des nanocapsules lipidiques sous forme gel. La tête polaire de la Gem-C12 (la gemcitabine), est orientée vers la phase aqueuse, tandis que la chaine laurique est orientée vers le cœur de la LNC. La gemcitabine est ainsi responsable des liaisons hydrogènes conduisant à la formation d'un réseau tridimensionnel prenant la forme d'un « collier de perles ».

L'encapsulation de gemcitabine lipophile dans des systèmes nanoparticulaires n'est pas une nouveauté [12–16] , en revanche la gélification du système en est une. De nombreuses équipes de recherche ont travaillé sur des modifications de la gemcitabine couplées à son encapsulation. Ainsi des micelles polymériques, des nanoémulsions, des liposomes ou encore des nanoparticules ont encapsulé de la gemcitabine modifiée par une chaine alkyle mais aucune de ces études n'ont fait part d'une quelconque gélification [12–19]. Cela peut s'expliquer de deux manières. Il a été démontré dans la publication n°1 « *Gemcitabine-loaded lipid nanocapsule hydrogel: when the drug is a key player of the nanomedicine structure* » que la gélification était dépendante de la concentration en particule et également de la concentration en Gem-C12. Dans ce travail de thèse, de fortes concentrations en particules (445

mg.mL^{-1}) et en principe actif ont été utilisées. Les études précédemment citées n'ont pas utilisé de telles concentrations, ce qui peut expliquer qu'on ne retrouve pas de gélification. De plus, ces études ont utilisé une forme plus lipophile que la Gem-C12 et le fait d'augmenter cette lipophilicité entraîne peut-être le principe actif modifié à être encapsulé au cœur des nano-objets (perte de son amphiphilie).

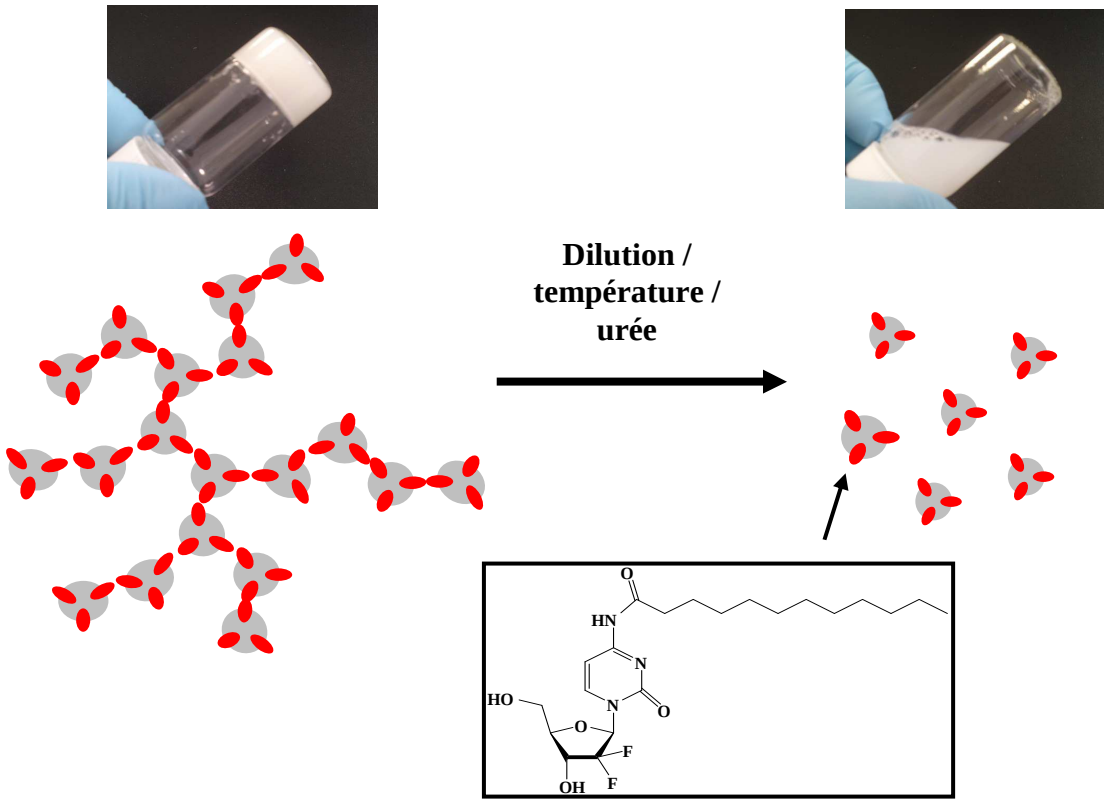

Figure 2: Représentation schématique du gel obtenu avec des LNCs chargées en Gem-C12.

Le gel développé dans cette étude est considéré comme un hydrogel. En effet, un hydrogel peut être défini comme une formulation semi-solide ayant une phase externe polaire (ici une phase aqueuse), immobilisée dans l'espace par un réseau tridimensionnel. Dans le cadre de cet hydrogel, le réseau tridimensionnel est formé par les LNCs reliées par des liaisons inter-nanoparticulaires.

2.1. Application des hydrogels

A l'origine, Wichterle et Lim ont introduit les hydrogels pour des utilisations biologiques dans les années 1960 [20]. Depuis, leur intérêt dans le domaine pharmaceutique et médical n'a fait qu'augmenter au fil des années [21,22]. En effet, le nombre de publications qui leurs sont consacrés est en constante augmentation avec plus de 2000 références en 2010 [23]. L'application topique de nombreuses molécules (lipophiles ou hydrophiles) a été améliorée : meilleures pénétration et absorption, en utilisant un hydrogel. Différentes applications sont retrouvées : cicatrisation [24,25], cosmétologie [26], administration locale de molécules [27,28], ingénierie tissulaire [29,30], ingénierie oculaire [31,32] ou encore délivrance d'anticancéreux [33–36]. L'administration par voie parentérale de molécules par le biais d'hydrogel a récemment gagné en importance en raison des nombreux avantages que représente ce mode d'administration. En effet, les injections locorégionales permettent d'éviter le premier passage hépatique, favorise une diffusion continue et plus longue du produit, limite les injections à haute dose et diminue les effets secondaires.

2.2. Chimiothérapie

En clinique humaine et vétérinaire, une seule injection rapide d'un hydrogel chargé en molécules thérapeutiques et s'hydrolysant sur plusieurs jours/semaines permettrait de pallier aux séances de perfusions lors de leur administration systémique qui sont la plupart du temps longues. De plus, dans le cadre d'une utilisation en médecine humaine la réduction des effets secondaires en évitant des administrations systémiques quotidiennes augmente l'attractivité de ce type de formulation. De nombreux hydrogels sont actuellement étudiés pour la délivrance d'anticancéreux. Il y a actuellement 202 études en phase clinique utilisant des « hydrogels » et seulement 11 pour une application dans le domaine des « cancers » (www.clinicaltrials.gov, consulté le 2 avril 2013). Cela montre l'intérêt grandissant des hydrogels et la faible avancée de leur utilisation dans le domaine de la cancérologie. Un exemple d'hydrogel testé en clinique humaine est l'Oncogel™. C'est un système de relargage contrôlé du paclitaxel, thermosensible, composé d'un copolymère d'acide polylactique-co-glycolique (PLGA) et de PEG avec la structure suivante PLGA–PEG–PLGA. Ce gel a été testé pour le traitement du cancer de l'œsophage

après injection intratumorale [37]. Ce gel permet une libération de paclitaxel continue pendant 6 semaines et permet d'obtenir ainsi une concentration plus élevée directement au niveau du site d'action. Cependant, les études menées ont été stoppées en phase clinique (décision du commanditaire de l'étude, non basée sur des donnés d'innocuité et d'efficacité). Un autre exemple d'hydrogel testé en clinique est le Vantas®. Il est utilisé comme traitement palliatif du cancer avancé de la prostate. Il s'agit d'un implant non biodégradable (composé de méthacrylate d'hydroxy-2 éthyle, de méthacrylate d'hydroxy-2 propyle et de triméthacrylate de triméthylolpropane) libérant de l'histréline (un analogue synthétique de la gonadoréline). Les études ont montré que l'implant permet une libération continue d'histréline pendant 1 an et une suppression de la testostérone plasmatique [38].

2.3. Hydrogels et nanoparticules

La forte quantité en eau de la plupart des hydrogels résulte en une libération relativement rapide en plusieurs heures/jours des molécules hydrophiles. Ainsi l'incorporation de particules dans les hydrogels est actuellement étudiée comme solution pour obtenir une libération à long terme (Figure 3). De plus, l'incorporation de nanoparticules dans les hydrogels permet également de protéger les drogues d'éventuelles dégradations chimiques/enzymatiques [39]. De nombreuses études sont actuellement menées sur l'incorporation de nanoparticules dans des hydrogels et plusieurs revues en font l'inventaire [39, 40]. La nouveauté de ce travail dans ce domaine est la participation active des nanoparticules dans la gélification. En effet, les gélifications dans toutes les études menées actuellement sont dues à l'ajout de polymères naturels (collagène, gélatine, laminine, Matrigel®, acide hyaluronique, alginate, chitosane, etc...) ou synthétiques (poly(éthylène glycol) (PEG), poly(acide lactique) (PLA), PLGA, polycaprolactone (PCL), polyacrylamide (PAAm), polyuréthane (PU), etc...). Dans cette étude, ce sont les nanocapsules qui permettent cette gélification. Cela permet de ne pas ajouter de polymères et d'éviter d'éventuelles toxicités. En effet, certains polymères naturels rentrant dans la composition des hydrogels sont immunogènes, et certains polymères synthétiques entrainent des réactions inflammatoires et ont des faibles taux de clairance [41].

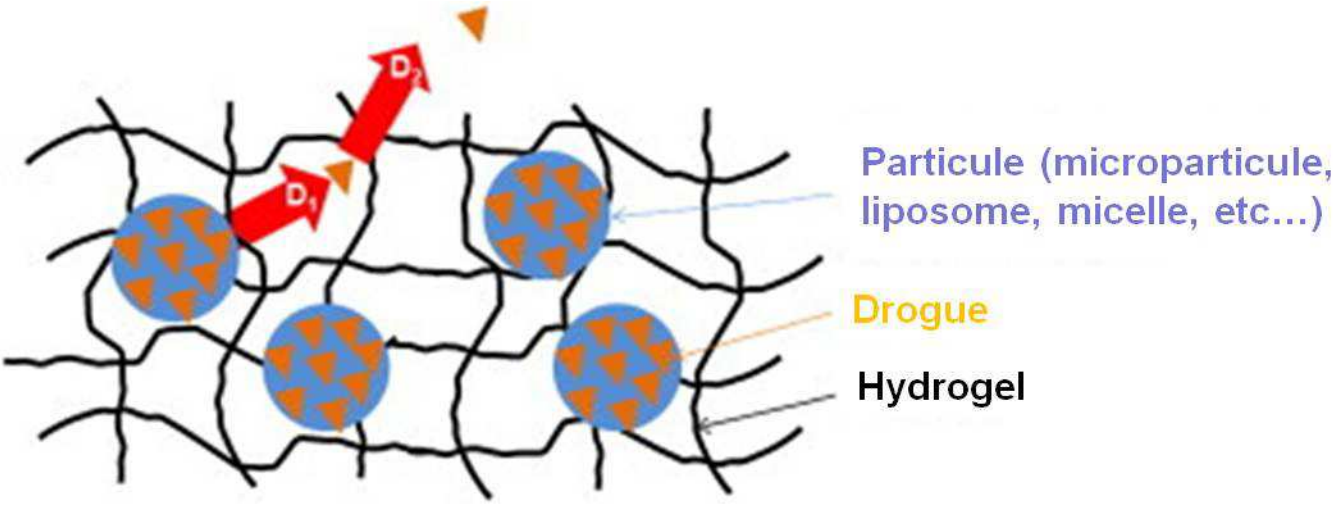

Figure 3 : Représentation schématique d'un hydrogel renfermant des particules renfermant elles-mêmes une drogue (D_1 : libération de la particule, D_2 : diffusion à travers l'hydrogel). *(D'après* Hoare *et al.,2008* [40]*)*

2.4. Universaliser notre hydrogel

A ce jour, l'obtention d'un hydrogel avec les nanocapsules lipidiques est uniquement due à l'encapsulation d'une forme lipophile de la gemcitabine. Or, la gemcitabine est un anticancéreux cytostatique appartenant aux CMR (cancérogène, mutagène et reprotoxique). En effet, des études *in vitro* et *in vivo* ont montré l'apparition d'aberrations chromosomiques [42]. De plus, des études expérimentales chez l'animal ont montré une reprotoxicité avec des anomalies congénitales et d'autres effets sur le développement de l'embryon [43]. Pour élargir la gamme d'utilisation de ce nouvel hydrogel à d'autres pathologies cancéreuses (non traitées par la gemcitabine) ou non, il serait intéressant de développer un hydrogel « non toxique ». La gemcitabine est un analogue de la désoxycytidine, un désoxynucléoside appartenant à la famille des pyrimidines. Il serait alors judicieux de greffer une chaine alkyle sur la fonction amine de cet analogue, tout comme sur la désoxyadénosine ou la désoxyguanosine. En effet, ces trois désoxynucléosides possèdent également sur leur cycle purique une fonction amine. Une fois encapsulées dans les nanocapsules lipidiques, il suffira d'étudier le comportement rhéologique de ces formulations.

Une fois un hydrogel non toxique obtenu, une multitude de possibilité s'ouvriront pour son utilisation comme par exemple le traitement des plaies, de l'ingénierie tissulaire,

l'apport de principes actifs *in situ*, etc. Il serait aussi envisageable de combiner une molécule hydrophobe et une molécule hydrophile. La molécule hydrophile se retrouverait piégée dans la partie aqueuse et la molécule hydrophobe dans le cœur des nanocapsules lipidiques. De plus, la vitesse d'érosion du gel ou de libération des LNCs pourrait être régulée en fonction de la durée souhaitée pour la diffusion et l'action du médicament en jouant sur la quantité de molécule gélifiante au sein des LNCs (voir publication n°2 : *Aqueous suspension and hydrogel of gemcitabine prodrug-loaded lipid nanocapsules: in vitro behavior and in vivo tissue distribution*).

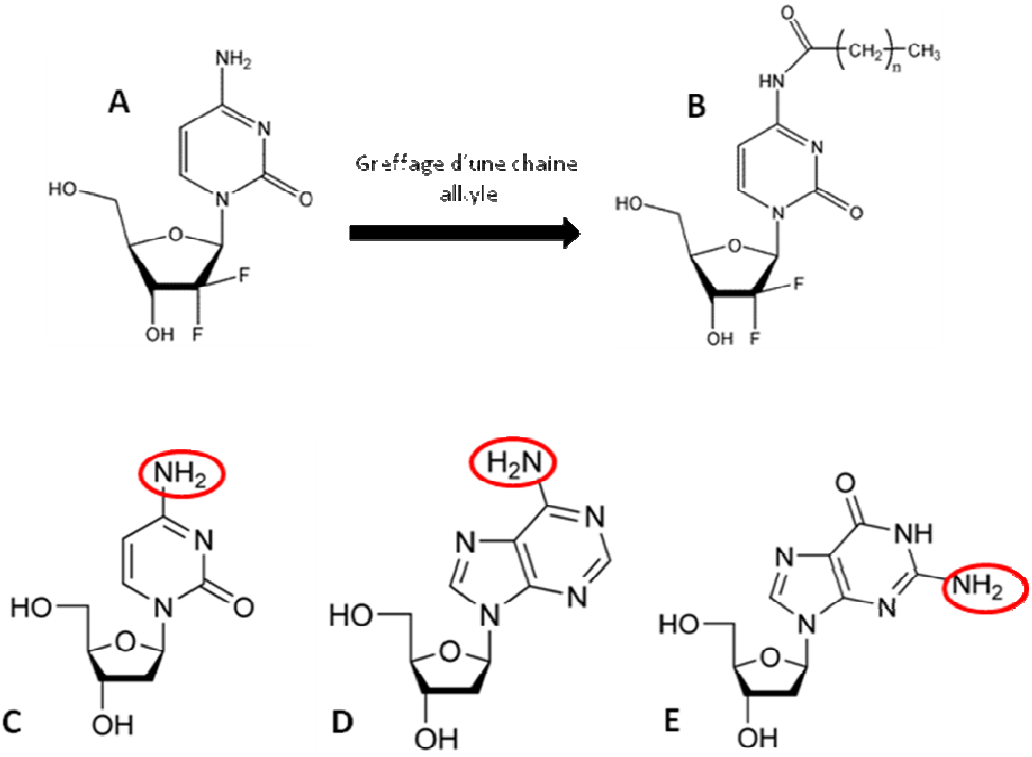

Figure 4: Représentation schématique de la réaction chimique rendant la gemcitabine (A) lipophile (B), et des candidats possibles pour remplacer la gemcitabine. (C: désoxycytidine, D: désoxyadénosine, E: désoxyguanosine).

3. Caractérisation de la gélification

Après la mise en évidence de liaisons hydrogène entre les têtes polaires de la gemcitabine, je me suis penché sur la présence ou non de Gem-C12 dans des micelles de Kolliphor® (hydroxystéarate de PEG_{660}). En effet, est-ce qu'a la fin de la formulation des nanocapsules lipidiques, il n'y a uniquement que des LNCs ou alors des LNCs et des micelles encapsulant toutes les deux la Gem-C12 ? Ces micelles de Kolliphor® chargées en Gem-C12 pourraient être responsables de la gélification du milieu, sachant que la Gem-C12 est insoluble dans l'eau. Pour cela des études de séparation des LNCs et de possibles micelles de Kolliphor® ont été réalisées.

Dans un premier temps, des tubes filtrants Amicon® ont été utilisés, mais aucun seuil de coupure disponible n'a réussi à séparer les micelles de Kolliphor® (12 nm) des LNCs (55 nm). Les micelles ne sont pas passées à travers le seuil de coupure de 30 KDa. Les tailles des objets dans le sous-nageant après centrifugation ne sont pas exploitables car l'intensité de la lumière diffusée est trop faible, signifiant une faible présence de matière. En revanche, le seuil de coupure de 100 KDa est trop grand pour séparer les micelles des LNCs. En effet des LNCs ont été retrouvées dans le sous-nageant après centrifugation (taille de 55 nm avec un PdI de 0,035). Dans un second temps, une séparation par exclusion stérique a été réalisée à l'aide de colonne de sépharose. Des LNCs et des micelles chargées en Nile Red ont été utilisées. Les LNC chargées en Nile Red sont éluées en premier suivi des micelles (Figure 5). Cependant cette méthode n'a permis qu'une séparation partielle car les micelles commencent à sortir avant même l'élution totale des LNCs (Figure 5).

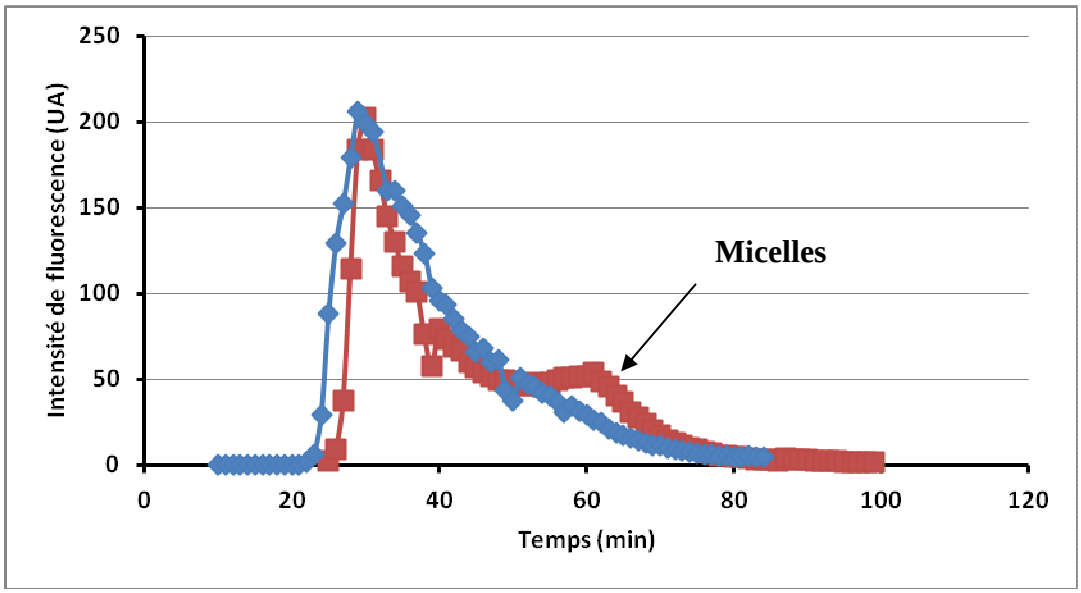

Figure 5 : Profil d'élution de LNCs chargées en Nile Red (courbe bleue) et d'un mélange de LNCs et de micelles (courbe rouge) par exclusion stérique sur colonne de sépharose.

Finalement, la dialyse a été choisie comme alternative aux deux précédentes méthodes de séparation. Des LNCs chargées en Nile Red (3ml) ont été dialysées avec un seuil de coupure de 100 KDa contre un grand volume d'eau (4L), changé 3 fois par jour pendant 7 jours pour accélérer la sortie d'éventuelles micelles. En parallèle, des micelles de Kolliphor® contenant du Nile Red ont également été dialysées de la même manière. De façon étonnante, après dialyse des micelles, une coloration rose de la membrane de dialyse a été observée. De plus, des objets (sans filtration de la solution dialysée) de plus de 5 µm de diamètre hydrodynamique ont été retrouvés dans le boudin de dialyse. Ces résultats indiquent que le processus de dialyse des micelles se fait par la sortie des chaînes libres de Kolliphor® (à la concentration micellaire critique dans le boudin de dialyse). Ainsi l'équilibre est déplacé et des micelles se détruisent à l'intérieur du boudin pour se reformer à l'extérieur. Finalement, le Nile Red libéré lors de la destruction des micelles de Kolliphor® se retrouve adsorbé sur la membrane de dialyse ou alors s'associe pour former des cristaux en solution. Lors de la dialyse des LNCs chargées en Nile Red sans ajout de micelle de Kolliphor®, aucune coloration de la membrane et aucune variation de la taille n'a été observé sur la solution dialysée. Ces derniers résultats démontrent qu'aucun passage de micelles ne s'est produit et donc qu'il ne semble pas y avoir de micelle de Kolliphor® libre lors de la formulation des LNCs.

Des dialyses similaires ont été effectuées avec des LNCs et des micelles chargées en Gem-C12. Après 7 jours de dialyse, les solutions dialysées ont été filtrées sur 0,2 µm pour éliminer d'éventuels cristaux de Gem-C12, puis analysées par UPLC. Les résultats ont montré une diminution de 48 ± 0,4% de la quantité en Gem-C12 dans les solutions contenant les micelles, alors qu'une diminution de seulement 7,8 ± 3,7% est obtenue avec les LNCs. Cette dernière expérience est à répéter pour confirmer les résultats obtenus mais l'ensemble des ces résultats semble indiquer qu'il n'y a pas de micelle encapsulant la Gem-C12 et que l'encapsulation de la prodrogue se fait uniquement dans les nanocapsules lipidiques. La gélification du système est bien due à des interactions entre les LNCs et non pas à des interactions LNCs-micelles.

Pour finir de caractériser l'hydrogel, une observation de la taille et de la morphologie des LNCs (sous forme liquide et sous forme gel) par microscopie électronique à transmission, par cryo-microscopie électronique à balayage et par microscopie à force atomique a été réalisée. Malheureusement aucun résultat exploitable n'a été obtenu, certainement dû à la dégradation provoquée par le rayonnement d'électrons. Des améliorations doivent être cependant réalisées dans ces études de microscopie car des publications ont déjà montré la possibilité d'observé des hydrogels chargées en nanoparticules lipidiques par cryo-microscopie [44].

4. Biodistribution

L'étude de biodistribution a été réalisée sur des souris immunodéficientes sans greffe tumorale. Il a été démontré un fort tropisme des LNCs vers les ganglions lymphatiques après injection sous-cutanée et intraveineuse. De façon intéressante, une injection sous-cutanée au niveau du cou a permis de cibler spécifiquement les ganglions du haut du corps (ganglions cervicaux, axillaires, médiastinaux, brachiaux) (Figure 6). En effet, il n'a pas été retrouvé ou très peu de fluorescence dans les ganglions inguinaux. Le peu de fluorescence retrouvé est certainement lié à l'entrée des nanocapsules lipidiques dans la circulation sanguine par le canal thoracique. Pour une utilisation thérapeutique, l'injection sous-cutanée a donc pour effet de cibler spécifiquement des ganglions proches du site d'injection et permet ainsi de ne pas toucher inutilement des ganglions sains avec des nanovecteurs contenant un anticancéreux.

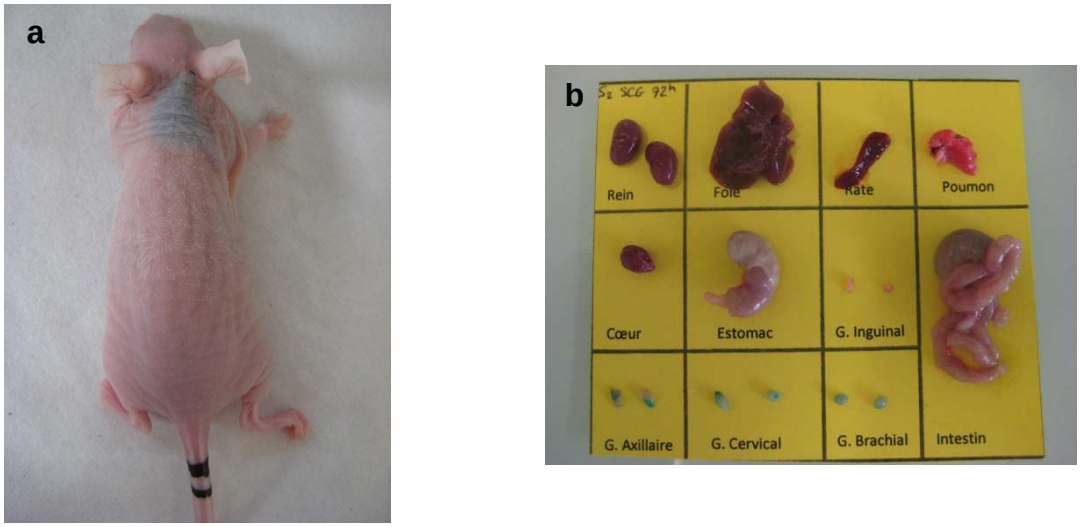

Figure 6 : Souris nude ayant reçu une injection sous-cutanée de LNCs chargées en Gem-C12 et DiD sous forme gel (a). Organes récupérés sur cette souris 72h après l'injection sous-cutanée (b). Les ganglions axillaires, cervicaux et brachiaux sont très clairement devenus bleus par la présence de DiD.

Deux précédentes études de biodistribution des LNCs ont également montré leurs accumulations dans des ganglions [45,46]. Des études histologiques ont révélé une

accumulation des LNCs dans les zones paracortex et les sinus trabéculaires. Cependant, aucune étude n'a encore été réalisée pour savoir quel type de cellules interagit avec les LNCs. Il serait donc intéressant de réaliser des co-marquages comme cela a déjà été fait par ailleurs avec d'autres types de nanoparticules [47] (Figure 7).

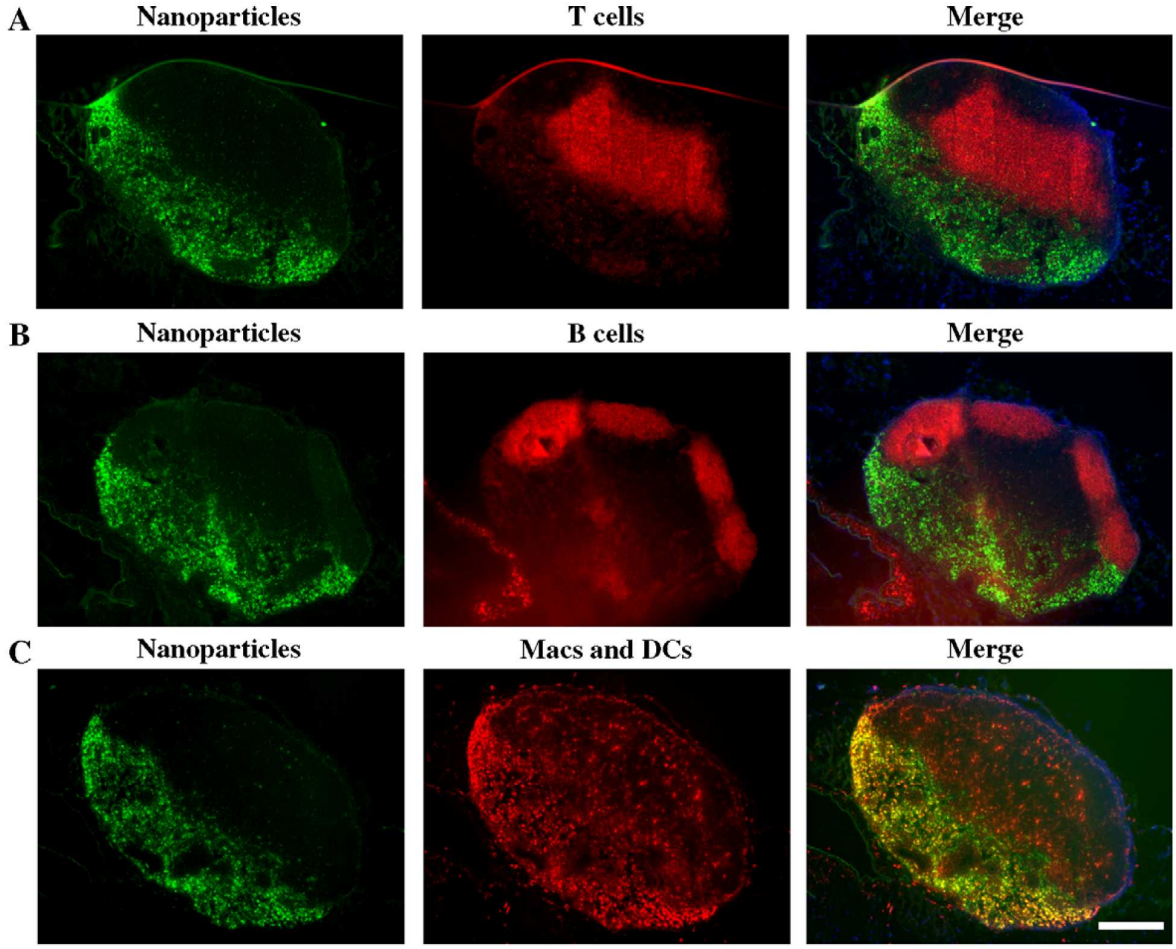

Figure 7 : Co-localisation de nanoparticules de poly(sulfure de phénylène) de 20 nm dans des ganglions lymphatiques (Macs : macrophages, DCs : cellules dendritiques). *(D'après* Reddy *et al.,2006* [47]*)*

Une très brève biodistribution sur 4h a été réalisée sur souris SCID porteuses de la greffe Ma44-3 après injection intraveineuse et sous-cutanée des LNCs chargées en Gem-C12. De très récents résultats non encore publiés ont montré l'induction de macrophages intravasculaires pulmonaires (PIMs) chez des souris porteuses de tumeurs, modifiant totalement la biodistribution des particules après injection

intraveineuse. Dans ce travail, aucune différence de biodistribution, notamment au niveau des poumons, n'a été observée entre des souris saines et porteuses d'une greffe. Il serait cependant intéressant de refaire cette biodistribution, avec plus de souris par groupe et des temps plus longs, pour visualiser au mieux l'interaction des nanocapsules lipidiques avec la tumeur et les métastases ganglionnaires.

Après implantation du gel, aucun signe visuel de réaction inflammatoire n'a été observé. Cependant, des études histologiques doivent être réalisées sur des souris non immunodéficientes pour quantifier de manière plus précise une éventuelle toxicité cutanée et/ou tissulaire. Sur des souris non immunodéficientes, une réaction physiologique cicatricielle peut se mettre en place autour de l'implant l'isolant des tissus environnants et empêchant la libération des LNCs et donc de l'anticancéreux. Cette étude histologique permettrait de déterminer le rapport bénéfice/risque qu'apporterait cette nouvelle thérapie.

5. Efficacité thérapeutique

Le modèle tumoral utilisé avec implantation orthotopique permet d'étudier le développement des tumeurs dans un environnement comparable à la clinique humaine contrairement aux xénogreffes ectopiques. D'un point de vue expérimental, la greffe des cellules Ma44-3 présente un fort taux de réussite et entraîne un développement reproductible et rapide des tumeurs ainsi que des métastases dans le médiastin. Néanmoins, l'agressivité du modèle fait que la fenêtre pendant laquelle les traitements peuvent être administrés est réduite, et les traitements appliqués doivent agir rapidement. Ce modèle tumoral reste intéressant pour évaluer l'efficacité de ce nouveau système, du fait de l'agressivité de la tumeur qui permet la production rapide de résultats.

Lors des études, un gel chargé à 5% en prodrogue a été choisi pour obtenir une libération totale des LNCs en moins de 24 heures. Cependant, pour des modèles animaux développant un cancer moins agressif, une libération plus longue serait possible en utilisant les LNCs chargées à 7,5% en Gem-C12 ou encore plus concentrées. Notre gel a l'avantage de pouvoir être injectable. En effet, une aiguille de 18, 19 ou 21 Gauge permet d'injecter le gel sans perte de ses propriétés viscoélastiques et de façon simple et rapide.

En clinique pour traiter le cancer du poumon non à petites cellules, une dose de 1250 mg/m^2 de gemcitabine est administrée ce qui correspond à une dose équivalente en gemcitabine de 400 mg/kg chez la souris. Des études préliminaires de toxicité ont été réalisées sur des souris SCID-CB17 saines. Comme les volumes à injecter chez la souris sont limités [48], l'étude préliminaire de dose maximale tolérée a commencé avec une dose de 130 mg/kg délivrée en sous-cutanée en une fois. Cette dose a provoqué une diminution du poids des animaux de plus de 20% et entrainé leur mort. La dose a été réduite de moitié sans succès. Finalement, la dose de 40 mg/kg a été utilisée lors de l'étude de biodistribution mais celle-ci présentait à nouveau des effets toxiques sur la souche SCID-CB17. Pour ne pas diminuer excessivement la dose, la dose de 40 mg/kg a été administrée en deux et trois fois sur une semaine par les voies sous-cutanée et intraveineuse, respectivement. Les résultats ont montré que deux injections sous-cutanées de l'hydrogel se sont avérées

aussi efficaces que trois injections intraveineuses de gemcitabine et que trois injections systémiques de LNCs chargées en Gem-C12 (en suspension) sur la survie des souris porteuses d'une greffe.

L'utilisation d'un système de libération local et prolongé est un mode d'administration particulièrement attractif. Bien que l'administration systémique soit le mode de délivrance le plus couramment utilisé en clinique, il nécessite des injections à de fortes concentrations, pour obtenir des concentrations intratumorales efficaces et pour surpasser les phénomènes de résistance. Cependant, l'injection à forte dose, et plus spécifiquement pour la gemcitabine, entraine un certain nombre d'effets secondaires. L'effet secondaire le plus décrit est la myélotoxicité. D'après nos résultats, la libération de la Gem-C12 via les nanocapsules limite le phénomène de myélosuppression donc améliorerait le confort des patients en cas d'utilisation clinique.

De nombreux cancers sont traités avec une bi voire une tri-chimiothérapie. La combinaison d'une seconde molécule, telle que le cisplatine ou le carboplatine, dans notre hydrogel pourrait être envisagée. En clinique, l'association d'une de ces deux molécules de deuxième génération avec la gemcitabine est le traitement standard pour les patients atteints de NSCLC de stade avancé. Mettre au point un hydrogel permettant la libération simultanée d'une polythérapie pourrait apporter aux cancérologues un outil d'intérêt. De plus, si un hydrogel « universel » est formulé, une multitude combinaison est envisageable.

Dans ce travail l'effet de LNCs chargées en Gem-C12 sur un cancer pulmonaire a été rapporté. Cependant, la gemcitabine est le traitement standard du cancer pancréatique. Ce cancer est difficile à traiter et son pronostic est mauvais, avec une survie à 5 ans inférieure à 5% et une médiane de survie d'environ 6 mois. La mortalité avoisine son incidence (rapport mortalité/incidence = 0,99). Bien que n'apportant qu'un très modeste gain de survie par rapport au 5-Fluoro-Uracile (5,6 mois *vs.* 4,4 mois) [49], l'utilisation de la gemcitabine montre surtout, chez un grand nombre de patients, une bonne tolérance [50]. Un test de survie cellulaire (MTS) a montré une forte amélioration de l'efficacité antitumorale des LNCs chargées en Gem-C12 sur la lignée MiaPaCa-2, comparativement à la gemcitabine. Il serait

intéressant de passer sur un modèle *in vivo* de cancer pancréatique pour évaluer le gain d'un traitement par des LNCs chargées en Gem-C12. De récentes études se sont intéressées au effet des nanoparticules chargées en anticancéreux sur des modèles orthotopique de cancer pancréatique. Yoshida *et al*. ont montré que des liposomes encapsulant du cisplatine ont efficacement délivré la drogue dans les cellules tumorales et ont permis une inhibition de la croissance tumorale ainsi qu'une augmentation de la survie des souris [51]. Lee *et al*. et Graeser *et al*. ont respectivement formulé des nanoparticules d'oxyde de fer et des liposomes encapsulant de la gemcitabine. Dans les deux cas, ils ont obtenu une diminution significative de la taille de la tumeur primaire, et également dans la deuxième étude une diminution de la diffusion de métastases [52,53].

6. Une application clinique est-elle possible?

L'hydrogel formulé dans cette étude est-il susceptible un jour d'être utilisable directement en clinique humaine? Telle est la question à laquelle nous allons essayer de répondre dans ce dernier chapitre de discussion.

Paradoxalement, l'innovation sous-tendant cette nouvelle formulation est aussi une contrainte. La voie systémique est la principale voie d'administration utilisée dans les traitements classiques de chimiothérapie anticancéreuse. Or l'ajout de la prodrogue de gemcitabine a pour effet de gélifier les nanocapsules. Pour une utilisation systémique par voie *i.v.*, une dilution suffisamment importante des nanocapsules lipidiques doit être réalisée. En effet, une préparation trop visqueuse ne pourra pas être injectée, au risque de perturber la circulation générale et de générer des thrombus. Mais une fois diluée, une diminution de la concentration en gemcitabine est obtenue avec pour conséquence un schéma thérapeutique impliquant de plus nombreuses injections, et donc un désagrément pour le patient.

L'utilisation de l'hydrogel, non dilué, semble donc être l'utilisation la plus prometteuse. Parmi les différentes voies parentérales, la voie sous-cutanée étudiée dans ce travail permet un passage dans la circulation lymphatique pour accéder aux métastases en migration dans les chaînes ganglionnaires. Cependant, en clinique humaine, retrouve-t-on des traitements sous cette forme ? Il existe à ce jour quelques traitements faisant appel à des implants sous-cutanés et ils sont spécifiques du cancer de la prostate : par exemple le Suprefact® et le Zoladex ® qui sont deux traitements par implants biocompatibles et biodégradables [54,55]. L'injection sous-cutanée de notre hydrogel dans le cadre d'un traitement anticancéreux chez des patients semble donc être une réalité envisageable. Une autre voie intéressante pour l'injection de notre gel, serait la voie intratumorale après résection de la tumeur. Comme pour les disques de Gliadel™, l'injection de l'hydrogel dans la cavité tumorale permettrait une libération continue du principe actif pour empêcher par exemple une reprise tumorale.

7. Conclusion

En conclusion, cette thèse a été un travail réalisé sur différents aspects du développement d'une formule permettant le traitement d'un cancer pulmonaire métastasant dans les ganglions lymphatiques. Premièrement, un aspect technologique a été le développement d'un vecteur capable d'encapsuler la gemcitabine lipophile et deuxièmement, un aspect plus expérimental s'est concrétisé par le développement et l'utilisation *in vivo* d'un modèle tumoral.

Les apports majeurs de ce travail sont i) d'avoir proposé une nouvelle stratégie permettant l'encapsulation d'une molécule à la base hydrophile dans des nanocapsules lipidiques, ii) d'avoir obtenu une forme hydrogel permettant la libération de LNCs intactes, iii) et d'avoir employé un nouveau modèle tumoral pulmonaire permettant l'obtention de métastases ganglionnaires après implantation orthotopique.

Par rapport aux objectifs qui étaient fixés, une formulation permettant une encapsulation totale et stable au cours du temps a été obtenue. Les LNCs formulées ont eu un fort tropisme naturel pour cibler les ganglions lymphatiques. Et finalement, les formulations injectées en suspension ou sous forme d'hydrogel ont été aussi efficaces que le traitement standard pour traiter des animaux ayant développé des tumeurs très agressives, avec l'avantage de limiter le phénomène de myélosuppression. Pour finir, l'obtention d'un hydrogel de nanocapsules lipidiques offre de nouvelles perspectives dans le traitement des cancers, qui aujourd'hui, restent des pathologies où de nombreux efforts doivent être menés pour améliorer la survie mais également la vie des patients.

8. Références

1. Perez-Soler, R. & Khokhar, A. R. Lipophilic cisplatin analogues entrapped in liposomes: role of intraliposomal drug activation in biological activity. *Cancer Res.* **52,** 6341–6347 (1992).

2. Mayhew, E., Franklin, J. ., Bhatia, S., Harmon, P. . & Janoff, A. . Hydrophobic taxane derivatives. Patent US6291690 (2001)

3. Lundberg, B. ., Risovic, V., Ramaswamy, M. & Wasan, K. . A lipophilic paclitaxel derivative incorporated in a lipid emulsion for parenteral administration. *J. Control. Release* **86,** 93–100 (2003).

4. Bergman, A. M. *et al.* Antiproliferative activity and mechanism of action of fatty acid derivatives of arabinofuranosylcytosine in leukemia and solid tumor cell lines. *Biochem. Pharmacol.* **67,** 503–511 (2004).

5. Roger, E., Lagarce, F. & Benoit, J.-P. Development and characterization of a novel lipid nanocapsule formulation of Sn38 for oral administration. *Eur. J. Pharm. Biopharm.* **79,** 181–188 (2011).

6. Murdan, S. Organogels in drug delivery. *Expert Opi. Drug Deliv.* **2,** 489–505 (2005).

7. Murdan, S., Gregoriadis, G. & Florence, A. T. Interaction of a nonionic surfactant-based organogel with aqueous media. *Int. J. Pharm.***180,** 211–214 (1999).

8. Murdan, S., Bergh, B. van den, Gregoriadis, G. & Florence, A. T. Water-in-sorbitan monostearate organogels (water-in-oil gels). *J. Pharm. Sci.***88,** 615–619 (1999).

9. Murdan, S. Organogels in drug delivery. *Expert Opin Drug Deliv* **2,** 489–505 (2005).

10. Murdan, S., Gregoriadis, G. & Florence, A. Non-ionic surfactant based organogels incorporating niosomes. *STP pharma sciences.* **6,** 44–48 (1996).

11. Kumar, R. & Katare, O. P. Lecithin organogels as a potential phospholipid-structured system for topical drug delivery: a review. *AAPS PharmSci Tech.* **6,** 298–310 (2005).

12. Brusa, P., Immordino, M. L., Rocco, F. & Cattel, L. Antitumor activity and pharmacokinetics of liposomes containing lipophilic gemcitabine prodrugs. *Anticancer Res.* **27,** 195–199 (2007).

13. Immordino, M. L. *et al.* Preparation, characterization, cytotoxicity and pharmacokinetics of liposomes containing lipophilic gemcitabine prodrugs. *J. Control. Release* **100,** 331–346 (2004).

14. Zhu, S., Lansakara-P., D. S. P., Li, X. & Cui, Z. Lysosomal Delivery of a Lipophilic Gemcitabine Prodrug Using Novel Acid-Sensitive Micelles Improved Its Antitumor Activity. *Bioconjugate Chem.* **23,** 966–980 (2012).

15. Sloat, B. R. *et al.* In vitro and in vivo anti-tumor activities of a gemcitabine derivative carried by nanoparticles. *Int. J. Pharm.* **409,** 278-288 (2001).

16. Chung, W.-G., Sandoval, M. A., Sloat, B. R., Lansakara-P, D. S. P. & Cui, Z. Stearoyl gemcitabine nanoparticles overcome resistance related to the over-expression of ribonucleotide reductase subunit M1. *J. Control. Release* ***157,*** *132-140* (2012).

17. Sandoval, M. A. *et al.* EGFR-targeted stearoyl gemcitabine nanoparticles show enhanced anti-tumor activity. *J. Control. Release* ***157,*** *287-296* (2012).

18. Stella, B. *et al.* Encapsulation of gemcitabine lipophilic derivatives into polycyanoacrylate nanospheres and nanocapsules. *Int. J. Pharm.* **344,** 71–77 (2007).

19. Castelli, F., Sarpietro, M. G., Ceruti, M., Rocco, F. & Cattel, L. Characterization of Lipophilic Gemcitabine Prodrug−Liposomal Membrane Interaction by Differential Scanning Calorimetry. *Mol. Pharmaceutics* **3,** 737–744 (2006).

20. Wichterle, O. & Lím, D. Hydrophilic Gels for Biological Use. *Nature* **185,** 117–118 (1960).

21. Kashyap, N., Kumar, N. & Kumar, M. N. V. R. Hydrogels for pharmaceutical and biomedical applications. *Crit. Rev. Ther. Drug Carrier Syst.* **22,** 107–149 (2005).

22. Hoffman, A. S. Hydrogels for biomedical applications. *Adv. Drug Deliv. Rev.* **54,** 3–12 (2002).

23. Van Vlierberghe, S., Dubruel, P. & Schacht, E. Biopolymer-Based Hydrogels As Scaffolds for Tissue Engineering Applications: A Review. *Biomacromolecules* **12,** 1387–1408 (2011).

24. Yusof, N., Ainul Hafiza, A. H., Zohdi, R. M. & Bakar, M. Z. A. Development of honey hydrogel dressing for enhanced wound healing. *Radiat. Phys. Chem.* **76,** 1767–1770 (2007).

25. Mukherjee, D. & Banthia, A. K. Preparation of Adrenochrome Hydrogel Patch, Gel, Ointment, and the Comparison of Their Blood Coagulating and Wound Healing Capability. *Mater. Manufac. Proc.***21,** 297–301 (2006).

26. Adams, T. S. T., Crook, T. & Cadier, M. A. M. A late complication following the insertion of hydrogel breast implants. *J. Plast. Reconstr. Aesthet. Surg.* **60,** 210–212 (2007).

27. Das, A., Wadhwa, S. & Srivastava, A. K. Cross-linked guar gum hydrogel discs for colon-specific delivery of ibuprofen: formulation and in vitro evaluation. *Drug Deliv.* **13,** 139–142 (2006).

28. Chang, J. Y. *et al.* Prolonged antifungal effects of clotrimazole-containing mucoadhesive thermosensitive gels on vaginitis. *J. Control. Release* **82,** 39–50 (2002).

29. Mathieu, E. *et al.* Intramyocardial delivery of mesenchymal stem cell-seeded hydrogel preserves cardiac function and attenuates ventricular remodeling after myocardial infarction. *PLoS ONE* **7,** e51991 (2012).

30. Sharma, B. *et al.* Human cartilage repair with a photoreactive adhesive-hydrogel composite. *Sci. Transl. Med.* **5,** 167ra6 (2013).

31. Nanjawade, B. K., Manvi, F. V. & Manjappa, A. S. In situ-forming hydrogels for sustained ophthalmic drug delivery. *J. Control. Release* **122,** 119–134 (2007).

32. Miyazaki, S. *et al.* In situ gelling xyloglucan formulations for sustained release ocular delivery of pilocarpine hydrochloride. *Int. J. Pharm.* **229,** 29–36 (2001).

33. Torres, A. J., Zhu, C., Shuler, M. L. & Pannullo, S. Paclitaxel delivery to brain tumors from hydrogels: a computational study. *Biotechnol. Prog.* **27,** 1478–1487 (2011).

34. Dadsetan, M. *et al.* A stimuli-responsive hydrogel for doxorubicin delivery. *Biomaterials* **31,** 8051–8062 (2010).

35. Al-Abd, A. M., Hong, K.-Y., Song, S.-C. & Kuh, H.-J. Pharmacokinetics of doxorubicin after intratumoral injection using a thermosensitive hydrogel in tumor-bearing mice. *J. Control. Release* **142,** 101–107 (2010).

36. Sťastný, M. *et al.* HPMA-hydrogels containing cytostatic drugs. Kinetics of the drug release and in vivo efficacy. *J. Control. Release* **81,** 101–111 (2002).

37. Zentner, G. M. *et al.* Biodegradable block copolymers for delivery of proteins and water-insoluble drugs. *J. Control. Release* **72,** 203–215 (2001).

38. Dineen, M. K., Tierney, D. S., Kuzma, P. & Pentikis, H. S. An evaluation of the pharmacokinetics and pharmacodynamics of the histrelin implant for the palliative treatment of prostate cancer. *J. Clin. Pharmacol.* **45,** 1245–1249 (2005).

39. Hamidi, M., Azadi, A. & Rafiei, P. Hydrogel nanoparticles in drug delivery. *Advanced Drug Deliv. Rev.* **60,** 1638–1649 (2008).

40. Hoare, T. R. & Kohane, D. S. Hydrogels in drug delivery: Progress and challenges. *Polymer* **49,** 1993–2007 (2008).

41. Ratner, B. . *Biomaterials Science: An Introduction Materials in Medicine*. (2004).

42. Aydemir, N. & Bilaloğlu, R. Genotoxicity of two anticancer drugs, gemcitabine and topotecan, in mouse bone marrow in vivo. *Mutat. Res.* **537,** 43–51 (2003).

43. Eudaly, J. A., Tizzano, J. P., Higdon, G. L. & Todd, G. C. Developmental toxicity of gemcitabine, an antimetabolite oncolytic, administered during gestation to CD-1 mice. *Teratology* **48,** 365–381 (1993).

44. Silva, A. C., Amaral, M. H., González-Mira, E., Santos, D. & Ferreira, D. Solid lipid nanoparticles (SLN) - based hydrogels as potential carriers for oral transmucosal delivery of Risperidone: Preparation and characterization studies. *Colloids and Surfaces B: Biointerfaces* **93,** 241–248 (2012).

45. Hirsjärvi, S. *et al.* Influence of size, surface coating and fine chemical composition on the in vitro reactivity and in vivo biodistribution of lipid nanocapsules versus lipid nanoemulsions in cancer models. *Nanomedicine* **9,** *375-387* (2012).

46. Hirsjärvi, S. *et al.* Surface modification of lipid nanocapsules with polysaccharides: From physicochemical characteristics to in vivo aspects. *Acta Biomater.* **9,** 6686-6693 (2013).

47. Reddy, S. T., Rehor, A., Schmoekel, H. G., Hubbell, J. A. & Swartz, M. A. In vivo targeting of dendritic cells in lymph nodes with poly(propylene sulfide) nanoparticles. *J. Control. Release* **112,** 26–34 (2006).

48. Diehl, K. H. *et al.* A good practice guide to the administration of substances and removal of blood, including routes and volumes. *J. Appl. Toxicol.* **21,** 15–23 (2001).

49. Burris, H. A., 3rd *et al.* Improvements in survival and clinical benefit with gemcitabine as first-line therapy for patients with advanced pancreas cancer: a randomized trial. *J. Clin. Oncol.* **15,** 2403–2413 (1997).

50. Heinemann, V. Gemcitabine: progress in the treatment of pancreatic cancer. *Oncology* **60,** 8–18 (2001).

51. Yoshida, M. *et al.* Targeting Anticancer Drug Delivery to Pancreatic Cancer Cells Using a Fucose-Bound Nanoparticle Approach. *PLoS ONE* **7,** e39545 (2012).

52. Lee, G. Y. *et al.* Theranostic nanoparticles with controlled release of gemcitabine for targeted therapy and MRI of pancreatic cancer. *ACS Nano* **7,** 2078–2089 (2013).

53. Graeser, R. *et al.* Antimetastatic effects of liposomal gemcitabine and empty liposomes in an orthotopic mouse model of pancreatic cancer. *Pancreas* **38,** 330–337 (2009).

54. http://www1.astrazeneca-us.com/pi/zoladex10_8.pdf. (2 avril 2013).

55. http://products.sanofi.ca/fr/suprefact-depot.pdf. (2 avril 2013).

Curriculum vitæ

M^lle MOYSAN Elodie
Le Roch Viannec
56550 Locoal-Mendon
06 25 95 90 43
moysan.elodie@hotmail.fr
Née le 17 Novembre 1986 à Lorient

FORMATIONS

Depuis Avril 2010 — **Université d'Angers**, Angers, France
Thèse en Pharmacologie Expérimentale et Clinique

2010 — **Ecole Nationale Vétérinaire, Agroalimentaire et de l'Alimentation Nantes-Atlantique – ONIRIS**, Nantes, France
Accréditation pour expérimentation animale niveau 1
Numéro d'autorisation : **A 49 -2011-09**

2007 – 2009 — **Université Joseph Fourier**, UFR Pharmacie, Grenoble, France
Master Recherche - Ingénieries pour la Santé et le Médicament - Spécialité « Biotechnologies et Ingénierie Diagnostiques et Thérapeutiques » - Parcours « Biotechnologie, Santé et Management »
Mention Bien

Diplôme délivré en partenariat avec Grenoble Ecole de Management (GEM) et l'Ecole de Pharmacie de Genève-Lausanne (EPGL)

2004 – 2007 — **Université de Bretagne Sud**, Vannes, France
Licence - Sciences et Technologies - Mention « Sciences de la Vie et de la Terre » - Spécialité « Biologie Appliquée »
Mention Assez Bien

EXPÉRIENCES PROFESSIONNELLES

2010-2013 (3ans) — **Doctorat de Pharmacologie Expérimentale et Clinique**
Université d'Angers, France
Unité de Micro et Nanomédecines Biomimétiques – UMR-S 1066
Directeurs de Thèse : Pr. Jean-Pierre Benoit et Dr. Guillaume Bastiat

- ✓ *Hydrogel de nanocapsules lipidiques chargées en gemcitabine : une technologie pharmaceutique pour cibler les ganglions de drainage des cancers*

Janvier – Juin 2009 **Stage de master 1 et 2 à l'Institut Albert Bonniot**
Avril – Juin 2008 Grenoble, France
Ontogenèse et Oncogenèse Moléculaire – Inserm U823
Directrices de recherche : Pr. Elisabeth Brambilla et Dr. Béatrice Eymin

- ✓ *Implication du facteur d'épissage SC35 dans la réponse des cellules tumorales de carcinomes pulmonaires aux agents génotoxiques*

Avril – Mai 2007 **Stage de Licence au laboratoire de CECALIMENT**
St Allouestre, France

- ✓ *Mise en place d'un protocole d'analyse de mycotoxines*

ACTIVITES D'ENSEIGNEMENT

2011 - 2013 **Vacataire** à l'IUT d'Angers, France

Cours magistraux aux 2ème années en section agronomie et section analyses biologiques et biochimiques
Encadrement des travaux pratiques des 2èmes années en section agronomie et section analyses biologiques et biochimiques

- ✓ *Cours : La culture in vitro (2 x 1,5h)*
- ✓ *TP : Culture in vitro appliquée au végétal et aux cellules animales (125h)*
- ✓ *Préparation et correction des contrôles continus*
- ✓ *Correction des comptes rendus de Tp*

2010 - 2011 **Doctorante Contractuelle à Activité Complémentaire d'Enseignement** à l'IUT d'Angers, France

Encadrement des travaux pratiques des 1ères et 2èmes années en section agronomie et section analyses biologiques et biochimiques

- ✓ *TP : Culture cellulaire végétale, 1ère année (12h)*
- ✓ *TP : Culture in vitro appliquée au végétal et aux cellules animales, 2ème année (52h)*
- ✓ *Correction des comptes rendus de Tp*

ENCADREMENT

2012 (1mois)	**Encadrement** de Véronika Csorba, étudiante en 3ème année de pharmacie à l'université de Budapeste en Hongrie
2012 (6mois)	**Encadrement** de Yolanda Gonzalez Fernandez, étudiante en 5ème année de pharmacie à l'université de Séville en Espagne
2011 (6mois)	**Encadrement** de Anna Cieślak, étudiante en 5ème année de pharmacie à l'université de médecine de Łódź en Pologne

COMPÉTENCES SCIENTIFIQUES

Galénique

- Nanocapsules lipidiques (NCL)
- Modification de surface

Physico-chimie

- Résonance magnétique nucléaire (RMN)
- Chromatographie en phase liquide à haute et ultra performance (HPLC et UPLC)
- Tensiomètre à goutte
- Rhéologie (Oscillation, écoulement, température)
- Mesure de taille nanométrique, d'indice de polydispersité et de potentiel zéta

Biologie cellulaire

- Culture de lignées cancéreuses humaines
- Développement de lignées cellulaires transgéniques stables par transfection.
- Immunofluorescence, microscopie
- Cytométrie en flux

Biologie moléculaire

- Extraction d'ADN, d'ARN et de protéines
- Analyse de l'expression génique par RT-PCR quantitative en temps réel
- Analyse de l'expression protéique par Western Blot
- Clonage moléculaire de vecteurs d'expression
- Immuno-précipitation

In vivo

- Implantation ectopique et orthotopique
- Injections *i.v* , *s.c* et *i.*p sur souris
- Récupération d'organes et de sang

Imagerie

- Visualisation *in vivo* et *ex vivo* de fluorescence
- Utilisation du Maestro System ®

PUBLICATIONS

Moysan E, Bastiat G, Benoit J.P. Gemcitabine versus modified gemcitabine: a review of several promising chemical modifications. *Molecular Pharmaceutics*. **2013**, 10, 430-44.

Edmond. V, **Moysan E**, Khochbin**.** S *et al*: Post-translational modifications of the SR protein SC35 through Tip60-, HDAC6- and SRPK-dependent signaling networks control cell fate decision in response to cisplatin. *EMBO J.* **2011**, *30*, 510-523.

COMMUNICATIONS ORALES

Moysan. E, Bejaud. J, Lautram. N, Bastiat. G, Benoit. J.P. Innovative gel formulation of lipid nanocapsules with modified gemcitabine: a new pharmaceutical technology for lung and pancreatic cancer therapy. Nanomedicine in oncology, 26-29 septembre 2012. Ile de Berder, France

Moysan. E, Cieślak. A, Bejaud. J, Lautram. N, Bastiat. G, Benoit. J.P. Innovative gel formulation of lipid nanocapsules with gemcitabine: A potential treatment of lung cancer. Journées de l'école doctorale, 7-8 novembre 2011. Thalmont-Saint-Hilaire, France.

COMMUNICATIONS POSTERS

Moysan. E, Wauthoz. N Bastiat. G, Benoit. J.P. An original nanomedicine to deliver gemcitabine in lymph nodes invaded by metastasis. XXVII$^{\text{ièmes}}$ Scientific GTRV meeting 3-5 décembre 2012. Paris, France.

Moysan. E, Bastiat. G, Cieslak. A, Lautram. N, Béjaud. J, Benoit. J.P. Modified Gemcitabine-loaded lipid nanocapsules: when a drug participates to the structure of a nanomedicine. 39$^{\text{th}}$ CRS annual meeting & exposition, July 15 – 18, 2012. Québec City, Canada.

Moysan. E Cieślak. A, Bejaud. J, Lautram. N, Bastiat. G, Benoit. J.P**.** Lipid nanocapsules loaded with gemcitabine: an innovative pharmaceutical technology for lung cancer treatment. XXVI^{ièmes} Scientific GTRV meeting 5-7 décembre 2011. Bruxelles, Belgique.

PRIX

Prix Debiopharm Group de la meilleure présentation de poster intitulée : Lipid nanocapsules loaded with gemcitabine: an innovative pharmaceutical technology for lung cancer treatment. XXVI^{ièmes} Scientific GTRV meeting 5-7 décembre 2011; Bruxelles, Belgique.

l'université nantes angers le mans
PÔLE DE RECHERCHE ET D'ENSEIGNEMENT SUPÉRIEUR

université angers

Thèse de Doctorat

Elodie Moysan

Hydrogel de nanocapsules lipidiques chargées en gemcitabine : une technologie pharmaceutique pour cibler les ganglions de drainage des cancers

Résumé

Un hydrogel de nanocapsules lipidiques (NCLs) chargées en gemcitabine a été utilisé afin de cibler les ganglions lymphatiques pour optimiser la chimiothérapie des cancers pulmonaires métastatiques. Une forme lipophile de la gemcitabine, ce principe actif étant modifié par une chaîne aliphatique en C_{12}, a été encapsulée dans les LNCs, et de façons intéressantes et inattendues, une gélification spontanée du système a été obtenue. Les propriétés viscoélastiques de l'hydrogel dépendent des concentrations en LNCs et en prodrogue. La gemcitabine modifiée se localise à l'interface huile/eau des LNCs et permet l'interaction des LNCs via des liaisons hydrogène. Ces liaisons permettent d'aboutir à une structure gélifiée, sans matrice extérieure, comme un « collier de perles ». Une fois dilué, les LNCs sont retrouvées en suspension. Ces LNCs chargées en prodrogue ont montré une efficacité *in vitro*, supérieure à la gemcitabine native, sur des cellules de carcinomes pulmonaires et pancréatiques. L'injection sous-cutanée de l'hydrogel représente une voie d'administration prometteuse pour la délivrance de principes actifs dans les ganglions. La proportion de LNCs dans les ganglions lymphatiques a été augmentée et prolongée et aucune accumulation dans le foie et la rate n'a été observée comparativement à une injection sous-cutanée ou intraveineuse de LNCs en suspension. Un modèle orthotopique de cancer pulmonaire métastasant de manière importante dans le médiastin a été utilisé pour des études d'efficacité. Le traitement avec les LNCs chargées en prodrogue a significativement augmenté la survie des souris sans développer de myélosuppression, qui est observée après injection de gemcitabine non encapsulée. Les LNCs encapsulant la gemcitabine modifiée pourraient être une nouvelle forme de nanomédecine bénéfique pour le traitement de cancer métastasant dans les ganglions lymphatiques.

Mots clés
Nanomédecine; Nanocapsules lipidiques; Gemcitabine, Hydrogel; Cancer pulmonaire; Métastases, Ganglions lymphatiques.

Abstract

Gemcitabine-loaded lipid nanocapsules (LNCs) hydrogel was used to target lymph nodes, with the aim to optimize the chemotherapy of metastases from lung cancers. A lipophilic form of gemcitabine, modified with lauroyl chain, was encapsulated inside LNCs, and interestingly a spontaneous gel system has been obtained. The viscoelastic properties were dependent on the LNCs and prodrug concentrations. The modified gemcitabine was localized at the oil/water interface of the LNCs. This particular assembly promoted the inter-LNC interaction via H-bond between gemcitabine moieties of prodrug to lead to LNC gel structure in water, without matrix, like a pearl necklace. Once diluted, the hydrogel provided nanoparticles in suspension. The *in vitro* citotoxicity of encapsulated gemcitabine was higher than for free gemcitabine, in regards of lung and pancreatic carcinoma cell lines. Subcutaneous hydrogel injection was a promising administration route to target lymph nodes. The amount of LNCs in lymph nodes was increased, and the accumulation in liver and spleen was prevented, in comparison to subcutaneous and intravenous injection of LNCs aqueous suspension. A human orthotopic xenograft of lung cancer, with high metastatic potential, was used for *in vivo* efficacy studies. Treatment with prodrug-loaded LNCs significantly increased the median survival time of treated mice, without developing myelosuppression as observed for free gemcitabine treatment. Modified gemcitabine-loaded LNCs could be a new technology of beneficial nanomedicine for the treatment of metastases in lymph nodes.

Key Words
Nanomedicine; Lipid nanocaspules; Gemcitabine; Hydrogel; Lung cancer; Metastasis; Lymph nodes.